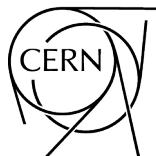


2015 European School of High-Energy Physics

Bansko, Bulgaria
2 – 15 September 2015

Editors: M. Mulders
G. Zanderighi



CERN Yellow Reports: School Proceedings
Published by CERN, CH-1211 Geneva 23, Switzerland

ISBN 978-92-9083-472-4 (paperback)

ISBN 978-92-9083-473-1 (PDF)

ISSN 2519-8041 (Print)


ISSN 2519-805X (Online)

DOI <https://doi.org/10.23730/CYRSP-2017-004>

Accepted for publication by the CERN Report Editorial Board (CREB) on 6 November 2017

Available online at <http://publishing.cern.ch/> and <http://cds.cern.ch/>

Copyright © CERN, 2017

 Creative Commons Attribution 4.0

Knowledge transfer is an integral part of CERN's mission.

CERN publishes this volume Open Access under the Creative Commons Attribution 4.0 license (<http://creativecommons.org/licenses/by/4.0/>) in order to permit its wide dissemination and use. The submission of a contribution to a CERN Yellow Report series shall be deemed to constitute the contributor's agreement to this copyright and license statement. Contributors are requested to obtain any clearances that may be necessary for this purpose.

This volume is indexed in: CERN Document Server (CDS), INSPIRE, Scopus.

This volume should be cited as:

Proceedings of the 2015 European School of High-Energy Physics, Bansko, Bulgaria, 2 – 15 September 2015, edited by M. Mulders and G. Zanderighi, CERN Yellow Reports: School Proceedings, Vol. 4/2017, CERN-2017-008-SP (CERN, Geneva, 2017), <https://doi.org/10.23730/CYRSP-2017-004>

A contribution in this volume should be cited as:

[Author name(s)], in Proceedings of the 2015 European School of High-Energy Physics, Bansko, Bulgaria, 2 – 15 September 2015, edited by M. Mulders and G. Zanderighi, CERN Yellow Reports: School Proceedings, Vol. 4/2017, CERN-2017-008-SP (CERN, Geneva, 2017), pp. [first page]–[last page], <https://doi.org/10.23730/CYRSP-2017-004>. [first page]

Abstract

The European School of High-Energy Physics is intended to give young physicists an introduction to the theoretical aspects of recent advances in elementary particle physics. These proceedings contain lecture notes on quantum field theory and the Electroweak Standard Model, Higgs physics, flavour physics and CP violation, theories 'behind' the Standard Model, heavy ion physics, and practical statistics for High Energy Physics.

Preface

The twenty-third event in the series of the European School of High-Energy Physics took place in Bansko, Bulgaria, from 2 to 15 September 2015. It was organized jointly by CERN, Geneva, Switzerland, and JINR, Dubna, Russia, with support from the Bulgarian Nuclear Regulatory Agency, St. Kliment Ohridski University of Sofia, and the Institute for Nuclear Research and Nuclear Energy of the Bulgarian Academy of Sciences. The local organization team was chaired by Prof. Roumen Tsenov who was greatly assisted by Mrs Gergana Mitkova on many administrative matters. The other members of the local committee were: P. Iaydjuev, I. Ilchev, L. Kostov, B. Pavlov, D. Tonev and G. Vankova-Kirilova.

A total of 92 students of 34 different nationalities attended the school, mainly from institutes in member states of CERN and/or JINR, but also some from other regions. The participants were generally students in experimental High-Energy Physics in the final years of work towards their PhDs.

The School was hosted at the St. Ivan Rilski hotel in Bansko, about 160 km to the south of Sofia. According to the tradition of the school, the students shared twin rooms mixing participants of different nationalities.

A total of 30 lectures were complemented by daily discussion sessions led by six discussion leaders. The students displayed their own research work in the form of posters in an evening session in the first week, and the posters stayed on display until the end of the School. The full scientific programme was arranged in the on-site conference facilities.

The School also included an element of outreach training, complementing the main scientific programme. This consisted of a two-part course from the Inside Edge media training company. In an after-dinner session, students had the opportunity to act out radio interviews under realistic conditions based on a hypothetical scenario.

The students from each discussion group subsequently carried out a collaborative project, preparing a talk on a physics-related topic at a level appropriate for a general audience. The talks were given by student representatives of each group in an evening session in the second week of the School. A jury, chaired by Svejina Dimitrova, Director of the Astronomic Observatory and Planetarium in Varna, judged and gave feedback on the presentations; other members of the jury were Andrea de Simone (lecturer at the School), Kate Ross (Schools Administrator), and Zornica Asanska and Klimentina Savova (high-school students who are studying physics at the Academician Kiril Popov Mathematical School in Plovdiv). We are very grateful to all of these people for their help.

Our thanks go to the local-organization team and, in particular, to Roumen Tsenov, for all of their work and assistance in preparing the School, on both scientific and practical matters, and for their presence throughout the event. Our thanks also go to the efficient and friendly hotel management and staff who assisted the School organizers and the participants in many ways.

Very great thanks are due to the lecturers and discussion leaders for their active participation in the School and for making the scientific programme so stimulating. The students, who in turn manifested their good spirits during two intense weeks, appreciated listening to and discussing with the teaching staff of world renown.

We would like to express our strong appreciation to Professor Rolf Heuer, Director General of CERN, and Professor Victor Matveev, Director of JINR, for their lectures on the scientific programmes of the two organizations and for discussing with the School participants. It is worth noting that Professor Heuer lectured at every European School of HEP during his seven-year mandate as Director General of CERN that ends in December 2015.

Our sincere thanks are also due to the following high-level visitors who participated in the opening ceremony of the School: Ms Genoveva Jecheva, Director, National Science Fund of the Ministry of Education and Science; Professor Latchesar Kostov, Chairman, Bulgarian Nuclear Regulatory Agency; and Professor Dimitar Tonev, Director, Institute for Nuclear Research and Nuclear Energy, Bulgarian Academy of Sciences.

In addition to the rich academic programme, the participants enjoyed numerous sports, leisure and cultural

activities in and around Bansko. Particularly noteworthy were the half-day excursion to the village of Dobursko, with its historic church and dancing grandmothers, and the town of Razlog, and the full-day excursion to the impressive Rila Monastery and the town of Blagoevgrad. Sports and leisure activities in and around the hotel, as well as the excursions, provided an excellent environment for informal interactions between staff and students.

We are very grateful to Kate Ross and Tatyana Donskova for their untiring efforts in the lengthy preparations for and the day-to-day operation of the School. Their continuous care of the participants and their needs during the School was highly appreciated.

The success of the School was to a large extent due to the students themselves. Their poster session was very well prepared and highly appreciated, their group projects were a huge success, and throughout the School they participated actively during the lectures, in the discussion sessions and in the different activities and excursions.

Nick Ellis
(On behalf of the Organizing Committee)





People in the photograph

1 Sergey Demidov	34 William Astill	67 Martijn Mulders
2 Alexander Bednyakov	35 Aysenur Gencer	68 Eldwan Brianne
3 Andrey Arbuzov	36 Abdelali El Jaoudi	69 Irina Cioara
4 Daniel Salerno	37 Veselin Filev	70 Philipp Millet
5 Shirin Chenarani	38 Christian Bourjau	71 Nataliia Kovalchuk
6 Daniel Buscher	39 Brian Amadio	72 Nick Ellis
7 Sophie Berkman	40 Anna Kowalewska	73 Francesco Giuli
8 Baishali Dutta	41 Joze Zobec	74 Michael Buttignol
9 Esmaeel Eskandari	42 Cristovao Da Cruz e Silva	75 Luca Cadamuro
10 Roger Naranjo	43 Elsayed Tayel	76 Andrew Ferrante
11 Royer Ticse Torres	44 Christine Mclean	77 Olga Grzymkowska
12 Ivan Orlov	45 Muhammad Shoaib	78 Carsten Burgard
13 Milan Stojanovic	46 Tatyana Donskova	79 Matic Lubej
14 Tobias Heck	47 Joao Pela	80 Juan Pedro Araque Espinosa
15 Mikhail Iliushin	48 Francisco Arduh	81 Georgiy Razuvaev
16 Elvire Bouvier	49 Violetta Sagun	82 Damian Alvarez Piqueras
17 Adam Morris	50 Balthasar Schachtner	83 Nikolay Geraksiev
18 Goran Kacarevic	51 Camilla Galloni	84 Othamane Rifki
19 Nataliia Kondrashova	52 Nikoloz Tsverava	85 Daniel Cervenkov
20 Orjan Dale	53 Emanuele Usai	86 Anna Maksymchuk
21 Maria Hoffmann	54 Marco Sessa	87 Nils Flaschel
22 Dmytro Levit	55 Daria Savrina	88 Leonor Cerda Alberich
23 Nicolas Koehler	56 Anna Lupato	89 Thea Aarrestad
24 Simon Fink	57 Ivan Angelozzi	90 Nikolay Atanov
25 Elena Ginina	58 Alexander Olshevskiy	91 Stefan Mladenov
26 Jonatan Rosten	59 Andrea Gaudiello	92 Klimentina Savova
27 Mathias Garny	60 Rishat Sultanov	93 Zornitsa Asanska
28 Katharina Ecker	61 Ali Harb	94 Francesco Riva
29 Rachel Hinman	62 Thomas Strebler	95 Tsvetan Vetsov
30 Sebastien Prince	63 Andrew Johnson	96 Yang Qin
31 Michael Ziegler	64 Josef Pacalt	97 Roumen Tsenov
32 Zakaria Chadi	65 Daniele Madaffari	
33 Vytautas Vislavicius	66 Nada Barakat	

Photographs (montage)



The 2015 European School of High-Energy Physics

Bansko, Bulgaria 2 – 15 September 2015





Contents

Preface	
<i>N. Ellis</i>	v
Photograph of participants	vii
Photographs (montage)	x
Quantum Field Theory and the Electroweak Standard Model	
<i>A.B. Arbuzov</i>	1
Higgs Physics, in the SM and Beyond	
<i>F. Riva</i>	35
Flavor and CP violation within and beyond the Standard Model	
<i>S. Gori</i>	65
Behind the Standard Model	
<i>A. Wulzer</i>	91
A very brief introduction to heavy ion physics	
<i>S. Floerchinger</i>	141
Practical Statistics for High Energy Physics	
<i>E. Gross</i>	165
Organizing Committee	187
Local Organizing Committee	187
List of Lecturers	187
List of Discussion Leaders	187
List of Students	188
List of Posters	189

Quantum Field Theory and the Electroweak Standard Model

A.B. Arbuzov

BLTP JINR, Dubna, Russia

Abstract

Lecture notes with a brief introduction to Quantum field theory and the Standard Model are presented. The lectures were given at the 2015 European School of High-Energy Physics. The main features, the present status, and problems of the Standard Model are discussed.

Keywords

Lectures; ESHEP; quantum field theory; Standard Model.

1 Introduction

The lecture course consists of four main parts. In the Introduction, we will discuss what is the Standard Model [1–3], its particle content, and the main principles of its construction. The second Section contains brief notes on Quantum Field Theory (QFT), where we remind the main objects and rules required further for construction of the SM. Sect. 3 describes some steps of the SM development. The Lagrangian of the model is derived and discussed. Phenomenology and high-precision tests of the model are overviewed in Sect. 4. The present status, problems, and prospects of the SM are summarized in Conclusions. Some simple useful exercises and questions are given for students in each Section. These lectures give only an overview of the subject while for details one should look in textbooks, e.g., [4–6], and modern scientific papers.

1.1 What is the Standard Model?

Let us start with the definition of the subject of the lecture course. It is the so-called *Standard Model* (SM). This name is quite widely accepted and commonly used to define a certain theoretical model in high energy physics. This model is suited to describe properties and interactions of *elementary* particles. One can say that at the present moment, the Standard Model is the most successful physical model ever. In fact it describes with a high precision hundreds and hundreds independent observables. The model made also a lot of predictions which have been verified later experimentally. Among other physical models pretending to describe fundamental properties of Nature, the SM has the highest predictive power. Moreover, the model is minimal: it is constructed using only fields, interactions and parameters which are necessary for consistency and/or observed experimentally. The minimality and in general the success of the model is provided to a great extent by application of symmetry principles.

In spite of the nice theoretical features and successful experimental verification of the SM, we hardly can believe that it is the true fundamental theory of Nature. First of all, it is only one of an infinite number of possible models within Quantum field theory. So it has well defined grounds but its uniqueness is questionable. Second, we will see that the SM and QFT itself do not seem to be the most adequate (mathematical) language to describe Nature. One can also remind that gravity is not (yet) joined uniformly with other interactions.

But in any case, the SM is presently the main theoretical tool in high-energy physics. Most likely this status will be preserved even if some new more fundamental physical model would be accepted by the community. In this case the SM can be treated as an approximation (a low-energy limit) of a more general theory.

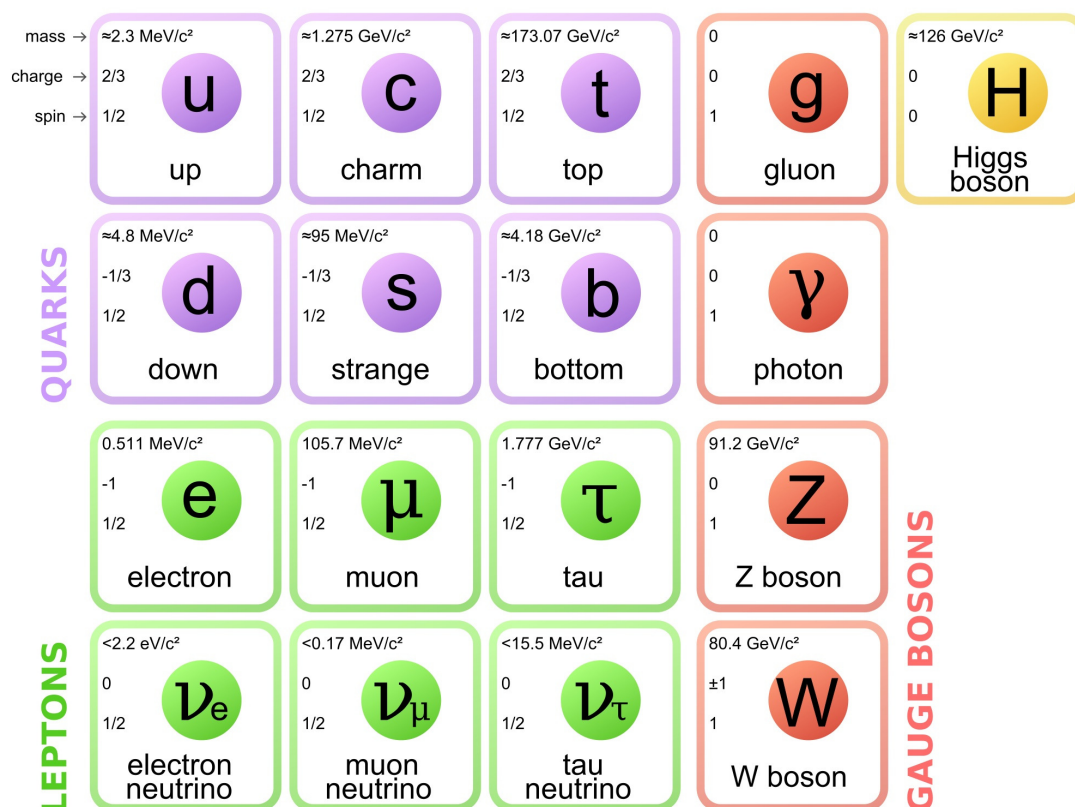


Fig. 1: Particle content of the Standard Model. Courtesy to Wikipedia: 'Standard Model of Elementary Particles' by MissMJ — Own work by uploader, PBS NOVA, Fermilab, Office of Science, United States Department of Energy, Particle Data Group.

1.2 Particle content of the Standard Model

Before construction of the SM, let us defined its content in the sense of fields and particles.

We would like to underline that the discovery of the Higgs boson at LHC in 2012 [7, 8] just finalized the list of SM particles from the experimental point of view. Meanwhile the Higgs boson is one of the key ingredients of the SM, so it was always in the list even so that its mass was unknown.

The particle content of the SM is given on Fig. 1. It consists of 12 fermions (spin = $1/2$), 4 vector gauge bosons (spin = 1), and one scalar Higgs boson (spin = 0). For each particle the chart contains information about its mass, electric charge, and spin. One can see that the data on neutrino masses is represented in the form of upper limits, since they have not been yet measured. Strictly speaking the information about neutrino masses should be treated with care. According to the present knowledge, as discussed in the course of lectures given by S. Petcov, a neutrino particle of a given lepton flavor e.g., ν_τ , is not a mass eigenstate but a superposition of (at least) three states with different masses.

Fermions are of two types: *leptons* and *quarks*. They are:

- 3 charged leptons (e, μ, τ);
- 3 neutrinos ν_e, ν_μ, ν_τ (or ν_1, ν_2, ν_3 , see lectures by S. Petcov);
- 6 quarks of different *flavors*, see lectures by S. Gori.

Each quark can have one of three *colours*, see lectures by A. Mitov. Each fermion has 2 degrees of freedom e.g., can have spin up or down, or can be either *left* or *right*. Each fermion particle in the SM has an *anti-particle*, $f \neq \bar{f}$. The later statement is not yet verified for neutrinos, they might be Majorana particles.

Traditionally fermions are called *matter fields*, contrary to the so-called *force fields*, i.e., intermediate vector bosons which mediate interactions. Please keep in mind that this notion doesn't correspond to the common sense directly. In fact most of fermions are unstable and do not form the 'ordinary matter' around us, while e.g., mass of nuclear matter is provided to a large extent by gluons. Moreover, looking at various Feynman diagrams we can see that fermions can serve as intermediate particles in interaction processes.

In the SM we have the following boson fields:

- 8 vector (spin=1) *gluons*;
- 4 vector (spin=1) *electroweak bosons*: γ , Z , W^+ , W^- ;
- 1 scalar (spin=0) *Higgs boson*.

Gluons and photon are *massless* and have 2 degrees of freedom (polarizations), Z and W bosons are *massive* and have 3 degrees of freedom (polarizations). By saying massless or massive we mean the absence or presence of the corresponding terms in the Lagrangian of the SM. This is not always related to observables in a straightforward way: e.g., gluons are not observed as free asymptotic states, and masses of unstable W and Z bosons are defined indirectly from kinematics of their decay products.

Gluons and Electroweak (EW) bosons are *gauge bosons*, their interactions with fermions are fixed by certain symmetries of the Lagrangian. Note that electrically neutral bosons (H , γ , Z , and gluons) coincide with their anti-particles e.g., $\gamma \equiv \bar{\gamma}$.

Besides the particle content, we have to list the interactions which are described by the Standard Model. Our final goal would be to answer the question "*How many fundamental interactions are there in Nature?*" But we should understand that it is only a dream, a primary motivation of our studies. Being scientists we might be always unsure about the true answer to this question. On the other hand, we can certainly say, how many different interactions is there in a given model, for example the SM one. To answer this question we have to look at the Lagrangian of the model, see e.g., book [9]. For the SM it looks very long and cumbersome. The SM Lagrangian contains kinetic terms for all listed above fields and dozens of terms that describe interactions between them. Before trying to count the number of interactions we should understand the structure and symmetries of the Lagrangian.

1.3 Principles of the Standard Model

We are going to construct the SM Lagrangian. For this purpose, we have to define first the guiding principles. That is important for optimization of the procedure. The same principles might be used further in construction of other models.

First of all, we have to keep in mind that the SM is a model that is built within the local Quantum field theory. From the beginning this condition strongly limits the types of terms that can appear in the Lagrangian because of the Lorentz invariance, the Hermitian condition, the locality etc. One can make a long list of various conditions. Here I list only the main principles which will be exploited in our way of the SM construction:

- the *generalized correspondence* to various existing theories and models like Quantum Mechanics, QED, the Fermi model etc.;
- the *minimality*, i.e., only observed and/or unavoidable objects (fields and interactions) are involved;
- the *unitarity* which is a general condition for cross sections and various transformations of fields related to the fact that any probability is limited from above by unity;
- the *renormalizability* is necessary for derivation of finite prediction of observable quantities at the quantum level;
- the *gauge* principle for introduction of interactions.

The main guiding principle is the *symmetry* one. The SM possesses several different symmetries:

- the Lorentz (and Poincaré) symmetry,
- the CPT symmetry,
- three gauge symmetries $SU(3)_C \otimes SU(2)_L \otimes U(1)_Y$,
- the global $SU(2)_L \times SU(2)_R$ symmetry in the Higgs sector (it is broken spontaneously);
- some other symmetries, like the one between three generation of fermions, the one that provides cancellation of anomalies etc.

In this context, one can mention also the conformal symmetry which is obviously broken in the SM, but the mechanism of its breaking and the consequences are very important for the model.

2 Brief notes on Quantum field theory

The Standard Model is a model constructed within the local relativistic Quantum field theory. It means that the SM obeys the general QFT rules. We should keep in mind that there are many other possible QFT models, and the SM is distinguished between them mostly because of its successful experimental verifications but also because of a number of its features like renormalizability, unitarity, and cancellation of axial anomalies. I assume that all students of the ESHEP school had courses on Quantum field theory. Here we will just remind several features of QFT which are important for further construction of the SM Lagrangian.

As it was already mentioned, we are going to preserve the correspondence to Quantum Mechanics (QM). Historically, QFT was developed on the base of QM, in particular using the quantum oscillator ansatz. But by itself QFT can be considered as a more profound fundamental construction, so one should be able to define this theory without referring to QM. In fact, QFT can be formulated starting from the basic classification of fields as unitary irreducible representations of the Lorentz group.

Let us first of all fix the notation. We will work in the natural system of units where the speed of light $c = 1$ and the reduced Planck constant $\hbar = 1$. The Lorentz indexes will be denoted by Greek letters, like $\mu = 0, 1, 2, 3$; p_μ is a four-momentum of a particle, $\mathbf{p} = (p_1, p_2, p_3)$ is a three-momentum, $p_0 = E$ is the particle energy.

The metric tensor of the Minkowsky space is chosen in the form

$$g_{\mu\nu} = \begin{pmatrix} 1 & 0 & 0 & 0 \\ 0 & -1 & 0 & 0 \\ 0 & 0 & -1 & 0 \\ 0 & 0 & 0 & -1 \end{pmatrix}, \quad g_{\mu\nu}p_\nu = p_\mu, \quad g_{\mu\mu} = 4. \quad (1)$$

We will always assume summation over a Lorentz index if it is repeated twice: $A_\mu B_\mu \equiv A_0 B_0 - A_1 B_1 - A_2 B_2 - A_3 B_3$, where the metric tensor is used. In particular, the scalar product of two four-vectors is defined as $pq = p_\mu q_\mu = p_0 q_0 - p_1 q_1 - p_2 q_2 - p_3 q_3$. It is a relativistic *invariant*.

We will assume that there exist so-called asymptotic free final states for particle-like excitation of quantum fields. These asymptotic states will be associated with initial or final state (elementary) particles which fly in a free space without interactions. For such states we apply the *on-mass-shell condition* $p^2 = pp = p_0^2 - \mathbf{p}^2 = E^2 - \mathbf{p}^2 = m^2$ where m is the mass of the particle.

Now we will postulate the properties of the fields that are required for the construction of the SM. A neutral scalar field can be defined as

$$\varphi(x) = \frac{1}{(2\pi)^{3/2}} \int \frac{d\mathbf{p}}{\sqrt{2p_0}} (e^{-ipx} a^-(\mathbf{p}) + e^{+ipx} a^+(\mathbf{p})), \quad (2)$$

where $a^\pm(\mathbf{p})$ are *creation* and *annihilation* operators. Their commutation relations read

$$\begin{aligned} [a^-(\mathbf{p}), a^+(\mathbf{p}')] &\equiv a^-(\mathbf{p})a^+(\mathbf{p}') - a^+(\mathbf{p}')a^-(\mathbf{p}) = \delta(\mathbf{p} - \mathbf{p}'), \\ [a^-(\mathbf{p}), a^-(\mathbf{p}')] &= [a^+(\mathbf{p}), a^+(\mathbf{p}')] = 0. \end{aligned} \quad (3)$$

The field is a function of four-coordinate x in the Minkowsky space. It behaves as a plane wave in the whole space. The Lagrangian¹ for the neutral scalar field can be chosen in the form

$$\mathcal{L}(x) = \frac{1}{2}(\partial_\mu\varphi\partial_\mu\varphi - m^2\varphi^2). \quad (4)$$

Note that it depends only on the field and its first derivative. Variation of the action $A \equiv \int d^4\mathcal{L}(x)$ with respect to variations of the field $\varphi \rightarrow \varphi + \delta\varphi$ according to the *least action principle* gives

$$\delta \int dx \mathcal{L}(x) = \int dx \left(\frac{\partial \mathcal{L}}{\partial \varphi} \delta\varphi + \frac{\partial \mathcal{L}}{\partial(\partial_\mu\varphi)} \delta(\partial_\mu\varphi) \right) = 0. \quad (5)$$

Here we apply quite natural for QFT zero boundary conditions for the field and its derivative at infinity and get the well-known Klein–Gordon equation of motion

$$(\partial_\mu^2 + m^2)\varphi(x) = 0. \quad (6)$$

EXERCISE: Check that the postulated above field $\varphi(x)$ satisfies the equation.

Creation and annihilation operators act in the Fock space which consists of *vacuum* ground state denoted as $|0\rangle$ and *excitations* over it. For the vacuum state we postulate

$$a^-(\mathbf{p})|0\rangle = 0, \quad \langle 0|a^+(\mathbf{p}) = 0, \quad \langle 0|0\rangle = 1. \quad (7)$$

Actually, $a^-(\mathbf{p})|0\rangle = 0 \cdot |0\rangle$ but the vacuum state can be dropped since finally all observable quantities are proportional to $\langle 0|0\rangle$. The field excitations are states of the form

$$|f\rangle = \int d\mathbf{p} f(\mathbf{p})a^+(\mathbf{p})|0\rangle, \quad |g\rangle = \int d\mathbf{p}d\mathbf{q} g(\mathbf{p}, \mathbf{q})a^+(\mathbf{p})a^+(\mathbf{q})|0\rangle, \quad \dots \quad (8)$$

The most simple excitation $a^+(\mathbf{p})|0\rangle \equiv |p\rangle$ is used to describe a single on-mass-shell particle with momentum \mathbf{p} . Then $a^+(\mathbf{p})a^+(\mathbf{q})|0\rangle$ is a two-particle state and so on. Because of the presence of modulating functions like $f(\mathbf{p})$ and $g(\mathbf{p}, \mathbf{q})$, the Fock space is infinite-dimensional.

EXERCISES: 1) Find the norm $\langle p|p\rangle$; 2) check that operator $\hat{N} = \int d\mathbf{p} a^+(\mathbf{p})a^-(\mathbf{p})$ acts as a particle number operator.

A charged scalar field is defined as

$$\begin{aligned} \varphi(x) &= \frac{1}{(2\pi)^{3/2}} \int \frac{d\mathbf{p}}{\sqrt{2p_0}} (e^{-ipx} a^-(\mathbf{p}) + e^{+ipx} b^+(\mathbf{p})), \\ \varphi^*(x) &= \frac{1}{(2\pi)^{3/2}} \int \frac{d\mathbf{p}}{\sqrt{2p_0}} (e^{-ipx} b^-(\mathbf{p}) + e^{+ipx} a^+(\mathbf{p})), \\ [a^-(\mathbf{p}), a^+(\mathbf{p}')] &= [b^-(\mathbf{p}), b^+(\mathbf{p}')] = \delta(\mathbf{p} - \mathbf{p}'), \quad [a^\pm, b^\pm] = 0, \end{aligned}$$

where operators $a^\pm(\mathbf{p})$ create and annihilate particles, while operators $b^\pm(\mathbf{p})$ are used for the same purpose for *anti-particles*. The corresponding Lagrangian reads

$$\mathcal{L}(\phi, \phi^*) = \partial_\mu\varphi^*\partial_\mu\varphi - m^2\varphi^*\varphi. \quad (9)$$

Note that φ and φ^* are related by a generalized conjugation which involves operator transformations: $(a^\pm)^* = a^\mp$ and $(b^\pm)^* = b^\mp$. It is worth no to note also that φ and φ^* are not ‘‘a particle and an anti-particle’’.

¹Actually it is a Lagrangian density.

A massive charged vector field (remind W bosons) is defined as

$$\begin{aligned}
U_\mu(x) &= \frac{1}{(2\pi)^{3/2}} \int \frac{d\mathbf{p}}{\sqrt{2p_0}} \sum_{n=1,2,3} e_\mu^n(\mathbf{p}) (e^{-ipx} a_n^-(\mathbf{p}) + e^{+ipx} b_n^+(\mathbf{p})), \\
U_\mu^*(x) &= \frac{1}{(2\pi)^{3/2}} \int \frac{d\mathbf{p}}{\sqrt{2p_0}} \sum_{n=1,2,3} e_\mu^n(\mathbf{p}) (e^{-ipx} b_n^-(\mathbf{p}) + e^{+ipx} a_n^+(\mathbf{p})), \\
[a_n^-(\mathbf{p}), a_l^+(\mathbf{p}')] &= [b_n^-(\mathbf{p}), b_l^+(\mathbf{p}')] = \delta_{nl} \delta(\mathbf{p} - \mathbf{p}'), \quad [a^\pm, b^\pm] = 0.
\end{aligned}$$

For *polarization vectors* $e_\mu^n(\mathbf{p})$ the following conditions are applied:

$$e_\mu^n(\mathbf{p}) e_\mu^l(\mathbf{p}) = -\delta_{nl}, \quad p_\mu e_\mu^n(\mathbf{p}) = 0. \quad (10)$$

EXERCISE: Using the above orthogonality conditions, show that

$$\sum_{n=1,2,3} e_\mu^n(\mathbf{p}) e_\nu^n(\mathbf{p}) = -\left(g_{\mu\nu} - \frac{p_\mu p_\nu}{m^2}\right). \quad (11)$$

The Lagrangian for a massive charged vector field takes the form

$$\mathcal{L} = -\frac{1}{2} \left(\partial_\mu U_\nu^* - \partial_\nu U_\mu^* \right) \left(\partial_\mu U_\nu - \partial_\nu U_\mu \right) + m^2 U_\mu^* U_\mu. \quad (12)$$

The corresponding Euler-Lagrange equation reads

$$-\partial_\mu (\partial_\mu U_\nu - \partial_\nu U_\mu) - m^2 U_\mu = 0.$$

EXERCISE: Using the above equation, show that $\partial_\nu U_\nu(x) = 0$, i.e., derive the Lorentz condition. Note that the Lorentz condition removes from the field one of four independent degrees of freedom (components).

A massless neutral vector field (a photon) is defined as

$$\begin{aligned}
A_\mu(x) &= \frac{1}{(2\pi)^{3/2}} \int \frac{d\mathbf{p}}{\sqrt{2p_0}} e_\mu^\lambda(\mathbf{p}) (e^{-ipx} a_\lambda^-(\mathbf{p}) + e^{+ipx} a_\lambda^+(\mathbf{p})), \\
[a_\lambda^-(\mathbf{p}), a_\nu^+(\mathbf{p}')] &= -g_{\lambda\nu} \delta(\mathbf{p} - \mathbf{p}') \quad e_\mu^\lambda(\mathbf{p}) e_\nu^\lambda(\mathbf{p}) = g_{\mu\nu}, \quad e_\mu^\lambda(\mathbf{p}) e_\mu^\nu(\mathbf{p}) = g_{\lambda\nu}.
\end{aligned} \quad (13)$$

Formally this field has four polarizations, but only two of them correspond to physical degrees of freedom. The corresponding Lagrangian reads

$$\mathcal{L} = -\frac{1}{4} F_{\mu\nu} F_{\mu\nu}, \quad F_{\mu\nu} \equiv \partial_\mu A_\nu - \partial_\nu A_\mu. \quad (14)$$

A Dirac fermion field is defined as

$$\begin{aligned}
\Psi(x) &= \frac{1}{(2\pi)^{3/2}} \int \frac{d\mathbf{p}}{\sqrt{2p_0}} \sum_{r=1,2} (e^{-ipx} a_r^-(\mathbf{p}) u_r(\mathbf{p}) + e^{+ipx} b_r^+(\mathbf{p}) v_r(\mathbf{p})), \\
\bar{\Psi}(x) &= \frac{1}{(2\pi)^{3/2}} \int \frac{d\mathbf{p}}{\sqrt{2p_0}} \sum_{r=1,2} (e^{-ipx} b_r^-(\mathbf{p}) \bar{v}_r(\mathbf{p}) + e^{+ipx} a_r^+(\mathbf{p}) \bar{u}_r(\mathbf{p})), \\
[a_r^-(\mathbf{p}), a_s^+(\mathbf{p}')]_+ &= [b_r^-(\mathbf{p}), b_s^+(\mathbf{p}')]_+ = \delta_{rs} \delta(\mathbf{p} - \mathbf{p}'), \\
[a_r^+(\mathbf{p}), a_s^+(\mathbf{p}')]_+ &= [a_r^-(\mathbf{p}), b_s^+(\mathbf{p}')]_+ = \dots = 0.
\end{aligned} \quad (15)$$

EXERCISE: Show that $a_r^+(\mathbf{p}) a_r^+(\mathbf{p}) = 0$, i.e., verify the Pauli principle.

Here, u_r , u_r , \bar{u}_r , and \bar{v}_r are four-component spinors, so $\Psi(x) \equiv \{\Psi_\alpha(x)\}$ is a four-vector column, $\alpha = 1, 2, 3, 4$, and $\bar{\Psi}(x)$ is a four-vector row,

$$\bar{u}u = \sum_{\alpha=1}^4 \bar{u}_\alpha u_\alpha = \sum_{\alpha=1}^4 u_\alpha \bar{u}_\alpha = \text{Tr}(u\bar{u}).$$

Spinors are solutions of the (Dirac) equations:

$$\begin{aligned} (\hat{p} - m)u_r(\mathbf{p}) &= 0, & \bar{u}_r(\mathbf{p})(\hat{p} - m) &= 0, \\ (\hat{p} + m)v_r(\mathbf{p}) &= 0, & \bar{v}_r(\mathbf{p})(\hat{p} + m) &= 0, \\ \hat{p} &\equiv p_\mu \gamma_\mu = p_0 \gamma_0 - p_1 \gamma_1 - p_2 \gamma_2 - p_3 \gamma_3, & m &\equiv m\mathbf{1}, \end{aligned} \quad (16)$$

where $\mathbf{1}$ is the unit four-by-four matrix. For the solutions of the above equations we impose the normalization conditions

$$\bar{u}_r(\mathbf{p})u_s(\mathbf{p}) = -\bar{v}_r(\mathbf{p})v_s(\mathbf{p}) = 2m\delta_{rs}.$$

The gamma matrixes (should) satisfy the commutation condition

$$[\gamma_\mu, \gamma_\nu]_+ = 2g_{\mu\nu}\mathbf{1} \quad \Rightarrow \quad \gamma_0^2 = \mathbf{1}, \quad \gamma_1^2 = \gamma_2^2 = \gamma_3^2 = -\mathbf{1}$$

and the condition of Hermitian conjugation

$$\gamma_\mu^\dagger = \gamma_0 \gamma_\mu \gamma_0.$$

The latter leads to the rule of the *Dirac conjugation*:

$$\bar{\Psi} = \Psi^\dagger \gamma_0, \quad \bar{u} = u^\dagger \gamma_0, \quad \bar{v} = v^\dagger \gamma_0. \quad (17)$$

EXERCISE: Show that the Dirac conjugation rule is consistent with the set of Dirac equations (16).

Note that explicit expressions for gamma matrixes are not unique, but they are not necessary for construction of observables, *QUESTION: Why is that so?* The most common representations are the so-called Dirac's (standard) and Weyl's (spinor) ones.

Two values of index r in Eq. (15) correspond to two independent degrees of freedom for each spinor in other words to two independent solutions of the Dirac equations. These two degrees of freedom can be treated as two polarization states like 'spin up' and 'spin down'. But in the Standard Model, there is one special choice of the basis for spinors, namely we will distinguish *Left* (L) and *Right* (R) spinors. By definition,

$$\Psi_L \equiv P_L \Psi, \quad \Psi_R \equiv P_R \Psi, \quad P_{L,R} \equiv \frac{1 \mp \gamma_5}{2}, \quad \Psi = \Psi_L + \Psi_R. \quad (18)$$

Here $\gamma_5 \equiv i\gamma_0\gamma_1\gamma_2\gamma_3$, this gamma-matrix has the properties

$$[\gamma_\mu, \gamma_5]_+ = 0, \quad \gamma_5^2 = \mathbf{1}, \quad \gamma_5^\dagger = \gamma_5. \quad (19)$$

As can be seen from Eq. (18), $P_{L,R}$ form a complete set of orthogonal projection operators,

$$P_{L,R}^2 = P_{L,R} \quad P_L P_R = P_R P_L = 0, \quad P_L + P_R = \mathbf{1}. \quad (20)$$

The sign before γ_5 in the definition of the projection operators in Eq. (18) corresponds to the standard representation of gamma matrixes². The Dirac conjugation (17) of left and right spinors gives

$$\bar{\Psi}_L \equiv \bar{\Psi} \frac{1 + \gamma_5}{2}, \quad \bar{\Psi}_R \equiv \bar{\Psi} \frac{1 - \gamma_5}{2}.$$

²In the spinor representation the sign is opposite: $P_L \equiv (1 + \gamma_5)/2$ and $P_R \equiv (1 - \gamma_5)/2$.

Remind some properties of gamma matrixes

$$\begin{aligned} \text{Tr}\gamma_\mu &= \text{Tr}\gamma_5 = 0, & \text{Tr}\gamma_\mu\gamma_\nu &= 4g_{\mu\nu}, & \text{Tr}\gamma_5\gamma_\mu\gamma_\nu &= 0, \\ \text{Tr}\gamma_\mu\gamma_\nu\gamma_\alpha\gamma_\beta &= 4(g_{\mu\nu}g_{\alpha\beta} - g_{\mu\alpha}g_{\nu\beta} + g_{\mu\beta}g_{\nu\alpha}), & \text{Tr}\gamma_5\gamma_\mu\gamma_\nu\gamma_\alpha\gamma_\beta &= -4i\varepsilon_{\mu\nu\alpha\beta}. \end{aligned}$$

The equations for u and v are chosen so that we get the conventional *Dirac equations*

$$(i\gamma_\mu\partial_\mu - m)\Psi(x) = 0, \quad i\partial_\mu\bar{\Psi}(x)\gamma_\mu + m\bar{\Psi}(x) = 0.$$

These equations follow also from the Lagrangian

$$\mathcal{L} = \frac{i}{2} \left[\bar{\Psi}\gamma_\mu(\partial_\mu\Psi) - (\partial_\mu\bar{\Psi})\gamma_\mu\Psi \right] - m\bar{\Psi}\Psi \equiv i\bar{\Psi}\gamma_\mu\partial_\mu\Psi - m\bar{\Psi}\Psi.$$

Note that the right-hand side is a short notation for the true Lagrangian which is given in the middle.

In QFT Lagrangians (Hamiltonians) should be Hermitian: $\mathcal{L}^\dagger = \mathcal{L}$. *QUESTION: What kind of problems one can have with a non-Hermitian Hamiltonian?*

Up to now we considered only *free* non-interacting fields. Studies of transitions between free states is the main task of QFT³.

Let us postulate the transition *amplitude* (matrix element) \mathcal{M} of a physical process:

$$\mathcal{M} \equiv \langle out|S|in\rangle, \quad S \equiv T \exp\left(i \int dx \mathcal{L}_I(\varphi(x))\right). \quad (21)$$

Here S is the so-called S-matrix which is the general evolution operator of quantum states. Letter T means the *time ordering* operator, it will be discussed a bit later. The initial and final states are

$$|in\rangle = a^+(\mathbf{p}_1) \dots a^+(\mathbf{p}_s)|0\rangle, \quad |out\rangle = a^+(\mathbf{p}'_1) \dots a^+(\mathbf{p}'_r)|0\rangle. \quad (22)$$

The differential probability to evolve from $|in\rangle$ to $|out\rangle$ is

$$dw = (2\pi)^4 \delta\left(\sum p'_i\right) \frac{n_1 \dots n_s}{2E_1 \dots E_s} |\mathcal{M}|^2 \prod_{j=1}^r \frac{d\mathbf{p}'_j}{(2\pi)^3 2E'_j}.$$

Here n_i is the particle number density of i^{th} particle beam.

Nontrivial transitions happen due to interactions of fields. QFT prefers dealing with *local* interactions $\Rightarrow \mathcal{L}_I = \mathcal{L}_I(\varphi(x))$. By 'local' we mean that all interaction terms in the Lagrangian are constructed as products of fields (or their first derivatives) taken the same space-time coordinate.

Examples of interaction Lagrangians:

$$\begin{aligned} g\varphi^3(x), & \quad h\varphi^4(x), & y\varphi(x)\bar{\Psi}(x)\Psi(x), \\ e\bar{\Psi}(x)\gamma_\mu\Psi(x)A_\mu(x), & & G\bar{\Psi}_1(x)\gamma_\mu\Psi_1(x) \cdot \bar{\Psi}_2(x)\gamma_\mu\Psi_2(x). \end{aligned}$$

IMPORTANT: Always keep in mind the dimension of your objects! The reference unit is the dimension of energy (mass):

$$[E] = [m] = 1 \quad \Rightarrow \quad [p] = 1, \quad [x] = -1. \quad (23)$$

An action should be dimensionless

$$\left[\int dx \mathcal{L}(x) \right] = 0 \quad \Rightarrow \quad [\mathcal{L}] = 4. \quad (24)$$

³Collective, nonperturbative effects, bound states etc. are also of interest, but that goes beyond the scope of these lectures.

EXERCISE: Show that $[\varphi] = [A_\mu] = 1$ and $[\Psi] = 3/2$. Find the dimensions of the coupling constants g, h, y, e , and G in the examples above.

By definition the time ordering operator acts as follows:

$$T A_1(x_1) \dots A_n(x_n) = (-1)^l A_{i_1}(x_{i_1}) \dots A_{i_n}(x_{i_n}) \quad \text{with } x_{i_1}^0 > \dots > x_{i_n}^0, \quad (25)$$

where l is the number of fermion field permutations.

The perturbative expansion of the S matrix exponent (21) leads to terms like

$$\frac{i^n g^n}{n!} \langle 0 | a^-(\mathbf{p}'_1) \dots a^-(\mathbf{p}'_r) \int dx_1 \dots dx_n T \varphi^3(x_1) \dots \varphi^3(x_n) a^+(\mathbf{p}_1) \dots a^+(\mathbf{p}_s) | 0 \rangle.$$

Remind that fields φ also contain creation and annihilation operators. By permutation of operators $a^-(\mathbf{p})a^+(\mathbf{p}') = a^+(\mathbf{p}')a^-(\mathbf{p}) + \delta(\mathbf{p} - \mathbf{p}')$ we move a^- to the right and a^+ to the left. At the end we get either 0 because $a^-|0\rangle = 0$ or some terms proportional to $\langle 0|0\rangle = 1$.

$$*EXERCISE: Show that $[a^-(\mathbf{p}), \varphi(x)] = \frac{e^{ipx}}{(2\pi)^{3/2}\sqrt{2p_0}}$ and $[a_r^-(\mathbf{p}), \bar{\Psi}(x)]_+ = \frac{e^{ipx}\bar{u}_r(\mathbf{p})}{(2\pi)^{3/2}\sqrt{2p_0}}$.*$$

By definition the *causal Green function* is given by

$$\langle 0 | T \varphi(x) \varphi(y) | 0 \rangle \equiv -i D^c(x - y). \quad (26)$$

It is a building block for construction of amplitudes. One can show (see textbooks) that

$$(\partial^2 + m^2) D^c(x) = \delta(x), \quad (27)$$

so that D^c is the Green function of the Klein-Gordon operator,

$$D^c(x) = \frac{-1}{(2\pi)^4} \int \frac{dp e^{-ipx}}{p^2 - m^2 + i0}, \quad (28)$$

where $+i0$ is an infinitesimally small quantity imaginary quantity which shifts the poles of the Green function from the real axis. The sign of this quantity is chosen to fulfil the requirement of the time ordering operation in Eq. (26).

For other fields we have

$$\begin{aligned} \langle 0 | T \Psi(x) \bar{\Psi}(y) | 0 \rangle &= \frac{i}{(2\pi)^4} \int \frac{dp e^{-ip(x-y)} (\hat{p} + m)}{p^2 - m^2 + i0}, \\ \langle 0 | T U_\mu(x) U_\nu^*(y) | 0 \rangle &= \frac{-i}{(2\pi)^4} \int \frac{dp e^{-ip(x-y)} (g_{\mu\nu} - p_\mu p_\nu / m^2)}{p^2 - m^2 + i0}, \\ \langle 0 | T A_\mu(x) A_\nu(y) | 0 \rangle &= \frac{-i}{(2\pi)^4} \int \frac{dp e^{-ip(x-y)} g_{\mu\nu}}{p^2 + i0}. \end{aligned} \quad (29)$$

The Wick theorem states that for any combinations of fields

$$T A_1 \dots A_n \equiv \sum (-1)^l \langle 0 | T A_{i_1} A_{i_2} | 0 \rangle \dots \langle 0 | T A_{i_{k-1}} A_{i_k} | 0 \rangle : A_{i_k} \dots A_{i_n} : \quad (30)$$

The sum is taken over all possible ways to pair the fields.

The *normal ordering* operation acts as

$$: a_1^- a_2^+ a_3^- a_4^- a_5^+ a_6^- a_7^+ : = (-1)^l a_2^+ a_5^+ a_7^+ a_1^- a_3^- a_4^- a_6^- \quad (31)$$

so that all annihilation operators go to the left and all creation operators go to the right. The number of fermion operator permutations l provides the factor $(-1)^l$.

Using the Wick theorem we construct the *Feynman rules* for simple $g\phi^3$ and $h\phi^4$ interactions. But for the case of gauge interactions we need something more as we will see below.

It appears that symmetries play the crucial role in QFT. There are two major types of symmetries in the SM: *global* and *local* ones. By a global symmetry we mean invariance of a Lagrangian and observables with respect to certain transformations of coordinates and/or fields if the transformations are the same in each space-time point. If the transformations do depend on coordinates, the corresponding symmetry is called local.

The 1st Noether (Nöther) theorem:

If an action is invariant with respect to transformations of a global Lie group G_r with r parameters, then there are r linearly independent combinations of Lagrange derivatives which become complete divergences; and vice versa.

If the field satisfies the Euler–Lagrange equations, then $\text{div}J = \nabla J = 0$, i.e., the *Noether currents* are conserved. Integration of those divergences over a 3-dimensional volume (with certain boundary conditions) leads to r *conserved charges*. Remind that conservation of the electric charge in QED is related to the global $U(1)$ symmetry of this model, and that Poincaré symmetries lead to conservation of energy, momentum, and angular momentum.

Much more involved and actually important for us is the **2nd Noether theorem:**

If the action is invariant with respect to the infinite-dimensional r -parametric group $G_{\infty,r}$ with derivatives up to the k^{th} order, then there are r independent relations between Lagrange derivatives and derivatives of them up to the k^{th} order; and vice versa.

The importance of the second theorem is justified by the fact that gauge groups (and also the general coordinate transformation in Einstein’s gravitational theory) are infinite-dimensional groups. The 2nd Noether theorem provides r conditions on the fields which are additional to the standard Euler–Lagrange equations. These conditions should be used to exclude *double counting* of physically *equivalent* field configurations.

2.1 Gauge symmetries

Let us start the discussion of local gauge symmetries with Quantum electrodynamics (QED). The free Lagrangians for electrons and photons

$$\mathcal{L}_0(\Psi) = i\bar{\Psi}\gamma_\mu\partial_\mu\Psi - m\bar{\Psi}\Psi, \quad \mathcal{L}_0(A) = -\frac{1}{4}F_{\mu\nu}F_{\mu\nu} \quad (32)$$

are invariant with respect to the *global* $U(1)$ transformations

$$\Psi(x) \rightarrow \exp(ie\theta)\Psi(x), \quad \bar{\Psi}(x) \rightarrow \exp(-ie\theta)\bar{\Psi}(x), \quad A_\mu(x) \rightarrow A_\mu(x). \quad (33)$$

One can note that $F_{\mu\nu}$ is invariant also with respect to *local* transformations $A_\mu(x) \rightarrow A_\mu(x) + \partial_\mu\omega(x)$. For fermions the corresponding transformations are

$$\Psi(x) \rightarrow \exp(ie\omega(x))\Psi(x), \quad \bar{\Psi}(x) \rightarrow \exp(-ie\omega(x))\bar{\Psi}(x), \quad (34)$$

i.e., the global constant angle θ in Eq. (33) is substituted by a local function $\omega(x)$ which varies from one space-time point to another.

The question is how to make the fermion Lagrangian being also invariant? The answer is to introduce the so-called *covariant derivative*:

$$\partial_\mu \rightarrow D_\mu, \quad D_\mu\Psi \equiv (\partial_\mu - ieA_\mu)\Psi, \quad D_\mu\bar{\Psi} \equiv (\partial_\mu + ieA_\mu)\bar{\Psi}. \quad (35)$$

Then we get the QED Lagrangian:

$$\mathcal{L}_{\text{QED}} = -\frac{1}{4}F_{\mu\nu}F_{\mu\nu} + i\bar{\Psi}\gamma_\mu D_\mu\Psi - m\bar{\Psi}\Psi$$

$$= -\frac{1}{4}F_{\mu\nu}F_{\mu\nu} + i\bar{\Psi}\gamma_\mu\partial_\mu\Psi - m\bar{\Psi}\Psi + e\bar{\Psi}\gamma_\mu\Psi A_\mu,$$

where the last term describes interaction of electrons and positrons with photons. The most important point here is that the structure of the interaction term is completely fixed by the gauge symmetry. Nevertheless, there is one specific feature of the abelian $U(1)$ case, namely the values of electric charges (coupling constants) can be different e.g., for up and down quarks.

One can note that local transformations are more natural because of causality of Special relativity.

EXERCISES: 1) Check the covariance: $D_\mu\Psi \rightarrow e^{ie\omega(x)}(D_\mu\Psi)$; 2) construct the Lagrangian of scalar QED (use Eqs. (9) and (14)).

Let's look now again at the free photon Lagrangian

$$\begin{aligned}\mathcal{L}_0(A) &= -\frac{1}{4}(\partial_\mu A_\nu - \partial_\nu A_\mu)^2 = -\frac{1}{2}A_\nu K_{\mu\nu}A_\nu, \\ K_{\mu\nu} &= g_{\mu\nu}\partial^2 - \partial_\mu\partial_\nu \Rightarrow K_{\mu\nu}(p) = p_\mu p_\nu - g_{\mu\nu}p^2.\end{aligned}$$

Operator $K_{\mu\nu}(p)$ has zero modes (since $p_\mu K_{\mu\nu} = 0$), so it is not invertable. Definition of the photon propagator within the *functional integral formalism* becomes impossible. The reason is the unresolved symmetry. The solution is to introduce a *gauge fixing term* into the Lagrangian:

$$\begin{aligned}\mathcal{L}(A) &= -\frac{1}{4}F_{\mu\nu}F_{\mu\nu} - \frac{1}{2\alpha}(\partial_\mu A_\mu)^2 \Rightarrow \\ \langle 0|T A_\mu(x)A_\nu(y)|0\rangle &= \frac{-i}{(2\pi)^4} \int dp e^{-ip(x-y)} \frac{g_{\mu\nu} + (\alpha - 1)p_\mu p_\nu / p^2}{p^2 + i0}.\end{aligned}$$

It is very important that physical quantities do not depend on the value of α .

Let us briefly discuss the features of non-abelian Gauge symmetries which will be also used in the construction of the SM. Transformations for a *non-abelian* case read

$$\begin{aligned}\Psi_i &\rightarrow \exp ig\omega^a t_{ij}^a \Psi_j, \quad [t^a, t^b] = i f^{abc} t^c, \\ B_\mu^a &\rightarrow B_\mu^a + \partial_\mu\omega^a + g f^{abc} B_\mu^b \omega^c, \quad F_{\mu\nu} \equiv \partial_\mu B_\nu^a - \partial_\nu B_\mu^a + g f^{abc} B_\mu^b B_\nu^c,\end{aligned}$$

where t^a are the group generators, f^{abc} are the structure constants (see details in the lectures by A. Mitov).

We introduce the covariant derivative

$$\partial_\mu\Psi \rightarrow D_\mu\Psi \equiv (\partial_\mu - igB_\mu^a t^a)\Psi$$

and get

$$\begin{aligned}\mathcal{L}(\Psi, B) &= i\bar{\Psi}\gamma_\mu D_\mu\Psi + \mathcal{L}(B), \\ \mathcal{L}(B) &= -\frac{1}{4}F_{\mu\nu}^a F_{\mu\nu}^a - \frac{1}{2\alpha}(\partial_\mu B_\mu^a)^2 = -\frac{1}{4}(\partial_\mu B_\nu^a - \partial_\nu B_\mu^a)^2 - \frac{1}{2\alpha}(\partial_\mu B_\mu^a)^2 \\ &\quad - \frac{g}{2} f^{abc} (\partial_\mu B_\nu^a - \partial_\nu B_\mu^a) B_\mu^b B_\nu^c - \frac{g^2}{4} f^{abc} f^{ade} B_\mu^b B_\nu^c B_\mu^d B_\nu^e.\end{aligned}$$

Note that $\mathcal{L}(B)$ contains self-interactions and can not be treated as a 'free Lagrangian'. There is no any mass term for the gauge field in the Lagrangian, $m_B \equiv 0$, because such a mass term would be not gauge-invariant. It is worth to note that the non-abelian charge g is *universal*, i.e., it is the same for all fields which are transformed by the given group.

Exclusion of double-counting due to the physical equivalence of the field configurations related to each other by non-abelian gauge transformations is nontrivial. Functional integration over those identical

configurations (or application of the BRST method) leads to the appearance of the so-called *Faddeev–Popov ghosts*:

$$\begin{aligned}\mathcal{L}(\Psi, B) &\rightarrow \mathcal{L}(\Psi, B) + \mathcal{L}_{gh}, \\ \mathcal{L}_{gh} &= -\partial_\mu \bar{c}^a \partial_\mu c^a + g f^{acb} \bar{c}^a B_\mu^c \partial_\mu c^a = -\partial_\mu \bar{c}^a \partial_\mu c^a - g f^{acb} \partial_\mu \bar{c}^a B_\mu^c c^a,\end{aligned}\quad (36)$$

where c and \bar{c} are ghost fields, they are fermions with a boson-like kinetic term. Keep in mind that Faddeev–Popov ghosts are *fictitious* particles. In the Feynman rules they (should) appear only as virtual states in propagators but not in the initial and final states. Formally, ghosts can be found also in QED, but they are non-interacting since $f^{abc} = 0$ there and can be totally omitted.

2.2 Regularization and renormalization

Higher-order terms in the perturbative series contain loop integrals e.g.,

$$I_2 \equiv \int \frac{d^4 p}{(p^2 + i0)((k-p)^2 + i0)} \sim \int \frac{|p|^3 d|p|}{|p|^4} \sim \ln \infty. \quad (37)$$

Introduction of a cut-off M leads to a finite, i.e., *regularized* value of the integral:

$$I_2^{\text{cut-off}} = i\pi^2 \left(\ln \frac{M^2}{k^2} + 1 \right) + \mathcal{O} \left(\frac{k^2}{M^2} \right) = i\pi^2 \left(\ln \frac{M^2}{\mu^2} - \ln \frac{k^2}{\mu^2} + 1 \right) + \mathcal{O} \left(\frac{k^2}{M^2} \right). \quad (38)$$

Another possibility is the *dimensional regularization* where $\dim = 4 \rightarrow \dim = 4 - 2\varepsilon$

$$I_2^{\text{dim.reg.}} = \mu^{2\varepsilon} \int \frac{d^{4-2\varepsilon} p}{(p^2 + i0)((k-p)^2 + i0)} = i\pi^2 \left(\frac{1}{\varepsilon} - \ln \frac{k^2}{\mu^2} + 2 \right) + \mathcal{O}(\varepsilon). \quad (39)$$

Here the divergence is parameterized by the ε^{-1} term. The origin of UV divergences is the *locality* of interactions in QFT.

Let's consider a three-point (vertex) function in the $g\phi^3$ model, it looks like

$$\begin{aligned}G &= \int dx dy dz \varphi(x)\varphi(y)\varphi(z)F(x, y, z), \\ F^{\text{dim.reg.}} &= \frac{A}{\varepsilon} \delta(y-x)\delta(z-x) + \dots\end{aligned}$$

IMPORTANT: Divergent terms are *local* because of the delta-functions.

A QFT model is called **renormalizable** if all UV-divergent terms are of the type of the ones existing in the (semi)classical Lagrangian. Otherwise the model is **non-renormalizable**.

EXAMPLES:

- a) renormalizable models: QED, QCD, the SM [proved by 't Hooft & Veltman], $h\varphi^4$, $g\varphi^3$;
- b) non-renormalizable models: the Fermi model with $\mathcal{L} \sim G(\bar{\Psi}\gamma_\mu\Psi)^2$ and General Relativity.

It can be shown that models with dimensionful ($[G] < 0$) coupling constants are non-renormalizable.

In renormalizable models all UV divergences can be *subtracted* from amplitudes and shifted into *counter terms* in \mathcal{L} . Each term in \mathcal{L} gets a *renormalization constant*:

$$\mathcal{L} = \frac{Z_2}{2}(\partial\varphi)^2 - \frac{Z_m m^2}{2}\varphi^2 + Z_4 h\varphi^4 = \frac{1}{2}(\partial\varphi_B)^2 - \frac{m_B^2}{2}\varphi^2 + h_B\varphi^4,$$

where $\varphi_B = \sqrt{Z_2}\varphi$, $m_B^2 = m^2 Z_M Z_2^{-1}$, $h_B = h Z_4 Z_2^{-2}$ are *bare* field, mass, and charge,

$$Z_i(h, \varepsilon) = 1 + \frac{Ah}{\varepsilon} + \frac{Bh^2}{\varepsilon^2} + \frac{Ch^3}{\varepsilon} + \mathcal{O}(h^3).$$

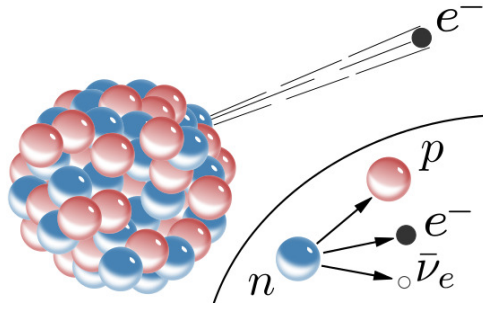


Fig. 2: Beta decay.

Renormalization constants are chosen in such a way that divergences in amplitudes are *cancelled out* with divergences in Z_i . This happens order by order.

R. Feynman said once: “*I think that the renormalization theory is simply a way to sweep the difficulties of the divergences of electrodynamics under the rug.*” Physicists are still not fully satisfied by the renormalization procedure, but the method has been verified in many models. Moreover, renormalizable models including the SM appear to be the most successful ones in description of phenomenology.

Physical results should not depend on the auxiliary scale μ :

$$F(k, g, m) \xrightarrow{\infty} F_{\text{reg}}(k, M, g, m) \xrightarrow{M \rightarrow \infty} F_{\text{ren}}(k, \mu, g, m) \xrightarrow{RG} F_{\text{phys}}(k, \Lambda, m),$$

where Λ is a dimensionful scale.

Charge (and mass) become *running*, i.e., energy-dependent:

$$g \rightarrow g\left(g, \frac{\mu'}{\mu}\right), \quad \beta(g) \equiv \left. \frac{dg}{d \ln \mu} \right|_{g_B = \text{Const}}. \quad (40)$$

Note that the renormalization scale μ unavoidably appears in any scheme. Scheme and scale dependencies are reduced after including higher and higher orders of the perturbation theory.

At this point we stop the brief introduction to Quantum field theory, comprehensive details can be found in textbooks, e.g., Refs. [4, 6].

3 Construction of the Standard Model

3.1 The Fermi model and Cabibbo–Kobayashi–Maskawa mixing matrix

To describe the β decay $n \rightarrow p + e^- + \nu_e$ in 1933, see Fig. 2, Enrico Fermi suggested a simple model:

$$\mathcal{L}_{\text{int}} = G \underbrace{\bar{\Psi}_n \gamma_\rho \Psi_p}_{J_\rho^{(N)}} \cdot \underbrace{\bar{\Psi}_\nu \gamma_\rho \Psi_e}_{J_\rho^{(l)\dagger}} + h.c.$$

with interactions in the form of a product of two vector currents. This model was inspired by QED where similar vector currents appear.

In 1957 R. Marshak & G. Sudarshan; and R. Feynman & M. Gell-Mann modified the model:

$$\begin{aligned} \mathcal{L}_{\text{Fermi}} &= \frac{G_{\text{Fermi}}}{\sqrt{2}} J_\mu J_\mu^\dagger, \\ J_\mu &= \bar{\Psi}_e \gamma_\rho \frac{1 - \gamma_5}{2} \Psi_{\nu_e} + \bar{\Psi}_\mu \gamma_\rho \frac{1 - \gamma_5}{2} \Psi_{\nu_\mu} + (V - A)_{\text{nucleons}} + h.c. \end{aligned} \quad (41)$$

Explicit $V-A$ (Vector minus Axial–vector) form of weak interactions means the 100% violation of parity. In fact, it appears that only left fermions participate in weak interactions, while right fermions don't. The modification of the model was required to describe differential distributions of beta decays. Note that the CP symmetry in Lagrangian (41) is still preserved.

The modern form of the Fermi Lagrangian includes 3 fermion generations:

$$\mathcal{L}_{\text{Fermi}} = \frac{G_{\text{Fermi}}}{\sqrt{2}} (\bar{e}_L \bar{\mu}_L \bar{\tau}_L) \gamma_\rho \begin{pmatrix} \nu_{e,L} \\ \nu_{\mu,L} \\ \nu_{\tau,L} \end{pmatrix} \cdot (\bar{u}'_L \bar{c}'_L \bar{t}'_L) V_u^\dagger \gamma_\rho V_d \begin{pmatrix} d'_L \\ s'_L \\ b'_L \end{pmatrix} + \dots$$

Quarks $\{q'\}$ are the *eigenstates* of strong interactions, and $\{q\}$ are the eigenstates of the weak ones.

Matrixes V_d and V_u describe quark mixing (see details in lectures by S. Gori):

$$\begin{pmatrix} d \\ s \\ b \end{pmatrix} = V_d \times \begin{pmatrix} d' \\ s' \\ b' \end{pmatrix}, \quad V_u^\dagger V_d \equiv V_{\text{CKM}} = \begin{pmatrix} V_{ud} & V_{us} & V_{ub} \\ V_{cd} & V_{cs} & V_{cb} \\ V_{td} & V_{ts} & V_{tb} \end{pmatrix}.$$

By construction, in this model (and further in the SM) the mixing matrixes are unitary: $V_i^\dagger V_i = \mathbf{1}$. In a sense, this property just keeps the number of quarks to be conserved. V_{CKM} contains 4 independent parameters: 3 angles and 1 phase.

QUESTION: What is mixed by V_{CKM} ? E.g., what is mixed by the V_{ud} element of V_{CKM} ?

The Fermi model describes β -decays and the muon decay $\mu \rightarrow e + \bar{\nu}_e + \nu_\mu$ with a very high precision. Nevertheless, there are two critical problems:

1. The model is non-renormalizable, remind that the dimension of the Fermi coupling constant $[G_{\text{Fermi}}] = -2$.
2. Unitarity in this model is violated: consider e.g., electron-neutrino scattering

$$\sigma_{\text{total}}(e\nu_e \rightarrow e\nu_e) \sim \frac{G_{\text{Fermi}}^2}{\pi} s, \quad s = (p_e + p_{\nu_e})^2. \quad (42)$$

This cross section obviously growth with energy. Meanwhile the unitarity condition for l^{th} partial wave in the scattering theory requires that $\sigma_l < \frac{4\pi(2l+1)}{s}$. For $l = 1$ we reach the *unitarity limit* at $s_0 = 2\pi\sqrt{3}/G_{\text{Fermi}} \approx 0.9 \cdot 10^6 \text{ GeV}^2$. So at energies above $\sim 10^3 \text{ GeV}$ the Fermi model is completely senseless.

3.2 (Electro)Weak interactions in SM

The modern point of view is: *a renormalizable model which preserves unitarity is a Yang–Mills (non-abelian) gauge model*. So we have to try to construct an interaction Lagrangian using the principle of gauge symmetry.

Let's try to do that for description of weak interactions The 1st step: we introduce a massive vector W boson

$$\mathcal{L}_{\text{int}} = -g_w (J_\alpha W_\alpha + J_\alpha^\dagger W_\alpha^\dagger). \quad (43)$$

Then the scattering amplitude, see Fig. 3, takes the form

$$T = i(2\pi)^4 g_w^2 J_\alpha \frac{g_{\alpha\beta} - k_\alpha k_\beta / M_W^2}{k^2 - M_W^2} J_\beta^\dagger, \quad (44)$$

where k is the W boson momentum. If $|k| \ll M_W$ we reproduce the Fermi model with

$$\frac{G_{\text{Fermi}}}{\sqrt{2}} = \frac{g_w^2}{M_W^2}.$$

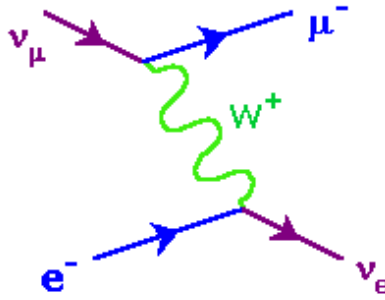


Fig. 3: Feynman diagram for electron-neutrino scattering with W boson exchange.

However such a way to introduce interactions again leads to a non-renormalizable model. The problem appears due to the specific momentum dependence in the propagator of a massive vector particle, see Eq. (29).

The minimal way to introduce electromagnetic and weak interactions as gauge ones is to take the group $SU(2) \otimes U(1)$. The abelian group $U(1)$ is the same as gives conservation of charge in QED. Instead of electric charge Q we introduce now the *hypercharge* Y . $U(1)$ gauge symmetry provides interactions of fermions with a massless vector (photon-like) field B_μ . The non-abelian group $SU(2)$ is the same as used for description of spinors in Quantum mechanics. Instead of spin we use here the *weak isospin* I . There are three massless vector Yang–Mills bosons in the adjoint representation of this group: W_μ^a , $a = 1, 2, 3$. Two of them can be charge and the third one should be neutral. Introduction of the third (electro)weak boson is unavoidable, even so that we did not have experimental evidences of weak neutral currents at the times of the SM invention.

QUESTION: Why weak interactions in the charged current (like muon and beta decays) were discovered experimentally much earlier than the neutral current ones?

One can show that the model built for gauge $SU(2) \otimes U(1)$ interactions of fermions and vector bosons is renormalizable and unitary. But this model doesn't describe the reality since all gauge bosons should be massless because of the symmetry condition. To resolve this problem we need a mechanism that will provide masses for some vector bosons without an explicit breaking of the gauge symmetry.

3.3 The Brout-Englert-Higgs mechanism

Let's consider the simple abelian $U(1)$ symmetry for interaction of a charged scalar field φ with a vector field A_μ :

$$\mathcal{L} = \partial_\mu \varphi^* \partial_\mu \varphi - V(\varphi) - \frac{1}{4} F_{\mu\nu}^2 + ie(\varphi^* \partial_\mu \varphi - \partial_\mu \varphi^* \varphi) A_\mu + e^2 A_\mu A_\mu \varphi^* \varphi.$$

If $V(\varphi) \equiv V(\varphi^* \cdot \varphi)$, \mathcal{L} is invariant with respect to local $U(1)$ gauge transformations

$$\varphi \rightarrow e^{ie\omega(x)} \varphi, \quad \varphi^* \rightarrow e^{-ie\omega(x)} \varphi^*, \quad A_\mu \rightarrow A_\mu + \partial_\mu \omega(x). \quad (45)$$

In polar coordinates $\varphi \equiv \sigma(x) e^{i\theta(x)}$ and $\varphi^* \equiv \sigma(x) e^{-i\theta(x)}$ and the Lagrangian takes the form

$$\mathcal{L} = \partial_\mu \sigma \partial_\mu \sigma + e^2 \sigma^2 \underbrace{\left(A_\mu + \frac{1}{e} \partial_\mu \theta \right)}_{\equiv B_\mu} \underbrace{\left(A_\mu + \frac{1}{e} \partial_\mu \theta \right)}_{\equiv B_\mu} - V(\varphi^* \varphi) - \frac{1}{4} F_{\mu\nu}^2. \quad (46)$$

Note that after the change of variables $A_\mu + \frac{1}{e} \partial_\mu \theta \rightarrow B_\mu$, we have $F_{\mu\nu}(A) = F_{\mu\nu}(B)$.

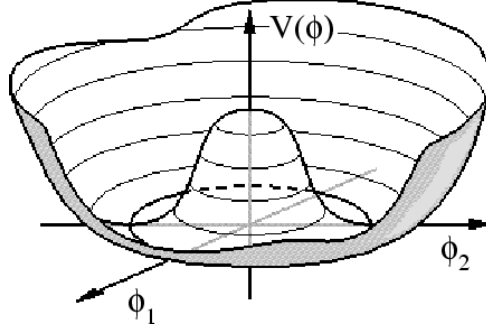


Fig. 4: The Higgs field potential. Picture courtesy: E.P.S. Shellard, DAMTP, Cambridge. From <http://www.geocities.com/CapeCanaveral/2123/breaking.htm>.

We see that $\theta(x)$ is completely swallowed by the field $B_\mu(x)$. So we made a change of variables. But which set of variables is the true physical one? This question is related to the choice of variables in which the secondary quantization should be performed. And the answer can be given by measurements. In fact, according to Quantum mechanics only quantum eigenstates can be observed, so we have a reference point.

R. Brout & F. Englert [10], and P. Higgs [11], see also a brief review in the Scientific Background on the Nobel Prize in Physics 2013 [12], suggested to take the scalar potential in the form

$$V(\varphi^* \varphi) = \lambda(\varphi^* \varphi)^2 + m^2 \varphi^* \varphi. \quad (47)$$

For $\lambda > 0$ and $m^2 < 0$ we get the shape of a *Mexican hat*, see Fig. 4. We have chosen a potential for which $V(\varphi^* \varphi) = V(\sigma^2)$, while $\theta(x)$ corresponds to the rotational symmetry of the potential.

By looking at the derivative of the potential $\frac{dV(\sigma)}{d\sigma} = 0$, we find two critical points: $\sigma = 0$ is the local maximum and $\sigma_0 = \sqrt{-\frac{m^2}{2\lambda}}$ is the global minimum. We have to shift to the global minimum: $\sigma(x) \rightarrow h(x) + \sigma_0$. So we get

$$\mathcal{L} = \partial_\mu h \partial_\mu h + e^2 h^2 B_\mu B_\mu + 2e^2 \sigma_0 h B_\mu B_\mu + e^2 \sigma_0^2 B_\mu B_\mu - V(h) - \frac{1}{4} F_{\mu\nu}^2. \quad (48)$$

We see that field B_μ got the mass:

$$m_B^2 = 2e^2 \sigma_0^2 = -\frac{e^2 m^2}{\lambda} > 0. \quad (49)$$

So, we generated a mass term for the vector field without putting it into the Lagrangian by hand. That is the core of the Brout–Englert–Higgs mechanism.

The quantity $\sigma_0 \equiv v$ is the *vacuum expectation value* (vev) of $\sigma(x)$,

$$v \equiv \langle 0 | \sigma | 0 \rangle, \quad v = \frac{1}{V_0} \int_{V_0} d^3x \sigma(x). \quad (50)$$

Look now at the potential (keep in mind $m^2 = -2\lambda v^2$)

$$\begin{aligned} V(h) &= \lambda(h+v)^4 + m^2(h+v)^2 \\ &= \lambda h^4 + 4\lambda v h^3 + h^2 \underbrace{(6\lambda v^2 + m^2)}_{2m_h^2 = 4\lambda v^2} + h \underbrace{(4\lambda v^3 + 2m^2 v)}_{=0} + \lambda v^4 + m^2 v^2. \end{aligned}$$

So the scalar field h has a normal (not tachyon-like) ($m_h^2 > 0$) mass term. One can see that the initial tachyons φ are not observable.

It is worth to note that even so the field content of the Lagrangian is changed, but the number of degrees of freedom is conserved. In fact initially we had two components of the scalar field and two components of the massless vector field, and after the change of variables we have a single scalar field plus a massive vector field with 3 independent components: $2 + 2 = 1 + 3$.

The field $\theta(x)$ is a *Nambu–Goldstone boson*. It is massless, $m_\theta = 0$, and corresponds to effortless rotations around the symmetry axis of the potential. In general, the Goldstone theorem claims that in a model with spontaneous breaking of a continuous global symmetry G_n (remind the first Noether theorem) there exist as many massless modes, as there are group generators which do not preserve the vacuum invariance.

The constant term $\lambda v^4 + m^2 v^2$ obviously doesn't affect equations of motion, but it contributes to the Universe energy density (too much, actually). That makes a problem for Cosmology. Formally, one can make a shift of the initial Lagrangian just by this term and avoid the problem.

Now let us return to the case of the Standard Model. To generate masses for 3 vector bosons we need at least 3 goldstones. The minimal possibility is to introduce one complex scalar doublet field:

$$\Phi \equiv \begin{pmatrix} \Phi_1 \\ \Phi_2 \end{pmatrix}, \quad \Phi^\dagger = (\Phi_1^* \ \Phi_2^*). \quad (51)$$

Then the following Lagrangian is $SU(2) \otimes U(1)$ invariant

$$\begin{aligned} \mathcal{L} &= (D_\mu \Phi)^\dagger (D_\mu \Phi) - m^2 \Phi^\dagger \Phi - \lambda (\Phi^\dagger \Phi)^2 - \frac{1}{4} W_{\mu\nu}^a W_{\mu\nu}^a - \frac{1}{4} B_{\mu\nu} B_{\mu\nu}, \\ B_{\mu\nu} &\equiv \partial_\mu B_\nu - \partial_\nu B_\mu, \quad W_{\mu\nu}^a \equiv \partial_\mu W_\nu^a - \partial_\nu W_\mu^a + g \varepsilon^{abc} W_\mu^b W_\nu^c, \\ D_\mu \Phi &\equiv \partial_\mu \Phi + ig W_\mu^a \frac{\tau^a}{2} \Phi + \frac{i}{2} g' B_\mu \Phi. \end{aligned} \quad (52)$$

Again for $m^2 < 0$ there is a non-trivial minimum of the Higgs potential and a non-zero vev of a component: $\langle 0 | \Phi_2 | 0 \rangle = \eta / \sqrt{2}$. In accord with the Goldstone theorem, three massless bosons appear. The global $SU(2) \times SU(2)$ symmetry of the Higgs sector is reduced to the *custodial* $SU(2)$ symmetry.

3.4 Electroweak bosons

The gauge bosons of the $SU(2) \otimes U(1)$ group can be represented as

$$W_\mu^+ = \frac{W_\mu^1 + iW_\mu^2}{\sqrt{2}}, \quad W_\mu^- = \frac{W_\mu^1 - iW_\mu^2}{\sqrt{2}}, \quad W_\mu^0 = W_\mu^3, \quad B_\mu. \quad (53)$$

W_μ^0 and B_μ are both neutral and have the same quantum numbers, so they can mix. In a quantum world, 'can' means 'do':

$$\begin{aligned} W_\mu^0 &= \cos \theta_w Z_\mu + \sin \theta_w A_\mu, \\ B_\mu &= -\sin \theta_w Z_\mu + \cos \theta_w A_\mu, \end{aligned} \quad (54)$$

where θ_w is the *weak mixing angle*, introduced first by S. Glashow, θ_w is known also the Weinberg angle. Remind that we have to choose variables which correspond to observables. Vector bosons Z_μ and A_μ are linear combinations of the primary fields W_μ^0 and B_μ .

It is interesting to note that Sheldon Glashow, Abdus Salam, and Steven Weinberg got the Nobel Prize in 1979, *before* the discovery of Z and W bosons in 1983, and even longer before the discovery of the Higgs boson. So the Standard Model has been distinguished before experimental confirmation of its key components.

Look now at the scalar fields:

$$\Phi \equiv \frac{1}{\sqrt{2}} \begin{pmatrix} \Psi_2(x) + i\Psi_1(x) \\ \eta + \sigma(x) + i\xi(x) \end{pmatrix}, \quad \Phi^\dagger = \dots$$

Fields $\Psi_{1,2}$ and ξ become massless Goldstone bosons. We *hide* them into the vector fields:

$$\begin{aligned} W_\mu^i &\rightarrow W_\mu^i + \frac{2}{g\eta} \partial_\mu \Psi_i \Rightarrow M_W = \frac{g\eta}{2}, \\ Z_\mu &= \frac{g}{\sqrt{g^2 + g'^2}} W_\mu^0 - \frac{g'}{\sqrt{g^2 + g'^2}} B_\mu - \frac{2}{\eta\sqrt{g^2 + g'^2}} \partial_\mu \xi \Rightarrow M_Z = \frac{\eta\sqrt{g^2 + g'^2}}{2}. \end{aligned} \quad (55)$$

The photon field appears massless by construction. Looking at the mixing we get

$$\cos \theta_w = \frac{g}{\sqrt{g^2 + g'^2}} = \frac{M_W}{M_Z}.$$

The non-abelian tensor

$$W_{\mu\nu}^a \equiv \partial_\mu W_\nu^a - \partial_\nu W_\mu^a + g\varepsilon^{abc} W_\mu^b W_\nu^c$$

leads to triple and quartic self-interactions of the *primary* W_μ^a bosons, since

$$\mathcal{L} = -\frac{1}{4} W_{\mu\nu}^a W_{\mu\nu}^a + \dots \quad (56)$$

Fields B_μ and W_μ^a were not interacting between each other. But after the spontaneous breaking of the global symmetry in the Higgs sector, and the consequent change of the basis $\{W_\mu^0, B_\mu\} \rightarrow \{Z_\mu, A_\mu\}$, we get interactions of charged W_μ^\pm bosons with photons. That allows to fix the relation between the constants:

$$e = \frac{gg'}{\sqrt{g^2 + g'^2}} = g \sin \theta_w. \quad (57)$$

The value of the W boson charge ($\pm e$) is known from β decays. The very construction of the SM requires phenomenological input. So on the way of the SM building, not everything comes out automatically from symmetry principles etc.

3.5 EW interactions of fermions

We have chosen the $SU(2) \otimes U(1)$ symmetry group. To account for parity violation in weak decays, we assume different behavior of left and right fermions under $SU(2)_L$ transformations:

$$\begin{aligned} \text{left doublets} &\quad \left(\begin{array}{c} \nu_e \\ e \end{array} \right)_L, \left(\begin{array}{c} u \\ d \end{array} \right)_L + 2 \text{ generations}, \\ \text{right singlets} &\quad e_R, u_R, d_R, (\nu_{e,R}) + 2 \text{ generations}. \end{aligned}$$

The fermion Lagrangian is constructed with the help of covariant derivatives:

$$\begin{aligned} \mathcal{L}(\Psi) &= \sum_{\Psi_i} \left[\frac{i}{2} \left(\bar{\Psi}_L \gamma_\alpha D_\alpha \Psi_L - D_\alpha \bar{\Psi}_L \gamma_\alpha \Psi_L \right) + \frac{i}{2} \left(\bar{\Psi}_R \gamma_\alpha D_\alpha \Psi_R - D_\alpha \bar{\Psi}_R \gamma_\alpha \Psi_R \right) \right], \\ D_\alpha \Psi_L &\equiv \partial_\alpha \Psi_L + \frac{ig\tau^b}{2} W_\alpha^b \Psi_L - ig_1 B_\alpha \Psi_L, \quad D_\alpha \Psi_R \equiv \partial_\alpha \Psi_R - ig_2 B_\alpha \Psi_L. \end{aligned}$$

All interactions of the SM fermions with the vector bosons are here. But coupling constants $g_{1,2}$ still have to be fixed.

Fermions have weak isospins and hypercharges:

$$\Psi_L : \quad \left(\frac{1}{2}, -\frac{2g_1}{g'} \right), \quad \Psi_R : \quad \left(0, -\frac{2g_2}{g'} \right). \quad (58)$$

Looking at interactions of e with A_μ in $\mathcal{L}(\Psi)$ we fix its hypercharges:

$$e_L : \left(-\frac{1}{2}, -1 \right), \quad e_R : \left(0, -2 \right). \quad (59)$$

The *Gell-Mann–Nishijima formula* works for all fermions:

$$Q = I_3 + \frac{Y}{2}, \quad (60)$$

where Q is the electric charge, I_3 is the weak isospin projection, and Y is the hypercharge.

Interactions of leptons with W^\pm and Z bosons come out in the form

$$\begin{aligned} \mathcal{L}_I &= -\frac{g}{\sqrt{2}} \bar{e}_L \gamma_\mu \nu_{e,L} W_\mu^- + h.c. - \frac{g Z_\mu}{2 \cos \theta_w} \left[\bar{\nu}_{e,L} \gamma_\mu \nu_{e,L} \right. \\ &\quad \left. + \bar{e} \gamma_\mu \left(-(1 - 2 \sin^2 \theta_w) \frac{1 - \gamma_5}{2} + 2 \sin^2 \theta_w \frac{1 + \gamma_5}{2} \right) e \right] \\ \Rightarrow g_w &= \frac{g}{2\sqrt{2}}, \quad M_W^2 = \frac{g^2 \sqrt{2}}{8 G_{\text{Fermi}}} = \frac{e^2 \sqrt{2}}{8 G_{\text{Fermi}} \sin^2 \theta_w} = \frac{\pi \alpha}{\sqrt{2} G_{\text{Fermi}} \sin^2 \theta_w}. \end{aligned}$$

That gives $M_W = \frac{38.5}{\sin \theta_w}$ GeV, remind $M_Z = \frac{M_W}{\cos \theta_w}$.

We can see that the Higgs boson vev is directly related to the Fermi coupling constant:

$$v = (\sqrt{2} G_{\text{Fermi}})^{-1/2} \approx 246.22 \text{ GeV}. \quad (61)$$

So this quantity has been known with a high precision long before the discovery of the Higgs boson and measurement of its mass.

QUESTION: Why neutral weak currents in the SM do not change flavour?

3.6 Self-interactions of EW bosons and Faddeev–Popov ghosts

Because of the non-abelian $SU(2)_L$ group and mixing of the neutral vector bosons, we have a rather rich structure of EW boson self-interactions, see Fig. 5. The corresponding contributions to the SM Lagrangian look as follows:

$$\begin{aligned} \mathcal{L}_3 &\sim ie \frac{\cos \theta_w}{\sin \theta_w} \left[(\partial_\mu W_\nu^- - \partial_\nu W_\mu^-) W_\mu^+ Z_\nu - (\partial_\mu W_\nu^+ - \partial_\nu W_\mu^+) W_\mu^- Z_\nu \right. \\ &\quad \left. + W_\mu^- W_\nu^+ (\partial_\mu Z_\nu - \partial_\nu Z_\mu) \right] \\ \mathcal{L}_4 &\sim -\frac{e^2}{2 \sin^2 \theta_w} \left[(W_\mu^+ W_\mu^-)^2 - W_\mu^+ W_\mu^+ W_\nu^- W_\nu^- \right], \\ &\quad -\frac{e^2 \cos^2 \theta_w}{\sin^2 \theta_w} \left[W_\mu^+ W_\mu^- Z_\nu Z_\nu - W_\mu^+ Z_\mu W_\mu^- Z_\nu \right] \\ &\quad -\frac{e^2 \cos^2 \theta_w}{\sin^2 \theta_w} \left[2W_\mu^+ W_\mu^- Z_\nu A_\nu - W_\mu^+ Z_\mu W_\mu^- A_\nu - W_\mu^+ A_\mu W_\mu^- Z_\nu \right] \\ &\quad -e^2 \left[W_\mu^+ W_\mu^- A_\nu A_\nu - W_\mu^+ A_\mu W_\mu^- A_\nu \right]. \end{aligned}$$

As we discussed earlier, an accurate treatment of non-abelian gauge symmetries leads to introduction of Faddeev–Popov ghosts. For the $SU(2)$ case we obtain 3 ghosts: $c_a(x)$, $a = 1, 2, 3$,

$$c_1 = \frac{X^+ + X^-}{\sqrt{2}}, \quad c_2 = \frac{X^+ - X^-}{\sqrt{2}}, \quad c_3 = Y_Z \cos \theta_w - Y_A \sin \theta_w,$$

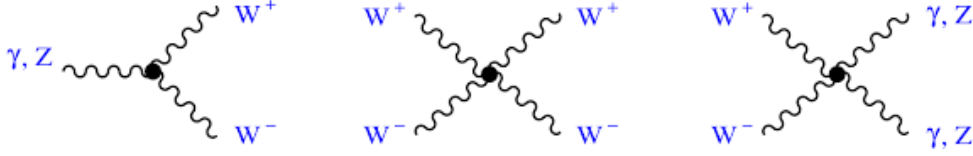


Fig. 5: Vertices of EW boson self-interactions.

$$\mathcal{L}_{gh} = \underbrace{\partial_\mu \bar{c}_i (\partial_\mu c_i - g \varepsilon_{ijk} c_j W_\mu^k)}_{\text{kinetic} + \text{int. with } W^a} + \underbrace{\text{int. with } \Phi}_{M_{gh}, \text{ int. with } H}.$$

Propagators of the ghost fields read

$$D_{Y_\gamma}(k) = \frac{i}{k^2 + i0}, \quad D_{Y_Z}(k) = \frac{i}{k^2 - \xi_Z M_Z^2 + i0}, \quad D_X(k) = \frac{i}{k^2 - \xi_W M_W^2 + i0},$$

where ξ_i are the gauge parameters. Note that masses of the ghosts Y_γ , Y_Z , and X^\pm coincide with the ones of photon, Z , and W^\pm , respectively. That is important for *gauge invariance* of total amplitudes. The ghosts appear only in propagators, but not in the final or initial states.

3.7 Generation of fermion masses

We observe massive fermions, but the $SU(2)_L$ gauge symmetry forbids fermion mass terms, since

$$m \bar{\Psi} \Psi = m \left(\bar{\Psi} \frac{1 + \gamma_5}{2} + \bar{\Psi} \frac{1 - \gamma_5}{2} \right) \left(\frac{1 + \gamma_5}{2} \Psi + \frac{1 - \gamma_5}{2} \Psi \right) = m (\bar{\Psi}_L \Psi_R + \bar{\Psi}_R \Psi_L) \quad (62)$$

while Ψ_L and Ψ_R are transformed in different ways under $SU(2)_L$. The SM solution is to introduce Yukawa interactions:

$$\begin{aligned} \mathcal{L}_Y = & -y_d (\bar{u}_L \bar{d}_L) \begin{pmatrix} \phi^+ \\ \phi^0 \end{pmatrix} d_R - y_u (\bar{u}_L \bar{d}_L) \begin{pmatrix} \phi^{0*} \\ -\phi^- \end{pmatrix} u_R \\ & - y_l (\bar{\nu}_L \bar{l}_L) \begin{pmatrix} \phi^+ \\ \phi^0 \end{pmatrix} l_R - y_\nu (\bar{\nu}_L \bar{l}_L) \begin{pmatrix} \phi^{0*} \\ -\phi^- \end{pmatrix} \nu_R + h.c. \end{aligned}$$

This form of this Lagrangian is fixed by the condition of the $SU(2)_L$ gauge invariance. It is worth to note that neutrino masses can be generated in the same way as the up-quark ones. Of course, that requires introduction of additional Yukawa constants y_ν .

QUESTION: Why do we need 'h.c.' in \mathcal{L}_Y ?

Spontaneous breaking of the global symmetry in the Higgs sector provides in \mathcal{L} mass terms for fermions and Yukawa interactions of fermions with the Higgs boson:

$$\mathcal{L}_Y = -\frac{v+H}{\sqrt{2}} [y_d \bar{d}d + y_u \bar{u}u + y_l \bar{l}l + y_\nu \bar{\nu}\nu] \Rightarrow m_f = \frac{y_f}{\sqrt{2}} v.$$

By construction, the coupling of the Higgs boson to a fermion is proportional its mass m_f . It is interesting to note that the top quark Yukawa coupling is very close to 1. And there is a very strong hierarchy of fermion masses:

$$y_t \approx 0.99 \gg y_e \approx 3 \cdot 10^{-6} \gg y_\nu \approx ?$$

The question mark in the last case is given not only because we do not know neutrino masses, but also since we are not sure the they are generated by the same mechanism.

Quarks can mix and Yukawa interactions are not necessarily diagonal neither in the basis of weak interaction eigenstates, nor in the basis of the strong ones. In the eigenstate basis of a given interaction for the case of three generations, the Yukawa coupling constants are 3×3 matrixes:

$$\begin{aligned} \mathcal{L}_Y = & - \sum_{j,k=1}^3 \left\{ (\bar{u}_{jL} \bar{d}_{jL}) \left[\begin{pmatrix} \phi^+ \\ \phi^0 \end{pmatrix} y_{jk}^{(d)} d_{kR} + \begin{pmatrix} \phi^{0*} \\ -\phi^- \end{pmatrix} y_{jk}^{(u)} u_{kR} \right] \right. \\ & \left. + (\bar{\nu}_{jL} \bar{l}_{jL}) \left[\begin{pmatrix} \phi^+ \\ \phi^0 \end{pmatrix} y_{jk}^{(l)} l_{kR} + \begin{pmatrix} \phi^{0*} \\ -\phi^- \end{pmatrix} y_{jk}^{(\nu)} \nu_{kR} \right] \right\} + h.c. \end{aligned}$$

where indexes j and k mark the generation number.

Charged lepton mixing is formally allowed in the SM, but not (yet) observed experimentally. Searches for lepton flavour violating processes, like the $\mu \rightarrow e\gamma$ decay, are being performed. The Pontecorvo–Maki–Nakagawa–Sakata (PMNS) mixing matrix for (Dirac) neutrinos can be embedded in the SM.

3.8 Short form of the SM Lagrangian

At CERN one can buy souvenirs with the Standard Model Lagrangian represented in a very short compressed form:

$$\begin{aligned} \mathcal{L}_{\text{SM}} = & -\frac{1}{4} F_{\mu\nu} F^{\mu\nu} \\ & + \bar{\Psi} \not{D} \Psi + h.c. \\ & + \Psi_i y_{ij} \Psi_j \Phi + h.c. \\ & + |D_\mu \Phi|^2 - V(\Phi). \end{aligned} \tag{63}$$

We can understand now the meaning of each term. First of all, we see that the Lagrangian is given in the initial form before the spontaneous symmetry breaking. Summation over $SU(3)_C$, $SU(2)_L$, and $U(1)_Y$ gauge groups is implicitly assumed in the first term. The second line represents the gauge interactions of fermions provided by the covariant derivative(s). The third line is the Yukawa interaction of fermions with the scalar field. And the fourth line represent the kinetic and potential term of the primary scalar doublet field.

EXERCISE: Find two 'misprints' in the Lagrangian (63) which break the commonly accepted QFT notation discussed in Sect. 2.

3.9 Axial anomaly

There are *axial-vector* currents in the SM:

$$J_\mu^A = \bar{\Psi} \gamma_\mu \gamma_5 \Psi. \tag{64}$$

In the case of massless fermions, the unbroken global symmetry (via the Noether theorem) leads to conservation of these currents: $\partial_\mu J_\mu^A = 0$. For massive fermions $\partial_\mu J_\mu^A = 2im \bar{\Psi} \gamma_5 \Psi$. But *one-loop corrections*, see Fig. 6, give

$$\partial_\mu J_\mu^A = 2im \bar{\Psi} \gamma_5 \Psi + \frac{\alpha}{2\pi} F_{\mu\nu} \tilde{F}_{\mu\nu}, \quad \tilde{F}_{\mu\nu} \equiv \frac{1}{2} \varepsilon_{\mu\nu\alpha\beta} F_{\alpha\beta}. \tag{65}$$

That fact is known as *axial* or *chiral* or *triangular* Adler–Bell–Jackiw anomaly. So at the quantum level the classical symmetry is lost. That is a problem for the theory. In simple words, such a symmetry breaking makes the classical and quantum levels of the theory being inconsistent to each other.

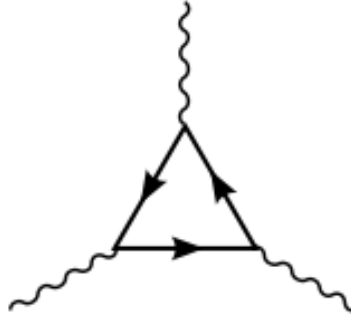


Fig. 6: Triangular anomaly diagram.

But in the SM the axial anomalies apparently cancel out. This can be seen for all possible combination of external gauge bosons:

- 1) $(W W W)$ and $(W W B)$ — automatically since left leptons and quarks are doublets;
- 2) $(B W W)$ — since $Q_e + Q_u + Q_d = 0$;
- 3) $(B B B)$ — since $Q_e = -1$, $Q_\nu = 0$, $Q_u = \frac{2}{3}$, $Q_d = -\frac{1}{3}$;
- 4) $(B g g)$ — automatically ($g = \text{gluon}$);
- 5) $(B g r g r)$ — the same as '3)' ($g r = \text{graviton}$).

Here B and W are the primary $U(1)$ and $SU(2)_L$ gauge bosons. Note that anomalies cancel out in each generation separately. It is interesting to note that condition '2)' means that the hydrogen atom is neutral.

It is very important that the axial anomalies cancel out in the *complete SM*: with the $SU(3)_C \otimes SU(2)_L \otimes U(1)_Y$ gauge symmetries. So there is a nontrivial connection between the QCD and EW sectors of the model.

QUESTION: Where is γ_5 in the $(B B B)$ case?

3.10 Parameters and interactions in the SM

The SM has quite a lot of parameters. We do not know (yet) where do they come from and have to define their values from observations. Let us first count the number of independent free parameters in the SM. It is convenient to perform this exercise by looking at the initial form of the SM Lagrangian before the change of variables invoked by the spontaneous symmetry breaking. So, we have:

- 3 gauge charges (g_1, g_2, g_s);
- 2 parameters in the Higgs potential;
- 9 Yukawa couplings for charged fermions;
- 4 parameters in the CKM matrix.

It makes in total 18 free parameters for the *canonical* Standard Model. Usually, we add also as a free parameter the Λ_{QCD} scale, which is required for calculations in perturbative QCD (see lectures by A. Mitov). Moreover, we can include neutrino masses and mixing, as described above. That would give in addition 4 (or 6 for the Majorana case) parameters in the PMNS matrix and 3 more Yukawa couplings.

QUESTION: How many independent dimensionful parameters is there in the SM?

Most likely that many of the listed parameters are not true independent ones. There should be some hidden symmetries and relations. Those certainly go beyond the SM. In spite of a large number of parameters the SM is distinguished between many other models by its minimality and predictive power. For example, the supersymmetric extension of the SM formally has more than one hundred free parameters, and for this reason it is not able to provide unambiguous predictions for concrete observables.

Let us now count the interactions in the SM. Obviously, we should do that in accord with the QFT rules. The key point is to exploit symmetries, first of all the gauge ones. But looking at the Lagrangian it might be not clear what actually should be counted:

- number of *different vertexes* in Feynman rules?
- number of particle which *mediate* interactions?
- number of *coupling constants*?

Our choice here is to count coupling constants. In fact that will automatically help us to avoid double coupling of the same interactions. So we have:

- 3 gauge charges (g_1, g_2, g_s);
- 1 self-coupling λ in the Higgs potential;
- 9 Yukawa couplings for charged fermions.

If required we can add 3 Yukawa couplings for neutrinos. We see that the SM contains 5 types of interactions: 3 gauge one, the self-interaction of scalar bosons, and the Yukawa interactions of the scalar bosons with fermions. Note also that even we like some interactions e.g., the gauge ones, in the SM more than others, we can not say that any of them is more fundamental than others just since they all are in the same Lagrangian.

3.11 The naturalness problem in the SM

The most serious, actually the only one real theoretical problem of the SM is the *naturalness* known also as *fine-tuning* or *hierarchy problem*. Note that all but one masses in the SM are generated due to the spontaneous symmetry breaking in the Higgs sector. While the scalar boson mass itself has been introduced *by hands* (of Peter Higgs et al.) from the beginning. The tachyon mass term breaks the scale invariance (the conformal symmetry) *explicitly*.

So the running of all but one masses is suppressed by the classical symmetries. As the result, the masses run with energy only logarithmically, but the Higgs mass runs quadratically. In the one-loop approximation we get

$$M_H^2 = (M_H^0)^2 + \frac{3\Lambda^2}{8\pi^2 v^2} \left[M_H^2 + 2M_W^2 + M_Z^2 - 4m_t^2 \right].$$

It is unnatural to have $\Lambda \gg M_H$. The most natural option would be $\Lambda \sim M_H$ e.g., everything is defined by the EW scale. But that is not the case of the SM. . . There are two general ways to solve the problem:

- either to exploit some (super)symmetry to cancel out the huge terms;
- or to introduce some new physics at a scale not very far from the electroweak one, i.e., making Λ being not large. One can find in the literature quite a lot of models for both options. But the experimental data coming from modern accelerators and rare decay studies disfavors most of scenarios of new physics with scales up to about 1 TeV and even higher. Moreover, it was shown that the measured value of the Higgs boson mass makes the SM being self-consistent up to very high energies up to the Planck mass scale [13]. Direct and indirect experimental searches push up and up possible energy scale of new physical phenomena. So the naturalness problem becomes nowadays more and more prominent. And the question, why the top quark mass, the Higgs boson mass and and vacuum expectation value v are of the same order becomes more and more intriguing.

After the discovery of the Higgs boson and measurement of its mass, we found some remarkable empirical relation between parameters of the SM. In particular the equality

$$v = \sqrt{M_H^2 + M_W^2 + M_Z^2 + m_t^2} \quad (66)$$

holds within the experimental errors: $246.22 = 246 \pm 1$ GeV. Obviously, there should be some tight clear relation between the top quark mass and the Higgs boson one (or the EW scale in general). The present version of the SM does not explain this puzzle.

EXERCISE: Divide both sides of Eq. (66) by v and find a relation between coupling constants.

Another interesting relation also involves the Higgs boson and the top quark:

$$2 \frac{m_h^2}{m_t^2} = 1.05 \approx 1 \approx 2 \frac{m_t^2}{v^2} \equiv y_t^2 = 0.99. \quad (67)$$

It might be that these relations are of a pure numerological nature, but they certainly indicate some hidden properties of the SM.

4 Phenomenology of the Standard Model

Let us discuss input parameters of the SM. It was convenient to count their number in the *primary* form of the Lagrangian. But for *practical* applications we use different sets, see e.g., Table 1. Different *EW schemes* with different sets of practical input parameters are possible, since there are relations between them. One should keep in mind that the result of calculations does depend on the choice because we usually work in a limited order of the perturbation theory, while the true relations between the parameters (and between observed quantities) involve the complete series. So simple relations appear at the lowest order, quantum effects (radiative corrections) make them complicated.

Table 1: Input parameters of the SM.

18(19)=	1	1	1	1	1	9	4	(1)
primary:	g'	g	g_s	m_Φ	λ	y_f	y_{jk}	none
practical:	α	M_W	α_s	G_{Fermi}	M_H	m_f	V_{CKM}	Λ_{QCD}

A comprehensive up-to-date set of the SM parameters can be found in the Review of Particle Physics published by the Particle Data Group Collaboration [14]. Let us look at some values of input parameters extracted from experiments:

- The *fine structure constant*: $\alpha^{-1}(0) = 137.035999074(44)$ from $(g - 2)_e$;
- The SM predicts $M_W = M_Z \cos \theta_w \Rightarrow M_W < M_Z$, we have now
 $M_Z = 91.1876(21)$ GeV from LEP1/SLC, $M_W = 80.385(15)$ GeV from LEP2/Tevatron/LHC;
- The Fermi coupling constant: $G_{\text{Fermi}} = 1.1663787(6) \cdot 10^{-5}$ GeV⁻² from muon decay,
- The top quark mass: $m_t = 173.21(51)(71)$ GeV from Tevatron/LHC;
- The Higgs boson mass: $M_H = 125.09(21)(11)$ GeV from ATLAS & CMS (March 2015).

One can see that the precision in definition of the parameters varies by several orders of magnitude. That is related to experimental uncertainties and to the limited accuracy of theoretical calculations which are required to extract the parameter values from the data. *QUESTION: What parameter of the (canonical) SM is known now with the least precision?*

4.1 The muon decay

Let us consider a few examples of particle interaction processes and start with the muon decay $\mu^- \rightarrow e^- + \bar{\nu}_e + \nu_\mu$, see Fig. 7. It is the most clean weak interaction process. One can say that this process is one of keystones of particle physics. The muon decay width reads

$$\Gamma_\mu = \frac{1}{\tau_\mu} = \frac{G_{\text{Fermi}}^2 m_\mu^5}{192\pi^3} \left[f(m_e^2/m_\mu^2) + \mathcal{O}(m_\mu^2/M_W^2) + \mathcal{O}(\alpha) \right],$$

$$f(x) = 1 - 8x + 8x^3 - x^4 - 12x^2 \ln x,$$

$$\mathcal{O}(m_\mu^2/M_W^2) \sim 10^{-6}, \quad \mathcal{O}(\alpha) \sim 10^{-3},$$

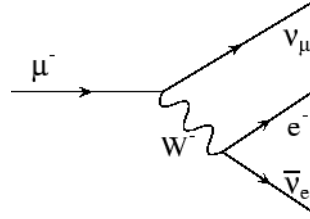


Fig. 7: The Feynman diagram for muon decay in the SM.

where $\mathcal{O}(\alpha)$ includes effects of radiative corrections due to loop (virtual) effects and real photon and/or e^+e^- pair emission.

As mentioned above, the value of the Fermi coupling constant is extracted from the data on muon lifetime, $G_{\text{Fermi}} = 1.1663787(6) \cdot 10^{-5} \text{ GeV}^{-2}$. The high precision is provided by a large experimental statistics, low systematical errors of the final state electron observation, and by accurate theoretical calculations of radiative corrections. But impressive precision ($\sim 1 \cdot 10^{-6}$) in the measurement of the muon life time doesn't give by itself any valuable test of the SM. *QUESTION: Why is that so?* On the other hand, studies of differential distributions in electron energy and angle do allow to test the $V - A$ structure of weak interactions and look for other possible types of interactions which can be parameterized in a model-independent way by the so-called *Michel parameters*.

4.2 Electron and muon anomalous magnetic moments

The Dirac equations predict gyromagnetic ratio $g_f = 2$ in the fermion magnetic moment $\vec{M} = g_f \frac{e}{2m_f} \vec{s}$. Julian Schwinger in 1948 found that one-loop QED correction the vertex function gives the so called *anomalous magnetic moment*:

$$a_f \equiv \frac{g_f - 2}{2} \approx \frac{\alpha}{2\pi} = 0.001\,161\, \dots \quad (68)$$

For the electron case, the Harvard experiment [15] obtained

$$a_e^{\text{exp}} = 1\,159\,652\,180.73(28) \cdot 10^{-12} \text{ [0.24ppb]}.$$

The SM predicts [16]

$$a_e^{\text{SM}} = 1\,159\,652\,181.643(25)_{8th}(23)_{10th}(16)_{EW+had.}(763)_{\delta\alpha} \cdot 10^{-12}.$$

The perfect agreement between the measurement and the theoretical prediction is a triumph of Quantum electrodynamics. In particular, we note that $a_f \neq 0$ is a pure quantum loop effect which is absent as in classical physics as well as in Quantum mechanics.

It is worth to note that the extremely high precision in the experimental measurement of the electron anomalous magnetic moment allows to use it as a reference point for definition of the fine structure constant: $a_e^{\text{exp}} \Rightarrow \alpha^{-1}(0) = 137.035999074(44)$.

For the anomalous magnetic moment of muon, the E821 experiment at BNL in 2006 published the following result of data analysis:

$$a_\mu^{\text{exp}} = 116\,592\,089(54)(33) \cdot 10^{-11} \text{ [0.5ppm]}.$$

The corresponding theoretical value and the difference are

$$\begin{aligned} a_\mu^{\text{SM}} &= 116\,591\,840(59) \cdot 10^{-11} \text{ [0.5ppm]} \\ \Delta a_\mu &\equiv a_\mu^{\text{exp}} - a_\mu^{\text{SM}} = 249(87) \cdot 10^{-11} \text{ } [\sim 3\sigma]. \end{aligned} \quad (69)$$

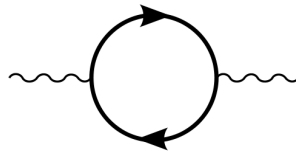


Fig. 8: The one-loop Feynman diagram for QED vacuum polarization.

First, one can see that both experimental and theoretical values are very accurate. Second, there is a discrepancy of the order of three standard deviations. That is a rather rare case for the SM tests. Moreover, this discrepancy remains for a long period of time in spite of intensive efforts of instrumentalists and theoreticians.

The SM prediction consists of the QED, hadronic and weak contributions:

$$\begin{aligned}
 a_\mu &= a_\mu(\text{QED}) + a_\mu(\text{hadronic}) + a_\mu(\text{weak}), & (70) \\
 a_\mu(\text{QED}) &= 116\,584\,718\,845\,(9)(19)(7)(30) \cdot 10^{-14} & [5 \text{ loops}], \\
 a_\mu(\text{hadronic}) &= a_\mu(\text{had. vac.pol.}) + a_\mu(\text{had. l.b.l.}), = 6949\,(37)(21) \cdot 10^{-11} + 116\,(40) \cdot 10^{-11}, \\
 a_\mu(\text{weak}) &= 154\,(2) \cdot 10^{-11} & [2 \text{ loops}].
 \end{aligned}$$

Note that the QED contribution to the muon anomalous magnetic moment is essentially the same as the one to the electron magnetic moment. The only difference is coming from the dependence on electron and muon masses. As concerning the hadronic and weak interaction contributions, they are enhanced by the factor m_μ^2/m_e^2 with respect to the electron case. The same factor typically appears for hypothetical contributions of new interactions beyond the SM. For this reason anomalous magnetic moments of muon and tau lepton are potentially more sensitive to new physics contributions.

One can see that the difference between the theoretical prediction and the experimental data is almost twice the contribution of weak interactions: $\Delta a_\mu \sim 2 \times a_\mu(\text{weak})$. Here by 'weak' we mean the complete electroweak calculation minus the pure QED contribution. The weak interactions have been directly tested with high precision experimentally. So it is not so simple to attribute the difference to an effect of new physics. Nevertheless, there is a bunch of theoretical models that try to resolve the problem by introduction of new interactions and/or new particles.

4.3 Vacuum polarization

By direct calculation in QED, one can see that virtual charged fermion anti-fermion pairs provide a screening effect for the electric force between probe charges. Resummation of bubbles, see Fig. 8, gives

$$\begin{aligned}
 \alpha(q^2) &= \frac{\alpha(0)}{1 - \Pi(q^2)}, & \text{e.g. } \alpha^{-1}(M_Z^2) \approx 128.944(19), \\
 \Pi(q^2) &= \frac{\alpha(0)}{\pi} \left(\frac{1}{3} \ln \left(\frac{-q^2}{m_e^2} \right) - \frac{5}{9} + \delta(q^2) \right) + \mathcal{O}(\alpha^2), \\
 \delta(q^2) &= \delta_\mu(q^2) + \delta_\tau(q^2) + \delta_W(q^2) + \delta_{\text{hadr.}}(q^2). & (71)
 \end{aligned}$$

The hadronic contribution to vacuum polarization $\delta_{\text{hadr.}}(q^2)$ for $|q^2|$ below a few GeV^2 is not calculable within the perturbation theory. Now we get it from experimental data on $e^+e^- \rightarrow \text{hadrons}$ and $\tau \rightarrow \nu_\tau + \text{hadrons}$ with the help of dispersion relations, see e.g., review [17]. Lattice results for this quantity are approaching.

Note that screening, i.e., an effective reduction of the observed charge with increasing of distance, is related to the minus sign attributed to a fermion loop in the Feynman rules.

QUESTION: Estimate the value of q_0^2 at which $\alpha(q_0^2) = \infty$.

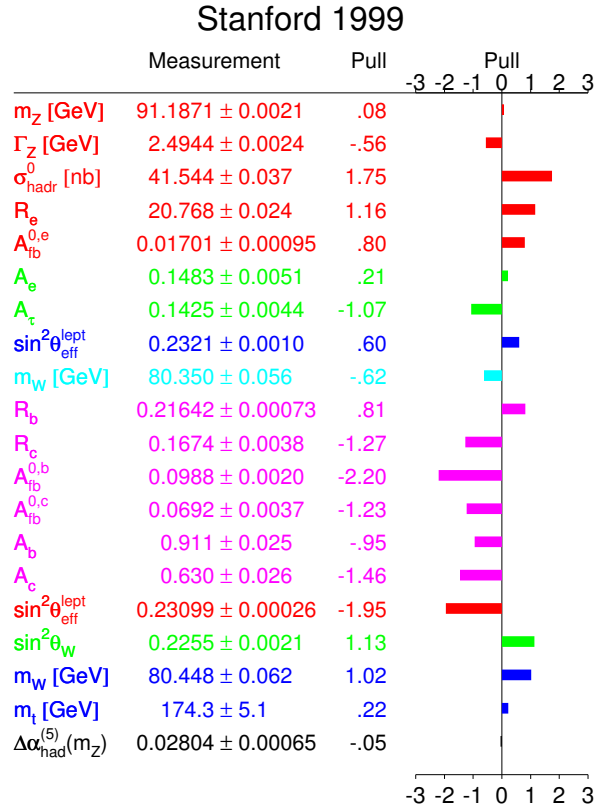


Fig. 9: Pulls of pseudo-observables at LEP [18].

This singularity is known as the *Landau pole*. Formally, such a behaviour of QED brakes unitarity at large energies. But that happens at energies much higher than any practical energy scale including the Planck mass and the mass of the visible part of the Universe. So we keep this problem in mind as a theoretical issue which stimulates our searches for a more fundamental description of Nature.

4.4 Experimental tests of the SM at LEP

After the analysis of LEP1 and LEP2 experimental data, the LEP Electroweak Working Group (LEP-EWWG) [18] illustrated the overall status of the Standard Model by the so-called *pulls*, see Fig. 9. The pulls are defined as differences between the measurement and the SM prediction calculated for the central values of the fitted SM input parameters [$\alpha(M_Z^2) = 1/128.878$, $\alpha_s(M_Z^2) = 0.1194$, $M_Z = 91.1865$ GeV, $m_t = 171.1$ GeV] divided by the experimental error. Although there are several points where deviations between the theory and experiment approach two standard deviations, the average situation should be ranked as extremely good. We note that the level of precision reached is of the order of $\sim 10^{-3}$, and that it is extremely non-trivial to control all experimental systematics at this level.

Through quantum effects the observed cross sections of electron-positron annihilation at LEP depend on all parameters of the Standard Model including the Higgs boson mass. The so called yellow band plot Fig. 10 shows the fit of M_H performed by LEPEWWG [18] with the LEP data in March 2012. The left yellow area has been excluded by direct searches at LEP, and the right one was also excluded by LHC. The plot is derived from a combined fit of all the world experimental data to the SM exploiting the best knowledge of precision theoretical calculations which is realized in computer codes ZFITTER [19] and TOPAZO [20]. One can see that the data was not very sensitive to M_H , but the fit unambiguously

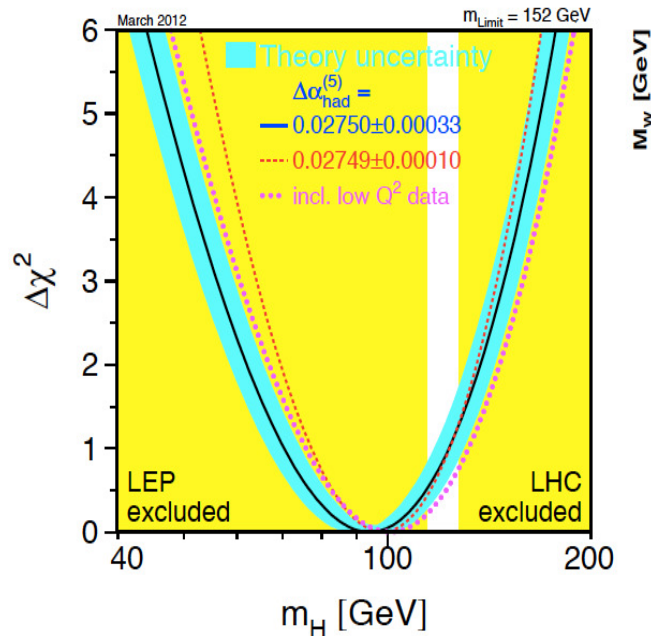


Fig. 10: The curve shows $\Delta\chi_{\min}^2(M_H^2) = \chi_{\min}^2(M_H^2) - \chi_{\min}^2$ as a function of M_H . The width of the shaded band around the curve shows the theoretical uncertainty. The vertical bands show the 95% CL exclusion limit on M_H from the direct searches at LEP (left) and at LHC (right). The dashed curve is the result obtained using the evaluation of $\Delta\alpha^{(5)}(M_Z^2)$. The dotted curve corresponds to a fit including also the low- Q^2 data.

prefers a relatively light Higgs boson. Now we can say that the measured value of this parameter agrees very well with the LEP fit. That indirectly confirms again the consistency and the power of the Standard Model.

It is interesting also to look at the behavior of the cross sections of electron-positron annihilation into hadrons as a function of energy Fig. 11. A clear peak at the Z boson mass is seen. The excellent agreement of the experimental data with the SM predictions is achieved only after inclusion of QCD and electroweak radiative corrections which reach dozens of percent in the vicinity of the peak.

A peculiar result was obtained at LEP for number of (light) neutrinos, see Fig. 12. Even so that the final state neutrinos in the process $e^+ + e^- \rightarrow Z \rightarrow \nu + \bar{\nu}$ was not observed, the corresponding cross section was restored with the help of the separately measured total, hadronic, and leptonic cross sections [18].

It appears that to dependence of LEP observables on quantum loop effects involving top quark is rather strong. So even without approaching the direct production of top quark, LEP experiments were able to extract information about its mass. The top quark mass 'history' (till 2006) is shown by Fig. 13.

In general, all LEP measurements of various cross-sections of electroweak SM processes were found in a very good agreement with theoretical predictions obtained within the SM, see plot Fig. 14 from the LEPWWG [18] 2013 report. The dots show the measurements and curves are the SM predictions with radiative corrections taken into account.

4.5 Measurements of SM processes at LHC

The Large Hadron Collider is not only a discovery machine. In fact the large luminosity and advanced detectors allow to perform there high-precision tests of the Standard Model. High statistics on many SM

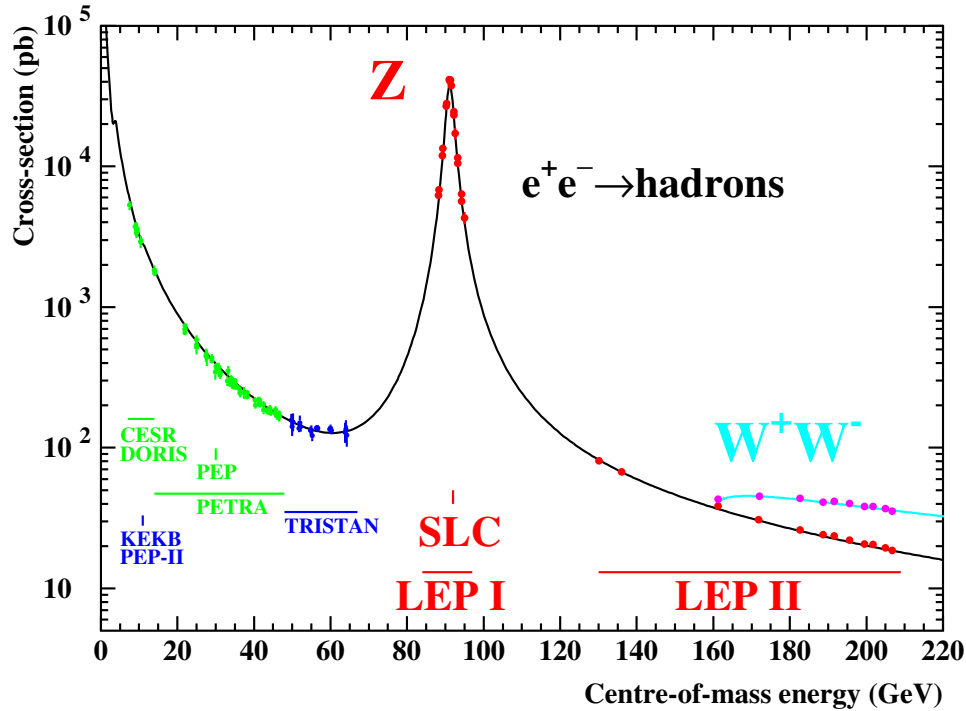


Fig. 11: Measurements of the $e^+e^- \rightarrow \text{hadrons}$ cross section.

processes is collected. Plots Fig. 15 and Fig. 16 show the public preliminary results of the ATLAS and CMS collaborations. One can see that we again have a good agreement for all channels. Certainly, the tests of the SM will be continued at LHC at higher energies and luminosity. That is one of the main tasks the LHC physical programme. The proton-antiproton collider Tevatron has proven that hadronic colliders can do high-precision studies of the SM. In particular, CDF and D0 experiments at Tevatron managed to exceed LEP in the precision of the W boson mass measurement.

At LHC the best precision in SM processes measurement is reached for the Drell–Yan-like processes. A schematic diagram for such a process is shown on Fig. 17. These processes are distinguished by production of final state leptons which can be accurately detected. We distinguish the neutral current (NC) Drell–Yan-like processes which involve intermediate Z bosons and photons, and the charged current (CC) ones which go through W bosons. The main contribution to the (observed) total cross section of these processes comes from the domain where the invariant mass of the final state lepton pair is close to the masses of Z and W bosons. So these processes are also known as single Z and W production reactions. The CC and NC Drell–Yan-like processes at LHC are used for:

- luminosity monitoring;
- W mass and width measurements;
- extraction of parton density functions;
- detector calibration;
- background to many other processes;
- and new physics searches.

In particular, a new peak in the observed invariant-mass distribution of final leptons can indicate the presence of a new intermediate particle.

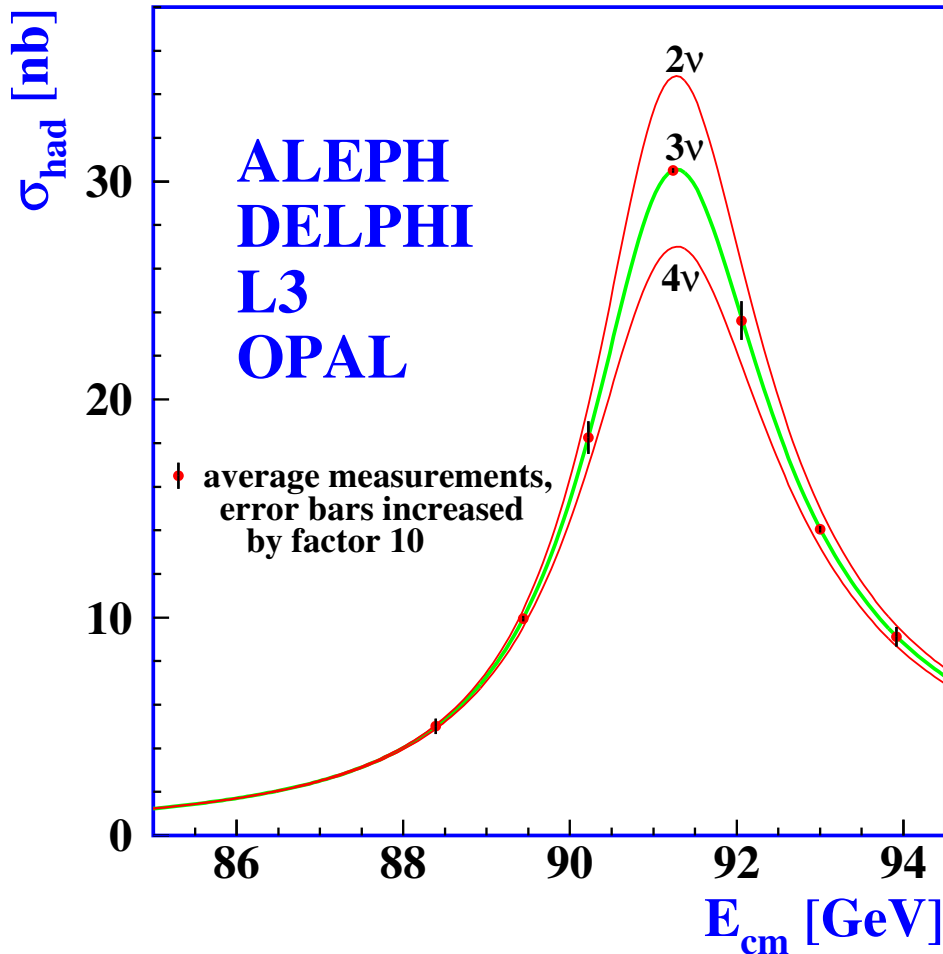


Fig. 12: Annihilation cross section $e^+e^- \rightarrow \text{hadrons}$ for different numbers of light neutrinos: measured distribution vs. the SM prediction.

5 Conclusions

Let us summarize the status of the SM. We see that it is a rather elegant construction which allows making systematic predictions for an extremely wide range of observables in particle physics. The energy range of its applicability covers the whole domain which is explored experimentally while the limits remain unknown. We do not understand all features of the model, the origin of its symmetries, and parameter values. But we see that the SM has the highest predictive power among all models in particle physics and it successfully passed verification at thousands of experiments.

There are several particularly nice features of the SM:

- it is renormalizable and unitary \Rightarrow it gives finite predictions;
- its predictions do agree with experimental data;
- symmetry principles are extensively exploited;
- it is minimal;
- all its particles are discovered;
- the structure of interactions is fixed (but not yet tested everywhere);
- not so many free parameters, all are fixed;
- CP violation is allowed;

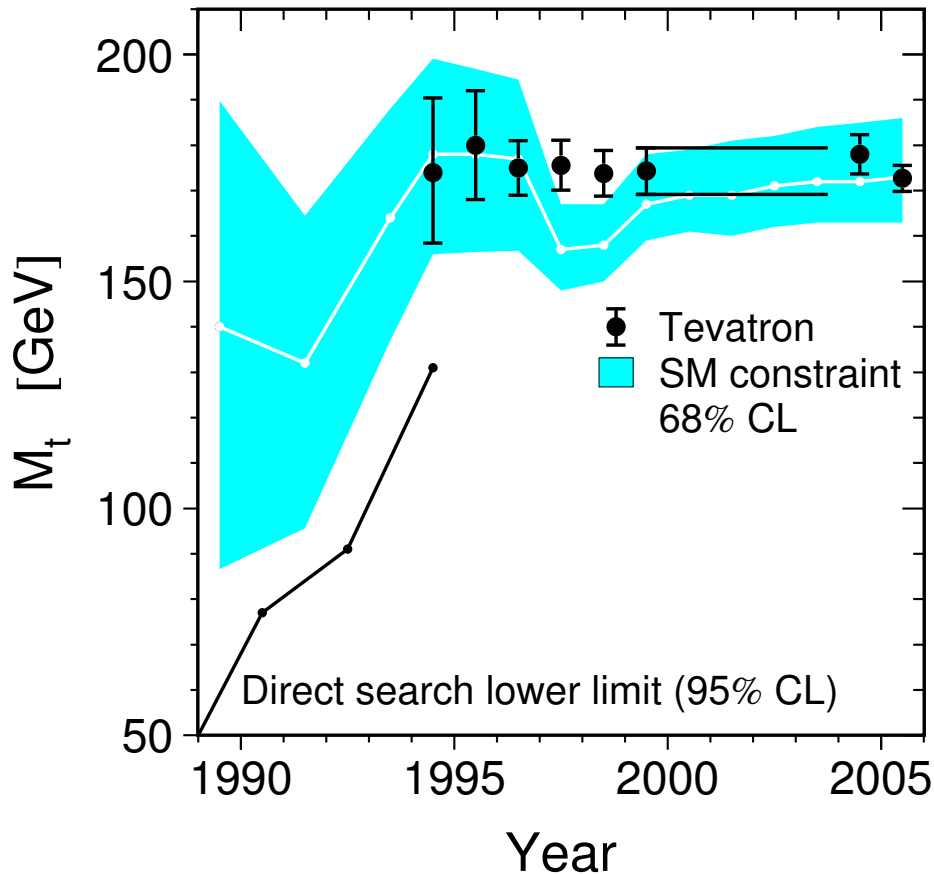


Fig. 13: Indirect (LEP) and direct (Tevatron) measurements of the top quark mass.

- tree-level flavor-changing neutral currents are not present;
- there is a room to incorporate neutrino masses and mixing.

In principle in the future, the SM can be embedded into a more general theory as an effective low-energy approximation.

For many reasons we do not believe that the SM is the final 'theory of everything'. Of course first of all, we have to mention that the SM is not joined with General Relativity. But frankly speaking, that is mostly the problem of GR, the SM itself is ready to be incorporated into a generalized joint QFT construction. The naturalness problem discussed above in Sect. 3.11 indicates that either some new physics should be very close to the EW energy scale, or we do not understand features of the renormalization procedure in the SM. In general, we have a lot of open questions within the SM:

- the origin of symmetries;
- the origin of energy scales;
- the origin of 3 fermion generations;
- the origin of neutrino masses;
- the hierarchy of lepton masses;

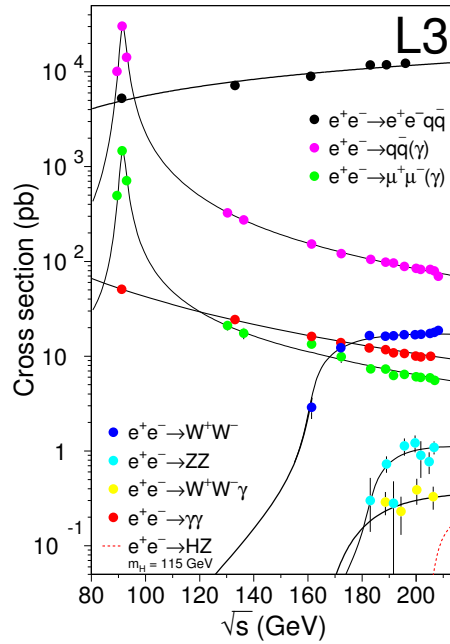


Fig. 14: Cross-sections of electroweak SM processes at LEP2.

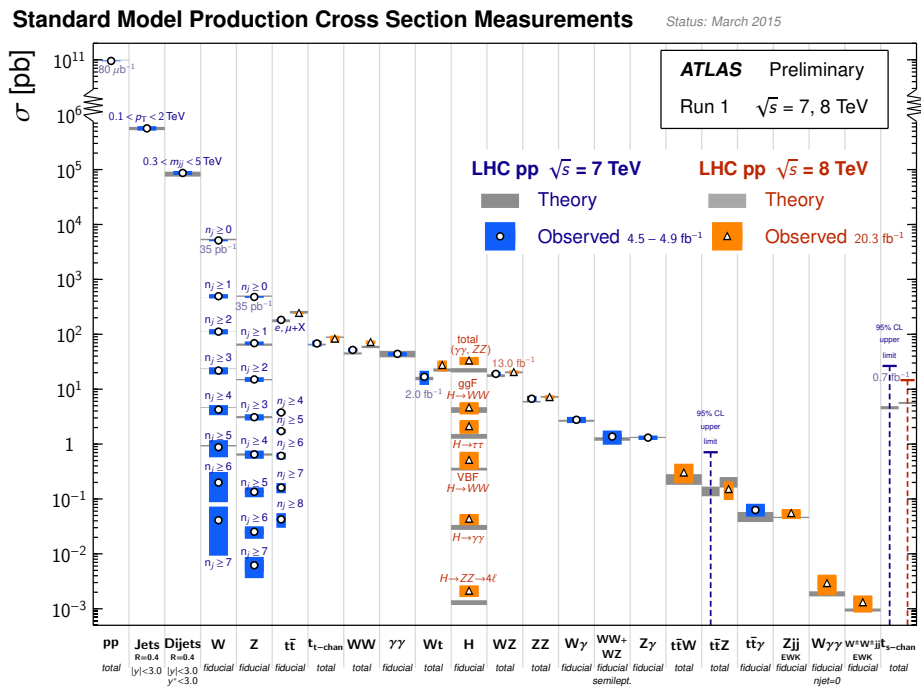


Fig. 15: SM cross sections measured by ATLAS (public results).

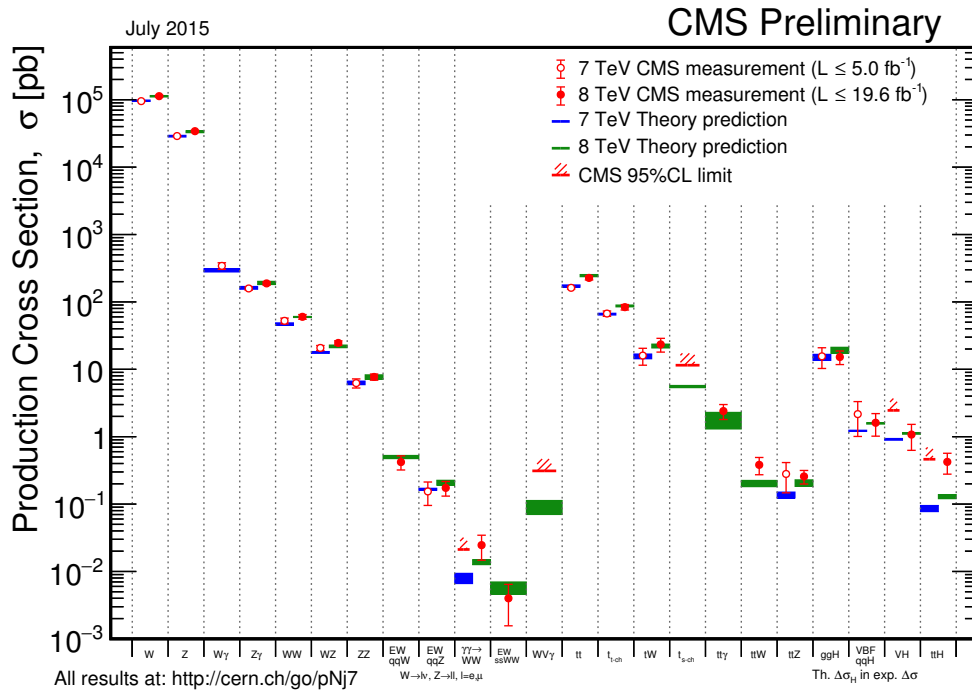


Fig. 16: SM cross sections measured by CMS (public results).

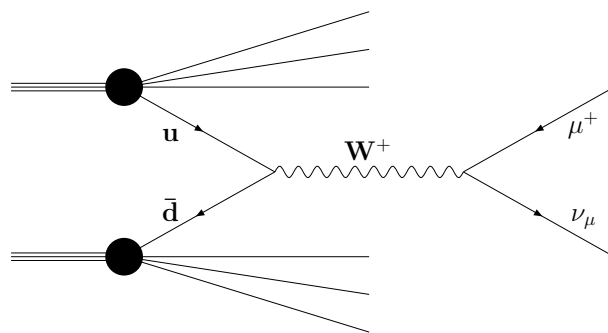


Fig. 17: Schematic Feynman diagram for the charged current Drell–Yan-like process.

- the absence of strong CP violation in the QCD sector;
- confinement in QCD, and so on. . .

There are also some phenomenological issues:

- the baryon asymmetry in the Universe;
- the dark matter;
- the dark energy;
- the proton charge radius, $(g - 2)_\mu$, and not much else. . .

The first three items above are related to Cosmology, see lectures by A. De Simone. We should note also that most of observations in Cosmology and Astrophysics are well described within the Standard Model (and General Relativity). But for the listed cases we need most likely something beyond the SM. The last item in the list claims that there are some tensions in the predictions of the SM and measurements at experiments in particle physics.

So we see that the SM is build using nice fundamental principles but with a substantial phenomenological input. The most *valuable task* for high-energy physicists now is to find the energy domain limit(s)

of the SM applicability. We hope to discover soon new physical phenomena. But any kind of new physics has to preserve the correspondence to the SM. The SM contains good mechanisms to generate masses of vector bosons and fermions, but it doesn't show the *origin(s)* of the energy scales.

So, the SM can not be the full story in particle physics, we still have a lot to explore.

References

- [1] S. L. Glashow, Nucl. Phys. **22** (1961) 579.
- [2] S. Weinberg, Phys. Rev. Lett. **19** (1967) 1264.
- [3] A. Salam, Conf. Proc. C **680519** (1968) 367.
- [4] N. N. Bogoliubov, D. V. Shirkov, *Introduction to the theory of quantized fields*, Interscience Publishers, 1959.
- [5] L. H. Ryder, *Quantum Field Theory*, 2nd Edition, Cambridge University Press, 1996.
- [6] M. E. Peskin, D. V. Schroeder, *An Introduction to Quantum Field Theory*, Westview Press, 1995.
- [7] G. Aad *et al.* [ATLAS Collaboration], Phys. Lett. B **716** (2012) 1.
- [8] S. Chatrchyan *et al.* [CMS Collaboration], Phys. Lett. B **716** (2012) 30.
- [9] D. Y. Bardin and G. Passarino, *The standard model in the making: Precision study of the electroweak interactions*, Oxford University Press, International series of monographs on physics, 104 Oxford, 1999.
- [10] F. Englert and R. Brout, Phys. Rev. Lett. **13** (1964) 321.
- [11] P. W. Higgs, Phys. Rev. Lett. **13** (1964) 508.
- [12] Scientific Background on the Nobel Prize in Physics 2013: The BEH-Mechanism, Interactions with Short Range Forces and Scalar Particles, http://www.nobelprize.org/nobel_prizes/physics/laureates/2013/advanced-physicsprize2013.pdf.
- [13] A. V. Bednyakov, B. A. Kniehl, A. F. Pikelner and O. L. Veretin, Phys. Rev. Lett. **115** (2015) 20, 201802.
- [14] K. A. Olive *et al.* [Particle Data Group Collaboration], Chin. Phys. C **38** (2014) 090001.
- [15] D. Hanneke, S. F. Hoogerheide and G. Gabrielse, Phys. Rev. A **83** (2011) 052122.
- [16] T. Aoyama, M. Hayakawa, T. Kinoshita and M. Nio, Phys. Rev. Lett. **109** (2012) 111807.
- [17] S. Actis *et al.* [Working Group on Radiative Corrections and Monte Carlo Generators for Low Energies Collaboration], Eur. Phys. J. C **66** (2010) 585.
- [18] The LEP Electroweak Working Group, <http://lepewwg.web.cern.ch/LEPEWWG/>.
- [19] A. B. Arbuzov, M. Awramik, M. Czakon, A. Freitas, M. W. Grunewald, K. Monig, S. Riemann and T. Riemann, Comput. Phys. Commun. **174** (2006) 728.
- [20] G. Montagna, O. Nicrosini, F. Piccinini and G. Passarino, Comput. Phys. Commun. **117** (1999) 278.

Higgs Physics, in the SM and Beyond

F. Riva

CERN, Theory Department, CH-1211 Geneva, Switzerland

Abstract

A lecture on Higgs boson physics to highlight why it is necessary and how it looks like. I review the Standard Model and why a small electroweak scale is our strongest indication for an extended Higgs sector, that can be searched for by a precise study of Higgs properties. To this goal, I discuss effective field theories and how they capture the most relevant effects in large classes of scenarios beyond the Standard Model.

Keywords

Standard model: High-Energy Physics; Higgs Physics.

1 Motivation

1964-1967: A quantum field theoretical (QFT) description of the electroweak (EW) interactions is developed; among a handful of models that can give mass to the W^\pm and Z bosons, one stands out for its predictiveness, simplicity and for seemingly getting as close as possible to a fundamental theory: the Standard Model (SM) of particle physics [1–3]. Its most distinctive prediction is the existence of a resonance, the Higgs boson, whose properties are uniquely fixed by parameters that are already known, except for one, the Higgs boson mass m_h .

2009-2012: the Large Hadron Collider (LHC) is built to collide protons up to 14 TeV energies, and to search explicitly for the Higgs boson, or any alternative source for the EW masses. A discovery is guaranteed by theoretical inconsistency of the EW massive theory above ≈ 3 TeV. And is indeed made on July 4, 2012 [4,5]. The last parameter of the SM is now measured, $m_h = 125.09$ [6]. With this mass, the Higgs boson properties are just right for a rich experimental program to be carried out, as Higgs decays in a rather equilibrated way to all SM particles. With this mass, we can compute the quantum lifetime of our universe, and find that it is just right to last 13.7 billion years [7].

The most relevant aspect of the Higgs discovery, however, is that it constitutes the last brick of the SM, and this brick is just right, that the theory has in principle a very large range of validity. For this reason, the Higgs discovery interrupts an important trend in particle physics, where well-established fundamental principles were pointing the finger towards guaranteed discoveries.

In these lecture notes I will try to give a feeling of physics before the SM, in the SM, and Beyond the SM, to appreciate the necessity for a Higgs boson, but also its limitations. I think they provide a nice little story to understand why we are interested in studying Higgs physics, and how we are going to do so at the LHC and future colliders. Hundreds of relevant references will be omitted, sorry, and loads of interesting physics will not even be mentioned, sorry - see for instance the complementary reviews Refs. [8–11].

The notes are organized as follows. The QFT of massless and massive spin-1 states, and the necessity for a Higgs mechanism is reviewed in section 2, leading to the SM in section 3. The reader familiar with the SM and interested in the most modern aspects of Higgs physics, relevant for colliders, can skip to section 4, where I discuss the motivations why the SM might not be the end of the story. This section includes a discussion of Effective Field Theories (EFTs) relevant for Higgs physics, ranging from practical aspects relevant for global fits in SM precision tests, to power-counting rules to identify what are the relevant high-energy features that we can test in low-energy experiments.

2 bSM - before the Standard Model

To appreciate the importance of the Higgs mechanism, and of its SM realization, I must first discuss how the SM looks like without a Higgs boson. In particular I want to discuss the difficulties of providing a QFT description of the massless and massive spin-1 states/resonances observed in Nature: the photon γ and W, Z bosons respectively.

2.1 Gauge Invariance – 4 Legs Good, 2 Legs Better

The observation that physics is invariant under the Poincaré symmetry $\mathcal{P} = \mathbb{R}^4 \ltimes SO(1, 3)$ of translations, rotations and boosts, shapes most of our understanding of nature [12]. We realize this symmetry by building objects with well-defined transformation properties and combine them in an invariant way. An important mismatch strikes us at the very start of this program. Physical states $|p\rangle = a^\dagger(\vec{p})|0\rangle$ at finite momentum \vec{p} and spin s , and their scattering amplitudes, transform accordingly to the Little group, the subgroup of Lorentz that leaves the momentum of a particle unchanged (we can think of the momentum as spontaneously breaking the Lorentz group $SO(1, 3)$, the Little group is what is left). On the other hand, the fields $\Phi_{\{\mu\}}(x)$ appearing in the Lagrangian in position space, and Feynman diagrams, appear in full representations of $SO(1, 3)$ (denoted here with generic indices $\{\mu\}$). The two are however related,

$$\Phi_{\{\mu\}}(x) = \sum_s \int d^3p \epsilon_{\{\mu\}}(x; \vec{p}, s) a(\vec{p}, s), \quad (1)$$

with $\epsilon_{\{\mu\}}(x; \vec{p}, s)$ the polarization vectors, that define how representations of Lorentz break into representations of the Little group $LG \subset SO(1, 3)$. For $\Lambda_\nu^\mu \in SO(1, 3)$,

$$\Phi_{\{\mu\}}(x) \rightarrow D(\Lambda^{-1})\Phi_{\{\mu\}}(\Lambda x) \quad a(\vec{p}, s) \rightarrow \sum_{s'} U_{s, s'}^j(\Lambda^{Little}) a(\Lambda \vec{p}, s), \quad (2)$$

where $D(\Lambda)$ and $U(\Lambda^{Little})$ are representations of the full and Little Lorentz group respectively, that typically differ from one another.

Massive vectors. In this case, the Little group is the group of rotations $SO(3)$. Its representations are well known and classified according to their dimension $2j + 1$, where j is half-integer and refers to the spin of the particle annihilated by $a(\vec{p}, s)$ (and it bounds the sum in Eq. (2) into $s, s' \leq j$). The spin-1 representation, in which we are interested to describe W and Z bosons, is 3-dimensional, corresponding in practice to the two transverse and one longitudinal polarizations of massive vectors.

The smallest full representation of $SO(1, 3)$ that can accommodate these 3 states, is the vector field $\Phi_{\{\mu\}} = V^\mu$, with $D(\Lambda) = \Lambda_\nu^\mu$, that can source 4 degrees of freedom. The remaining one, $4 = 3 \oplus 1$ under $SO(1, 3) \rightarrow SO(3)$, corresponds to a $j = 1$ state and has a polarization $\epsilon_\mu(p) \propto p_\mu$ in Eq. (1). This is equivalent to the state sourced by the derivative of a scalar $\Phi_{\{\mu\}}(x) = \partial_\mu \phi(x)$ and it does not interest us in the description of spin-1 states. Luckily, it is easy to eliminate it: on the physical states, $p^\mu \epsilon_\mu(p) = 0$ singles out the spin-1 polarizations (for the scalar $p^\mu \epsilon_\mu(p) \propto p^\mu p_\mu = m^2 \neq 0$), which is equivalent to,

$$\langle \psi^{phys'} | \partial_\mu V^\mu | \psi^{phys} \rangle = 0 \quad (3)$$

on physical states, that separates the Hilbert space into two disjoint parts.

The most general Lagrangian (up to dimension-4 and bilinear in V^μ – so as to describe a free field) compatible with the Lorentz transformation of V^μ , can be written as

$$\mathcal{L} = -\frac{1}{4g^2} F_{\mu\nu} F^{\mu\nu} - \frac{\xi}{2} (\partial_\mu V^\mu)^2 - \frac{v^2}{2} V_\mu V^\mu, \quad (4)$$

where we have defined $F_{\mu\nu} \equiv \partial_\mu V_\nu - \partial_\nu V_\mu$ and introduced generic parameters g, v, ξ . Clearly Eq. (4) describes four dynamical degrees of freedom, since it contains the time derivative of all 4 components of V^μ . If we call $\chi = \partial_\mu V^\mu$, the equations of motion for V^μ read

$$-\xi \partial^\nu \chi - v^2 V^\nu = \partial_\mu F^{\mu\nu} / g^2 \quad \Rightarrow^{\partial^\nu} \quad -\xi \square \chi - v^2 \chi = 0, \quad (5)$$

where in the second equation we have exploited the fact that $F^{\mu\nu}$ is antisymmetric¹ Eq. (5) is interesting because it shows that the fields χ is not sourced by the other components of the vector field, it is a free field. For this reason it is consistent to have it vanish at all times, Eq. (3). In fact, the (Proca) Lagrangian

$$\mathcal{L} = -\frac{1}{4g^2} F_{\mu\nu} F^{\mu\nu} - \frac{v^2}{2} V_\mu V^\mu, \quad (6)$$

automatically provides this condition Eq. (3) as a consequence of the equations of motion (Eq. (5) with $\xi = 0$), and can be thought as the correct Lagrangian to describe the dynamics of one massive vector with $m = vg$.

Massless vectors. For massless particles the little group is $ISO(2)$, the isometries of a 2-dimensional plane, and its representations are 2-dimensional² and labelled by the helicity of the state: a spin-1 state has 2 degrees of freedom.

The problem is that in this peculiar case, it is not possible to find polarization vectors $\epsilon_\mu(x, \vec{p})$, such that the left-hand and the right hand side of Eq. (1) have the right transformation properties: no 4-vector field can be constructed with annihilation/creation operators of a spin-1 massless particle [12]. If one tries to force so, the resulting monster will do the following under a Lorentz transformation:

$$V_\mu(x) \rightarrow \Lambda^\nu_\mu V_\nu(\Lambda x) + \partial_\mu \Omega(x, \Lambda), \quad (7)$$

for a function $\Omega(x, \Lambda)$. This second piece in the transformation law for V_μ clearly differentiates it from a Lorentz vector, but its peculiar form suggests that, if a theory can be defined modulo transformations of the type

$$V_\mu(x) \rightarrow V_\mu(x) + \partial_\mu \alpha(x) \quad (8)$$

for any function $\alpha(x)$, then Eq. (7) might be concealed with the correct Lorentz transformation for a 4-vector. This is called *gauge* invariance/redundancy and plays a central rôle in our understanding of the fundamental interactions: it is an inevitable consequence of Lorentz invariance and the existence of massless spin-1 states (in this sense, symmetries are a consequence of dynamics, rather than the opposite) and leads to a unique Lagrangian,

$$\mathcal{L} = -\frac{1}{4g^2} F_{\mu\nu} F^{\mu\nu}. \quad (9)$$

In fact, this symmetry also accounts for the disappearance of the one degree of freedom w.r.t. the massive case. This type of symmetry is perhaps better referred to as a *redundancy*, since it characterizes a situation in which different mathematical descriptions correspond to the same physical system. In fact, there is even so much of this redundancy (since $\alpha(x)$ is a complete set of functions) that an entire degree of freedom becomes unphysical.

In summary, a massless spin-1 state has 2 degrees of freedom, and its description in terms of a quantum field requires the introduction of gauge invariance. A massive spin-1 state has instead 3 degrees of freedom and gauge invariance is not apparently manifest; its description in terms of a quantum 4-vector Lorentz field requires the additional Lorentz covariant condition Eq. (3).

¹This argument is not modified if V_μ couples to a conserved current $gV^\mu J_\mu$ in Eq. (4), since this cancels Eq. (5) because $\partial_\nu J^\nu = 0$.

²The representations are in fact 1-dimensional, but since parity interchanges helicity $h \rightarrow -h$, a manifestly parity preserving description must include multiplets with states of opposite helicity (for $h = 0$ this is trivially satisfied and the representation is in fact 1-dimensional)

2.2 The Higgs Mechanism: $4 + 1 - 2 = 3$

There is an interesting way of writing the Lagrangian for a massive spin-1 field, that is surprisingly equivalent to Eq. (6), but it involves an additional degree of freedom, in the form of a scalar $U(x) = \exp i\phi(x)$, and the Lagrangian

$$\mathcal{L} = -\frac{1}{4g^2}F_{\mu\nu}F^{\mu\nu} + \frac{v^2}{2}(D_\mu U)^2 = -\frac{1}{4g^2}F_{\mu\nu}F^{\mu\nu} - \frac{v^2}{2}(\partial_\mu\phi - V_\mu)^2 \quad (10)$$

where $D_\mu = \partial_\mu - iV_\mu$. This is, in fact, invariant under the symmetry

$$U(x) \rightarrow e^{i\alpha(x)}U(x) \quad \phi(x) \rightarrow \phi(x) + \alpha(x) \quad V_\mu(x) \rightarrow V_\mu(x) - \partial_\mu\alpha(x) \quad (11)$$

which includes the gauge invariance Eq. (8) for vector fields, and extends it to the scalar field. The theory described by Eq. (10) must therefore describe $4 - 2 + 1 = 3$ degrees of freedom (gauge invariance removing two degrees of freedom from a 4-vector, and the scalar adds one), equivalently to Eq. (6). That it is equivalent can also be understood by exploiting the gauge invariance and perform a transformation Eq. (11) on Eq. (10) with $\alpha = \phi$: this results in Eq. (6). This equivalence allows us to compare the theories for massive and massless vectors on an equal footing, both of them being based on intrinsic gauge invariance, and differing by the addition of a scalar degree of freedom, with the appropriate transformation properties. This is the essence of the *Higgs mechanism* and, in this form, provides a description of individual massive vectors, associated with Abelian gauge symmetries (such as in massive Quantum Electrodynamics – QED). In particular, the theory described by Eq. (6) or Eq. (10), and their extension to couplings with fermions based on gauge symmetry, can be extrapolated to arbitrary high energy.

Non-Abelian symmetries. We are interested however in providing a description of Nature and of the W^\pm, Z bosons, whose gauge symmetry $SU(2)_L$ is in fact non-abelian. This can be described in a generalization of Eq. (10),

$$\mathcal{L} = -\frac{1}{4g^2}\text{tr}[F_{\mu\nu}F^{\mu\nu}] + \frac{(v + ah)^2}{2}\text{tr}[D_\mu U^\dagger D^\mu U] \quad (12)$$

where now $F_{\mu\nu} = \partial_\mu V_\nu - \partial_\nu V_\mu - i[V_\mu, V_\nu]$ for $V_\mu = V_\mu^i \sigma^i$, σ^i the Pauli matrices, and

$$U = e^{i\phi^i \sigma^i} \quad (13)$$

for three scalars ϕ^a , so that the Lagrangian is invariant under $g_L \in SU(2)_L$

$$U \rightarrow g_L U, \quad V_\mu \rightarrow g_L V_\mu g_L^\dagger - ig_L^\dagger \partial_\mu g_L. \quad (14)$$

Notice that I've included an additional scalar h in Eq. (12), whose importance will become clear later, but for the moment we can take $a = 0$. Contrary to the abelian case of Eq. (10), that is basically a free theory, Eq. (12) has self-interactions, that contribute for instance to the $2 \rightarrow 2$ scattering between four spin-1 states. In this process, a surprising feature appears in the particular channel involving their longitudinal polarization. As shown in the left panel of Fig. 1, this theory predicts an uncontrolled rise with energy in the scattering probability in this channel. In fact, for

$$E \gtrsim \Lambda_{cut} = \frac{4\pi v}{\sqrt{|1-a|}} \quad (15)$$

the theory doesn't make sense anymore as a Lagrangian weakly coupled description of this scattering process (the amplitude calculated with this theory would appear to violate unitarity).

Why does the amplitude grow? Scalar fields that appear in the Lagrangian through the exponential representation Eq. (13) (the non-linear sigma-model), are in fact very special in Nature: their interactions

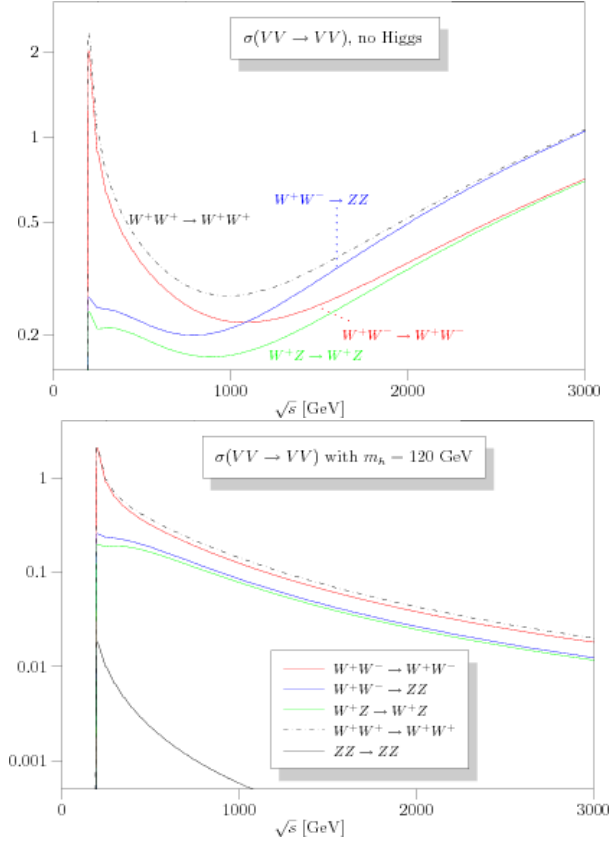


Fig. 1: Taken from [13]. Cross sections (in nanobarns) $\sigma(V_L V_L \rightarrow V_L V_L)$ for the longitudinal polarization of vectors in the SM, $V = W^\pm, Z$. The LEFT panel shows the energy-growth in the absence of a Higgs boson, while the RIGHT panel includes a Higgs bosons with $m_h = 120$ GeV.

are always associated with derivatives, and this leads to the rapid energy growth observed above. In fact, fields like these are Nambu-Goldstone bosons of spontaneously broken symmetries, and they always correspond to the low energy manifestation of a more complicated microscopic theory. This is where the unphysical behavior of Fig. 1 is bringing us: at high energy the theory of massive vectors does not describe Nature.

a=0 – Pions. A familiar example where we find the necessary scalar Eq. (13), is the pion Lagrangian from quantum chromodynamics (QCD). Here, for small $m_{u,d}$, QCD is almost invariant under the symmetry $\mathcal{G} = SU(2)_L \times SU(2)_R$, independently acting on the left- and right-handed up and down quark doublet

$$\Psi_{L,R} \equiv \begin{pmatrix} u \\ d \end{pmatrix}_{L,R}. \quad (16)$$

At low energy the quarks are no longer the relevant degrees of freedom, they condense at $E \sim \Lambda_{QCD}$ and define a new QCD vacuum, so that, at low energy, only the symmetry $SU(2)_L = SU(2)_R \equiv SU(2)_V = \mathcal{H}$ survives, while independent LR transformations are spontaneously broken. Goldstone theorem predicts three associated Nambu Goldstone bosons (NGB) corresponding to the pions π^a , which are the relevant degrees of freedom at low energy, as opposed to the quarks being the appropriate degrees of freedom at high-energy. These NGBs span the coset manifold \mathcal{G}/\mathcal{H} , which can be parametrized by $U = \exp i\pi^a \sigma^a$, transforming as $U \rightarrow g_L U g_R$. This is equivalent to Eq. (13), since the quark global $SU(2)_L$ corresponds indeed to the gauged weak interactions, while $U(1)_Y$ can be identified with a

subgroup of $SU(2)_R$. So, QCD gives mass to the EW bosons: at $E \lesssim \Lambda_{QCD}$ Eq. (12) (with $a = 0$) describes massive W, Z bosons, while at $E \gtrsim \Lambda_{QCD}$ they appear massless, and the anomalous behavior of Fig. 1 is not realized. Eq. (12) is an effective field theory (EFT) with a finite range of validity. The problem with QCD is that v in Eq. (12) is not a free parameter, but determines also other pion interactions and has been measured $v = f_\pi \approx 130$ MeV, so that $m_{W^\pm} = g \frac{f}{2} \approx 40$ MeV...

This is clearly not what we observe in Nature, but this example remains illustrative as it provides an important proof of principle, that led the physics community to speculate on the existence of a new strong interaction, called Technicolor [14, 15], with new (techni)quarks in addition to the SM ones, such that the magic of QCD is repeated at a higher scale

$$v = f_{TC} = 246 \text{ GeV} \quad (17)$$

thus reproducing the correct mass spectrum for the EW gauge bosons.

a=1 – Higgs. Recall that in Eq. (12) I've included the interaction with an additional real scalar h (with assumed canonical kinetic term). The reason for doing so is that it is easy to see that this gives an additional contribution to the amplitude for $V_L V_L$ scattering, that at high-energy has the opposite sign compared to the $a = 0$ one, and leads to Eq. (15). For $a = 1$, the high-energy behavior cancels and Eq. (12) goes from an EFT with a small cutoff to a theory that in principle has an arbitrarily large range of validity $\Lambda_{cut} \rightarrow \infty$.

The reason is the following. For $a = 1$ we can write

$$(v + h)U \equiv \Sigma = (\tilde{H}, H), \quad \Rightarrow \quad \frac{(v + h)^2}{2} \text{tr} [D_\mu U^\dagger D^\mu U] = |D^\mu H|^2 \quad (18)$$

where we have rewritten the fields using a different parametrization,

$$H = \exp(i\pi^a \sigma^a / \phi) \begin{pmatrix} 0 \\ \phi \end{pmatrix} = U \begin{pmatrix} 0 \\ \phi \end{pmatrix} = \frac{1}{\sqrt{2}} \begin{pmatrix} \phi_1 + i\phi_2 \\ \phi_3 + i\phi_4 \end{pmatrix}, \quad (19)$$

and $\tilde{H} = \epsilon H^\dagger$ (ϵ the antisymmetric tensor). This map works only when $|H| \equiv \phi \neq 0$, and is singular in $\phi = 0$. The important aspect is that now H transforms as a fundamental representation $\mathbf{2}$ of $SU(2)_L$ and his own Lagrangian at dimension ≤ 4 is simply

$$\mathcal{L}_H = \partial_\mu H^\dagger \partial^\mu H - V(H), \quad V(H) = -m_H^2 |H|^2 + \lambda |H|^4, \quad (20)$$

which describes four real scalars with non-pathological self interactions, whose scattering amplitudes are well-behaved also at high-energy. This has to be contrasted with the Lagrangian for U only, $v^2 \text{tr} [\partial_\mu U \partial^\mu U] / \xi$ that has instead a cutoff at $4\pi v$.

In some sense, we have found a different UV completion for our effective Lagrangian Eq. (12), that simply involves an additional scalar $\phi = v + h$, that however renders the amplitude physical, thanks to its contribution to scattering processes. This is illustrated in the right panel of figure 1. Now, what guarantees $|H| \neq 0$ everywhere so that the field H has a vacuum expectation value $\langle 0 | H^\dagger H | 0 \rangle \neq 0$? This is revealed from the H potential $V(H)$ in Eq. (20). Notice that this is independent of the NGBs, which cancel in $|H|^2$; this is why they are massless NGBs, because they don't appear in the potential. Then we see that for positive $m^2 > 0$ and positive $\lambda > 0$ the potential has a minimum at

$$\langle \phi \rangle \equiv v = \frac{\sqrt{m^2}}{\lambda} \quad (21)$$

and this is the average value of the field everywhere in spacetime. Because of this value, the low-energy Lagrangian has $SU(2)_L \times U(1)_Y$ symmetry realized non-linearly: we say that EW symmetry is

	SM Fields		$SU(3)_C, SU(2)_L, U(1)_Y$
spin-0	Higgs	H	$(\mathbf{1}, \mathbf{2}, -\frac{1}{2})$
spin-1/2	Quarks ($\times 3$ families)	$Q_L = (u_L \ d_L)$ u_R^\dagger d_R^\dagger	$(\mathbf{3}, \mathbf{2}, \frac{1}{6})$ $(\bar{\mathbf{3}}, \mathbf{1}, -\frac{2}{3})$ $(\bar{\mathbf{3}}, \mathbf{1}, \frac{1}{3})$
	Leptons ($\times 3$ families)	$L_L = (\nu \ e_L)$ e_R^\dagger	$(\mathbf{1}, \mathbf{2}, -\frac{1}{2})$ $(\mathbf{1}, \mathbf{1}, 1)$
spin-1	Gluon	g	$(\mathbf{8}, \mathbf{1}, 0)$
	W bosons	$W^\pm \ W^0$	$(\mathbf{1}, \mathbf{3}, 0)$
	B boson	B^0	$(\mathbf{1}, \mathbf{1}, 0)$

Table 1: The SM field content and quantum numbers.

spontaneously broken (EWSB). Now field excitations have to be considered around this minimum, and we see that $\delta\phi \equiv h$ has mass

$$m_h^2 = \lambda v^2. \quad (22)$$

So, this theory gives the 3 massive vectors and one massive scalar, a prediction summarized by Higgs in his original article [2], as *the prediction of incomplete multiplets of scalar and vector bosons*, which granted him and Englert [3] the Nobel prize in 2013.

In this introduction to the Higgs mechanism, I have tried to give a feeling for the necessity of gauge invariance and the Higgs mechanism, and then exposed to examples of the latter. We do not know yet with certitude how the EW symmetry breaking sector looks like, although we already know that it is not of the form of a purely technicolor interaction. Indeed, in 2012, an *incomplete multiplet* – called the Higgs boson – has been discovered at the LHC, suggesting that a field in the linear representation of the EW group provides an appropriate description of nature, at least in the regime of energy tested at the LHC so far.

3 The Standard Model

In a seminal article, Weinberg [1] proposed a model in which fermions and vectors interact with the Higgs field H . He pointed out the well-behaved high-energy limit of amplitudes, saying that *this model may be renormalizable*: this is now the definition of the Standard Model of particle physics. The field content includes gauge bosons $V = G, W, B$ associated with the SM gauge symmetry $SU(3) \times SU(2)_L \times U(1)_Y$, matter fermions $\psi = Q, u, d, L, e$, and of course the Higgs field. The quantum numbers are reported in table 1, while their dynamics is described by a very simple Lagrangian which, at least at first sight, appears to plausibly describe the behavior of elementary particles:

$$\mathcal{L}_{SM} = \sum_{\psi} i\bar{\psi}\mathcal{D}\psi + h.c. - \sum_V \frac{1}{4}V_{\mu\nu}V^{\mu\nu} + |D_{\mu}H|^2 - V(H) + y_{ij}^{D,L}H\bar{\psi}_i\psi_j + y_{ij}^U\tilde{H}\bar{\psi}_i\psi_j, \quad (23)$$

where $D_{\mu} = (\partial_{\mu} + ig'YB_{\mu} + igW_{\mu}^a\sigma^a + ig_sG_{\mu}^a\lambda^a)$. Notice that Left- and Right-handed fermion have different quantum numbers (they are referred to as *chiral*), implying that a standard mass term $m(\bar{\psi}_L\psi_R + \bar{\psi}_R\psi_L)$ would not respect gauge symmetry. In this sense, the Higgs field becomes necessary also to provide a mass to the fermions: indeed $\bar{\psi}_L H\psi_R$ is a gauge singlet, and induces a fermion mass after EWSB, $\phi \rightarrow h + v$.

3.1 Accidental and Approximate Symmetries

The SM Lagrangian Eq. (23) consists of only relevant and marginal operators (that is, operators with dimension $D \leq 4$). This is its defining feature, that allows it to be a valid theory over many orders of

magnitude in distance (in principle) and also that makes it such a predictive theory. Indeed, the limited number of interactions Eq. (23) implies many relations and structures that can be tested. An interesting way of keeping track of these relations, and to understand to what extent these relations are solid, is to identify the symmetries of the SM Lagrangian (some of which might be only approximate).

The SM Lagrangian Eq. (23) is invariant under a $U(1)_B$ symmetry, called *Baryon symmetry* or Baryon number, that acts on quarks and anti-quarks with opposite charge, as well as three $U(1)_{L_i}$ global symmetries that act on the three families of leptons, called *lepton numbers*. These symmetries are *accidental*, in the sense that they follow from the fact that only interactions of dimension ≤ 4 appear in Eq. (23), but they are *exact*. Indeed an operator of dimension-5, $LHLL$, called Weinberg operator, violates the lepton numbers (and gives mass to neutrinos), while at dimension-6, there are operators that violate baryon number. These symmetries imply important predictions in the SM: the absence of proton decay and vanishing neutrino masses.

Many other relations, especially in the context of Higgs physics, can instead be understood in terms of *custodial symmetry* $SU(2)_c$. This is an accidental and approximate symmetry of the Lagrangian. Custodial symmetry is best understood by writing the Higgs field as the 2×2 matrix Σ in Eq. (18). Now, Σ transforms as $\Sigma \rightarrow g_L \Sigma$ under $g_L \in SU(2)_L$, but we can conceive an extended (global) transformation $\Sigma \rightarrow \Sigma \rightarrow g_L \Sigma g_R$ for $g_{L,R} \in SU(2)_{L,R}$. For $g' \rightarrow 0$ and vanishing Yukawas, the SM Lagrangian involving the Higgs field can be written as

$$\mathcal{L}_{SM}^{\Sigma} = \text{tr} (D_{\mu} \Sigma^{\dagger} D^{\mu} \Sigma) - V(|\Sigma|) \quad (24)$$

and respects this symmetry. The Higgs vev $\langle \Sigma \rangle = \text{diag}(v, v)$ breaks it spontaneously to the diagonal subgroup $SU(2)_c = SU(2)_L = SU(2)_R$. This is called *custodial symmetry* because it implies that the mass of the W and Z bosons be identical. We can now keep track of the parameters that do not respect this symmetry by attributing them spurious transformation properties [16]

$$g' \sim (\mathbf{1}_L, \mathbf{3}_R) \quad Y^U \sim (\mathbf{1}_L, \mathbf{2}_R). \quad (25)$$

This can help to keep track of the size of certain effects in the SM. For instance, the W boson mass matrix $m_W^{ab} W^a W^b$ reduces into $\mathbf{3} \otimes \mathbf{3} = \mathbf{1} \oplus \mathbf{3} \oplus \mathbf{5}$, and the Z/W mass difference $m_Z^2 - m_{W\pm}^2 = (m_W^2)^{33} - (m_W^2)^{11}$, can only appear in the $\mathbf{5}$ of $SU(2)_L = SU(2)_R = SU(2)_c$. Using Eq. (25) we can see that, in the SM, we can have effects $m_Z^2 - m_{W\pm}^2 \propto (g')^2$. Indeed, at tree-level,³

$$\frac{m_Z^2}{m_W^2} = 1 + \frac{g'^2}{g^2} \quad (27)$$

This is particularly important for BSM physics, where custodial symmetry is no longer accidental and the ratio Eq. (27) can be modified.

3.2 Higgs Physics in the SM

Other *accidental* relations that characterize the SM cannot be attributed directly to symmetries, yet they can be considered on the same footing as defining features of the SM.

³At loop-level, effects involving the top-Yukawa become manifest. Our power-counting suggests that these $\propto (Y^t)^4$, but the explicit computation gives, for $m_t \gg m_b$,

$$\Delta \frac{m_Z^2}{m_W^2} = -\frac{3}{2} \frac{(Y^t)^2}{16\pi^2} \cos^2 \theta_w. \quad (26)$$

This is due to the fact that this contribution is related to an IR effect, regulated by m_t^2 in the propagator, that removes two powers of Y_t from our power-counting. In other words, Y_t cannot be considered a small spurion compatibly with the $m_t \gg m_b$ assumption: in the limit $Y_t \rightarrow 0$, the approximated expression Eq. (26) actually becomes infinite, but an exact computation with $m_b, m_t \rightarrow 0$ would show the expected behaviour.

The classical Lagrangian Eq. (23) can be expanded as $\phi \rightarrow h + v$, and the Goldstone bosons can be absorbed through an $SU(2)_L$ transformation (unitary gauge).

$$|D_\mu H|^2 \supset (m_W^2 W_\mu^+ W^{-\mu} + \frac{1}{2} m_Z^2 Z_\mu Z^\mu) \left(1 + 2\frac{h}{v} + \frac{h^2}{v^2}\right) \quad (28)$$

$$V(H) \supset -\frac{1}{2} m_h^2 h^2 \left(1 + 2\frac{h}{v} + \frac{h^2}{v^2}\right) \quad (29)$$

$$H \bar{\psi}_i \psi \supset m_\psi \bar{\psi}_i \psi \left(1 + \frac{h}{v}\right), \quad (30)$$

where $m_W = gv/2$, $m_Z = m_W/\cos\theta_W$ ($\cos\theta_W = g/\sqrt{g^2 + g'^2}$), $m_h = \lambda v/2$ and $m_\psi = yv/2$ in terms of the Lagrangian parameters. Interestingly, once the masses of the SM particles are measured, Eqs. (28-30) fix uniquely their coupling to physical Higgs bosons, in such a way that it is proportional to their mass. The fact that h interactions are naturally aligned with the fermion masses plays a crucial rôle for the phenomenology of the SM, forbidding to very high accuracy Flavor Changing Neutral Currents (FCNCs).

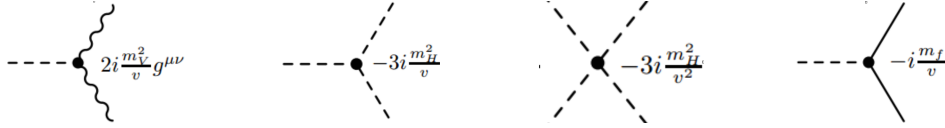


Fig. 2: Tree-level Higgs couplings in the SM.

The SM is a renormalizable theory. In practice this means that *infinite* quantum effects must be unobservable, as they cancel against infinite Lagrangian counter-terms and relate to input (measured) parameters of the theory. On the contrary, *finite* quantum effects are physical and observable: these constitute a robust prediction of the theory and an important test of its structure. For instance, quantum

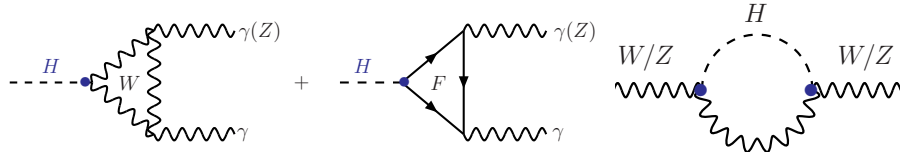


Fig. 3: Some loop effects involving the Higgs in the SM.

effects imply small (finite) departures of the tree-level relations in Fig. 2, that can be ignored for the purpose of this review. They are however important when they are associated with effects that are not present at tree level. I will discuss the most important here, though keep in mind that experiments can be designed to be sensitive also to other effects that I am here neglecting. First of all, the Higgs doesn't couple to photons, to gluons, nor to $Z\gamma$ at tree-level; all these are generated by loop effects, some of which are reported in Fig. 3. The exact expressions can be found e.g. in [11]; what matters to us is that the resulting expressions are completely determined by the tree-level couplings Eqs. (28-30) and are therefore a prediction of the SM. For these reason, knowledge of the SM particle masses gives us a concrete prediction on the physics of the Higgs boson, as shown in Fig. 4 that shows the different branching ratios for Higgs decays in the SM, for different values of m_h (computed before the discovery of the Higgs boson).

It is interesting to point out that loop effects allowed to test the physics of the Higgs boson, even before its discovery. Indeed, the last diagram of Fig. 3 shows a loop effect that contributes a finite amount

to processes involving a Z or a W boson. Since H propagate in the loop, these effects are $\propto \log m_h$. Precise measurements of the Z -boson properties at LEP [17], allowed therefore to extract the information of the RH side of Fig. 4, $m_h = 94_{-24}^{+29}$ GeV.

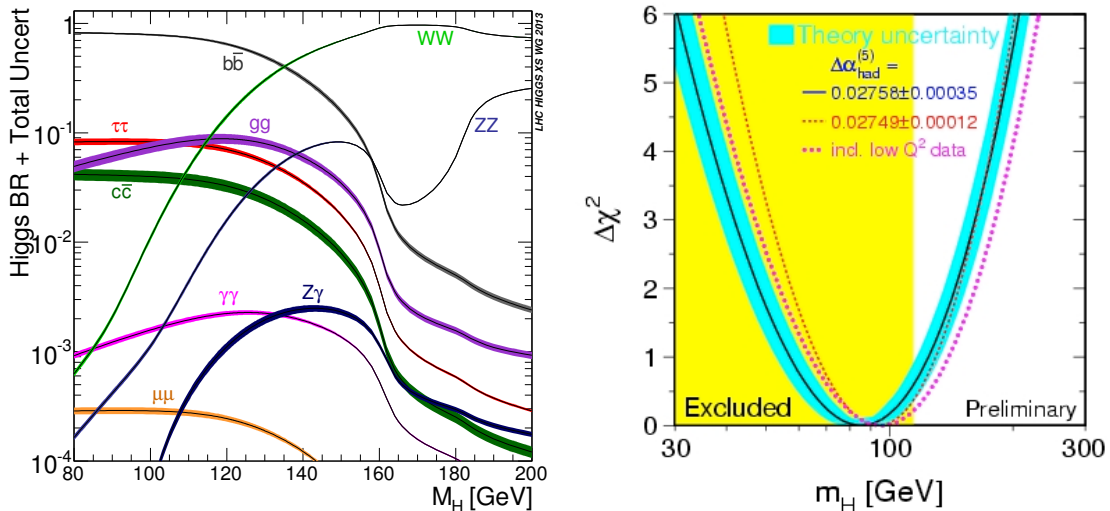


Fig. 4: LEFT: Higgs branching ratios in the SM, for different values of m_h [18]. RIGHT: preferred value of m_h , from a global fit to EW data; the yellow band corresponds to the direct LEP constraints $m_h > 114.4$ GeV [19].

So, when produced, a Higgs boson decays predominantly in b -quarks, W -bosons, gluons, etc. But how is it produced, to begin with? Amusingly, the dominant production mode at the LHC is through a loop effect: the cross-section for gluon fusion $gg \rightarrow h$ is large $\sigma_{gg \rightarrow h} \approx 44(19)$ pb at 13(8) TeV, simply because the proton content of gluons is very large. This is followed by tree-level, but electroweak, processes: vector boson fusion $qq \rightarrow VVqq \rightarrow hqq$ has $\sigma_{VBF} \approx 3.7(1.6)$ pb, while vector-associated production $\bar{q}q \rightarrow V^* \rightarrow Vh$ has $\sigma_{VH} \approx 2.2(1.1)$ pb; yet these are the dominant production modes at e^+e^- colliders. Finally, production in association with top quarks $pp \rightarrow t\bar{t}h$ constitute a small fraction of the total cross-section $\sigma_{t\bar{t}h} \approx 0.51(0.13)$ pb.

For what concerns the SM, the only information that was still missing before the LHC was m_h . This could be measured with extreme precision

$$m_h = 125.09 \pm 0.24 \text{ GeV} \quad [6] \quad (31)$$

thanks to the Higgs decaying to $\gamma\gamma$ and ZZ , which have the best mass-resolution (decays to W -bosons are instead penalized by the impossibility to detect neutrinos and hence to reconstruct the invariant mass of the W -pair).

As we will see in the next section, from a BSM point of view, all channels are important, because they allow us to test alternative hypotheses in which the Higgs couplings might depart from the SM ones. In this sense (borrowing Fabiola Gianotti words), *Nature has been kind to us*, because the Higgs mass happens to be such that all decay channels are more or less important. Indeed, had m_h be for instance 170 GeV, we would have been dominated by the WW mode, with no hope to ever observing $\gamma\gamma$ decays.

In the BSM-motivated quest of testing the Higgs couplings, it is important to keep in mind that the LHC is a complicated machine, in which size does not always matter. For instance, the process $gg \rightarrow h \rightarrow b\bar{b}$ has by far the largest cross-section, but the same is true for the QCD-dominated background, which renders this channel practically invisible. Decays into $b\bar{b}$ have therefore to be tested in the VH production mode, where the leptonic decays of the associated vector allow the event to be detected (or in VBF, where the same rôle is played by the special kinematics of the qq pair).

A convenient way to express the results of this exploration, is portrayed in Fig. 5. Here the Higgs couplings to the SM particles are multiplied by an arbitrary factor μ , the *signal strength*, such that the SM coincides with $\mu = 1$; then the μ_i are fitted as if they were free parameters of the theory. The information contained in these fits, will form the basis for our BSM exploration in the next section.

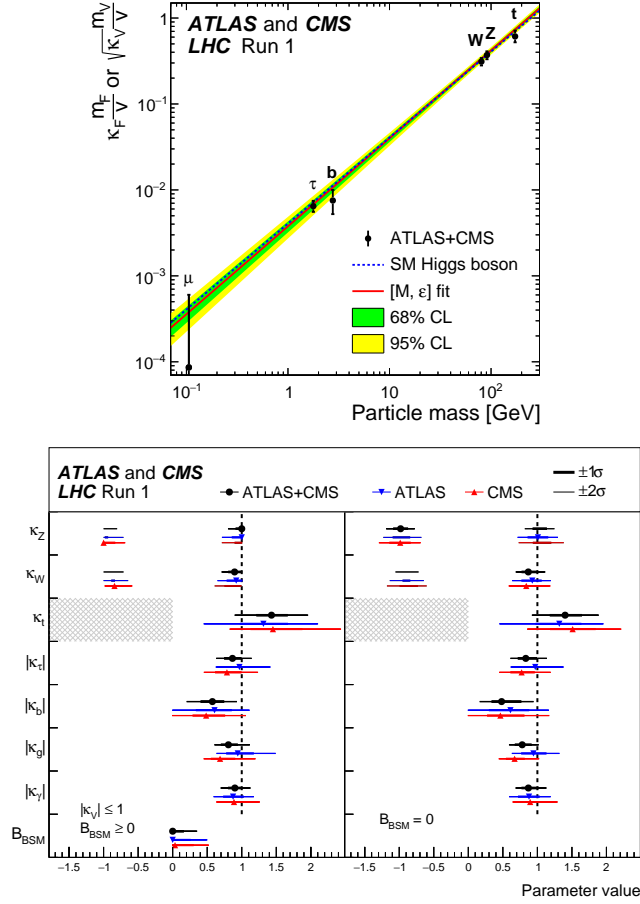


Fig. 5: One of the rare ATLAS+CMS combinations from [20]. LEFT: fit to tree-level Higgs couplings, testing the coupling/mass relation as predicted in the SM, Eqs. (28-30). RIGHT: test of the SM Higgs couplings, performed with a global fit by rescaling each SM tree-level coupling to particle i by a factor κ_i (the " κ " framework) - B_{BSM} denotes a branching ratio into undetected particles.

4 Beyond the Standard Model

I mentioned before that the defining feature of the SM is the possibility, given its matter content, to extrapolate it to very high-energy, thus allowing it to be (very close to) a fundamental theory.⁴ First of all, this is just a possibility: nothing forbids the presence of new structure at distances close to the ones probed today. Secondly, we have indications that such structure exists. For instance, electric charge runs towards higher values as the energy is increased, and eventually becomes strong and non-perturbative at $M_{Landau} \approx 10^{275}$ GeV, signaling the existence of new dynamics. Gravity, must ultimately become part of the SM, but it's known to become strong at energies of order $M_{Planck} \approx 10^{19}$ GeV. Other in-

⁴More precisely, the SM includes only relevant and marginal operators that represent a finite theory keeping their couplings fixed and sending the cutoff to ∞ .

dications include the existence of Dark Matter, the neutrino masses, the necessity for a mechanism for baryo(lepto)genesis, all of which are not accommodated in the SM.

All these reasons motivate searches for physics beyond the SM, in all its possible incarnations. There is however one additional reason, that pushes us to search for BSM physics explicitly *at the LHC* and in particular in *Higgs physics*: Naturalness. This much disputed principle has to do with the hierarchy problem, expressed by Wilson [21] as the impossibility for the existence of light scalar particles that are not associated with the breaking of some symmetry. This argument includes an elementary Higgs scalar, such as the one appearing in the SM, and is a consequence of the fact that the Higgs mass term $|H|^2$ in the Lagrangian has dimension-2 and is therefore a very relevant operator. Relevant operators are UV-sensitive, so that the value of the Higgs mass we observe is related to quantities at high-energy; for instance changing the value of $m_h^2(M_{Planck})$ - the Higgs mass parameter measured at the Planck scale - by a factor of two within the SM, corresponds to changing $m_h^2(\text{TeV})$ by a factor $M_{Planck}^2/\text{TeV}^2 = 10^{32}$! This Wilsonian point of view is the formal implementation of reductionist thinking, that is: low-energy quantities such as $m_h^2(\text{TeV})$ can be computed in terms of more fundamental quantities $m_h^2(M_{Planck})$; in this sense the observed value $m_h^2 \equiv m_h^2(\text{TeV}) \approx (100\text{GeV})^2 \ll 10^{4+32}\text{GeV}^2$ appears to be finely tuned in the UV and this is the essence of the hierarchy problem.⁵

More concretely, in a fundamental theory that predicts m_h^2 in terms of more fundamental parameters, we could integrate $m_h^2(E)$ along the renormalization group flow (denoted here with E , to highlight the physical Wilsonian interpretation of E as the momentum of particles in the loops), to obtain its value at small energy (see e.g. [9]):

$$m_h^2 = \int_0^\infty dE \frac{dm_h^2(E)}{dE} = \int_0^{\Lambda_{UV}} \frac{dm_h^2(E)}{dE} + \underbrace{\int_{\Lambda_{UV}}^\infty dE \frac{dm_h^2(E)}{dE}}_{\equiv m_h^2(\Lambda_{UV})}, \quad (32)$$

where we have separated the contribution from below/above an arbitrarily chosen physical scale Λ_{UV} . The point is that we can compute the first integral in the RH side of Eq. (32) with the observation that at low-energy the SM describes properly Higgs physics; for $\Lambda_{UV} = M_{Planck}$ we obtain a contribution $\Delta m_h^2 = 10^{36}\text{GeV}^2$ as mentioned above, that must be finely cancelled against an (uncorrelated, in the Wilsonian point of view!) contribution from $m_h^2(\Lambda_{UV})$.

Paradoxically, the best way to formulate the hierarchy problem, is in models that solve it, i.e. models that do exhibit additional symmetry, such as composite Higgs models (CHM) or Supersymmetry (SUSY), such that

$$m_h^2(\Lambda_{UV}) = 0. \quad (33)$$

This is achieved in CHM because $|H|^2$ is a composite operator in the theory above Λ_{UV} and is in fact irrelevant. In SUSY, instead, non-renormalization theorems imply that $dm_h^2(E)/dE = 0$ and hence Eq. (33). In both cases, however the dominant contribution to m_h^2 comes from the first integral in the RH side of Eq. (32) that is typically a loop factor smaller than Λ_{UV}^2 (in strongly coupled CHM this is possible only if the Higgs is a PNGB of a global SSB [23]). Given the Higgs couplings in the SM, this part can be calculated and one finds that no fine-tuning corresponds to

$$\Lambda_{UV} \lesssim 450 \text{ GeV}, \quad (34)$$

that is: new dynamics has to modify Higgs physics at a physical scale accessible to the LHC.

Now, we can tolerate some level of fine-tuning (this can be quantified using the definition of Ref. [24] and increases quadratically with the new physics scale), but these arguments clearly single out different directions for the future of particle physics:

⁵In the SM, this relevant operator is very sensitive to the UV, but in principle one could imagine a modification of the SM where this sensitivity is tamed, because the dimension of the $|H|^2$ operator is smaller. First principles exclude this possibility [22].

- Rethink the Wilsonian approach in the grander scheme of things
- Search directly for the new states at Λ_{UV}
- Test the properties of the Higgs boson, which are expected to depart from the SM ones, signaling a modification of the first integral in Eq. (32)

The first approach has recently provided promising directions that take into account the cosmological history of the universe [25] with or without the inclusion of anthropic arguments [26], and it is not clear how wide the spectrum of possibilities is. The search of direct states in the TeV region constitutes instead the bulk of the LHC search program; its different ramifications depend very much on how we think this different dynamics will be, I refer to reviews on CHM or SUSY.

Instead, testing the properties of the Higgs boson is a well-defined and compact field of research. Indeed, from an experimental point of view, there is only a limited number of observables that can be tested in the context of Higgs physics. Interestingly, also from a theoretical point of view, independently from the details of the UV dynamics, there is only a limited number of ways in which Higgs physics can be modified. This is a consequence, again, of the Wilsonian point of view: integrating out new physics at the scale Λ_{UV} generates a set of local operators, corresponding to an Effective Field Theory (EFT). Given that only the more relevant ones survive at low-energy and given that there is only a finite number of operators of a given relevance, there can be only a finite number of effects that is worth studying in Higgs physics. We discuss this in detail in what follows.

4.1 BSM Higgs Phenomenology

An important thing to keep in mind, when thinking about Higgs phenomenology, is that the structure of the SM is rather unique: the relation between the different couplings, implied mostly by gauge-invariance, allow the theory to be valid to high-scales. So,

Any modification of the SM couplings reduces the cut-off of the theory.

This has to be read together with the definition that

Any theory with a cutoff is an Effective Field Theory,

that can be written as an expansion in local field operators of different dimensionality

$$\mathcal{L}_{\text{eff}} = \mathcal{L}_{\text{SM}} + \sum_i \frac{c_i^{(6)}}{M^2} \mathcal{O}_i^{(6)} + \sum_j \frac{c_j^{(8)}}{M^4} \mathcal{O}_j^{(8)} + \dots, \quad (35)$$

where $c_i^{(D)}$ are called Wilson coefficients and the leading (relevant) contribution $\mathcal{L}_{\text{SM}} \equiv \mathcal{L}_{\leq 4}$ is the one surviving in the limit where M , which is here the mass of new physical states, is taken $\rightarrow \infty$.⁶

In other words, what we can learn from testing different aspects of Higgs physics, can be captured in the language of EFTs. For instance, the ‘ κ ’ framework [18], where all SM Higgs couplings are rescaled (as in $\kappa_Z = g_{hZZ}/g_{hZZ}^{SM}$ for the $hZ_\mu Z^\mu$ coupling to Z -bosons), lowers the cutoff of the theory for $\kappa \neq 1$, and eventually corresponds to an EFT, despite the fact that no scale appears explicitly in its formulation (we had an example of this for $a \neq 1$ in Eq. (12)).

From a practical, experimental, point of view, there have been different proposals to parametrize the experimental information that can be extracted from measurements of the Higgs properties, but ultimately, the information they carry can be matched to EFTs. Most notably, pseudo-observables - POs

⁶Here I’ll discuss only theories that have a well defined decoupling-limit, see however [27] for an interesting case, with a naturally light Higgs, that cannot be captured by such an EFT. Moreover, I refer to Refs. [28, 29] (and to the appendix of [30]) for parameterizations in which EW symmetry is never linearly realized (useful for instance to capture Technicolor theories with an accidentally light Higgs).

- [31, 32] are designed as EFT-inspired expansions around the poles of certain scattering amplitudes involving h ; as such they are physical quantities and can be used as an important tool to extract information about EFTs from experiment. They are particularly useful in processes involving on/off-shell EW bosons, such as $h \rightarrow V\bar{\psi}\psi$, because their measurement depends on a minimum of theoretical input: precision QCD/EW calculations can then be used to extract from them information about the Wilson coefficients c_i , but since the precision of such computations constantly improve, measurements in terms of POs constitute a durable legacy.

For processes involving QCD states, POs are unfortunately less effective, since the experimental information is encoded in objects -jets- that correspond to a multiplicity of states at the fundamental level. In this case, simplified template or fiducial cross-section measurements [33] try to package the experimental information in a way that has reduced sensitivity to theoretical uncertainties (which are prone to improve when future calculations will be available) and enhanced sensitivity to the effects induced by EFTs.

Having said this, let us discuss what EFTs for Higgs physics really are, were we are interested in theories which have the same field content as the SM (see table 1). EFTs are all about formulating hypotheses about microscopic physics and to follow how these hypotheses can be tested with low-energy experiments. The assumptions I'll make in what follows are:

- There are no states beyond the SM ones at the energies relevant for these experiments, i.e. $E \ll M$. This assumption is motivated by the so far null results of the LHC.
- There is well-defined decoupling limit $M \rightarrow \infty$ in which the SM is recovered; in particular the Higgs field behaves (at least approximately) like an $SU(2)_L$ SM linear doublet. This is motivated by the left panel of Fig. 5: experimental data implies that departures from this limit must be small and presumably associated with a small expansion parameter.
- New physics is flavor-universal. This is motivated by the difficulty of accommodating experimental constraints in models with flavor non-universal new physics, but also from simplicity. See Ref. [34] where this assumption is relaxed in the context of Higgs/EW physics. Similarly we assume here that new physics conserves CP.
- We assume, to begin with, that the new physics is such as to generate all allowed operators, so that the leading effects are necessarily given at dimension-6, all higher dimension effects being irrelevant.

This last assumption is the least motivated: typically scenarios of new physics affect different sectors of the SM in different ways, symmetries can forbid some operators in favor of others, and large couplings can enhance effects that would otherwise be small. We will discuss these aspects below, but for the moment this hypotheses provides a conservative way for exploring the new physics landscape without much commitment.

4.1.1 Dimension-6 Effects

An important aspect of EFTs is that some (combinations of) effective couplings are redundant and do not induce any physical effect. Consider an infinitesimal (small ϵ) local transformation

$$\phi(x) \rightarrow \phi(x) + \epsilon F(\phi(x), \partial\phi(x)) \quad (36)$$

for a generic function F . Such field redefinition does not change the S -matrix, as long as the redefined field has non-vanishing matrix elements with the states sourced by the original one, but it changes the action by

$$\delta\mathcal{S}[\phi] = \epsilon \int d^4x \frac{\delta\mathcal{S}[\phi]}{\delta\phi(x)} F(\phi(x), \partial\phi(x)). \quad (37)$$

This implies that pieces of the action that can be written in the form of Eq. (37), can be eliminated by such field redefinition without changing the physics: they are therefore redundant. An example can clarify this better:

$$\mathcal{S} = \int d^4x \frac{(\partial_\mu \phi)^2}{2} + \frac{c_\phi}{M^2} \phi^3 \square \phi \xrightarrow{(\phi \rightarrow \phi - c_\phi \frac{\phi^3}{M^2})} \mathcal{S} = \int d^4x \frac{(\partial_\mu \phi)^2}{2} + O\left(\frac{1}{M^4}\right). \quad (38)$$

The irrelevant interaction c_ϕ is proportional to the leading-order equations of motion and can be eliminated, up to higher order effects in the $1/M^2$ expansion (which here plays the ϵ role). From a practical point of view, such redundancy can be thought (together with integration by parts) as the freedom of choosing different forms of the Lagrangian (similarly to gauge invariance), to highlight different properties of the theory under scrutiny.

So, under the above assumptions, and focussing on non-redundant sets of operators, there is only a handful of operators that can modify Higgs physics. These are summarized in Table 2 where we exploit the above-mentioned freedom to write them in three different bases, corresponding to SILH [35, 36], Warsaw [37], and BSM primaries/Higgs basis [33, 38, 39]. Integration by parts and field redefinitions allow to swap the blue operators in the SILH basis with the red ones in the Warsaw basis (plus a redefinition of other Wilson coefficients).

It is sometimes useful to classify these effects according to their transformation properties under the SM $SU(2)_L \times SU(2)_R$ accidental symmetry, which derive from

$SU(2)_L \times SU(2)_R$	Higgs only	Higgs and Derivative
$(\mathbf{1}_L, \mathbf{1}_R)$	$\text{tr}(\Sigma^\dagger \Sigma) = H^\dagger H$	$\text{tr}(\Sigma^\dagger D_\mu \Sigma) = D_\mu(H^\dagger H)/2$
$(\mathbf{1}_L, \mathbf{3}_R)_{Y=0}$	$\text{tr}(\Sigma^\dagger \Sigma \sigma^b) = 0$	$\text{tr}(\Sigma^\dagger D_\mu \Sigma \sigma^b) \xrightarrow{b=3} -H^\dagger \overset{\leftrightarrow}{D}_\mu H/2$
$(\mathbf{3}_L, \mathbf{1}_R)$	$\text{tr}(\Sigma^\dagger \sigma^a \Sigma) = 0$	$\text{tr}(\Sigma^\dagger \sigma^a D_\mu \Sigma) = H^\dagger \sigma^a \overset{\leftrightarrow}{D}_\mu H/2$
$(\mathbf{3}_L, \mathbf{3}_R)_{Y=0}$	$\text{tr}(\Sigma^\dagger \sigma^a \Sigma \sigma^b) \xrightarrow{b=3} -(H^\dagger \sigma^a H)$	$\text{tr}(\Sigma^\dagger \sigma^a D_\mu \Sigma \sigma^b) \xrightarrow{b=3} -D_\mu(H^\dagger \sigma^a H)$

(39)

where the $\mathbf{3}_R$ is broken down to its components, since $SU(2)_R$ is not necessarily a BSM symmetry.⁷ For instance, in the SILH basis, the operator \mathcal{O}_T is $(\mathbf{1}_L, \mathbf{3}_R) \otimes (\mathbf{1}_L, \mathbf{3}_R) \supset \mathbf{5}_R$ and is indeed associated with maximal custodial symmetry breaking. Similarly, $\mathcal{O}_{H\psi_R}$ and $\mathcal{O}_{H\psi_L}$ are $\sim \mathbf{3}_R$ and also break custodial. On the other hand, using the spurious transformation properties of g' from Eq. (25), \mathcal{O}_B is a singlet, in the sense that it doesn't introduce further custodial symmetry breaking than the SM. All other operators are singlets too. This classification is important because $SU(2)_c$ in the SM implies some relations (see section 3.1) that are well preserved at loop level (as discussed below Eq. (25)); departures from these relations can be well measured and constitute accurate BSM probes.

Clearly each individual operator contributes to different physical processes; for instance \mathcal{O}_{HQ} modifies the Z couplings to left-handed quarks, but also contributes directly to $h \rightarrow Z\bar{Q}Q$ decays, etc. This fact complicates a global fit, but also makes its results difficult to present and to interpret, as marginalized constraints are often dominated by the poorest observables.⁸ For this reason it is useful to identify the most relevant experiments that can test the operators of Table 2 and organize them according to their precision, and the operators they are sensitive to.

⁷In Eq. (39) we have kept the third one $b = 3$ that is associated with vanishing hypercharge $Y = 0$, but keep in mind that operators, like \mathcal{O}_R^{ud} in the caption of Table 2, can be formed also with the \pm components that give $\bar{H}^\dagger \sigma^a H$ with hypercharge $Y = \pm 1$

⁸In principle the $n \times n$ correlation matrix relating measurements of n Wilson coefficients carries all the necessary information. In practice, however, results are often presented as marginalized over $n - 1$ parameters so that, when the correlation matrix has large off-diagonal components, constraints are dominated by the least sensitive measurements and appear, therefore, artificially weak. These are sometimes called "blind directions".

	SILH	Warsaw	BSM Primaries
LHC Higgs 10%	$\mathcal{O}_6 = \lambda H ^6$ $\mathcal{O}_{BB} = g'^2 H ^2 B_{\mu\nu} B^{\mu\nu}$ $\mathcal{O}_{GG} = g_s^2 H ^2 G_{\mu\nu}^A G^{A\mu\nu}$ $\mathcal{O}_{y\psi} = y_e H ^2 (\bar{\psi}_L H \psi_R)_{\psi=u,d,e}$ $\mathcal{O}_H = \frac{1}{2} (\partial^\mu H ^2)^2$ $\mathcal{O}_{HB} = ig' (D^\mu H)^\dagger (D^\nu H) B_{\mu\nu}$	\mathcal{O}_6 \mathcal{O}_{BB} \mathcal{O}_{GG} $\mathcal{O}_{y\psi}$ \mathcal{O}_H $\mathcal{O}_{WW} = g^2 H ^2 W_{\mu\nu}^a W^{\mu\nu a}$	$\Delta\mathcal{L}_{3h}$ $\Delta\mathcal{L}_{\gamma\gamma}^h$ $\Delta\mathcal{L}_{GG}^h$ $\Delta\mathcal{L}_{\psi\psi}^h$ $\Delta\mathcal{L}_{VV}^h$ $\Delta\mathcal{L}_{Z\gamma}^h$
LEP I %	$\mathcal{O}_{HW} = ig (\bar{D}^\mu H)^\dagger \sigma^a (\bar{D}^\nu H) W_{\mu\nu}^a$ $\mathcal{O}_W = \frac{ig}{2} \left(H^\dagger \sigma^a \overleftrightarrow{D}^\mu H \right) D^\nu W_{\mu\nu}^a$	$\mathcal{O}_{WB} = g' g H^\dagger \sigma^a H W_{\mu\nu}^a B^{\mu\nu}$ $\mathcal{O}_{HL} = (iH^\dagger \overleftrightarrow{D}_\mu H) (\bar{L}_L \gamma^\mu L_L)$	$\Delta\mathcal{L}_{\kappa\gamma}$ $\Delta\mathcal{L}_{g_1^Z}$
LEP I %	$\mathcal{O}_B = \frac{ig'}{2} \left(H^\dagger \overleftrightarrow{D}^\mu H \right) \partial^\nu B_{\mu\nu}$ $\mathcal{O}_T = \frac{1}{2} \left(H^\dagger \overleftrightarrow{D}_\mu H \right)^2$ $\mathcal{O}_{H\psi_R} = (iH^\dagger \overleftrightarrow{D}_\mu H) (\bar{\psi}_R \gamma^\mu \psi_R)_{\psi=u,d,e}$ $\mathcal{O}_{HQ} = (iH^\dagger \overleftrightarrow{D}_\mu H) (\bar{Q}_L \gamma^\mu Q_L)$ $\mathcal{O}'_{HQ} = (iH^\dagger \sigma^a \overleftrightarrow{D}_\mu H) (\bar{Q}_L \sigma^a \gamma^\mu Q_L)$	$\mathcal{O}'_{HL} = (iH^\dagger \sigma^a \overleftrightarrow{D}_\mu H) (\bar{L}_L \sigma^a \gamma^\mu L_L)$ \mathcal{O}_T $\mathcal{O}_{H\psi_R}$ \mathcal{O}_{HQ} \mathcal{O}'_{HQ}	$\Delta\mathcal{L}_{eL}^Z$ $\Delta\mathcal{L}_\nu^Z$ $\Delta\mathcal{L}_{uR,dR,eR}^Z$ $\Delta\mathcal{L}_{uL}^Z$ $\Delta\mathcal{L}_{dL}^Z$

Table 2: CP-even dimension-6 operators that affects Higgs physics. We omit dipole operators for fermions and $\mathcal{O}_R^{ud} = y_u^\dagger y_d (i\tilde{H}^\dagger \overleftrightarrow{D}_\mu H) (\bar{u}_R \gamma^\mu d_R)$ since they are suppressed by light fermion Yukawas under the MFV assumption. A complete set of operators can be found in Refs. [16, 37].

Higgs Physics. In principle Higgs physics can test all effects induced by the above operators. However, the sensitivity of present measurements of Higgs properties at the LHC is generally smaller than that of EW tests at LEP. For this reason it is useful to identify *Higgs-only* operators that do not contribute to EW precision observables and are therefore the genuine target of the LHC Higgs program, unconstrained by other experiments. Operators of the form $|H|^2 \mathcal{O}_{SM}$, with \mathcal{O}_{SM} a SM operator, only contribute to Higgs physics since, according to the classification Eq. (39), $|H|^2$ is an EW singlet that does not induce EW breaking effects. It is instructive to see why: the operator \mathcal{O}_{GG} for instance appears in the effective Lagrangian (with G in non-canonical normalization) as

$$-\frac{1}{4g_s^2} G_{\mu\nu}^A G^{A\mu\nu} + \frac{c_{GG}}{M^2} |H|^2 G_{\mu\nu}^A G^{A\mu\nu} = -\frac{1}{4} \left(\frac{1}{g_s^2} - 2 \frac{v^2}{M^2} \right) G_{\mu\nu}^A G^{A\mu\nu} + \frac{c_{GG}}{2M^2} (2vh + h^2) G_{\mu\nu}^A G^{A\mu\nu}.$$

The piece proportional to v^2 can be reabsorbed into a redefinition of g_s , which is an input parameter for the SM and has therefore no physical meaning until measured. In our flavor-universal framework we can think of the SM as having 8 input parameters, e.g. g' , g , g_s , m_W , $m_{u,d,e}$ and m_h , implying the existence of 8 Higgs-only operators

$$\text{Higgs-only: } \{ \mathcal{O}_{BB}, \mathcal{O}_{WW}, \mathcal{O}_{GG}, \mathcal{O}_H, \mathcal{O}_{y_{u,d,e}}, \mathcal{O}_6 \} \quad (40)$$

that are explicitly manifest in the Warsaw basis (upper-center box in Table 2). These can be tested at the LHC principally through the following rates

$$h \rightarrow \gamma\gamma, \quad h \rightarrow Z\gamma, \quad gg \rightarrow h \quad h \rightarrow ZZ, WW, \quad gg \rightarrow \bar{t}th, \quad h \rightarrow \bar{b}b, \quad h \rightarrow \bar{\tau}\tau, \quad gg \rightarrow hh \quad (41)$$

which contribute to the results from the right panel of Fig. 5, in addition with constraints from the $h \rightarrow Z\gamma$ channel [40] and $pp \rightarrow hh$ processes (the latter will test the Higgs cubic interaction that is affected uniquely by \mathcal{O}_6 , experimental results in this channel are not available yet, see Ref. [41] and references therein).

Notice that Higgs physics has in principle many more observables than the free parameters implied by the EFT, meaning that at this level in the $1/M$ expansion the EFT is in fact predictive and provides relations that can be tested. For instance, the EFT operators Eq. (40) imply that only one operator \mathcal{O}_H modifies both the $hZ_\mu Z^\mu$ and $hW_\mu^+ W^{-\mu}$ couplings. Similarly, two operators $\mathcal{O}_{BB}, \mathcal{O}_{WW}$ affect the four $hZ_{\mu\nu} Z^{\mu\nu}$, $hW_{\mu\nu}^+ W^{-\mu\nu}$, $hZ_{\mu\nu} A^{\mu\nu}$ and $hA_{\mu\nu} A^{\mu\nu}$ structures. These, and many more, are accidental relations that will be broken by the dimension-8 Lagrangian and they can be thought as the defining features of our assumptions on page 14. These relations can be made more explicit in the mass eigenbasis, writing combination of the 8 operators Eq. (40) as

$$\begin{aligned}
 \Delta\mathcal{L}_{\gamma\gamma}^h &= \kappa_{\gamma\gamma} \left(\frac{h}{v} + \frac{h^2}{2v^2} \right) \left[A_{\mu\nu} A^{\mu\nu} + Z_{\mu\nu} Z^{\mu\nu} + 2W_{\mu\nu}^+ W^{-\mu\nu} \right], \\
 \Delta\mathcal{L}_{Z\gamma}^h &= \kappa_{Z\gamma} \left(\frac{h}{v} + \frac{h^2}{2v^2} \right) \left[t_{\theta_W} A_{\mu\nu} Z^{\mu\nu} + \frac{c_{2\theta_W}}{2c_{\theta_W}^2} Z_{\mu\nu} Z^{\mu\nu} + W_{\mu\nu}^+ W^{-\mu\nu} \right], \\
 \Delta\mathcal{L}_{GG}^h &= \kappa_{GG} \left(\frac{h}{v} + \frac{h^2}{2v^2} \right) G_{\mu\nu}^A G^{A\mu\nu}, \\
 \Delta\mathcal{L}_{ff}^h &= \delta g_{ff}^h (h \bar{f}_L f_R + \text{h.c.}) \left(1 + \frac{3h}{2v} + \frac{h^2}{2v^2} \right), \\
 \Delta\mathcal{L}_{3h} &= \delta g_{3h} h^3 \left(1 + \frac{3h}{2v} + \frac{3h^2}{4v^2} + \frac{h^3}{8v^3} \right), \\
 \Delta\mathcal{L}_{VV}^h &= \delta g_{VV}^h 2m_W \left[h \left(W^{+\mu} W_\mu^- + \frac{Z^\mu Z_\mu}{2c_{\theta_W}^2} \right) + \Delta_h \right],
 \end{aligned} \tag{42}$$

with Δ_h contributing to processes with at least two physical Higgses. Here we have made sure that, for instance, only $\Delta\mathcal{L}_{\gamma\gamma}^h$ contributes to the $h \rightarrow \gamma\gamma$ rate and that only $\Delta\mathcal{L}_{3h}$ modifies the Higgs cubic. Then, these relations imply predictions: for instance the $hZ_{\mu\nu} Z^{\mu\nu}$ structure receives contributions that are proportional to $\kappa_{Z\gamma}$ and $\kappa_{\gamma\gamma}$ that are both well constrained.

This way of writing the EFT operators has the unique purpose of making manifest the relations between modification to different observables that persist in the dimension-6 Lagrangian. It is a way of writing *observables in terms of observables* that is analogous to defining the SM through the relation between W and Z masses Eq. (27), or the relations between Higgs couplings and masses Eqs. (28-30) that are accidental to the dimension-4 Lagrangian. In practice, these *BSM Primaries* [38], provide a useful way to express the results of a global fit in terms of parameters that are as close as possible to experiments, but at the same time maintain the information about the accidental relations of the dimension-6 Lagrangian. A global fit to Run-1 Higgs data reads [42] (see also [43–49])

$$\delta g_{VV}^h = 1.04 \pm 0.03, \quad \delta g_{tt}^h = 1.1_{-3.0}^{+0.9}, \quad \delta g_{bb}^h = 1.06_{-0.23}^{+0.30}, \quad \delta g_{\tau\tau}^h = 1.04 \pm 0.22 \tag{43}$$

$$\kappa_{gg} = 0.0005 \pm 0.008, \quad \kappa_{\gamma\gamma} = -0.0003_{-0.0007}^{+0.0005}, \quad \kappa_{Z\gamma} = 0.000_{-0.019}^{+0.035}. \tag{44}$$

This can be written in terms of constraints on the above operators, implying that $(c_H, c_{y_{u,d,e}}) \frac{v^2}{M^2} \sim 10^{-1}$, $c_G \frac{m_W^2}{M^2} \sim 10^{-3}$, while $(c_{WW}, c_{BB}) \frac{v^2}{M^2} \sim 10^{-2}$ (notice that c_{WW}, c_{BB} affect both $\gamma\gamma$ and the poorer $Z\gamma$; it is the latter that dominates this marginalized constraint); see also Fig. 6.

LEPI Electroweak Precision Tests (EWPT). A peculiarity of the Higgs field is that it acquires an expectation value that modifies the symmetry of the vacuum and the propagation of the EW bosons. Physics that modifies the Higgs sector can therefore also contribute to observables in EW physics, through the operators of Table 2 with $\langle H \rangle \rightarrow v/\sqrt{2}$.

LEP-I, operating on the Z -pole, provides the most precise measurements in this context, reaching the permille level. From an experimental point of view, we can think of these measurements of $e^+e^- \rightarrow$

$Z \rightarrow \text{fermions}$ as testing the couplings of Z to all the 7 SM (left and right) fermions $\nu, e_L, e_R, u_L, u_R, d_L, d_R$ (the Z couplings to these define a set of 7 pseudo-observables for LEP-I). Using (α_{em}, m_W, m_Z) as EW input parameters, it is easy to get convinced that there is no additional experimental information that can be extracted from LEP-I on flavor universal theories; in particular, information on custodial symmetry breaking (often presented as T parameter, that measures departures from the m_Z/m_W mass difference of Eq. (27)) or effects from $Z - B$ mixing (the S parameter [50, 51]) is contained in the Z -coupling measurements.

In the SILH basis, there turn out to be 7 operators contributing to these observables⁹, reported in the bottom-left block of Table 2 - more precisely, only the combination $\mathcal{O}_W + \mathcal{O}_B$ affects this type physics, while the orthogonal combination $\mathcal{O}_W - \mathcal{O}_B$ does not,

$$\text{LEP-I: } \{ \mathcal{O}_W + \mathcal{O}_B, \mathcal{O}_T, \mathcal{O}_{HQ}, \mathcal{O}'_{HQ}, \mathcal{O}_{Hu}, \mathcal{O}_{Hd}, \mathcal{O}_{He} \} \quad (45)$$

There could have been more operators (as in the Warsaw basis, where there naively appear to be 8 operators contributing), implying that one combination will necessarily remain unconstrained and it will affect the results of global fits with marginalized coefficients (see footnote 8). In this sense, the SILH basis appears as a favorable choice for EWPT. The result of a global fit, restricted to these operators and to LEP-I data [17], implies that the coefficients c_i of the operators of Eq. (45) are constrained at the permille level [52–54],

$$c_i \frac{m_W^2}{M^2} \sim f_{ew} \times 10^{-3} \quad (46)$$

as illustrated in Fig. 6.

LEP-II vs LHC. We have seen that out of the 17 operators that involve H , Table 2, 7 are constrained by LEP-I measurements and are well described in the SILH basis, while other 8 can be tested with Higgs physics only, and are well described in the Warsaw basis. Two (combinations of) operators remain yet unconstrained. To understand what effects they induce, it is useful to think of the 17 operators in Table 2 as a 17-dimensional sub-manifold in the ∞ -dimensional space of all possible observables and single out the 2-dimensional plane that belongs to this 17-dimensional manifold, but does not contribute to any observables measured at LEP-I or to the Higgs-only measurements of the Right panel of Fig. 5. The result of this exercise is a continuation of what we began in Eq. (42), expressing the EFT in the mass eigenstate basis and unitary gauge. We find that [38]

$$\begin{aligned} \Delta \mathcal{L}_{ee}^V &= \delta g_{eR}^Z \frac{\hat{h}^2}{v^2} Z^\mu \bar{e}_R \gamma_\mu e_R + \delta g_{eL}^Z \frac{\hat{h}^2}{v^2} \left[Z^\mu \bar{e}_L \gamma_\mu e_L - \frac{c_{\theta_W}}{\sqrt{2}} (W^{+\mu} \bar{\nu}_L \gamma_\mu e_L + \text{h.c.}) \right] \\ &+ \delta g_{\nu L}^Z \frac{\hat{h}^2}{v^2} \left[Z^\mu \bar{\nu}_L \gamma_\mu \nu_L + \frac{c_{\theta_W}}{\sqrt{2}} (W^{+\mu} \bar{\nu}_L \gamma_\mu e_L + \text{h.c.}) \right], \end{aligned} \quad (47)$$

$$\begin{aligned} \Delta \mathcal{L}_{qq}^V &= \delta g_{uR}^Z \frac{\hat{h}^2}{v^2} Z^\mu \bar{u}_R \gamma_\mu u_R + \delta g_{dR}^Z \frac{\hat{h}^2}{v^2} Z^\mu \bar{d}_R \gamma_\mu d_R \\ &+ \delta g_{dL}^Z \frac{\hat{h}^2}{v^2} \left[Z^\mu \bar{d}_L \gamma_\mu d_L - \frac{c_{\theta_W}}{\sqrt{2}} (W^{+\mu} \bar{u}_L \gamma_\mu d_L + \text{h.c.}) \right] \\ &+ \delta g_{uL}^Z \frac{\hat{h}^2}{v^2} \left[Z^\mu \bar{u}_L \gamma_\mu u_L + \frac{c_{\theta_W}}{\sqrt{2}} (W^{+\mu} \bar{u}_L \gamma_\mu d_L + \text{h.c.}) \right] \end{aligned} \quad (48)$$

$$\Delta \mathcal{L}_{g_1^Z} = \delta g_1^Z \left[igc_{\theta_W} (Z^\mu (W^{+\nu} W_{\mu\nu}^- - \text{h.c.}) + Z^{\mu\nu} W_\mu^+ W_\nu^-) \right] \quad (49)$$

⁹This is true when performing EW fits using (α_{em}, m_W, m_Z) as EW input parameters; if instead one uses (α_{em}, G_F, m_Z) there is an additional non-Higgs operator $(\bar{L}_L \sigma^\alpha \gamma^\mu L_L) (\bar{L}_L \sigma^\alpha \gamma_\mu L_L)$ that enters the fit at dimension-6 level, but also has an additional measurement that constrains it: the muon lifetime is used to extract G_F .

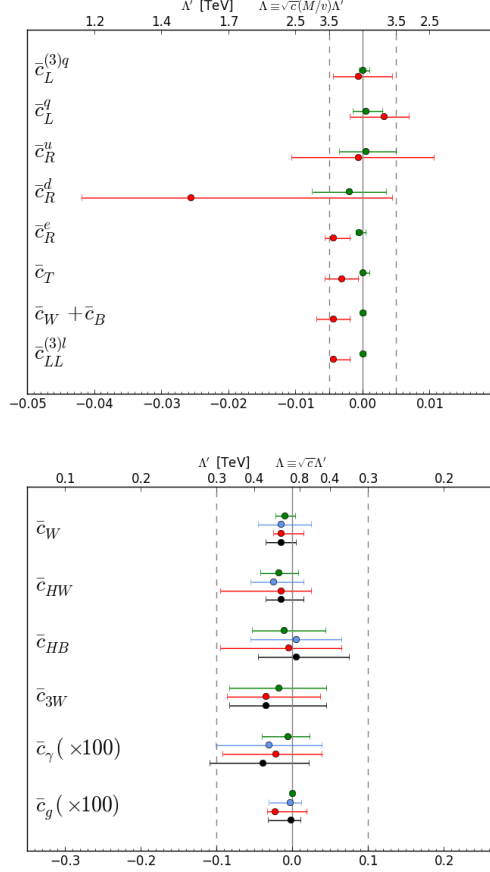


Fig. 6: 95% confidence intervals from a global fit, from Ref. [54]. The green lines denote fits with one coefficient only, while red bars denote fits with multi coefficients, marginalized (in our notation $c_{R,L}^\psi$ is $c_{H\psi}$).

$$\begin{aligned}
 \Delta\mathcal{L}_{\kappa\gamma} = & -2gc_{\theta_W}^2 \frac{h}{v} \left(W_\mu^- J_\mu^+ + \text{h.c.} + \frac{c_{2\theta_W}}{c_{\theta_W}^3} Z_\mu J_Z^\mu + \frac{2s_{\theta_W}^2}{c_{\theta_W}} Z_\mu J_{em}^\mu \right) \left(1 + \frac{h}{2v} \right) + \frac{e^2 v}{2c_{\theta_W}^2} h Z_\mu Z^\mu + \Delta_{h^2} \Big] \\
 = & \delta\kappa_\gamma \left[ie \left(1 + \frac{h}{v} \right)^2 (A_{\mu\nu} - t_{\theta_W} Z_{\mu\nu}) W^{+\mu} W^{-\nu} + 2Z_\nu \partial_\mu \left(\frac{h}{v} + \frac{h^2}{2v^2} \right) (t_{\theta_W} A^{\mu\nu} - t_{\theta_W}^2 Z^{\mu\nu}) \right. \\
 & \left. + \left(\frac{h}{v} + \frac{h^2}{2v^2} \right) \left(t_{\theta_W} Z_{\mu\nu} A^{\mu\nu} + \frac{c_{2\theta_W}}{2c_{\theta_W}^2} Z_{\mu\nu} Z^{\mu\nu} + W_{\mu\nu}^+ W^{-\mu\nu} \right) \right], \quad (50)
 \end{aligned}$$

complete Eq. (42) to span the entire space of dimension-6 operators, in a way that aligns with EW and Higgs observables. Here h corresponds to the physical Higgs and Δ_{h^2} includes interactions with at least two h that are irrelevant for experiments in the near future.

From Eqs. (49,50) we can read that the two remaining directions modify the trilinear gauge couplings (TGCs) between ZW^+W^- and γW^+W^- , as well as the $hV\bar{\psi}\psi$ ($V = W, Z$) amplitude. The reason that both these observables appear simultaneously modified can be traced to the fact that Higgs and the eaten Goldstones belong to the same multiplet, so that some BSM deformations in the Higgs sector can modify also processes with longitudinal W, Z bosons, at least at a fixed order in the $1/M$ expansion. TGCs can be tested in diboson processes at LEP-II or at the LHC, while deformation in $hV\bar{\psi}\psi$ are tested in $pp \rightarrow VH$ associated production at the LHC.¹⁰ The constraints from these two search modes

¹⁰In principle the same amplitude can be tested in $h \rightarrow V\bar{\psi}\psi$ decays [55] but, as shown in Fig. 7, constraints from LEP-II

are at present comparable, although the latter are typically extracted from the high-energy regime [56], so that certain conditions regarding the validity of our EFT assumption limit their interpretability [57]. From LEP-II data [58] we read

$$\delta g_{1,Z} = -0.05^{+0.05}_{-0.07}, \quad \delta \kappa_\gamma = 0.05^{+0.04}_{-0.04}. \quad (51)$$

These directions Eqs. (49,50) can be translated into combinations of operators in the SILH or Warsaw basis (see Ref. [39] for a gauge-invariant formulation in terms of the above operators), where $\delta g_{1,Z}, \delta \kappa_\gamma \sim c m_W^2/M^2$, for c a combination of Wilson coefficients, and are included in Fig. 6.

To conclude, let me reiterate the arguments of this section. Global fits are useful to explore the impact of experimental data on broad BSM hypotheses, that in our case we have defined with the assumptions in page 14 that we hope are able to capture large classes of BSM theories. If the theoretical parameters are not aligned with the experimental observables, the results of a global fit with n parameters, $n - 1$ of which are normalized, will be dominated by the poorest experiment. For this reason we have divided experiments with different sensitivity in correlated blocks (LEP-I, LEP-II and Higgs physics) and identified the operators they constrain. In fact, the best way to do this is to align the theoretical parameters to the most precise experiments, as in the BSM primaries/Higgs basis.

The outcome of this discussion is two-fold. First of all, it allowed us to identify the relations that persist in the effective Lagrangian at the level of dimension-6 operators, relations that can be tested or used as a check, if a deviation is found, or can be used to better constraint a given parameter. An example of such relation is reported in Fig. 7, which shows the differential distribution of Higgs decaying to a vector and a pair of fermions, such as in the golden channel. This distribution is affected by many dimension-6 operators, but all of them are bounded by other experiments, either at LEP-I, LEP-II or in Higgs physics; therefore this distribution cannot be arbitrarily modified, and a prediction of the dimension-6 EFT analysis is that, if any deviations are found there, they must be within the blue band, or violate some of our assumptions.

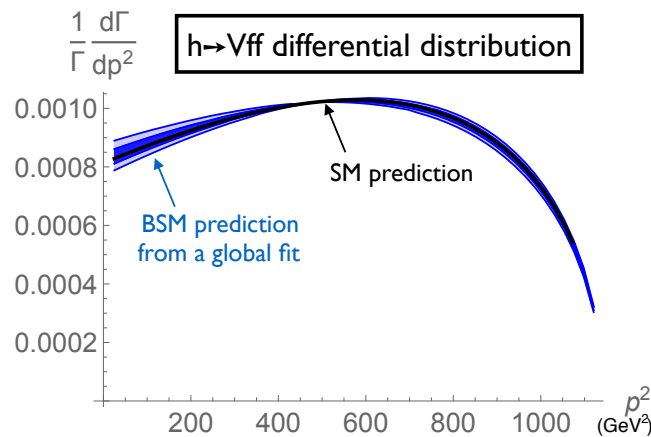


Fig. 7: Normalized differential distribution for Higgs decays in the golden channel. The black line corresponds to the SM prediction, while the blue bands correspond to the $(1,2\text{-}\sigma)$ contours of the BSM-deformation, as allowed by constraints from a global fit on possible dimension-6 modifications, that includes LEP-I and LEP-II data, as well as constraints on $h \rightarrow Z\gamma$. From the data in [52] (see also [59]).

are stronger than what can currently be measured in that channel

Secondly, this discussion, shows the most that we can get, in terms of experimental constraints, out of the *most conservative* hypotheses that all operators are democratically generated, and that they can even cancel each other in their contribution to a given observable. Even in this limiting hypothesis we could identify classes of operators that are already very well tested and constrained.

4.2 BSM Perspective

In realistic set-ups, based on physical microscopic hypotheses, only subsets of operators are typically generated, thus providing concrete scenarios that can be tested more precisely, and from which something can be learned. There is no limit in how specific and complicated a BSM model can be, but there is instead a limit in how simple it can be. Here we want to identify the minimal set of ingredients that can characterize a microscopic model and that can, at the same time, represent broad features of more generic BSM scenarios. These ingredients are,

$$\textit{One New Mass Scale } M, \quad \textit{One New Coupling } g_*, \quad \textit{Symmetries and Selection Rules}^{11}$$

where we assume that the UV completion admits some perturbative expansion in its couplings. These microscopic properties will be imprinted into the Wilson coefficients of the operators of Table 2. In lack of a specific model in which to compute this UV \rightarrow IR matching, we can still estimate them through a procedure known as *power-counting* or Naive Dimensional Analysis [60].

The idea is simple. Symmetries or properties of the underlying theory determine if an operator is generated or not. In weakly coupled theories this can simply boil down to whether or not the field mediating an interaction is present at the scale M (an example of this will be given below for SUSY), and can make the difference between large (tree-level) and small (loop-level) effects [61], while in strongly coupled theories a symmetry is typically necessary to generate a selection rule in the IR (for instance in composite Higgs models the Higgs is a psuedo-Goldstone boson with non-linearly realized global symmetry that generates mostly interactions with derivatives ∂H).

The dimension of the operator D determines that its coefficient will scale $\sim 1/M^{D-4}$, in order to make the action dimensionless, as we already know. What is perhaps more exotic is the fact that, counting powers of $\hbar \neq 1$ in the Lagrangian can tell us how many powers of couplings an operator might carry. Indeed, couplings, as well as fields, carry \hbar dimensions [35] (see also Refs. [9, 10]). It is easy to see that, since $[S] = \hbar$, fields have $[\phi] = \hbar^{1/2}$, while couplings have $[g] = \hbar^{-1/2}$. Any operator in the Lagrangian must have dimension $[c_i \mathcal{O}_i] = \hbar$, and we find that for an operator with n_i fields,

$$c_i \sim (\text{coupling})^{n_i-2} \tag{52}$$

In what follows we clarify the importance of power-counting through two examples ins SUSY and CH models, the most studied extensions of the Higgs sector that solve the hierarchy problem. Keep in mind that the selection rules discussed here, apply at the matching scale M , but the coefficients will run as they evolve towards lower energy. These effects can be computed entirely within the EFT, see [16, 62–66], and can have some important implications, in particular in situations where a poorly measured Wilson coefficient mixes through renormalization group flow into a very-well measure one.

4.2.1 SUSY

SUSY provides a great example of symmetries and selection rules in action. Superymmetry is compatible only with holomorphic interactions, thus forbidding the up-quark Yukawa $\propto \tilde{H} = \epsilon H^\dagger$ in the SM Lagrangian Eq. (23). Up-quark masses require therefore the presence of an additional Higgs doublet

¹¹Selection rules follow from microscopic symmetries that might or might not be realized (linearly or not) in the IR. Here I tend to refer to selection rules, as those that cannot be identified with symmetries from the low-energy point of view.

with opposite hypercharge $H_2 \in (\mathbf{1}, \mathbf{2}, 1/2)$, which can appear in the Lagrangian without complex conjugation.¹²

Moreover, the symmetry implies that the SM fields are part of super-multiplets containing fields of different spin. Some of these fields can potentially mediate proton decay, so that many SUSY incarnations invoke an accidental symmetry, R -parity, to forbid the relevant interactions responsible for this. Under R , the SM fields that we know, together with the scalar component of H_2 , are even, while all other states appearing in the SUSY multiplets are odd. This last observation is uniquely responsible for the EFT structure of SUSY models with R -parity. Indeed, any process between SM (R -even) states, can not be mediated at tree-level by an R -odd resonance, so that the only tree-level BSM effects are those associated with H_2 , the only R -even BSM particle. We show the relevant diagram in Fig. 8, where we identify h with the linear combination of H_1, H_2 that is closer to the SM one, and call H the heaviest combination (see Ref. [68]).

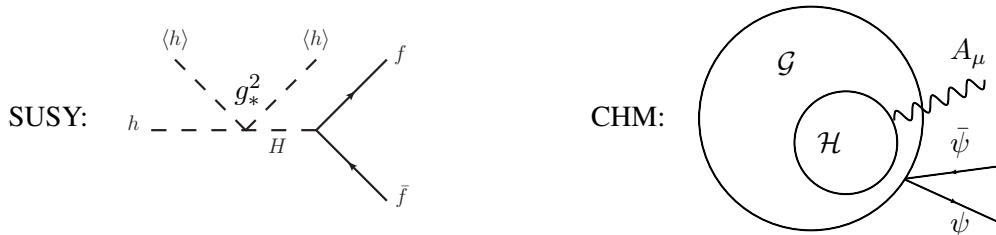


Fig. 8: LEFT: a modification of the Higgs couplings to SM fermion is the largest effect from integrating out BSM physics in SUSY models with R -parity. RIGHT: in CHM a strong sector brakes a global symmetry $\mathcal{G} \rightarrow \mathcal{H}$, while the gauge and Yukawa couplings break the symmetries explicitly, but weakly.

So, from the EFT perspective, R -symmetry translates in the *selection rule* that only a very special subset of new interactions is generated sizably at low energy: $\mathcal{O}_{y_u}, \mathcal{O}_{y_d}, \mathcal{O}_{y_e}$. What else can we say about this ‘New Physics’ sector? Flavor *symmetry* $U(3)^5$, is broken in the SM by the Yukawa couplings; the stringent constraints from flavor physics favor the possibility that the Yukawas be the only source of flavor symmetry breaking also in TeV-scale BSM: a possibility that is known as Minimal Flavor Violation [69] and is indeed realized in these SUSY models (the $H\bar{\psi}\psi$ couplings are aligned with the SM Yukawas). Finally, we can identify the microscopic coupling

$$\mathcal{L}_{UV}^{\text{SUSY}} \supset \frac{g_*^2}{4} h^3 H \quad (53)$$

with the generic g_* introduced on page 21, and m_H with M .

Now that we have identified the *relevant*¹³ features of SUSY models, in the generic language of page 21, we can estimate the low-energy EFT:

$$\text{SUSY} \sim \left\{ \begin{array}{l} \text{Selection rule from R-symmetry} \\ \text{Flavor symmetry, broken by } y_\psi \\ \text{New coupling: } g_*^2 \\ \text{Mass scale: } m_H \end{array} \right\} \Rightarrow \mathcal{L}_{eff}^{\text{SUSY}} = \tilde{c}_u \frac{g_*^2}{m_H^2} \mathcal{O}_{y_u} + \tilde{c}_d \frac{g_*^2}{m_H^2} \mathcal{O}_{y_d} + \tilde{c}_e \frac{g_*^2}{m_H^2} \mathcal{O}_{y_e} \quad (54)$$

where we have used the fact that the operators \mathcal{O}_{y_ψ} contain 5 fields so we expect their coefficient $\sim \text{coupling}^3$; since they brake flavor symmetries they must involve y_ψ (they are already weighted by one

¹²One of my favorite possibilities is that instead up-type quark Yukawas arise as SUSY breaking effects, while the Higgs doublet, which has quantum numbers $H_2 \in (\mathbf{1}, \mathbf{2}, -1/2)$ be the scalar supersymmetric partner of one of the leptons L , which has the same quantum numbers. In this case h would be the sneutrino [67], implying that we would have already discovered SUSY!

¹³On the most technical meaning of the word: features that are important at low-energy.

power of the Yukawas in Table 2), thus Eq. (52) reads here $\text{coupling}^3 \sim y_\psi g_*^2$. An explicit computation reproduces Eq. (54), with

$$\tilde{c}_u = -\cot \beta, \quad \tilde{c}_d = \tilde{c}_e = \tan \beta. \quad (55)$$

This example shows the impressive power of EFTs: 3 parameters are enough to capture the low-energy signatures of all SUSY models with R symmetry and minimal field content. It also shows the importance of being able to identify the relevant microscopic features that shape the Wilson coefficients at the matching scale, as in Eq. (54), for two reasons. Certainly, these power-counting rules provide a useful short-cut for the $BSM \rightarrow SM EFT$ matching. Most importantly, however, they allow us to identify which are the relevant hypotheses that we are actually testing when we use the EFT to parametrize SM precision tests; all other features of specific BSM models being *de facto* irrelevant. For this reason, we can refer to the assumptions in Eq. (54), as broad, in the sense that they are not specific to a single model.

4.2.2 Composite Higgs Models

Models of Composite Higgs solve the hierarchy problem in two steps. First of all they postulate a compositeness scale $M \sim \text{few} \times \text{TeV} \ll M_{Planck}$ that is naturally generated, e.g., by dimensional transmutation, like the QCD scale. As explained before, above M , $|H|^2$ is an irrelevant operator and hence small. A more physical picture is simply that the Higgs H is a composite particle that exists only in the low-energy EFT: the contribution to m_h^2 from loops of high virtuality is tamed when the particles in the loop probe Higgs compositeness. This would still imply $m_h \sim M$ naturally. As we will see below, EWPT constrain $M \gtrsim 3 \text{ TeV}$, thus creating a *little hierarchy problem*, that is solved if the H is also an approximate Nambu Goldstone boson of a spontaneously broken global symmetry \mathcal{G}/\mathcal{H} . Of course this is *natural*, as it mimics the pions of QCD, which have been observed in nature.

There are many explicit realizations of these models, but the gross picture is common to all of them. A strong sector confines at the scale M and breaks a symmetry $\mathcal{G} \rightarrow \mathcal{H}$, delivering at least 4 massless NGBs at low energy, and nothing else.¹⁴ The \mathcal{G}/\mathcal{H} symmetry is broken explicitly by how this sector couples to the SM: the EW gauge couplings g, g' are associated to the gauging of only a subgroup $SU(2)_L \times U(1) \subset \mathcal{H}$ (therefore breaking \mathcal{H} explicitly), and the SM Yukawas always break \mathcal{G} when the SM fermions are coupled to the strong sector. A pictorial representation is given in Fig. 8.

These ingredients are enough to estimate the low-energy EFT of composite Higgs models:

$$\text{CHM} \sim \left\{ \begin{array}{l} \mathcal{G}/\mathcal{H} \text{ symmetry, broken by } g, g', y \\ \text{New coupling in } H\text{-sector: } g_* \\ \text{Resonances mass scale: } M \end{array} \right\} \Rightarrow \mathcal{L}_{eff}^{\text{CHM}} = \frac{M^4}{g_*^2} L \left(\frac{g_* H}{M}, \frac{D_\mu}{M}, \frac{g F_{\mu\nu}}{M^2}, \frac{\lambda_\psi \psi}{M^{3/2}} \right) \quad (56)$$

where \mathcal{G}/\mathcal{H} -preserving Higgs interactions must be compatible with the goldstone symmetry and be functions of the CCWZ building blocks [72], that at the leading order read the same for all compact cosets,¹⁵

$$d_\mu = \partial_\mu H + \dots, \quad \epsilon_\mu = H \overleftrightarrow{D}_\mu H + \dots \quad (57)$$

More precisely, the Lagrangian for a Strongly Interacting Light Higgs reads [35],

$$\begin{aligned} \mathcal{L}_{\text{SILH}} = & \frac{\tilde{c}_H g_*^2}{M^2} \mathcal{O}_H + \frac{\tilde{c}_T g_*^2}{M^2} \mathcal{O}_T - \frac{\tilde{c}_6 g_*^2}{M^2} \mathcal{O}_6 + \left(\frac{\tilde{c}_y g_*^2}{M^2} \mathcal{O}_{y_\psi} + \text{h.c.} \right) + \frac{\tilde{c}_W}{M^2} \mathcal{O}_W + \frac{\tilde{c}_B}{M^2} \mathcal{O}_B \\ & + \frac{\tilde{c}_{HW}}{M^2} \mathcal{O}_{HW} + \frac{\tilde{c}_{HB}}{M^2} \mathcal{O}_{HB} + \frac{\tilde{c}_{BB}}{M^2} \mathcal{O}_{BB} + \frac{\tilde{c}_g}{M^2} \mathcal{O}_{GG}. \end{aligned} \quad (58)$$

¹⁴Non-minimal models with extended cosets predict more states in the IR, $SO(6)/SO(5)$ for instance includes an additional singlet in the light spectrum, that can in principle play important phenomenological rôles, such as being DM [70, 71].

¹⁵An interesting limiting case is that of $ISO(4)/SO(4)$: here the coset manifold is flat and $\epsilon_\mu = 0$, so that the first strong interactions involving H arise at dimension-8 [30].

This defines the basis the SILH basis previously introduced and explains the normalization of operators $\mathcal{O}_B, \mathcal{O}_{HB} \sim g'$, $\mathcal{O}_W, \mathcal{O}_{HW} \sim g$, while $\mathcal{O}_{BB} \sim g'^2$ and $\mathcal{O}_{GG} \sim g_s^2$, appearing in Table 2. Also, \mathcal{O}_6 shares the same symmetry as the Higgs quartic $\lambda|H|^2$: this is why we expect $\mathcal{O}_6 \sim \lambda$.

Further UV hypotheses can be easily translated into selection rules for SILH Wilson coefficients. For instance, both coset structures $SU(3)/SU(2) \times U(1)$ and $SO(5)/SO(4)$ are minimal, in the sense they only have 4 NGB degrees of freedom that can be identified with H . Yet they differ in that the latter case $\mathcal{H} = SO(4) \simeq SU(2)_L \times SU(2)_R$ contains custodial symmetry, implying that operators that transform non-trivially under $SU(2)_c$ must be suppressed. In the SILH basis we find,

$$\text{Custodial symmetry} \quad \Rightarrow \quad \tilde{c}_T = 0. \quad (59)$$

In many known theories (including weakly coupled 5D theories, and their holographic strongly coupled duals), the dominant effects come from integrating out particles of $\text{spin} \leq 1$ at tree-level, while other effects only arise at loop-level. This hypothesis, called *Minimal Coupling*, implies a further suppression

$$\text{Minimal Coupling} \quad \Rightarrow \quad \tilde{c}_{HW}, \tilde{c}_{HB} \sim \frac{g_*^2}{16\pi^2} \quad \tilde{c}_{BB}, \tilde{c}_{GG} \sim \frac{g_{SM}^2}{16\pi^2} \quad (60)$$

where we have taken into account that, for $\mathcal{O}_{BB}, \mathcal{O}_{GG}$ the couplings to such particles must also break the shift-symmetry and are therefore typically suppressed by a symmetry breaking SM coupling $g_{SM} = g', y_t, \dots$.

It is interesting to compare the power-counting of Eqs. (58,59,60) with the experimental observations from the previous section. From Fig. 6 we see that the best constraints are on c_{BB} and c_{GG} , that are predicted suppressed by several powers of the weak couplings, and on $c_W + c_B$ that are instead expected $\mathcal{O}(1)$, implying

$$M \gtrsim 2.5 \text{ TeV}. \quad (61)$$

Despite these stringent constraints, we notice that many Higgs-only operators are g_* enhanced allowing for sizeable effects in Higgs physics.¹⁶ A careful study of the Higgs properties will tell us more about these types of models.

We have seen the example of a weakly coupled BSM scenario, where loop-effects were suppressed, so that the dynamical field content and interactions (in this case dictated by R -parity) have an important impact on the low-energy EFT (also the minimal coupling assumption Eq. (60) relied on such weakly coupled picture). In other words, the EFT for weakly coupled BSM models is rather model-dependent.

On the other hand, in strongly coupled BSM scenarios, *everything that is not forbidden is compulsory*, as it might be generated by unsuppressed loop effects involving the strong coupling. In these scenarios, our power-counting rules that identify weak and strong couplings and symmetries, are not only useful, but rather necessary, as the underlying theory is incalculable. In these conditions, broad assumptions about the UV are enough to determine the resulting EFT, independently of the microscopic details.

There are many, more or less specific, assumptions that can characterize physics BSM and that can be captured by power-counting rules like those mentioned above. For instance, New physics can couple to the SM bosons only (this is sometimes called *universal*) [73] or only to the top quark [74], that plays the most important rôle in terms of loop effects to the Higgs mass parameter, or only to the transverse components of vector-bosons [30]. It is important to keep in mind that, when testing a specific property of the Higgs boson, we are specifically looking towards one of these specific BSM directions.

¹⁶This is in fact a chicken-egg situation: these models were thought in the LEP era with knowledge of EW constraints.

4.2.3 EFT Validity

Our complete discussion so far was based on the existence of a scale separation

$$E \ll M. \quad (62)$$

An experiment operating at energy E_{exp} , can provide a constraint (or measurement) on the combination

$$\frac{c_i}{M^2} < \frac{\delta_{exp}}{E_{exp}^2} \quad (63)$$

on the effects of an operator \mathcal{O}_i , with precision δ^{exp} . From this we can say that our original assumption Eq. (62) is indeed satisfied if the experimental precision $\delta_{exp} = c_i E_{exp}^2 / M^2 \ll c_i$. Vice versa, we can say that our measurement can be consistently interpreted in the EFT context, only in theories with

$$c_i \gg \delta_{exp}. \quad (64)$$

We have seen in the above examples that the Wilson coefficients c_i can vary enormously depending from the UV structure: they can be enhanced by a strong coupling or reduced by loop factors, and even vanish. Therefore, it is fair to say that:

There is no model-independent discussion about the EFT validity.

In this context, the power-counting arguments outlined above become particularly useful, because they allow us to identify the broadest features that can make a Wilson coefficient large or small, so that the question of whether the EFT provides a consistent interpretation of our measurement, can be answered in the most generic (less model-dependent) terms.

At the LHC, some experiments (e.g $2 \rightarrow 2$ scattering processes) are testing a large range of energies, and the question of whether Eq. (62) is satisfied becomes more subtle, as E_{exp} is in principle unknown. This can be obviated in a number of ways. The most systematic is to perform an additional cut $\sqrt{s} < M_{cut}$ at the level of the analysis on the center-of mass energy of the system.¹⁷ This procedure provides the necessary information on E_{exp} that is now bounded from above by M_{cut} and allows to discuss the EFT validity [57, 77].

In these high- E processes, EFT effects have the common property that they *grow* with some power of the energy, relatively to the SM. On the other hand, the precision of measurements of deviations from the SM, *decreases* with energy, principally due to the rapid fall-off in number of events at high-energy (since parton distribution functions decrease exponentially fast). In some instances this implies that the constraint is dominated by an energy region with little sensitivity, implying that only departures from the SM that exceed the SM itself can be tested,

$$\delta_{exp} = \frac{\delta\sigma}{\sigma_{SM}} \gtrsim 1. \quad (65)$$

This is often considered a limitation to test EFTs at hadronic colliders in high-energy processes, as it implies from Eq. (64) that such experiments can not be interpreted in theories with $c_i \lesssim 1$. This corresponds to weakly coupled theories that fill a special place in BSM model-building, as they are calculable and well under control. In this sense $\delta_{exp} \lesssim 1$ can be thought as a target for experiments, that opens the door to interpret their results in a wider and well-motivated context [77]. Yet this doesn't mean that high-energy low-resolution experiments that test EFT are necessarily inconsistent: they provide useful information about strongly coupled theories, where, e.g. $c_i \sim g_*^2 \gg 1$.

¹⁷In some systems, this might not be known, but a consistent analysis can still be performed along the lines of Refs. [75, 76].

5 Conclusions

I like Higgs physics because it is at the frontier of our exploration of the universe at small distances. As such, it can potentially hide information about structure beyond the SM. The hierarchy problem suggests the existence of such structure, that would imply modification of the Higgs properties. These can be studied in the formalism of EFTs and their power-counting, a dictionary that allows to recognize the relevant ingredients in microscopic theories and read their effects at low-energy.

EFTs can be thought as a structured and well motivated context to perform SM precision tests, the result of which gives us quantitative information on how well we know the SM, in terms of how strong are the constraints on certain classes of theories beyond the SM.

At the same time, EFTs, accompanied with their BSM perspective, provide an important search tool that extends the reach of the LHC beyond its direct reach. This is particularly true for strongly coupled BSM scenarios, that might induce large effects in low-energy processes, despite the scale of new physics being beyond kinematic reach.

References

- [1] S. Weinberg, Phys. Rev. Lett. **19** (1967) 1264.
- [2] P. W. Higgs, Phys. Rev. Lett. **13** (1964) 508.
- [3] F. Englert and R. Brout, Phys. Rev. Lett. **13** (1964) 321.
- [4] G. Aad *et al.* [ATLAS Collaboration], Phys. Lett. B **716** (2012) 1 [arXiv:1207.7214 [hep-ex]].
- [5] S. Chatrchyan *et al.* [CMS Collaboration], Phys. Lett. B **716** (2012) 30 [arXiv:1207.7235 [hep-ex]].
- [6] G. Aad *et al.* [ATLAS and CMS Collaborations], Phys. Rev. Lett. **114** (2015) 191803 [arXiv:1503.07589 [hep-ex]].
- [7] G. Degrossi, S. Di Vita, J. Elias-Miro, J. R. Espinosa, G. F. Giudice, G. Isidori and A. Strumia, JHEP **1208** (2012) 098 [arXiv:1205.6497 [hep-ph]].
- [8] R. Contino, “The Higgs as a Composite Nambu-Goldstone Boson,” arXiv:1005.4269 [hep-ph].
- [9] G. Panico and A. Wulzer, “The Composite Nambu-Goldstone Higgs,” Lect. Notes Phys. **913** (2016) pp.1 [arXiv:1506.01961 [hep-ph]].
- [10] A. Pomarol, “Higgs Physics,” arXiv:1412.4410 [hep-ph].
- [11] A. Djouadi, “The Anatomy of Electro-Weak Symmetry Breaking. I: the Higgs Boson in the Standard Model,” Phys. Rept. **457** (2008) 1 [hep-ph/0503172].
- [12] S. Weinberg, “The Quantum theory of fields. Vol. 1: Foundations,” Cambridge Press.
- [13] A. Alboteanu, W. Kilian and J. Reuter, JHEP **0811** (2008) 010 [arXiv:0806.4145 [hep-ph]].
- [14] S. Weinberg, Phys. Rev. D **13** (1976) 974.
- [15] L. Susskind, Phys. Rev. D **20** (1979) 2619.
- [16] J. Elias-Miro, J. R. Espinosa, E. Masso and A. Pomarol, “Higgs Windows to New Physics Through D=6 Operators: Constraints and One-Loop Anomalous Dimensions,” JHEP **1311** (2013) 066 [arXiv:1308.1879 [hep-ph]].
- [17] S. Schael *et al.* [ALEPH and DELPHI and L3 and OPAL and SLD and LEP Electroweak Working Group and SLD Electroweak Group and SLD Heavy Flavour Group Collaborations], “Precision Electroweak Measurements on the Z Resonance,” Phys. Rept. **427** (2006) 257 [hep-ex/0509008].
- [18] S. Heinemeyer *et al.* [LHC Higgs Cross Section Working Group], arXiv:1307.1347 [hep-ph].
- [19] LEP Electroweak Working Group, <http://lepewwg.web.cern.ch>.
- [20] G. Aad *et al.* [ATLAS and CMS Collaborations], JHEP **1608** (2016) 045 [arXiv:1606.02266 [hep-ex]].
- [21] K. G. Wilson, Phys. Rev. D **3** (1971) 1818.

- [22] R. Rattazzi, V. S. Rychkov, E. Tonni and A. Vichi, “Bounding Scalar Operator Dimensions in 4D CFT,” JHEP **0812** (2008) 031 [arXiv:0807.0004 [hep-th]].
- [23] D. B. Kaplan, H. Georgi, Phys. Lett. **B136** (1984) 183; D. B. Kaplan, H. Georgi, S. Dimopoulos, Phys. Lett. **B136** (1984) 187; H. Georgi, D. B. Kaplan, P. Galison, Phys. Lett. **B143** (1984) 152; T. Banks, Nucl. Phys. **B243** (1984) 125; H. Georgi, D. B. Kaplan, Phys. Lett. **B145** (1984) 216; M. J. Dugan, H. Georgi, D. B. Kaplan, Nucl. Phys. **B254** (1985) 299.
- [24] R. Barbieri and G. F. Giudice, Nucl. Phys. B **306** (1988) 63.
- [25] P. W. Graham, D. E. Kaplan and S. Rajendran, “Cosmological Relaxation of the Electroweak Scale,” Phys. Rev. Lett. **115** (2015) no.22, 221801 [arXiv:1504.07551 [hep-ph]].
- [26] A. Arvanitaki, S. Dimopoulos, V. Gorbenko, J. Huang and K. Van Tilburg, arXiv:1609.06320 [hep-ph].
- [27] J. Galloway, M. A. Luty, Y. Tsai and Y. Zhao, Phys. Rev. D **89** (2014) no.7, 075003 [arXiv:1306.6354 [hep-ph]].
- [28] R. Alonso, M. B. Gavela, L. Merlo, S. Rigolin and J. Yepes, “The Effective Chiral Lagrangian for a Light Dynamical “Higgs Particle”,” Phys. Lett. B **722** (2013) 330 Erratum: [Phys. Lett. B **726** (2013) 926] [arXiv:1212.3305 [hep-ph]].
- [29] G. Buchalla, O. Cat and C. Krause, Nucl. Phys. B **880** (2014) 552 Erratum: [Nucl. Phys. B **913** (2016) 475] [arXiv:1307.5017 [hep-ph]].
- [30] D. Liu, A. Pomarol, R. Rattazzi and F. Riva, “Patterns of Strong Coupling for Lhc Searches,” JHEP **1611** (2016) 141 [arXiv:1603.03064 [hep-ph]].
- [31] M. Gonzalez-Alonso, A. Greljo, G. Isidori and D. Marzocca, “Pseudo-Observables in Higgs Decays,” Eur. Phys. J. C **75** (2015) 3, 128 [arXiv:1412.6038 [hep-ph]].
- [32] G. Passarino, C. Sturm and S. Uccirati, Nucl. Phys. B **834** (2010) 77 [arXiv:1001.3360 [hep-ph]].
- [33] D. de Florian *et al.* [LHC Higgs Cross Section Working Group], arXiv:1610.07922 [hep-ph].
- [34] A. Efrati, A. Falkowski and Y. Soreq, JHEP **1507** (2015) 018 [arXiv:1503.07872 [hep-ph]].
- [35] G. F. Giudice, C. Grojean, A. Pomarol and R. Rattazzi, “The Strongly-Interacting Light Higgs,” JHEP **0706** (2007) 045 [hep-ph/0703164].
- [36] R. Contino, M. Ghezzi, C. Grojean, M. Muhlleitner and M. Spira, “Effective Lagrangian for a Light Higgs-Like Scalar,” JHEP **1307** (2013) 035 [arXiv:1303.3876 [hep-ph]].
- [37] B. Grzadkowski, M. Iskrzynski, M. Misiak and J. Rosiek, “Dimension-Six Terms in the Standard Model Lagrangian,” JHEP **1010** (2010) 085 [arXiv:1008.4884 [hep-ph]].
- [38] R. S. Gupta, A. Pomarol and F. Riva, “Bsm Primary Effects,” Phys. Rev. D **91** (2015) no.3, 035001 [arXiv:1405.0181 [hep-ph]].
- [39] E. Masso, “An Effective Guide to Beyond the Standard Model Physics,” JHEP **1410** (2014) 128 [arXiv:1406.6376 [hep-ph]].
- [40] G. Aad *et al.* [ATLAS Collaboration], Phys. Lett. B **732** (2014) 8 [arXiv:1402.3051 [hep-ex]].
- [41] S. Di Vita, C. Grojean, G. Panico, M. Riembau and T. Vantalon, “A Global View on the Higgs Self-Coupling,” arXiv:1704.01953 [hep-ph].
- [42] A. Falkowski, F. Riva and A. Urbano, “Higgs at Last,” JHEP **1311** (2013) 111 [arXiv:1303.1812 [hep-ph]].
- [43] J. Ellis, V. Sanz and T. You, “Complete Higgs Sector Constraints on Dimension-6 Operators,” JHEP **1407** (2014) 036 [arXiv:1404.3667 [hep-ph]].
- [44] A. Butter, O. J. P. boli, J. Gonzalez-Fraile, M. C. Gonzalez-Garcia, T. Plehn and M. Rauch, “The Gauge-Higgs Legacy of the Lhc Run I,” JHEP **1607** (2016) 152 [arXiv:1604.03105 [hep-ph]].
- [45] B. Dumont, S. Fichet and G. von Gersdorff, “A Bayesian View of the Higgs Sector with Higher Dimensional Operators,” JHEP **1307** (2013) 065 [arXiv:1304.3369 [hep-ph]].

- [46] J. de Blas, M. Ciuchini, E. Franco, D. Ghosh, S. Mishima, M. Pierini, L. Reina and L. Silvestrini, Nucl. Part. Phys. Proc. **273-275** (2016) 834 [arXiv:1410.4204 [hep-ph]].
- [47] T. Corbett, O. J. P. Eboli, J. Gonzalez-Fraile and M. C. Gonzalez-Garcia, Phys. Rev. D **87** (2013) 015022 [arXiv:1211.4580 [hep-ph]].
- [48] J. de Blas, M. Ciuchini, E. Franco, S. Mishima, M. Pierini, L. Reina and L. Silvestrini, JHEP **1612** (2016) 135 [arXiv:1608.01509 [hep-ph]].
- [49] H. Belusca-Maito, arXiv:1404.5343 [hep-ph].
- [50] M. E. Peskin and T. Takeuchi, “A New Constraint on a Strongly Interacting Higgs Sector,” Phys. Rev. Lett. **65** (1990) 964.
- [51] R. Barbieri, A. Pomarol, R. Rattazzi and A. Strumia, “Electroweak Symmetry Breaking After Lep-1 and Lep-2,” Nucl. Phys. B **703** (2004) 127 [hep-ph/0405040].
- [52] A. Pomarol and F. Riva, “Towards the Ultimate Sm Fit to Close in on Higgs Physics,” JHEP **1401** (2014) 151 [arXiv:1308.2803 [hep-ph]].
- [53] A. Falkowski and F. Riva, “Model-Independent Precision Constraints on Dimension-6 Operators,” JHEP **1502** (2015) 039 [arXiv:1411.0669 [hep-ph]].
- [54] J. Ellis, V. Sanz and T. You, “The Effective Standard Model After Lhc Run I,” JHEP **1503** (2015) 157 [arXiv:1410.7703 [hep-ph]].
- [55] G. Isidori, A. V. Manohar and M. Trott, Phys. Lett. B **728** (2014) 131 [arXiv:1305.0663 [hep-ph]].
- [56] A. Biekötter, A. Knochel, M. Krmer, D. Liu and F. Riva, “Vices and Virtues of Higgs Effective Field Theories at Large Energy,” Phys. Rev. D **91** (2015) 055029 [arXiv:1406.7320 [hep-ph]].
- [57] R. Contino, A. Falkowski, F. Goertz, C. Grojean and F. Riva, “On the Validity of the Effective Field Theory Approach to Sm Precision Tests,” JHEP **1607** (2016) 144 [arXiv:1604.06444 [hep-ph]].
- [58] S. Schael *et al.* [ALEPH and DELPHI and L3 and OPAL and LEP Electroweak Collaborations], “Electroweak Measurements in Electron-Positron Collisions at W-Boson-Pair Energies at Lep,” Phys. Rept. **532** (2013) 119 [arXiv:1302.3415 [hep-ex]].
- [59] M. Gonzalez-Alonso, A. Greljo, G. Isidori and D. Marzocca, “Electroweak Bounds on Higgs Pseudo-Observables and $h \rightarrow 4\ell$ Decays,” Eur. Phys. J. C **75** (2015) 341 [arXiv:1504.04018 [hep-ph]].
- [60] A. Manohar and H. Georgi, Nucl. Phys. B **234** (1984) 189.
- [61] M. B. Einhorn and J. Wudka, “The Bases of Effective Field Theories,” Nucl. Phys. B **876** (2013) 556 [arXiv:1307.0478 [hep-ph]].
- [62] J. Elias-Miro, J. R. Espinosa, E. Masso and A. Pomarol, JHEP **1308** (2013) 033 [arXiv:1302.5661 [hep-ph]].
- [63] E. E. Jenkins, A. V. Manohar and M. Trott, JHEP **1310** (2013) 087 [arXiv:1308.2627 [hep-ph]].
- [64] E. E. Jenkins, A. V. Manohar and M. Trott, JHEP **1401** (2014) 035 [arXiv:1310.4838 [hep-ph]].
- [65] R. Alonso, E. E. Jenkins, A. V. Manohar and M. Trott, JHEP **1404** (2014) 159 [arXiv:1312.2014 [hep-ph]].
- [66] J. Elias-Miro, C. Grojean, R. S. Gupta and D. Marzocca, JHEP **1405** (2014) 019 [arXiv:1312.2928 [hep-ph]].
- [67] F. Riva, C. Biggio and A. Pomarol, “Is the 125 GeV Higgs the Superpartner of a Neutrino?,” JHEP **1302** (2013) 081 [arXiv:1211.4526 [hep-ph]].
- [68] R. S. Gupta, M. Montull and F. Riva, “SUSY Faces Its Higgs Couplings,” JHEP **1304** (2013) 132 [arXiv:1212.5240 [hep-ph]].
- [69] G. D’Ambrosio, G. F. Giudice, G. Isidori and A. Strumia, Nucl. Phys. B **645** (2002) 155 [hep-ph/0207036].

- [70] S. Bruggisser, F. Riva and A. Urbano, “Strongly Interacting Light Dark Matter,” arXiv:1607.02474 [hep-ph]. “The Last Gasp of Dark Matter Effective Theory,” JHEP **1611** (2016) 069 [arXiv:1607.02475 [hep-ph]].
- [71] M. Frigerio, A. Pomarol, F. Riva and A. Urbano, “Composite Scalar Dark Matter,” JHEP **1207** (2012) 015 [arXiv:1204.2808 [hep-ph]].
- [72] S. R. Coleman, J. Wess and B. Zumino, Phys. Rev. **177** (1969) 2239; C. G. Callan, Jr., S. R. Coleman, J. Wess and B. Zumino, Phys. Rev. **177** (1969) 2247.
- [73] J. D. Wells and Z. Zhang, JHEP **1606** (2016) 122 [arXiv:1512.03056 [hep-ph]].
- [74] A. Pomarol and J. Serra, “Top Quark Compositeness: Feasibility and Implications,” Phys. Rev. D **78** (2008) 074026 [arXiv:0806.3247 [hep-ph]].
- [75] D. Racco, A. Wulzer and F. Zwirner, “Robust Collider Limits on Heavy-Mediator Dark Matter,” JHEP **1505** (2015) 009 [arXiv:1502.04701 [hep-ph]].
- [76] F. Pobbe, A. Wulzer and M. Zanetti, “Setting Limits on Effective Field Theories: the Case of Dark Matter,” arXiv:1704.00736 [hep-ph].
- [77] M. Farina, G. Panico, D. Pappadopulo, J. T. Ruderman, R. Torre and A. Wulzer, “Energy Helps Accuracy: Electroweak Precision Tests at Hadron Colliders,” arXiv:1609.08157 [hep-ph].

Three Lectures of Flavor and CP violation within and Beyond the Standard Model

S. Gori

Department of Physics, University of Cincinnati, Cincinnati, Ohio, USA

Abstract

In these lectures I discuss 1) flavor physics within the Standard Model, 2) effective field theories and Minimal Flavor Violation, 3) flavor physics in theories beyond the Standard Model and “high energy” flavor transitions of the top quark and of the Higgs boson. As a bi-product, I present the most updated constraints from the measurements of $B_s \rightarrow \mu^+ \mu^-$, as well as the most recent development in the LHC searches for top flavor changing couplings.

Keywords

Lectures; heavy flavor; CP violation; flavor changing couplings.

1 Introduction

My plan for these lectures is to introduce you to the basics of flavor physics and CP violation. These three lectures that I gave at the 2015 European School of High-Energy Physics are not comprehensive, but should serve to give an overview of the interesting open questions in flavor physics and of the huge experimental program measuring flavor and CP violating transitions. Hopefully they will spark your curiosity to learn more about flavor physics. There are many books and reviews about flavor physics for those of you interested [1–6].

Flavor physics is the study of different generations, or “flavors”, of quarks and leptons, their spectrum and their transitions. There are six different types of quarks: up (u), down (d), strange (s), charm (c), bottom (b) and top (t) and three different type of charged leptons: electron, muon and tau. In these lectures, I will concentrate on the discussion of quarks and the mesons that contain them. A recent review about lepton flavor violation can be found in [7].

The Large Hadron Collider (LHC) discovery of the Higgs boson in 2012 [8,9] and the subsequent early measurements of its couplings to the Standard Model (SM) gauge bosons and third generation quarks and leptons have been a remarkably successful confirmation of the SM and of its mechanism of electroweak symmetry breaking (EWSB). The LHC has been able to demonstrate that the Higgs does not couple universally with (some) quarks and leptons already with Run I data [10]. In fact, we know that in the SM $m_t \gg m_c \gg m_u$ and $m_b \gg m_s \gg m_d$, and that the same hierarchies hold for the Higgs Yukawa couplings with quarks and leptons. Our lack of understanding of why nature has exactly three generations of quarks and leptons and why their properties (masses and mixing angles) are described by such hierarchical values is the so called “Standard Model flavor puzzle”. In the limit of unbroken electroweak (EW) symmetry none of the basic constituent of matter would have a non-zero mass. The SM flavor puzzle is, therefore, intimately related to the other big open question in particle physics, i.e. which is the exact mechanism behind EWSB.

Once the SM quark and lepton masses, as well as quark mixing angles (3 plus a phase) have been fixed, the SM is a highly predictive theory for flavor transitions. Particularly, any flavor transition has to involve the exchange of at least a W boson and therefore flavor changing neutral transitions can only arise (at least) at the loop-level. In the last few years, tremendous progress has been reached in testing the mechanism of quark flavor mixing by several experiments (LHCb and B-factories (Belle and Babar) as well as the high energy experiments ATLAS and CMS), finding good agreement with the SM expectations. At the same time, there are a few flavor measurements that could be interpreted as

tantalizing hints for deviations if compared to the SM predictions. Particularly, lately there have been a lot of attention on the anomalies in angular observables in the decay $B_d \rightarrow K^* \mu \mu$ (involving a $b \rightarrow s$ flavor transition), as observed by the LHCb collaboration [11–13], as well as on the observables testing lepton flavor universality, $\text{BR}(B \rightarrow K \mu \mu)/\text{BR}(B \rightarrow K e e)$, as observed at LHCb [14] and on the rare decays $B \rightarrow D \tau \nu_\tau$ and $B \rightarrow D^* \tau \nu_\tau$ by Belle, Babar, and LHCb [15–19].

The coming years will be exciting since several low (and high) energy flavor experiments will collect a lot more data. In particular [6],

$$\frac{\text{LHCb upgrade}}{\text{LHCb, } 1\text{fb}^{-1}} \sim \frac{\text{Belle II data}}{\text{Belle data}} \sim 50, \quad \frac{\text{HL} - \text{LHC}}{\text{LHC, ICHEP 2016}} \sim 200 \quad (1)$$

in the time scale of ~ 20 years for the LHCb upgrade and for the High-Luminosity LHC and of ~ 10 years for Belle II.

Present and future flavor measurements will be able to probe, and eventually indirectly discover, New Physics (NP). Observing new sources of flavor mixing is, in fact, a natural expectation for any extension of the SM with new degrees of freedom not far from the TeV scale. While direct searches of new particles at high energies provide information on the mass spectrum of the possible new degrees of freedom, the indirect information from low energy flavor observables translates into unique constraints on their couplings.

The lectures are organized as follows: In Sec. 2, I will introduce the main ingredients of flavor physics and CP violation in the SM. I will both review the theory aspects and the experimental determination of the several SM flavor parameters. My second lecture, in Sec. 3, will discuss the role of flavor physics in testing effective field theories beyond the SM (BSM), where new degrees of freedom are heavy if compared to the EW scale, and they can be integrated out, to generate higher dimensional operators to be added to the SM Lagrangian. Sec. 4 is dedicated to the discussion of the flavor properties of specific BSM theories, i.e. models with multi-Higgs doublets and Supersymmetric models. I will also discuss the interplay between low energy flavor measurements and high energy flavor measurements involving top and Higgs flavor transitions, as it can be measured at ATLAS and CMS. Finally, I will conclude in Sec. 5.

2 Flavor physics in the Standard Model

2.1 The flavor sector of the Standard Model

The Standard Model (SM) Lagrangian can be divided in three main parts: the gauge, the Higgs, and the flavor sector. The first two parts are highly symmetric

$$\begin{aligned} \mathcal{L}_{\text{SM}}^{\text{gauge}} + \mathcal{L}_{\text{SM}}^{\text{Higgs}} &= i \sum_i \sum_\psi \bar{\psi}^i \not{D} \psi^i - \frac{1}{4} \sum_a G_{\mu\nu}^a G_{\mu\nu}^a - \frac{1}{4} \sum_a W_{\mu\nu}^a W_{\mu\nu}^a + \\ &\quad - \frac{1}{4} B_{\mu\nu} B_{\mu\nu} + |D_\mu \phi|^2 + (\mu^2 |\phi|^2 - \lambda |\phi|^4), \end{aligned} \quad (2)$$

and fully determined by a small set of free parameters: the three gauge couplings, g_3, g_2, g_1 corresponding to the SM gauge groups $SU(3) \times SU(2) \times U(1)_Y$, the Higgs (ϕ) mass, m_h , and the Higgs vacuum expectation value (VEV), v (or, equivalently, the Higgs mass term, μ , and the quartic coupling, λ). In this expression G, W , and B are the SM $SU(3), SU(2)$, and $U(1)_Y$ gauge fields, respectively, and we have defined the quark and lepton field content, ψ^i , as

$$\begin{aligned} \psi^i &\equiv Q_L^i, L_L^i, u_R^i, d_R^i, e_R^i, \quad \text{with} \\ Q_L^i &= (3, 2, 1/6), L_L^i = (1, 2, -1/2), u_R^i = (3, 1, 2/3), d_R^i = (3, 1, -1/3), e_R^i = (1, 1, -1), \end{aligned} \quad (3)$$

where $i = 1, 2, 3$ is the flavor (or generation) index and the three numbers refer to the representation under the SM gauge group.

The Lagrangian in (2) possesses a large flavor symmetry that can be decomposed as

$$\mathcal{G}_{\text{flavor}} = SU(3)^5 \times U(1)^5 = SU(3)_q^3 \times SU(3)_\ell^2 \times U(1)_B \times U(1)_L \times U(1)_Y \times U(1)_{\text{PQ}} \times U(1)_E, \quad (4)$$

where three $U(1)$ symmetries can be identified with baryon and lepton numbers, and hypercharge, the latter of which is broken spontaneously by the Higgs field. The two remaining $U(1)$ groups can be identified with the Peccei-Quinn symmetry [20] and with a global rotation of a single $SU(2)$ singlet (e_R in the case of Eq. (4)). The flavor sector of the SM Lagrangian breaks the $SU(3)^5$ symmetry through the Yukawa interactions

$$\mathcal{L}_{\text{yuk}} = -Y_d^{ij} \bar{Q}_L^i \phi D_R^j - Y_u^{ij} \bar{Q}_L^i \tilde{\phi} U_R^j - Y_e^{ij} \bar{L}_L^i \phi e_R^j + \text{h.c.}, \quad (5)$$

where ϕ is the Higgs field ($\phi = (1, 2, 1/2)$), $\tilde{\phi}$ is its conjugate representation $\tilde{\phi} = i\tau_2 \phi^\dagger$ and $Y_{d,u,e}$ are the three Yukawa couplings.

The diagonalization of each Yukawa coupling requires a bi-unitary transformation. Particularly, in the absence of right-handed (RH) neutrinos as in Eq. (3), the lepton sector Yukawa can be fully diagonalized by the transformation $U_{eL} Y_e U_{eR}^\dagger = \text{diag}(y_e^1, y_e^2, y_e^3) = \sqrt{2} \text{diag}(m_e, m_\mu, m_\tau)/v$. In the quark sector, it is not possible to simultaneously diagonalize the two Yukawa matrices Y_u and Y_d without breaking the $SU(2)$ gauge invariance. If, for example, we choose the basis in which the up Yukawa is diagonal, then

$$Y_u = \text{diag}(y_u^1, y_u^2, y_u^3) = \frac{\sqrt{2}}{v} (m_u, m_c, m_t), \quad Y_d = V \cdot \text{diag}(y_d^1, y_d^2, y_d^3) = \frac{\sqrt{2}}{v} V \cdot (m_d, m_s, m_b), \quad (6)$$

where we have defined the Cabibbo-Kobayashi-Maskawa (CKM) matrix as $V = U_{uL} U_{dL}^\dagger$.

However, in the SM the $SU(2)$ gauge symmetry is broken spontaneously by the Higgs field and therefore, we can equivalently rotate both left-handed (LH) up and down quarks independently, diagonalizing simultaneously up and down quark masses. By performing these transformations, the CKM dependence moves into the couplings of up and down quarks with the W boson. In particular, the charged-current part of the quark covariant derivative in (2) can be rewritten in the mass eigenstate basis as

$$-\frac{g}{2} \bar{Q}_L^i \gamma^\mu W_\mu^a \tau^a Q_L^i \xrightarrow{\text{mass-basis}} -\frac{g}{\sqrt{2}} (\bar{u}_L \quad \bar{c}_L \quad \bar{t}_L) \gamma^\mu W_\mu^+ V \begin{pmatrix} d_L \\ s_L \\ b_L \end{pmatrix}. \quad (7)$$

This equation shows that the appearance of W boson flavor changing couplings. This is the only flavor changing interaction in the SM. **Exercise:** prove that the neutral interactions of the photon, the Z boson, the gluons and the Higgs boson are flavor diagonal in the quark mass eigenbasis. We can therefore conclude that, in the SM,

- (a) the only interactions mediating flavor changing transitions are the charged interactions;
- (b) there are no tree-level flavor changing neutral interactions.

In spite of point (a), it must be stressed that V , the CKM matrix, originates from the Yukawa sector: in absence of Yukawa couplings, $V_{ij} = \delta_{ij}$ and therefore we have no flavor changing transitions.

We can now count the number of free parameters of the SM Lagrangian. As opposed to the five free parameters of the gauge and Higgs sector (g_1, g_2, g_3, v, m_h), the flavor part of the Lagrangian has a much larger number of free parameters. Particularly, the CKM matrix is defined by 4 free parameters: three real angles and one complex CP-violating phase. **Exercise:** Using the unitarity relations discussed

in the next subsection, demonstrate that the CKM matrix is fully described by 4 free parameters. This phase is the only source of CP violation in the SM, beyond the QCD phase, θ_{QCD} . The full set of parameters controlling the breaking of the quark flavor symmetry is composed by six quark masses and four parameters of CKM matrix (to be added to the three charged lepton masses, as obtained from the Yukawa coupling Y_e).

Many parameterizations of the CKM matrix have been proposed in the literature. In these lectures, we will focus on the standard parametrization [21] and on the Wolfenstein parametrization [22]. The CKM matrix is unitary and can be described by three rotation angles $\theta_{12}, \theta_{13}, \theta_{23}$ and a complex phase δ . In all generality, we can write the standard parametrization as product of three rotations with respect to three orthogonal axes

$$\begin{aligned} V &= \begin{pmatrix} V_{ud} & V_{us} & V_{ub} \\ V_{cd} & V_{cs} & V_{cb} \\ V_{td} & V_{ts} & V_{tb} \end{pmatrix} = \begin{pmatrix} 1 & 0 & 0 \\ 0 & c_{23} & s_{23} \\ 0 & -s_{23} & c_{23} \end{pmatrix} \begin{pmatrix} c_{13} & 0 & s_{13}e^{-i\delta} \\ 0 & 1 & 0 \\ -s_{13}e^{i\delta} & 0 & c_{13} \end{pmatrix} \begin{pmatrix} c_{12} & s_{12} & 0 \\ -s_{12} & c_{12} & 0 \\ 0 & 0 & 1 \end{pmatrix} = \\ &= \begin{pmatrix} c_{12}c_{13} & s_{12}c_{13} & s_{13}e^{-i\delta} \\ -s_{12}c_{23} - c_{12}s_{23}s_{13}e^{i\delta} & c_{12}c_{23} - s_{12}s_{23}s_{13}e^{i\delta} & s_{23}c_{13} \\ s_{12}s_{23} - c_{12}c_{23}s_{13}e^{i\delta} & -s_{23}c_{12} - s_{12}c_{23}s_{13}e^{i\delta} & c_{23}c_{13} \end{pmatrix}, \end{aligned} \quad (8)$$

where we have denoted $s_{ij} \equiv \sin \theta_{ij}$ and $c_{ij} \equiv \cos \theta_{ij}$, $i, j = 1, 2, 3$.

From measurements, we know that s_{12} , s_{13} and s_{23} are small numbers, therefore we can approximately write the CKM matrix in terms of an expansion in $|V_{us}|$

$$V = \begin{pmatrix} 1 - \frac{\lambda^2}{2} & \lambda & A\lambda^3(\rho - i\eta) \\ -\lambda & 1 - \frac{\lambda^2}{2} & A\lambda^2 \\ A\lambda^3(1 - \rho - i\eta) & -A\lambda^2 & 1 \end{pmatrix} + \mathcal{O}(\lambda^4), \quad (9)$$

with $\lambda \sim 0.23$ the Cabibbo angle and the parameters A, ρ, η of the order 1, defined as

$$\lambda \equiv s_{12}, \quad A\lambda^2 \equiv s_{23}, \quad A\lambda^3(\rho - i\eta) \equiv s_{13}e^{-i\delta}. \quad (10)$$

This is the Wolfenstein parametrization, that shows clearly the sizable hierarchies in between the several elements of the CKM matrix, that, at the zeroth order in λ is given by the identity matrix.

2.2 Tests of the CKM matrix

The unitarity of the CKM matrix implies the following relations between its elements:

$$\text{Phase independent : } \sum_{k=1,2,3} |V_{ik}|^2 = 1, \quad \text{Phase dependent : } \sum_{k=1,2,3} V_{ki}V_{kj}^* = 0, \quad j \neq i. \quad (11)$$

These relations are a distinctive feature of the SM, where the CKM matrix is the only source of quark flavor transitions. Each of the phase dependent relations, for fixed i and j , can be visualized as a triangle in the complex plane, where each side represents the complex number $V_{ki}V_{kj}^*$ for the three different $k = u, c, t$. The fact that the three vectors add up to form a closed triangle is the manifestation of the unitarity relation. Among the six phase dependent relations, the most stringent test is provided by the $i = 1$ and $j = 3$ case, since, in this case, the corresponding unitarity triangle has all sides of the same order in λ . Particularly, the unitarity relation can be written as

$$\frac{V_{ud}V_{ub}^*}{V_{cd}V_{cb}^*} + \frac{V_{td}V_{tb}^*}{V_{cd}V_{cb}^*} + 1 = 0 \quad \leftrightarrow \quad (\bar{\rho} + i\bar{\eta}) + (1 - \bar{\rho} - i\bar{\eta}) + 1 = 0, \quad (12)$$

where this defines the parameters $\bar{\rho}$ and $\bar{\eta}$, which are approximately given by

$$\bar{\rho} \simeq \rho \left(1 - \frac{\lambda^2}{2}\right), \quad \bar{\eta} \simeq \eta \left(1 - \frac{\lambda^2}{2}\right). \quad (13)$$

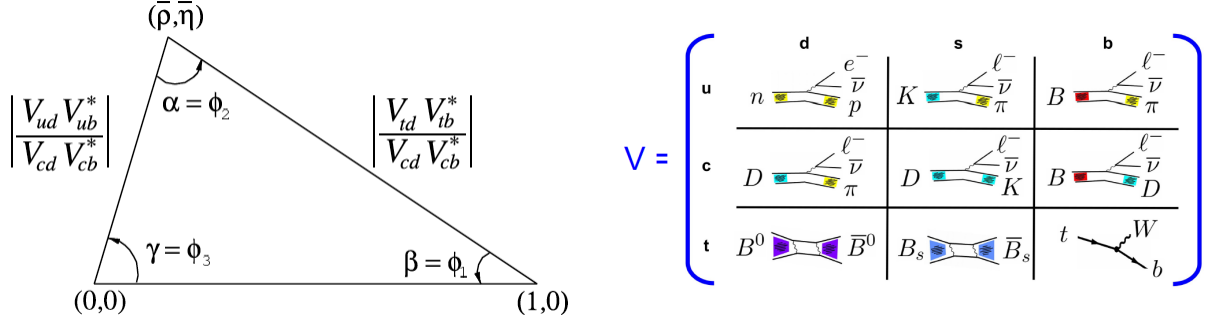


Fig. 1: **Left:** The unitarity triangle. **Right:** List of the most sensitive observables used to determine the several elements of the CKM matrix.

This unitarity triangle is represented on the left panel of Fig. 1. We have defined the angles of this triangle

$$\alpha \equiv \arg\left(-\frac{V_{td}V_{tb}^*}{V_{ud}V_{ub}^*}\right), \quad \beta \equiv \arg\left(-\frac{V_{cd}V_{cb}^*}{V_{td}V_{tb}^*}\right), \quad \gamma \equiv \arg\left(-\frac{V_{ud}V_{ub}^*}{V_{cd}V_{cb}^*}\right), \quad (14)$$

and also we can define one additional angle β_s as

$$\beta_s \equiv \arg\left(-\frac{V_{ts}V_{tb}^*}{V_{cs}V_{cb}^*}\right). \quad (15)$$

There are many measurements performed at different experiments (Babar, Belle, LHCb) that over-constrain the values of the elements of the CKM matrix. In the right panel of Fig. 1, we report a summary of the most stringent experimental constraints on the several CKM elements. Every element but V_{td} and V_{ts} are determined directly by tree-level processes. In particular

- V_{ud} is extracted through the measurement of a set of superallowed nuclear β decay;
- V_{us} , V_{ub} and V_{cs} are measured through the rates of inclusive and exclusive charmless semi-leptonic K , B and D decays to $\pi\ell\bar{\nu}$, respectively;
- V_{cb} is extracted through the measurement of the $B \rightarrow D\ell\bar{\nu}$ decay;
- V_{cs} and V_{tb} can be extracted from the measurements of $D \rightarrow K\ell\bar{\nu}$ and top decay to Wb , respectively. However, the corresponding constraint is not competitive with the constraint coming from the global fit of all the other observables.
- The one loop mass splittings in the neutral B and B_s systems are sensitive to the values of V_{td} and V_{ts} , respectively. Additional determinations include loop-mediated rare K and B decays.

V_{ud} is the best determined element of the CKM matrix with an error at the level of 0.02%. V_{us} , V_{cs} , and V_{cb} are also well determined with the corresponding observables with errors ranging in (0.1 – 2)%. The observables $B \rightarrow \pi\ell\bar{\nu}$ and $D \rightarrow \pi\ell\bar{\nu}$ determining V_{ub} and V_{cd} are, instead, the least accurately measured with an error at around $\sim 10\%$.

The consistency of different constraints on the CKM unitarity triangle is a powerful test of the SM in describing flavor changing phenomena. Fig. 2 shows the huge improvement in the determination of the unitarity triangle in the past 20 years: the left panel shows the present status and the right panel represents the situation back in 1995. In this fit, additional constraints beyond the ones discussed above are imposed. In particular, constraints on the CKM unitarity triangle come from the CP violation in $K \rightarrow \pi\pi$, the rates of the various $B \rightarrow \pi\pi, \rho\pi, \rho\rho$ decays (that depend on the phase α), the rates of various $B \rightarrow DK$ decays (that depends on the phase γ), the CP asymmetry in the decay $B \rightarrow \psi K_s$ (that

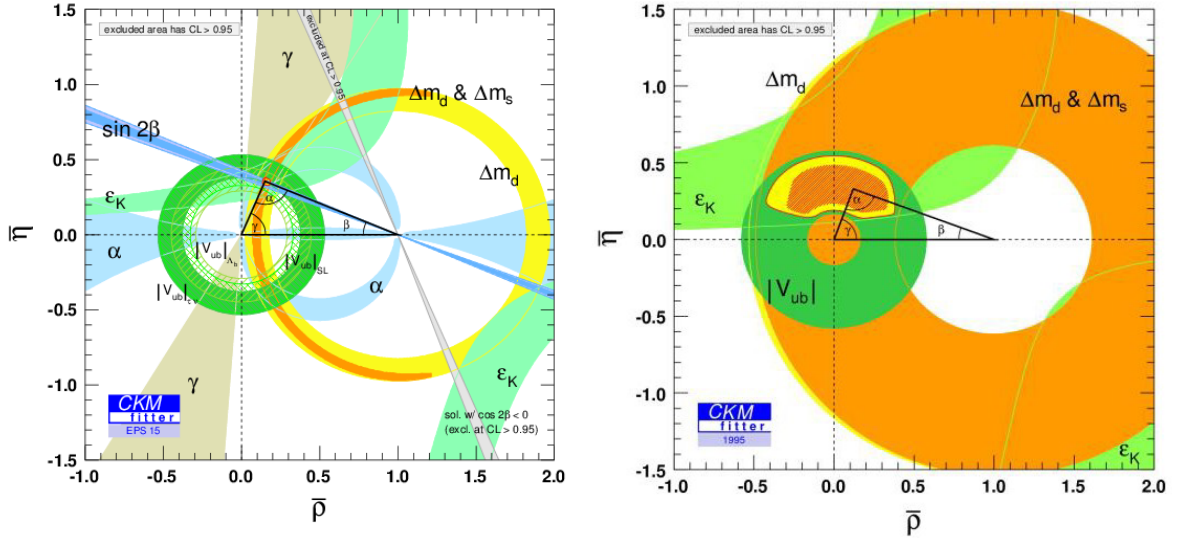


Fig. 2: Summary of the constraints on the CKM unitarity triangle as obtained by the CKMfitter collaboration [23] **Left:** in 2015, **Right:** in 1995.

depends on the phase β). From the figure, it is evident that there is little room for non-SM contributions in flavor changing transitions. The values of $\bar{\rho}$ and $\bar{\eta}$ are determined very accurately¹:

$$\bar{\rho} = 0.150^{+0.012}_{-0.006}, \quad \bar{\eta} = 0.354^{+0.007}_{-0.008}, \quad (16)$$

together with the parameters A and λ :

$$A = 0.823^{+0.007}_{-0.014}, \quad \lambda = 0.2254^{+0.0004}_{-0.0003}. \quad (17)$$

One can allow for arbitrary new physics (NP) in one or more flavor changing processes entering the CKM fit. This is particularly interesting in processes that appear in the SM at the loop-level. Then, one can quantitatively constrain the size of new physics contributions to processes such as neutral meson mixing. This is what we will discuss in the next section.

2.3 Meson mixing and the GIM mechanism

In the SM, in order for a flavor transition to take place, the exchange of at least a virtual W is necessary. A *Flavor-Changing-Neutral-Current* (FCNC) process is a process in which the electric charge does not change between initial and final states. As a consequence, in the SM such processes have a reduced rate relative to a normal weak interaction process. FCNCs are, however, not only suppressed by the loop, but also by the so called Glashow-Iliopoulos-Maiani (GIM) mechanism [26]. We will explain this mechanism through the discussion of meson mixing.

Let us take the K ($= d\bar{s}$) and \bar{K} ($= \bar{d}s$) meson system. These two flavor eigenstates are not mass eigenstates and, therefore, they mix. The leading order contributions to the mixing arise from box diagrams mediated by the exchange of the W boson and the up quarks. The corresponding effective Hamiltonian responsible of this mixing is given by

$$\mathcal{H}_K = \frac{G_F^2}{16\pi^2} m_W^2 \left[\sum_{i=u,c,t} F(x_i, x_i) \lambda_i^2 + \sum_{ij=u,c,t, i \neq j} F(x_i, x_j) \lambda_i \lambda_j \right] (\bar{s} \gamma_\mu (1 - \gamma_5) d)^2, \quad (18)$$

¹These numbers are taken from the CKMfitter collaboration [23]. Similar numbers are obtained by the UTFit collaboration [24] and by latticeaverages.org [25].

where we have defined $\lambda_i = V_{is}^* V_{id}$. $F(x_i, x_j)$ are loop functions, $x_q \equiv m_q^2/m_W^2$. In the limit of exact flavor symmetry ($m_d = m_s = m_b$) the several diagrams cancel, thanks to the unitarity of the CKM matrix (see Eqs. (11)). This is the so called *GIM mechanism*, that can be applied not only to the Kaon mixing system but to all SM flavor transitions. Historically, in 1970, at the time the GIM mechanism was proposed, only three quarks (up, down, and strange) were thought to exist. The GIM mechanism however, required the existence of a fourth quark, the charm, to explain the large suppression of FCNC processes.

The breaking of the flavor symmetry induces a mass difference between the quarks, so the sum of the diagrams responsible for meson mixing will be non-zero. We can use the unitarity relations (11) to eliminate the terms in the effective Hamiltonian that depend on λ_u , obtaining

$$\mathcal{H}_K = \frac{G_F^2}{16\pi^2} m_W^2 [S_0(x_t)\lambda_t^2 + S_0(x_c)\lambda_c^2 + 2S_0(x_c, x_t)\lambda_c\lambda_t] (\bar{s}\gamma_\mu(1 - \gamma_5)d)^2, \quad (19)$$

with $S_0(x_i)$ and $S_0(x_i, x_j)$ given by the combinations

$$S_0(x_i) \equiv F(x_i, x_i) + F(x_u, x_u) - 2F(x_i, x_u) \quad (20)$$

$$S_0(x_i, x_j) \equiv F(x_i, x_j) + F(x_u, x_u) - F(x_i, x_u) - F(x_j, x_u). \quad (21)$$

The explicit expressions can be found in e.g. [1]. All terms of this effective Hamiltonian are suppressed by, not only the loop factor, but also the small CKM elements, particularly suppressing the top loop contribution, and the small mass ratio m_c^2/m_W^2 in the case of the charm loop contribution, as predicted by the GIM mechanism.

This effective Hamiltonian leads to the oscillation of the two Kaons. The time evolution of the Kaon anti-Kaon system, $\psi = (K, \bar{K})$, reads

$$i\frac{d\psi(t)}{dt} = \hat{H}\psi(t), \quad \hat{H} = \hat{M} - i\frac{\hat{\Gamma}}{2} = \begin{pmatrix} M - i\Gamma/2 & M_{12} - i\Gamma_{12}/2 \\ M_{12}^* - i\Gamma_{12}^*/2 & M - i\Gamma/2 \end{pmatrix}, \quad (22)$$

with M and Γ the average mass and width of the two Kaons, respectively. The two eigenstates of the system (heavy and light, or, equivalently, long and short) have a mass and width given by

$$\begin{aligned} M_{H,L} &= M \pm \text{Re}(Q), \quad \Gamma_{H,L} = \Gamma \mp 2\text{Im}(Q), \\ Q &= \sqrt{\left(M_{12} - \frac{i}{2}\Gamma_{12}\right) \left(M_{12}^* - \frac{i}{2}\Gamma_{12}^*\right)}, \end{aligned} \quad (23)$$

and are a linear combination of the two K and \bar{K} states

$$|K_{H,L}\rangle = p|K\rangle \mp q|\bar{K}\rangle, \quad \frac{q}{p} = -\frac{2M_{12}^* - i\Gamma_{12}^*}{2\text{Re}(Q) + 2i\text{Im}(Q)}. \quad (24)$$

The difference in mass of the two Kaon states, ΔM_K , can be computed from the effective Hamiltonian in (19) by

$$m_K \Delta M_K = 2m_K \text{Re}(M_{12}) = \text{Re}(\langle \bar{K} | \mathcal{H}_K | K \rangle), \quad (25)$$

with m_K the average Kaon mass. Lattice QCD is essential to compute the matrix element of the four quark operator calculated between two quark bound states. We have [1]

$$\langle \bar{K} | (\bar{s}\gamma_\mu(1 - \gamma_5)d)^2 | K \rangle = \frac{8}{3} B_K(\mu) F_K^2 m_K^2, \quad (26)$$

with F_K the Kaon decay constant and $B_K(\mu)$ the Kaon bag parameter, evaluated at the scale μ . Putting these pieces together and including QCD corrections, one can find

$$M_{12} = \frac{G_F^2}{12\pi^2} F_K^2 \hat{B}_K m_K m_W^2 [(\lambda_c^*)^2 \eta_1 S_0(x_c) + (\lambda_t^*)^2 \eta_2 S_0(x_t) + 2\lambda_c^* \lambda_t^* \eta_3 S_0(x_c, x_t)], \quad (27)$$

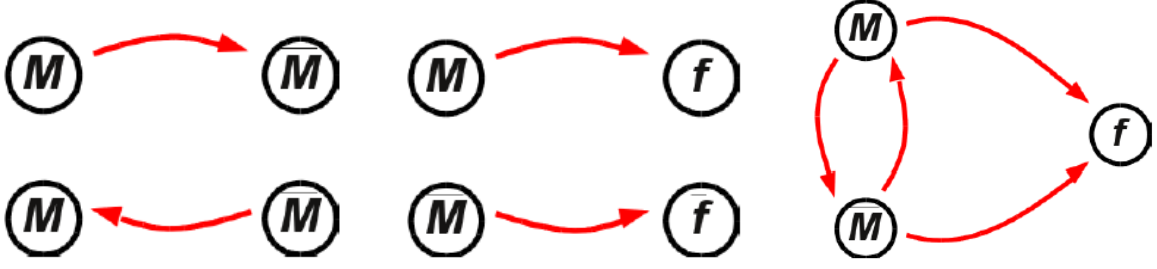


Fig. 3: **Left:** CP violation in mixing; **Middle:** CP violation in decay; **Right:** CP violation in interference, for meson decays to a final state f .

where $\eta_{1,2,3}$ are QCD correction factors given e.g. in [1] and we have defined the renormalization group invariant parameter

$$\hat{B}_K = B_K(\mu) [\alpha_s(\mu)]^{-2/9} \left[1 + \frac{\alpha_s(\mu)}{4\pi} J_3 \right], \quad (28)$$

with $J_3 \sim 1.9$ in the NDR-scheme [27]. In Sec. 3.1, we will discuss the bounds on New Physics theories arising from the measurement of the several observables of the meson mixing systems.

2.4 CP violation in meson decays

All CP-violating observables in K and \bar{K} decays, as well as in any $M - \bar{M}$ meson system, to final states f and \bar{f} can be expressed in terms of phase-convention-independent combinations of $A_f, \bar{A}_f, A_{\bar{f}}, \bar{A}_{\bar{f}}$, together with q/p of Eq. (24), in the case of neutral-mesons, where we define

$$A_f = \langle f | \mathcal{H} | M \rangle, \quad \bar{A}_f = \langle f | \mathcal{H} | \bar{M} \rangle, \quad A_{\bar{f}} = \langle \bar{f} | \mathcal{H} | M \rangle, \quad \bar{A}_{\bar{f}} = \langle \bar{f} | \mathcal{H} | \bar{M} \rangle. \quad (29)$$

As shown in Fig. 3, we distinguish three types of CP-violating effects in meson decays [4]:

- CP violation in mixing, defined by $|q/p| \neq 1$ and arising when the two neutral mass eigenstate admixtures cannot be chosen to be CP-eigenstates;
- CP violation in the decay of mesons, defined by $|\bar{A}_{\bar{f}}/A_f| \neq 1$;
- CP violation in interference between a decay without mixing, $M \rightarrow f$, and a decay with mixing $M \rightarrow \bar{M} \rightarrow f$. This is defined by $\text{Im}(q\bar{A}_f/pA_f) \neq 0$.

One example of CP violation in mixing (a) is the asymmetry in charged-current semi-leptonic neutral meson decays for which the “wrong sign” decays (i.e. decays to a lepton of charge opposite to the sign of the charge of the original b quark) are allowed only if there is a mixing between the meson and the anti-meson. For example, for a B_d meson

$$a_{\text{SL}}^d = \frac{\Gamma(\bar{B}_d(t) \rightarrow \ell^+ \nu X) - \Gamma(\bar{B}_d(t) \rightarrow \ell^- \bar{\nu} X)}{\Gamma(\bar{B}_d(t) \rightarrow \ell^+ \nu X) + \Gamma(\bar{B}_d(t) \rightarrow \ell^- \bar{\nu} X)} = \frac{1 - |q/p|^4}{1 + |q/p|^4}. \quad (30)$$

D0 performed several measurements of these asymmetries in B decays [28–30]. Combining all measurements, there is a long-standing anomaly with the SM prediction in the $a_{\text{SL}}^s - a_{\text{SL}}^d$ plane with a significance at the level of $\sim 2 - 3\sigma$ [31], mainly arising from the D0 measurement of the like-sign dimuon charge asymmetry [29] (see upper panel of Fig. 4).

In charged meson decays, where mixing effects are absent, the CP violation in decay (b) is the only possible source of CP asymmetries. For example, in the B meson system:

$$a_{f^\pm} = \frac{\Gamma(B^+ \rightarrow f^+) - \Gamma(B^- \rightarrow f^-)}{\Gamma(B^+ \rightarrow f^+) + \Gamma(B^- \rightarrow f^-)} = \frac{1 - |\bar{A}_{f^-}/A_{f^+}|^2}{1 + |\bar{A}_{f^-}/A_{f^+}|^2}. \quad (31)$$

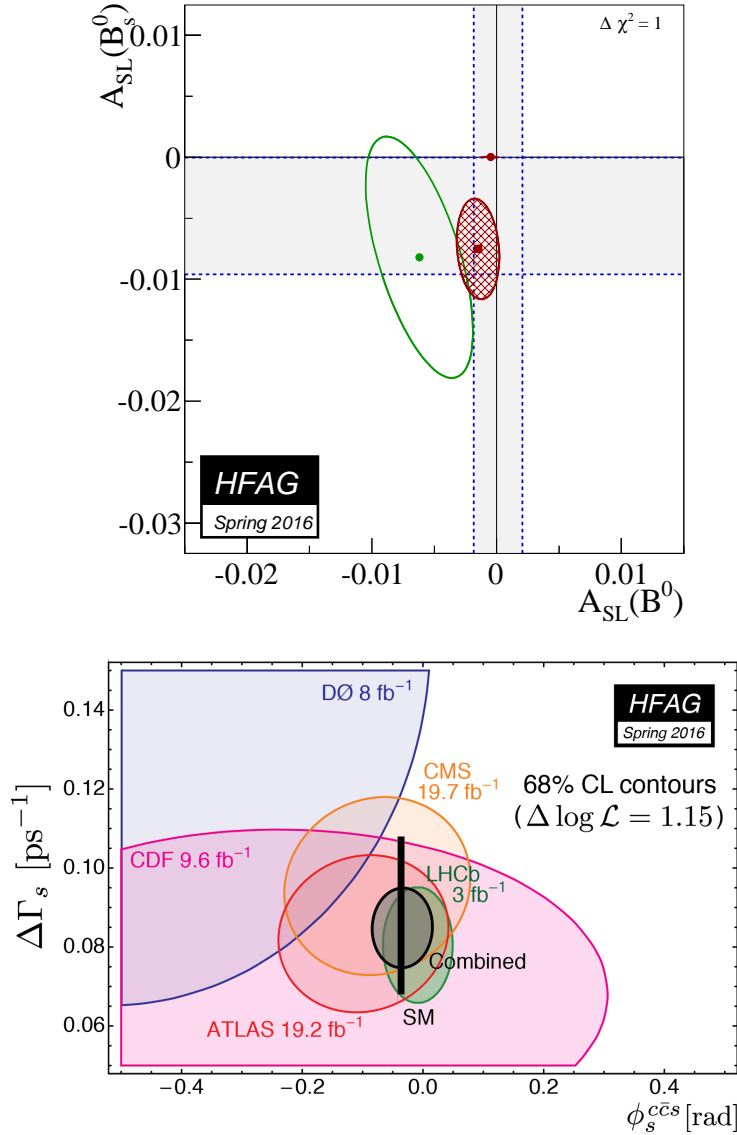


Fig. 4: Upper panel: Summary of the measurements of CLEO, BABAR, Belle, D0 and LHCb in the $a_{\text{SL}}^s - a_{\text{SL}}^d$ plane. **Lower panel:** $(\phi_s^{c\bar{c}s}, \Delta\Gamma_s)$ plane ($\Delta\Gamma_s$ is the difference in width in the $B_s - \bar{B}_s$ system), the individual 68% confidence-level contours of ATLAS, CMS, CDF, D0 and LHCb, their combined contour (solid line and shaded area), as well as the SM predictions (thin black rectangle) are shown (from [32]).

These asymmetries are different from zero only if at least two terms of the amplitude have different weak phases and different strong phases². Non-zero CP asymmetries have been observed in a few B meson decay modes by the LHCb collaboration: $B^+ \rightarrow K^+ K^- K^+$, $B^+ \rightarrow K^+ K^- \pi^+$ [33].

CP violation in interference (c) is measured through the decays of neutral mesons and anti-mesons to a final state that is a CP eigenstate (f_{CP})

$$a_{f_{\text{CP}}} = \frac{\Gamma(\bar{M}(t) \rightarrow f_{\text{CP}}) - \Gamma(M(t) \rightarrow f_{\text{CP}})}{\Gamma(\bar{M}(t) \rightarrow f_{\text{CP}}) + \Gamma(M(t) \rightarrow f_{\text{CP}})} \simeq \text{Im}(\lambda_{\text{CP}}) \sin(\Delta M_M t), \quad (32)$$

²Strong phases do not violate CP. Their origin is the contribution from intermediate on-shell states in the decay process, that is an absorptive part of an amplitude.

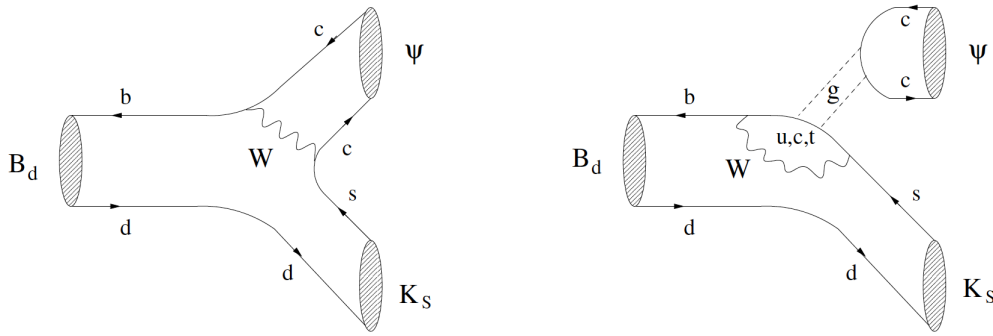


Fig. 5: The **Left:** tree diagram and the **Right:** penguin diagram contributing to $B_d \rightarrow \Psi K_S$ (from [37]).

where we have defined $\lambda_{\text{CP}} = \frac{q\bar{A}_f}{pA_f}$ and ΔM_M is the difference in mass of the meson anti-meson system. This type of CP violation has been observed in several B meson decays, as for example in $B_d \rightarrow J/\psi K_S$ at Babar [34], Belle [35] and by now by the LHCb, as well [36], leading to the measurement of the β angle of the CKM matrix $a_{J/\psi K_S} \simeq \sin(2\beta) \sin(\Delta M_d t)$. The Feynman diagrams contributing to this asymmetry are given in Fig. 5, where we show the tree (left panel) and the penguin (right panel) contributions. The current world average on the angle β is [32]

$$\sin(2\beta) = 0.69 \pm 0.02. \quad (33)$$

The corresponding CP asymmetry in B_s decay is $B_s \rightarrow \psi\phi$. The SM prediction is suppressed compared to the β angle by λ^2 , leading to $\beta_s^{\text{SM}} = 0.01882_{-0.00042}^{+0.00036}$ [23]. The latest LHCb result using 3 fb^{-1} data is in good agreement with this prediction and reads $\beta_s^{\text{LHCb}} = 0.005 \pm 0.0195$. A summary of all measurements of the mixing angle in the $B_s - \bar{B}_s$ system is reported in the lower panel of Fig. 4 and the world average is [32]

$$\beta_s = -\frac{\phi_s^{c\bar{c}s}}{2} = -0.00165 \pm 0.00165. \quad (34)$$

3 Effective field theories and flavor transitions

It is clear that the Standard Model is not a complete theory of Nature. Foremost arguments in favor of the existence of New Physics are

- It does not include gravity, and therefore it cannot be valid at energy scales above the Planck scale;
- It cannot explain the small value of the Higgs boson mass;
- It cannot account for neutrino masses and for the existence of Dark Matter (DM).

In particular, the DM and Higgs mass motivations suggest that the SM should be replaced by a new theory already at scales around the TeV scale. Given that the SM is only an effective low energy theory, non-renormalizable terms must be added to the SM Lagrangian. In the next subsection, we will discuss the flavor constraints on the NP scale associated to the higher dimensional operators contributing to flavor transitions.

3.1 The New Physics flavor puzzle

If we assume that the new degrees of freedom which complete the theory of Nature are heavier than the SM particles, we can integrate them out and describe physics beyond the SM by means of an effective

field theory (EFT) approach. The SM Lagrangian becomes the renormalizable part of this generalized Lagrangian which includes an infinite sum of operators with dimension $d \geq 5$, constructed in terms of SM fields and suppressed by inverse powers of the NP scale Λ ($\gg v$). This approach is a generalization of the Fermi theory of weak interactions, where the dimension six four-fermion operators describing weak decays are the results of having integrated out the W boson. The generic effective Lagrangian reads

$$\mathcal{L}_{\text{eff}} = \mathcal{L}_{\text{SM}} + \sum_n^{\geq 5} \frac{c_n^d}{\Lambda^{d-4}} \mathcal{O}_n^{(d)}(\text{SM}), \quad (35)$$

where \mathcal{L}_{SM} is the sum of (2) and (5) and $\mathcal{O}_n^{(d)}(\text{SM})$ are operators of dimension $d \geq 5$ containing SM fields only and compatible with the SM gauge symmetry. Generically, we would expect the Wilson coefficients $c_n^d = \mathcal{O}(1)$, however several of these operators contribute to flavor-changing processes and should be very suppressed to be in agreement with low energy flavor experiments. This is often denoted as the *NP flavor puzzle*.

As an example, we consider the dimension 6 operators contributing to Kaon mixing:

$$\begin{aligned} O_1^{\text{VLL}} &= (\bar{s}\gamma_\mu P_L d)^2, \\ O_1^{\text{LR}} &= (\bar{s}\gamma_\mu P_L d)(\bar{s}\gamma^\mu P_R d), \\ O_2^{\text{LR}} &= (\bar{s}P_L d)(\bar{s}P_R d), \\ O_1^{\text{SLL}} &= (\bar{s}P_L d)^2, \\ O_2^{\text{SLL}} &= (\bar{s}\gamma_{\mu\nu} P_L d)(\bar{s}\gamma^{\mu\nu} P_L d), \end{aligned} \quad (36)$$

plus the corresponding ones with the exchange $P_L \rightarrow P_R$ ($P_{L,R} = (1 \mp \gamma_5)/2$). The only operator that arises in the SM is O_1^{VLL} (see Sec. 2.3). As an example, a NP toy model containing a TeV scale new Z' gauge boson with coupling $g' Z'_\mu (\bar{s}\gamma^\mu (1 - \gamma_5) d)$ would produce a contribution to the operator O_1^{VLL} and, therefore, to the difference in mass of Kaon and anti-Kaon system that is equal to³

$$\Delta M_K = \Delta M_K^{\text{SM}} + \frac{8}{3} m_K F_K^2 \hat{B}_K \frac{(g')^2}{m_{Z'}^2}, \quad (37)$$

where ΔM_K^{SM} is the value predicted by the SM, as reported in Eqs. (25)-(28). For TeV-scale Z' 's coupled to a bottom and a strange quark with a EW strength coupling, the second piece of this equation is ~ 4 orders of magnitude larger than the SM contribution, and therefore, such gauge bosons are completely ruled out by Kaon mixing measurements. This shows the tension between a generic NP at around the TeV scale with EW-strength flavor violating couplings and low energy flavor measurements, the so called *NP flavor puzzle*.

A summary of the bounds for the four neutral meson systems (K, B_d, B_s, D) is shown in Table 1. Particularly, we show in the first two entries the bounds on the NP scale, Λ , having fixed the absolute value of the corresponding Wilson coefficient, c_n^6 of Eq (35), to one (the first column is for $c_n^6 = 1$, the second one for $c_n^6 = i$); the last two columns represent, instead, the bound on real part and on the imaginary part of the the Wilson coefficient, fixing the NP scale to 1 TeV. A few comments are in order. The bounds are weakest (strongest) for B_s (K) mesons, as mixing is the least (most) suppressed in the SM in that case. The bounds on the operators with a different chirality (left-right (LR) or right-left (RL)) are stronger, especially in the Kaon case, because of the larger hadronic matrix elements. Throughout the table, bounds on the NP scale Λ exceed the TeV scale by several orders of magnitude. Therefore, we can conclude that, if NP exists at around the TeV scale, it has to possess a highly non-generic flavor structure, to explain $c_n^d \ll 1$.

³**Exercise:** compute this contribution.

Operator	Bounds on Λ in TeV ($c_n^6 = 1$)		Bounds on c_n^6 ($\Lambda = 1$ TeV)	
	Re	Im	Re	Im
$(\bar{s}_L \gamma^\mu d_L)^2$	9.8×10^2	1.6×10^4	9.0×10^{-7}	3.4×10^{-9}
$(\bar{s}_R d_L)(\bar{s}_L d_R)$	1.8×10^4	3.2×10^5	6.9×10^{-9}	2.6×10^{-11}
$(\bar{c}_L \gamma^\mu u_L)^2$	1.2×10^3	2.9×10^3	5.6×10^{-7}	1.0×10^{-7}
$(\bar{c}_R u_L)(\bar{c}_L u_R)$	6.2×10^3	1.5×10^4	5.7×10^{-8}	1.1×10^{-8}
$(\bar{b}_L \gamma^\mu d_L)^2$	6.6×10^2	9.3×10^2	2.3×10^{-6}	1.1×10^{-6}
$(\bar{b}_R d_L)(\bar{b}_L d_R)$	2.5×10^3	3.6×10^3	3.9×10^{-7}	1.9×10^{-7}
$(\bar{b}_L \gamma^\mu s_L)^2$	1.4×10^2	2.5×10^2	5.0×10^{-5}	1.7×10^{-5}
$(\bar{b}_R s_L)(\bar{b}_L s_R)$	4.8×10^2	8.3×10^2	8.8×10^{-6}	2.9×10^{-6}

Table 1: Bounds on representative dimension-six operators that mediate meson mixing, assuming an effective coupling c_n^6/Λ^2 . The bounds quoted for Λ are obtained setting $|c_n^6| = 1$; those for c_{NP} are obtained setting $\Lambda = 1$ TeV. We define $q_{L,R} \equiv P_{L,R} q$. From [38] and [39].

3.2 The Minimal Flavor Violation ansatz

TeV scale New Physics could be invariant under some flavor symmetry, and, therefore, more easily in agreement with low energy flavor measurements. One example, of a class of such models are theories with Minimal Flavor Violation (MFV) [40–43]. Under this assumption, flavor violating interactions are linked to the known structure of the SM Yukawa couplings also beyond the SM. More specifically, the MFV ansatz can be implemented within the generic effective Lagrangian in Eq. (35), as well as to UV complete models, and it consists of two ingredients [43]: (i) a flavor symmetry and (ii) a set of symmetry-breaking terms. The symmetry is the SM global symmetry in absence of Yukawa couplings, as shown in Eq. (4). Since this global symmetry, and particularly the $SU(3)$ subgroups controlling quark flavor-changing transitions, is broken within the SM, it cannot be promoted to an exact symmetry of the NP model. Particularly, in the SM we can formally recover the flavor invariance under $\mathcal{G}_{\text{flavor}}$ by promoting the Yukawa couplings Y_d, Y_u, Y_e of (5) to dimensionless auxiliary fields (spurions) transforming under $SU(3)_q^3 = SU(3)_Q \times SU(3)_U \times SU(3)_D$ and under $SU(3)_\ell^2 = SU(3)_L \times SU(3)_e$ as

$$Y_Q \sim (3, 1, \bar{3})_{SU(3)_q^3}, Y_u \sim (3, \bar{3}, 1)_{SU(3)_q^3}, Y_e \sim (3, \bar{3})_{SU(3)_\ell^2}. \quad (38)$$

Exercise: Check that, with these transformations, the Yukawa Lagrangian of (4) is invariant under $SU(3)_q^3 \times SU(3)_\ell^2$.

Employing an effective field theory language, a theory satisfies the MFV ansatz, if all higher-dimensional operators, constructed from SM and $Y_{u,d,e}$ fields, are invariant under the flavor group, $\mathcal{G}_{\text{flavor}}$. The invariance under CP of the NP operators may or may not be imposed in addition to this criterion. In the down quark sector, the several operators will be combinations of the invariants

$$\bar{Q}_L Y_u Y_u^\dagger Q_L, \bar{D}_R Y_d^\dagger Y_u Y_u^\dagger Q_L, \bar{D}_R Y_d^\dagger Y_u Y_u^\dagger Y_d D_R. \quad (39)$$

As an example, let us take the operators in (36) and impose the MFV hypothesis. The corresponding Wilson coefficients cannot be generic order one numbers, since the operators are not invariant under the flavor symmetry $\mathcal{G}_{\text{flavor}}$. The leading term for the first operator reads

$$(c_1^{\text{VLL}})_{\text{MFV}} \mathcal{O}_1^{\text{VLL}} = Z y_t^4 (V_{ts}^* V_{td})^2 (\bar{s} \gamma_\mu P_L d)^2, \quad (40)$$

where y_t is the SM top Yukawa ($= m_t/v$) and Z is a (flavor independent) coefficient, generically of $\mathcal{O}(1)$. Thanks to the suppression by the small CKM elements V_{ts} and V_{td} , the bound on the NP scale

Λ of this operator is relatively weak $\Lambda \gtrsim 5$ TeV, to be compared to the bound of 1.6×10^4 TeV, as shown in Tab. 1. The other operators have, instead, a much smaller Wilson coefficient as they are suppressed by either the strange Yukawa square ($\mathcal{O}_1^{\text{SLL}}, \mathcal{O}_2^{\text{SLL}}$) or the product of down and strange Yukawas ($\mathcal{O}_1^{\text{LR}}, \mathcal{O}_2^{\text{LR}}$), resulting also in weak bounds on the NP scale Λ . **Exercise:** write the leading term of the Wilson coefficient of each operator in (36), according to the MFV ansatz and demonstrate that they are much smaller than $(c_1^{\text{VLL}})_{\text{MFV}}$.

This structure can be generalized to any higher dimensional operator mediating a flavor transition. Thus, generically in MFV models, flavor changing operators automatically have their SM-like suppressions, proportional to the same CKM elements and quark masses as in the SM and this can naturally address the NP flavor puzzle, as the NP scale of MFV models can be $\mathcal{O}(1 \text{ TeV})$ without violating flavor physics bounds.

To conclude, the MFV ansatz is remarkably successful in satisfying the constraints from low energy flavor observables. However, it does not address the question *Why do quark and lepton masses, as well as quark mixing, have such a hierarchical pattern* (SM flavor puzzle), since it simply states that the NP flavor violation has to have the same structure of the SM flavor violation.

3.3 Effective field theories for rare B decays

Rare B_d and B_s decays based on the $b \rightarrow s$ flavor changing neutral-current transition are very sensitive to BSM, as they are very suppressed in the SM [44]. In the last few years, measurements at the LHC, complementing earlier B-factory results, have hugely increased the available experimental information on these decays. In these lectures, we will focus on the golden channels: the B_s and B_d decays to two muons as they are among the rarest B decays. (see [45] for a recent review, that discusses additional B rare decays, as for example $B_s \rightarrow K \mu^+ \mu^-$ and $B_s \rightarrow K^* \mu^+ \mu^-$).

In the SM, these decays are dominated by the Z penguin and box diagrams involving top quark exchanges. The resulting effective Hamiltonian depends, therefore, on the loop function $Y(x_t)$ (see e.g. [46] for its definition), with $x_t \equiv m_t^2/m_W^2$ and reads

$$\mathcal{H}_{\text{eff}} = -\frac{G_F}{\sqrt{2}} \frac{\alpha}{\pi \sin^2 \theta} V_{tb}^* V_{ts} Y(x_t) (\bar{b} \gamma_\mu P_L s) (\bar{\mu} \gamma_\mu \gamma_5 \mu) + \text{h.c.}, \quad (41)$$

with s replaced by d in the case of $B_d \rightarrow \mu^+ \mu^-$. Evaluating the two matrix elements of the quark current and of the muon current leads to the branching ratio

$$\text{BR}(B_s \rightarrow \mu^+ \mu^-) = \frac{G_F^2}{\pi} \left(\frac{\alpha}{4\pi \sin^2 \theta} \right)^2 |V_{tb}^* V_{ts}|^2 Y^2(x_t) m_\mu^2 m_{B_s} \sqrt{1 - \frac{4m_\mu^2}{m_{B_s}^2}} F_{B_s} \tau_{B_s}, \quad (42)$$

and analogously for the B_d decay. In this equation, m_{B_s} is the mass of the B_s meson, τ_{B_s} its life time (1.6 ps), and F_{B_s} the corresponding decay constant. The main theoretical uncertainties in this branching ratio result from the uncertainties in the decay constant ($\sim 4\%$ for B_d and $\sim 3\%$ for B_s , using the latest lattice computations [47]), and in the CKM elements V_{td} and V_{ts} (both at the level of several % [23]). Inserting numbers and including the $\mathcal{O}(\alpha)$ and $\mathcal{O}(\alpha_s^2)$ corrections, the latest SM predictions read [48]

$$\text{BR}(B_s \rightarrow \mu^+ \mu^-)_{\text{SM}} = (3.65 \pm 0.23) \times 10^{-9}, \quad \text{BR}(B_d \rightarrow \mu^+ \mu^-)_{\text{SM}} = (1.06 \pm 0.09) \times 10^{-10}. \quad (43)$$

As shown by Eq. (42), the tiny branching ratios of these decays in the SM are due to several factors: (i) loop suppression, (ii) CKM suppression, and (iii) helicity suppression (by the small muon mass, m_μ). As we will discuss later in this section, extensions of the SM do not necessarily contain any of these suppression mechanisms, and, more in particular, the helicity suppression (iii).

Experimentally, searches for $B_{s,d} \rightarrow \mu^+ \mu^-$ have been performed by 11 experiments, spanning more than three decades (see upper panel of Fig. 6 for a summary of all bounds and measurements). In

the figure, markers without error bars denote upper limits on the branching fractions at 90% confidence level, while measurements are denoted with error bars delimiting 68% confidence intervals. The first hint for a non-zero B_s decay was reported in 2011 by the CDF collaboration [49]: $\text{BR}(B_s \rightarrow \mu^+ \mu^-)_{\text{CDF}} = 1.3_{-0.7}^{+0.9} \times 10^{-8}$. This was followed by several measurements by ATLAS, CMS and LHCb and by the first evidence for a non-zero B_d decay, as observed by the combination of CMS and LHCb Run I analyses [50]: $\text{BR}(B_d \rightarrow \mu^+ \mu^-)_{\text{CMS+LHCb}} = 3.9_{-1.4}^{+1.6} \times 10^{-10}$. In the lower panel of Fig. 6, we show the latest status of the measurement of the B_s and B_d decay mode. Particularly, by now, we have a 6.2σ evidence for $B_s \rightarrow \mu^+ \mu^-$ with

$$\text{BR}(B_s \rightarrow \mu^+ \mu^-)_{\text{CMS+LHCb}} = 2.8_{-0.6}^{+0.7} \times 10^{-9}, \quad \text{BR}(B_s \rightarrow \mu^+ \mu^-)_{\text{ATLAS}} = 0.9_{-0.8}^{+1.1} \times 10^{-9}, \quad (44)$$

showing a good agreement with the SM prediction (see [51] for the ATLAS analysis).

In BSM theories, several additional operators can contribute to the $B_{s,d}$ decays: \mathcal{O}'_{10} , obtained from the SM operator in (41) with $P_L \rightarrow P_R$ and

$$\begin{aligned} \mathcal{O}_S &= (\bar{b}P_L s)(\bar{\mu}\mu), \\ \mathcal{O}_P &= (\bar{b}P_L s)(\bar{\mu}\gamma_5\mu), \end{aligned} \quad (45)$$

and the corresponding prime operators obtained by $P_L \rightarrow P_R$. Using these additional operators, one can compute the branching ratio [52]

$$\begin{aligned} \frac{\text{BR}(B_s \rightarrow \mu^+ \mu^-)}{\text{BR}(B_s \rightarrow \mu^+ \mu^-)_{\text{SM}}} &\simeq (|S_s|^2 + |P_s|^2) \\ &\times \left(1 + y_s \frac{\text{Re}(P_s^2) - \text{Re}(S_s^2)}{|S_s|^2 + |P_s|^2} \right) \left(\frac{1}{1 + y_s} \right), \end{aligned} \quad (46)$$

where $y_s = (8.8 \pm 1.4)\%$ ($y_d \sim 0$ for the B_d system) have to be taken into account when comparing experimental and theoretical results, and

$$S_s \equiv \frac{m_{B_s}}{2m_\mu} \frac{(C_s^S - C_s'^S)}{C_{10s,d}^{\text{SM}}} \sqrt{1 - \frac{4m_\mu^2}{m_{B_s}^2}}, \quad (47)$$

$$P_s \equiv \frac{m_{B_s}}{2m_\mu} \frac{(C_s^P - C_s'^P)}{C_{10s,d}^{\text{SM}}} + \frac{(C_s^{10} - C_s'^{10})}{C_{10s}^{\text{SM}}}, \quad (48)$$

with the several Wilson coefficients defined using the normalization

$$\mathcal{H}_{\text{eff}} = -4 \frac{G_F}{\sqrt{2}} V_{tb} V_{ts}^* \frac{e^2}{16\pi^2} \sum_i (C_i \mathcal{O}_i + C_i' \mathcal{O}_i') + \text{h.c.} \quad (49)$$

Similar expressions hold for the B_d system. It is evident that the helicity suppression of the branching ratio can be eliminated thanks to the scalar and pseudoscalar operators and, therefore, large enhancements can be obtained. Comparing with the latest measurement of $B_s \rightarrow \mu^+ \mu^-$, one can find the bounds on the Wilson coefficients of the scalar and pseudoscalar operators, as shown in Fig. 7. The Wilson coefficients of the scalar operators are strongly constrained by the measurement of the B_s rare decay with a bound at the level of $\text{Re}(C_s^S - C_s'^S) < 0.071$ and $\text{Im}(C_s^S - C_s'^S) < 0.065$. Scalar NP contributions always increase the branching ratio and, for this reason, the 1σ region does not appear in the left panel of Fig. 7 (the present measurement is smaller than the SM prediction at the 1σ level, see Eqs. (43) and (44)). The pseudoscalar Wilson coefficients are instead more weakly constrained (see right panel of Fig. 7), and are consistent with 0 at the 1σ level. Scalar and pseudoscalar Wilson coefficients for the B_d meson decay are only weakly constrained, at the level of $\mathcal{O}(0.5)$.

As it is well known, the measurement of the ratio between $\text{BR}(B_s \rightarrow \mu^+ \mu^-)$ and $\text{BR}(B_d \rightarrow \mu^+ \mu^-)$ gives a very clean probe of new sources of flavor violation beyond the CKM matrix. Indeed, in

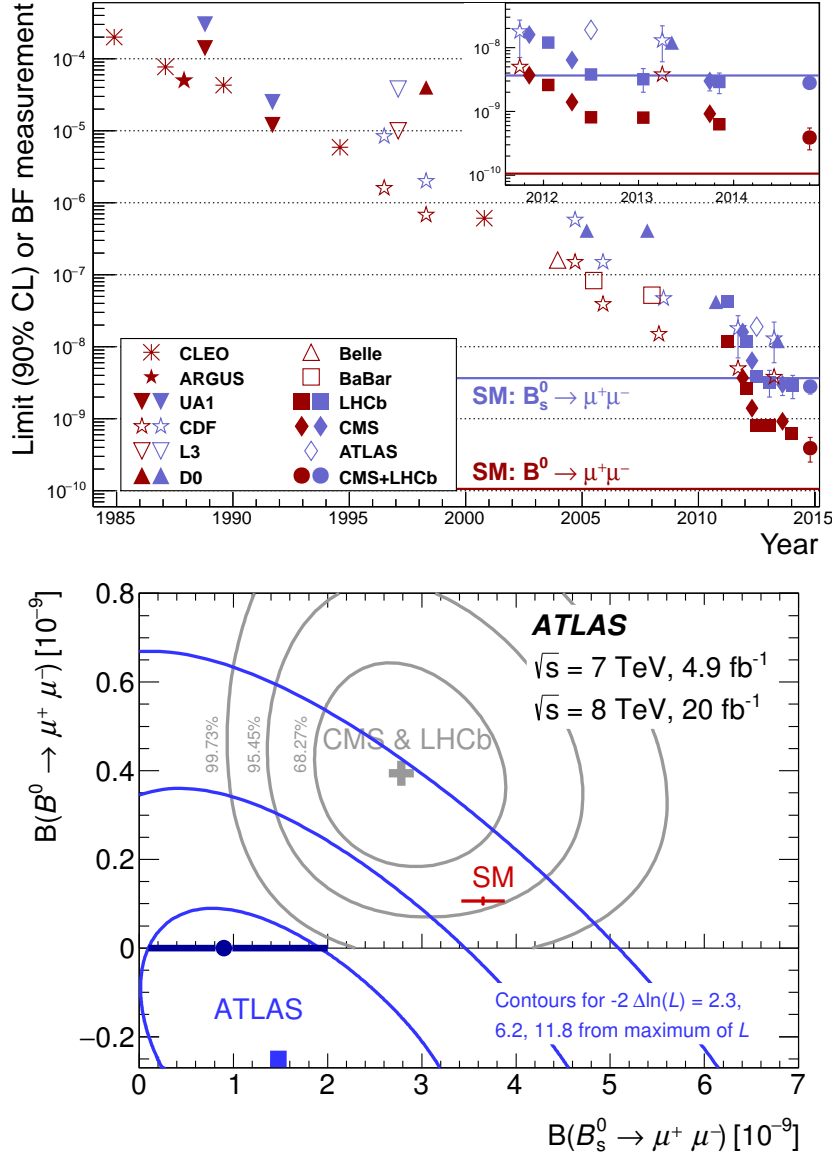


Fig. 6: Upper panel: Searches for $B_{s,d} \rightarrow \mu^+\mu^-$ from 1985 to 2015. Markers without error bars denote upper limits on the branching fractions at 90% confidence level, while measurements are denoted with errors bars delimiting 68% confidence intervals. The horizontal lines represent the SM predictions for the $B_s \rightarrow \mu^+\mu^-$ and $B_d \rightarrow \mu^+\mu^-$ branching fractions (from [50]); **Lower panel:** Present status of the measurements of $B_{s,d} \rightarrow \mu^+\mu^-$ at the 1, 2, 3 σ contours. Shown are the corresponding contours for the combined result of the CMS and LHCb experiments, the ATLAS measurement, and the SM prediction (from [51]).

all MFV models (see Sec. 4.1 of these lectures and e.g. [53] for some examples of MFV models), the ratio is determined by [54]

$$\frac{\text{BR}(B_d \rightarrow \mu^+\mu^-)}{\text{BR}(B_s \rightarrow \mu^+\mu^-)} = \frac{\tau_{B_d} m_{B_d} F_{B_d}^2 |V_{td}|^2}{\tau_{B_s} m_{B_s} F_{B_s}^2 |V_{ts}|^2} \sim 0.03, \quad (50)$$

and has a relatively small theoretical uncertainty at the level of $\sim 5\%$. Presently, the measurement of this ratio by CMS and LHCb is given by 0.14 ± 0.05 . In the coming years, the LHCb, ATLAS and CMS collaborations will be able to produce a more accurate test of this relation and, therefore, of the MFV

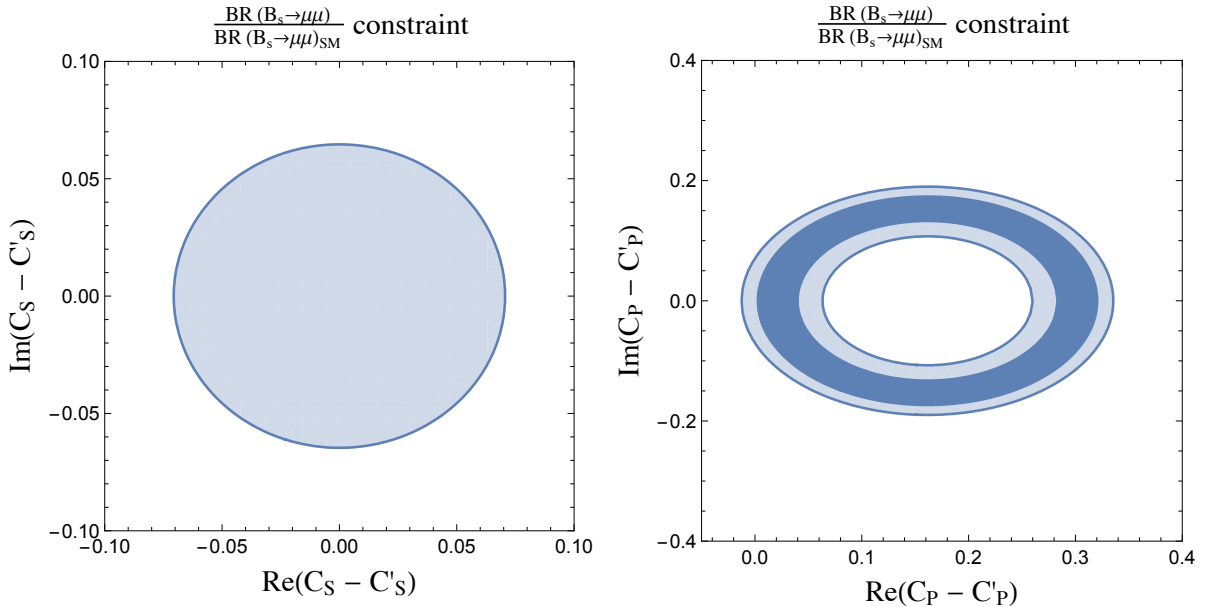


Fig. 7: One (dark blue) and two (light blue) σ bounds on the Wilson coefficients of the **Left:** scalar operator and **Right:** pseudoscalar operator, as obtained using the latest measurement of $B_s \rightarrow \mu^+ \mu^-$, assuming no new physics in $C_{10} - C'_{10}$ and switching on one set of operators at a time. Note the change in the axis range in the two panels.

ansatz. More specifically, the LHCb upgrade (50 fb $^{-1}$ data) will measure the SM prediction of this ratio with an uncertainty of $\sim 35\%$ [55].

4 Flavor at high energy: NP models and predictions

In this section we discuss the synergy between *direct searches* for NP particles at the LHC and *indirect searches* for NP through the measurement of flavor transitions at B-factories and at the LHCb. We will focus on specific NP frameworks: Two Higgs doublet models (2HDMs) in Sec. 4.1 and Supersymmetric (SUSY) models in Sec. 4.2, with new particles with masses at around the EW scale, that generically can not be integrated out to match the effective theories presented in the previous section. Historically, a few particles have been discovered first indirectly. In 1970, the measurement of the tiny branching ratio for the decay $K_L \rightarrow \mu^+ \mu^-$ lead to the prediction of the existence of the charm quark by Glashow, Iliopoulos and Maiani, before the direct discovery of the J/Ψ charm meson in 1974 by SLAC and BNL. Another remarkable example was the observation of CP violation in Kaon anti-Kaon oscillations that lead to the prediction of the existence of a third generation quarks by Kobayashi and Maskawa in 1973. The direct discovery of the bottom quark came four years later at Tevatron.

4.1 A Two Higgs doublet model with MFV

Two Higgs doublet models arise in several extensions of the SM, as for example Supersymmetric models. In the presence of more than one Higgs field the appearance of tree-level FCNC is not automatically forbidden by the GIM mechanism: additional conditions [56, 57] have to be imposed on the model in order to guarantee a sufficient suppression of FCNC processes. The most general 2HDM has, in fact, several new sources of flavor and of CP violation. Particularly, the Higgs potential is given by⁴

$$V(H_1, H_2) = \mu_1^2 |H_1|^2 + \mu_2^2 |H_2|^2 + (bH_1 H_2 + \text{h.c.}) + \frac{\lambda_1}{2} |H_1|^4 + \frac{\lambda_2}{2} |H_2|^4 + \lambda_3 |H_1|^2 |H_2|^2$$

⁴See [58] for a review about 2HDMs.

$$+ \lambda_4 |H_1 H_2|^2 + \left[\frac{\lambda_5}{2} (H_1 H_2)^2 + \lambda_6 |H_1|^2 H_1 H_2 + \lambda_7 |H_2|^2 H_1 H_2 + \text{h.c.} \right], \quad (51)$$

where $H_1 H_2 = H_1^T (i\sigma_2) H_2$. New sources of CP violation can arise from the terms $(H_1 H_2)^2$, $|H_1|^2 H_1 H_2$ and $|H_2|^2 H_1 H_2$, since, in all generality, $\lambda_{5,6,7}$ are complex coefficients. The most general Yukawa interaction Lagrangian can be written as

$$-\mathcal{L}_Y^{\text{gen}} = \bar{Q}_L X_{d1} D_R H_1 + \bar{Q}_L X_{u1} U_R H_1^c + \bar{Q}_L X_{d2} D_R H_2^c + \bar{Q}_L X_{u2} U_R H_2 + \text{h.c.}, \quad (52)$$

to which we can add the corresponding terms for the charged leptons (with $X_{\ell 1}, X_{\ell 2}$ Yukawas). After EWSB, quarks acquire mass from both H_1 ($\langle H_1 \rangle = v \cos \beta$) and H_2 ($\langle H_2 \rangle = v \sin \beta$). For generic X_i we cannot diagonalize simultaneously the two mass matrices:

$$M_i = \frac{v}{\sqrt{2}} (\cos \beta X_{i1} + \sin \beta X_{i2}), \quad (i = u, d) \quad (53)$$

and the couplings to the additional physical neutral Higgs fields, H, A , which are given in the decoupling (or alignment [59]) limit, $\cos(\alpha - \beta) = 0$, by

$$Z_i = \cos \beta X_{i2} - \sin \beta X_{i1}, \quad (i = u, d) \quad (54)$$

where we have defined the angle β as $\tan \beta = v_2/v_1^5$. Consequently we are left with dangerous FCNC couplings at the tree-level and with possible additional new sources of CP violation if (some of) the Yukawas are complex. FCNCs at the tree-level can be eliminated by imposing a discrete Z_2 symmetry, leading to a Type I, II, X or Y 2HDM [61] or by assuming the proportionality relations $X_{i1} \propto X_{i2}$, as in the *aligned 2HDM* [62]. This alignment condition is, however, not preserved by renormalization group equations, and, therefore, imposing the alignment condition at some high energy scale, as the GUT scale, will not result in an alignment model at the EW scale [63].

The MFV ansatz presented in Sec. 3.2 can be imposed to the 2HDM and this leads to interesting phenomenology both at low [53] and high energy [64]. The four Yukawa couplings $X_{u1}, X_{u2}, X_{d1}, X_{d2}$ will be a combination of the two Y_u, Y_d SM spurions. More specifically, without loss of generality we can define Y_u, Y_d to be the flavor structures appearing in X_{u2} and X_{d1} , respectively. Then we can express the two remaining Yukawa interactions as

$$\begin{aligned} X_{d1} &= Y_d, \\ X_{d2} &= \epsilon_0 Y_d + \epsilon_1 Y_d^\dagger Y_d Y_d + \epsilon_2 Y_u^\dagger Y_u Y_d + \dots, \\ X_{u1} &= \epsilon'_0 Y_u + \epsilon'_1 Y_u^\dagger Y_u Y_u + \epsilon'_2 Y_d^\dagger Y_d Y_u + \dots, \\ X_{u2} &= Y_u, \end{aligned} \quad (55)$$

with $\epsilon_i^{(r)}$ generic order one (flavor independent) complex coefficients, and where we have suppressed the higher order terms in $Y_d^\dagger Y_d$ and $Y_u^\dagger Y_u$ ⁶. If the expansions are truncated to the first order, one can recover the alignment condition, $X_{i1} \propto X_{i2}$. However, differently from the alignment model, quantum corrections cannot modify this functional form of the MFV expansion in (55), but they can only change the values of the $\epsilon_i^{(r)}$ at different energy scales. Additionally, for particular choices of the parameters $\epsilon_i^{(r)}$ in (55), one can recover the Type I, II, X and Y 2HDM. **Exercise:** convince your-self that, with the assumption in (55) and the transformation properties of the Yukawas in Eq. (38), the several Yukawa terms are invariant under the $SU(3)_q^3$ flavor symmetry.

⁵Strictly speaking $\tan \beta$ is not a physical parameter in a generic 2HDM [60], since the two Higgs doublets, H_1, H_2 , can be transformed into each other. In the following, we will describe the MFV 2HDM, in which $\tan \beta$ is a well defined quantity.

⁶See [65] for the discussion of the general MFV (GMFV), where both the top and bottom Yukawas are assumed to be of order one and their effects are re-summed to all orders.

The MFV 2HDM predicts Higgs-mediated FCNCs at the tree-level, arising from the terms $Y_u^\dagger Y_u Y_d$ and $Y_d^\dagger Y_d Y_u$ in (55). However, the flavor changing Higgs couplings are highly non-generic and, as we now discuss, generically leads to FCNCs in agreement with low energy data. Thanks to MFV, the contribution to meson mixing has the same dependence on the quark masses and CKM elements, as in the SM and, e.g. in the case of the difference in mass, reads

$$\begin{aligned}\Delta M_K^{\text{NP}} &\sim 2 \operatorname{Re}(M_{12}^K) = \frac{16}{3} M_K F_K^2 P_2^{LR}(K) \frac{|a_0|^2 m_s m_d m_t^4}{M_H^2 v^6} \operatorname{Re}[(V_{ts} V_{td}^*)^2] \tan^2 \beta, \\ \Delta M_{B_s}^{\text{NP}} &\sim 2 |M_{12}^s| = \frac{16}{3} M_{B_s} F_{B_s}^2 P_2^{LR}(B_s) \frac{|(a_0 + a_1)(a_0^* + a_2^*)| m_b m_s m_t^4}{M_H^2 v^6} |V_{tb} V_{ts}^*|^2 \tan^2 \beta,\end{aligned}\quad (56)$$

where a_0, a_1 and a_2 are functions of the expansion parameters ϵ_i (see [43] for their expression), P_2^{LR} are hadronic matrix elements and are given e.g. in [66]. M_H the mass of the heavy Higgs boson that is close to the mass of the pseudoscalar, A , in the alignment or decoupling limit $\cos(\alpha - \beta) = 0$. An analogous expression holds for the B_d system. Additional NP contributions can arise from the exchange of the light Higgs boson, h , but these are generically sub-dominant, as they are not enhanced by $\tan \beta$. These expressions show that larger NP effects arise in the B_s system, $\Delta M_{B_s}^{\text{NP}} \gg \Delta M_{B_d}^{\text{NP}} \gg \Delta M_K$, and that the NP contributions have the same dependence on the quark masses and CKM elements, as in the SM. This particular structure leads to not too strong constraints on the heavy Higgs boson masses. Even in the case of $\mathcal{O}(1)$ phases in the ϵ_i parameters, one finds the condition $\tan \beta (v/M_H) < \text{few}$, leading to EW scale heavy Higgs bosons, in the case of not too large values of $\tan \beta$ [53].

Similarly, Higgs exchange tree-level diagrams contribute to the rare $B_{s,d} \rightarrow \mu^+ \mu^-$ decays. If we assume the decoupling (or alignment limit), $\cos(\alpha - \beta) = 0$, and $m_H = m_A$, then the pseudoscalar and scalar contributions are the same and the branching ratios of the $B_{s,d}$ rare decays read [53]

$$\frac{\operatorname{BR}(B_{s,d} \rightarrow \mu^+ \mu^-)}{\operatorname{BR}(B_{s,d} \rightarrow \mu^+ \mu^-)_{\text{SM}}} \simeq |1 + R_{s,d}|^2 + |R_{s,d}|^2, \quad (57)$$

with

$$R_{s,d} = (a_0^* + a_1^*) \frac{2\pi^2 m_t^2}{Y(x_t) m_W^2} \frac{m_{B_{s,d}}^2 \tan^2 \beta}{(1 + m_{s,d}/m_b) M_H^2}, \quad (58)$$

where we have neglected the (small) contribution of the lightest Higgs, h , that is not $\tan^2 \beta$ enhanced. It is straightforward to demonstrate that the branching ratios predicted by this MFV 2HDM obey to the relation in (50), modulo corrections proportional to the ratios of masses $m_{s,d}/m_b$. These corrections are, however, well below the parametric uncertainties on the SM predictions for the two branching ratios. Using Eqs. (57) and (58), one can place constraints from the measurements of $B_s \rightarrow \mu^+ \mu^-$ in the famous $m_A - \tan \beta$ plane. As shown in e.g. [67], these constraints are complementary to the constraints that arise from the LHC direct searches of heavy new scalar/pseudoscalars (e.g. searches for $pp \rightarrow H, A \rightarrow \tau^+ \tau^-$ [68, 69]).

4.2 Flavor breaking in the SUSY models

In spite of the (so far) LHC null-results in searching for TeV-scale SUSY, Supersymmetry remains one of the best motivated theories beyond the SM. The particle content of the Minimal Supersymmetric Standard Model (MSSM) consists of the SM gauge and fermion fields plus a scalar partner for each quark and lepton (squarks and sleptons) and a spin-1/2 partner for each gauge field (gauginos). The Higgs sector has two Higgs doublets with the corresponding spin-1/2 partners (Higgsinos). Similarly to the SM (see Sec. 2.1), the MSSM Supersymmetry preserving Lagrangian is completely determined by symmetry principles and it has a relatively small set of free parameters. However, to make the MSSM phenomenologically viable, one also has to introduce soft SUSY breaking terms. The most general soft

SUSY breaking Lagrangian that is gauge invariant and respects R-parity reads

$$\begin{aligned}
 \mathcal{L}_{\text{soft}} &= \frac{1}{2}M_1\lambda_B\lambda_B + \frac{1}{2}M_2\lambda_W\lambda_W + \frac{1}{2}M_3\lambda_g\lambda_g - m_{H_d}^2|H_d|^2 - m_{H_u}^2|H_u|^2 \\
 &- \tilde{m}_Q^2\tilde{Q}_L^*\tilde{Q}_L - \tilde{m}_D^2\tilde{d}_R^*\tilde{d}_R - \tilde{m}_U^2\tilde{u}_R^*\tilde{u}_R - \tilde{m}_L^2\tilde{\ell}_L^*\tilde{\ell}_L - \tilde{m}_E^2\tilde{e}_R^*\tilde{e}_R \\
 &+ B\mu H_u H_d + \hat{A}_\ell\tilde{\ell}H_d\tilde{e}_R^* + \hat{A}_D\tilde{q}H_d\tilde{d}_R^* - \hat{A}_U\tilde{q}H_u\tilde{u}_R^*,
 \end{aligned} \tag{59}$$

with M_1, M_2, M_3 Majorana masses for the gauginos and m_{H_d}, m_{H_u} soft masses for the two Higgs boson doublets. In all generality, the squark and slepton soft masses ($\tilde{m}_Q, \tilde{m}_D, \tilde{m}_U, \tilde{m}_L, \tilde{m}_E$) as well as the trilinear couplings ($\hat{A}_\ell, \hat{A}_D, \hat{A}_U$) are 3×3 matrices in flavor space and introduce an additional very large number of free parameters (33 new angles and 47 new phases, of which 2 can be rotated away by field redefinitions). These soft terms lead to gluino, Higgsino and gaugino flavor changing couplings. It has been shown that low energy flavor measurements lead to bounds on the squark masses up to 10^3 TeV in the case of a completely generic flavor structure (see e.g [70]). In other words, in the case of TeV-scale SUSY, the rich flavor structure of the MSSM generically leads to large contributions to FCNC processes in conflict with available experimental data: the so-called *SUSY flavor problem*. Several models that address this problem have been proposed in the literature: models with mechanisms of SUSY breaking with flavor universality, such as in gauge mediation models [71], models with heavy squarks and sleptons, such as in (mini) split-SUSY [72–77], or models with alignment of quark with squark mass matrices [78].

MFV represents an interesting alternative. The MFV hypothesis can easily be implemented in the MSSM framework. The squark mass terms and the trilinear quark-squark-Higgs couplings can be expressed as follows

$$\begin{aligned}
 \tilde{m}_Q^2 &= \tilde{m}^2 \left(a_1 \mathbb{1} + b_1 Y_u Y_u^\dagger + b_2 Y_d Y_d^\dagger + b_3 Y_d Y_d^\dagger Y_u Y_u^\dagger + \dots \right), \\
 \tilde{m}_U^2 &= \tilde{m}^2 \left(a_2 \mathbb{1} + b_5 Y_u^\dagger Y_u + \dots \right), \\
 \tilde{m}_D^2 &= \tilde{m}^2 \left(a_3 \mathbb{1} + b_6 Y_d^\dagger Y_d + \dots \right), \\
 \hat{A}_U &= \tilde{A} \left(a_4 \mathbb{1} + b_7 Y_d Y_d^\dagger + \dots \right) Y_u, \\
 \hat{A}_D &= \tilde{A} \left(a_5 \mathbb{1} + b_8 Y_u Y_u^\dagger + \dots \right) Y_d,
 \end{aligned} \tag{60}$$

with the parameters \tilde{m} and \tilde{A} that set the the overall scale of the soft-breaking terms and the dimensionless coefficients a_i and b_i generic $\mathcal{O}(1)$ free complex parameters of the model. The several soft masses and trilinear terms are described by a matrix proportional to the identity plus (small) corrections, suppressed by small Yukawa couplings and CKM elements.

The NP effects in low energy flavor observables can, therefore, be computed using the so-called mass insertion approximation [79]. More specifically, every observable can be expressed by an expansion in $\delta = \Delta/\tilde{m}^2$, with Δ the off-diagonal terms in the sfermion mass matrices (proportional to the small Yukawas in the case of MFV). Using this method, one can demonstrate that, with the flavor structure in (60) and the corresponding one in the down sector, squark masses \tilde{m} at around the TeV scale are still consistent with flavor constraints [80]. We can then conclude that, if MFV holds, the present bounds on FCNCs do not exclude squarks in the LHC reach. LHC squark direct searches and low energy flavor observables are, therefore, two complementary probes of MFV SUSY models.

4.3 Top and Higgs flavor violating signatures

So far in these lectures, we have discussed low energy flavor observables that have been/will be measured by B-factories and by the LHCb. High energy flavor measurements by the ATLAS and CMS collaborations provide a complementary tool to test the underlying flavor structure of Nature. Particularly, in

Decay mode	SM prediction	LHC bound	Comments and References
$\text{BR}(t \rightarrow ch)$	3×10^{-15}	4.6×10^{-3}	$h \rightarrow \text{lept.}$ [81], $h \rightarrow b\bar{b}$ [82, 83], $h \rightarrow \gamma\gamma$ [84]
$\text{BR}(t \rightarrow uh)$	2×10^{-17}	4.2×10^{-3}	$h \rightarrow b\bar{b}$ [82, 83], $h \rightarrow \gamma\gamma$ [84]
$\text{BR}(t \rightarrow cg)$	5×10^{-12}	2×10^{-4}	Single top production [85]
$\text{BR}(t \rightarrow ug)$	4×10^{-14}	4×10^{-5}	Single top production [85]
$\text{BR}(t \rightarrow uZ)$	8×10^{-17}	1.7×10^{-4}	$Z \rightarrow \ell\ell$ [86, 87], tZ production [88]
$\text{BR}(t \rightarrow cZ)$	10^{-14}	2×10^{-4}	$Z \rightarrow \ell\ell$ [86, 87], tZ production [88]
$\text{BR}(t \rightarrow u\gamma)$	4×10^{-16}	1.3×10^{-4}	Single top production [89]
$\text{BR}(t \rightarrow c\gamma)$	5×10^{-14}	1.7×10^{-3}	Single top production [89]

Table 2: SM prediction for the several flavor changing top decay branching fractions (from [90]). Also shown the present LHC bounds, as well as a few details about the searches and the corresponding reference.

the last few years, a tremendous progress has been achieved in the measurement of Higgs and top flavor violating couplings. This is the topic of the last section of these lectures.

The top quark is the only quark whose Yukawa coupling to the Higgs boson is order of unity and the only one with a mass larger than the mass of the weak gauge bosons. Thanks to its heavy mass, the top mainly decays to a W boson and a bottom quark, with an extremely small life time of approximately 5×10^{-25} s. This is shorter than the hadronization time, making it impossible for the top quark to form bound states. For these reasons the top quark plays a special role in the Standard Model and in many BSM extensions thereof. An accurate knowledge of its properties can bring key information on fundamental interactions at the electroweak scale and beyond. So far, the flavor conserving properties of the top are known with a very good accuracy. Less is known about the flavor changing top couplings.

The flavor changing decays of the top quark are suppressed by the GIM mechanism, similarly to what happens to the other quarks. The decay of a top quark to a Z boson or a photon and an up or charm quark occurs only through higher-order diagrams. These processes should be compared to the tree-level decay to a W boson and a bottom quark, resulting in tiny top flavor changing branching ratios in the framework of the SM. In the second column of Tab. 2, we present the SM predictions for the flavor changing branching ratios of the top. All branching ratios are below the 10^{-13} level! A discovery of a flavor violating top decay in the foreseeable future would, therefore, unequivocally, imply the existence of New Physics.

Several searches for top flavor changing couplings have been performed at the LHC, and, so far, there is no evidence for non zero couplings. In the third column of Tab. 2 we show the state of the art of the most stringent constraints on the several branching ratios. All searches have been performed using the full 8 TeV luminosity. Some searches look directly for top flavor changing decays; some other for single top production, eventually in association with a Z or a photon. Projections of these constraints for the HL-LHC show that we could reach the sensitivity to flavor changing branching ratios at the level of $\text{BR}(t \rightarrow gc) \lesssim 4 \times 10^{-6}$ and $\text{BR}(t \rightarrow hq) \lesssim 2 \times 10^{-4}$ [91]. These values are still quite larger than the corresponding SM predictions, but will be crucial for testing the prediction of Randall-Sundrum models [92] and of 2HDMs with a generic flavor structure, that can predict branching ratios as large as $\text{BR}(t \rightarrow gc)_{2\text{HDM}} \sim 10^{-5}$ and $\text{BR}(t \rightarrow hq)_{2\text{HDM}} \sim 2 \times 10^{-3}$, $\text{BR}(t \rightarrow hq)_{\text{RS}} \sim 10^{-4}$, in agreement with the present low energy flavor constraints [93, 94].

As we have discussed in Sec. 2.1, the Higgs is intrinsically connected to the flavor puzzle, as without Yukawa interactions the SM flavor symmetry, $\mathcal{G}_{\text{flavor}}$, would be un-broken. For this reason, it is of paramount importance to test the couplings of the Higgs with quarks and leptons at the LHC. By now, we know that the masses of the third generation quarks and leptons are largely due to the 125 GeV

Higgs, as indicated by the measured values of Higgs couplings to the third generation fermions. Little is known about the origin of the masses of the first and second generation fermions and about flavor changing Higgs couplings.

In the SM, in spite of the very small Higgs width, flavor violating Higgs decays have a negligible branching ratio. Generically, flavor violating Yukawa couplings are well constrained by the low energy FCNC measurements [95, 96]. A notable exception are the flavor violating couplings involving a tau lepton. Models with extra sources of EWSB, can predict a sizable (% level) Higgs flavor violating decays to a tau and a lepton, while being in agreement with low energy flavor observables, as $\tau \rightarrow \mu\gamma$ [97].

A few searches for Higgs flavor violating decays $h \rightarrow \tau\mu$, $h \rightarrow \tau e$ have been performed by the LHC [98–102], so far not showing a convincing evidence for non-zero branching ratios (see, however, the initial small anomaly shown by the CMS collaboration in [98]). It will be very interesting to monitor these searches in the coming years of the LHC, as they could give a complementary probe of models with sizable flavor changing Higgs couplings to leptons.

5 Summary

An essential feature of flavor physics is its capability to probe very high scales, beyond the kinematical reach of high energy colliders. At the same time, flavor physics can teach us about properties of TeV-scale new physics (i.e. how new particles couple to the SM degrees of freedom), offering complementarity with searches of NP at colliders.

In these lectures, I discussed the flavor structure of the SM, particularly focusing on the symmetry principles of the SM Lagrangian and on how the flavor symmetry is broken. Flavor changing neutral processes in the SM are highly suppressed, both because they arise at least at the loop-level and because of the GIM mechanism that introduces the dependence of these processes on the small CKM off-diagonal elements and on the small quark masses.

Due to the SM suppression of FCNC processes, flavor transitions offer a unique opportunity to test the New Physics flavor structure. Generically NP models predict too large contributions to flavor transitions (the “New Physics flavor problem”) leading us to conclude that, if TeV-scale New Physics exists, it must have a highly non generic flavor structure, as for example it can obey to the Minimal Flavor Violation principle.

Several experiments are running and will be running in the coming years (LHCb, Belle II, NA62, KOTO and many lepton flavor experiments) and many more observables will be measured precisely. Some of the golden channels for the coming years are

- More precise measurement of the clean rare decays $B_s \rightarrow \mu^+\mu^-$ and $B_d \rightarrow \mu^+\mu^-$ at LHCb, ATLAS and CMS. The ratio of branching ratios will give us more insights on the validity of the MFV ansatz.
- Additional tests of the lepton universality relations in B decays at LHCb and Belle II: $\text{BR}(B \rightarrow Jee)/\text{BR}(B \rightarrow J\mu\mu)$ with $J = K, K^*, X_s, K\pi, \dots$. These are particularly clean tests of the SM, as the theory predictions are known to a very good precision and are not affected by hadronic uncertainties.
- Better measurements of $B \rightarrow D\tau\nu$ and $B \rightarrow D^*\tau\nu$, to confirm or disprove the present anomaly in these decays, as observed at Belle, Babar and LHCb [15, 16, 18, 19].
- Brand new measurements of $B \rightarrow K^{(*)}\nu\nu$ and $K \rightarrow \pi\nu\nu$ at Belle II and KOTO, respectively.
- Additional searches of top and Higgs flavor violating couplings at the LHC.

These channels (and several others) will be able either to set interesting constraints on NP, or to shed light into the existence of new degrees of freedom beyond the SM.

Acknowledgements

I would like to thank Wolfgang Altmannshofer and my student, Douglas Tuckler, for comments on the manuscript. I acknowledge support from the University of Cincinnati. I wish to thank the organizers of the 2015 European School of High-Energy Physics in Bansko for the invitation. I am also grateful to the students and the discussion leaders for interesting discussions.

References

- [1] A. J. Buras, “Weak Hamiltonian, CP violation and rare decays,” hep-ph/9806471.
- [2] G. Branco, L. Lavoura and J. Silva, “CP Violation”, Clarendon Press, Oxford, UK (1999)
- [3] A. V. Manohar and M. B. Wise, “Heavy quark physics,” Camb. Monogr. Part. Phys. Nucl. Phys. Cosmol. **10**, 1 (2000).
- [4] Y. Nir, “CP violation in meson decays,” hep-ph/0510413.
- [5] B. Grinstein, “TASI-2013 Lectures on Flavor Physics,” arXiv:1501.05283 [hep-ph].
- [6] Z. Ligeti, “TASI Lectures on Flavor Physics,” arXiv:1502.01372 [hep-ph].
- [7] A. de Gouvea and P. Vogel, “Lepton Flavor and Number Conservation, and Physics Beyond the Standard Model,” Prog. Part. Nucl. Phys. **71**, 75 (2013) [arXiv:1303.4097 [hep-ph]].
- [8] G. Aad *et al.* [ATLAS Collaboration], “Observation of a new particle in the search for the Standard Model Higgs boson with the ATLAS detector at the LHC,” Phys. Lett. B **716**, 1 (2012) [arXiv:1207.7214 [hep-ex]].
- [9] S. Chatrchyan *et al.* [CMS Collaboration], “Observation of a new boson at a mass of 125 GeV with the CMS experiment at the LHC,” Phys. Lett. B **716**, 30 (2012) [arXiv:1207.7235 [hep-ex]].
- [10] G. Aad *et al.* [ATLAS and CMS Collaborations], “Measurements of the Higgs boson production and decay rates and constraints on its couplings from a combined ATLAS and CMS analysis of the LHC pp collision data at $\sqrt{s} = 7$ and 8 TeV,” JHEP **1608**, 045 (2016) [arXiv:1606.02266 [hep-ex]].
- [11] R. Aaij *et al.* [LHCb Collaboration], “Measurement of Form-Factor-Independent Observables in the Decay $B^0 \rightarrow K^{*0} \mu^+ \mu^-$,” Phys. Rev. Lett. **111**, 191801 (2013) [arXiv:1308.1707 [hep-ex]].
- [12] R. Aaij *et al.* [LHCb Collaboration], “Angular analysis of the $B^0 \rightarrow K^{*0} \mu^+ \mu^-$ decay using 3 fb $^{-1}$ of integrated luminosity,” JHEP **1602**, 104 (2016) [arXiv:1512.04442 [hep-ex]].
- [13] A. Abdesselam *et al.* [Belle Collaboration], “Angular analysis of $B^0 \rightarrow K^*(892)^0 \ell^+ \ell^-$,” arXiv:1604.04042 [hep-ex].
- [14] R. Aaij *et al.* [LHCb Collaboration], “Test of lepton universality using $B^+ \rightarrow K^+ \ell^+ \ell^-$ decays,” Phys. Rev. Lett. **113**, 151601 (2014) [arXiv:1406.6482 [hep-ex]].
- [15] J. P. Lees *et al.* [BaBar Collaboration], “Measurement of an Excess of $\bar{B} \rightarrow D^{(*)} \tau^- \bar{\nu}_\tau$ Decays and Implications for Charged Higgs Bosons,” Phys. Rev. D **88**, no. 7, 072012 (2013) [arXiv:1303.0571 [hep-ex]].
- [16] M. Huschle *et al.* [Belle Collaboration], “Measurement of the branching ratio of $\bar{B} \rightarrow D^{(*)} \tau^- \bar{\nu}_\tau$ relative to $\bar{B} \rightarrow D^{(*)} \ell^- \bar{\nu}_\ell$ decays with hadronic tagging at Belle,” Phys. Rev. D **92**, no. 7, 072014 (2015) [arXiv:1507.03233 [hep-ex]].
- [17] A. Abdesselam *et al.* [Belle Collaboration], “Measurement of the branching ratio of $\bar{B}^0 \rightarrow D^{*+} \tau^- \bar{\nu}_\tau$ relative to $\bar{B}^0 \rightarrow D^{*+} \ell^- \bar{\nu}_\ell$ decays with a semileptonic tagging method,” arXiv:1603.06711 [hep-ex].
- [18] J. P. Lees *et al.* [BaBar Collaboration], “Evidence for an excess of $\bar{B} \rightarrow D^{(*)} \tau^- \bar{\nu}_\tau$ decays,” Phys. Rev. Lett. **109**, 101802 (2012) [arXiv:1205.5442 [hep-ex]].
- [19] R. Aaij *et al.* [LHCb Collaboration], “Measurement of the ratio of branching fractions $\mathcal{B}(\bar{B}^0 \rightarrow D^{*+} \tau^- \bar{\nu}_\tau) / \mathcal{B}(\bar{B}^0 \rightarrow D^{*+} \mu^- \bar{\nu}_\mu)$,” Phys. Rev. Lett. **115**, no. 11, 111803 (2015) Addendum: [Phys. Rev. Lett. **115**, no. 15, 159901 (2015)] [arXiv:1506.08614 [hep-ex]].

- [20] R. D. Peccei and H. R. Quinn, “Constraints Imposed by CP Conservation in the Presence of Instantons,” *Phys. Rev. D* **16**, 1791 (1977).
- [21] L. L. Chau and W. Y. Keung, “Comments on the Parametrization of the Kobayashi-Maskawa Matrix,” *Phys. Rev. Lett.* **53**, 1802 (1984).
- [22] L. Wolfenstein, “Parametrization of the Kobayashi-Maskawa Matrix,” *Phys. Rev. Lett.* **51**, 1945 (1983).
- [23] J. Charles *et al.* [CKMfitter Group Collaboration], “CP violation and the CKM matrix: Assessing the impact of the asymmetric B factories,” *Eur. Phys. J. C* **41**, no. 1, 1 (2005) [hep-ph/0406184]. Updated results and plots available at: <http://ckmfitter.in2p3.fr>.
- [24] M. Bona *et al.* [UTfit Collaboration], “The Unitarity Triangle Fit in the Standard Model and Hadronic Parameters from Lattice QCD: A Reappraisal after the Measurements of Δm_s and $\text{BR}(B \rightarrow \tau\nu_\tau)$,” *JHEP* **0610** (2006) 081 [hep-ph/0606167]. Updated results and plots available at: <http://www.utfit.org/UTfit/>
- [25] J. Laiho, E. Lunghi and R. S. Van de Water, “Lattice QCD inputs to the CKM unitarity triangle analysis,” *Phys. Rev. D* **81**, 034503 (2010) [arXiv:0910.2928 [hep-ph]].
- [26] S. L. Glashow, J. Iliopoulos and L. Maiani, “Weak Interactions with Lepton-Hadron Symmetry,” *Phys. Rev. D* **2**, 1285 (1970).
- [27] G. Buchalla, A. J. Buras and M. E. Lautenbacher, “Weak decays beyond leading logarithms,” *Rev. Mod. Phys.* **68**, 1125 (1996) [hep-ph/9512380].
- [28] V. M. Abazov *et al.* [D0 Collaboration], “Evidence for an anomalous like-sign dimuon charge asymmetry,” *Phys. Rev. Lett.* **105**, 081801 (2010) [arXiv:1007.0395 [hep-ex]].
- [29] V. M. Abazov *et al.* [D0 Collaboration], “Study of CP-violating charge asymmetries of single muons and like-sign dimuons in pp collisions,” *Phys. Rev. D* **89**, no. 1, 012002 (2014) [arXiv:1310.0447 [hep-ex]].
- [30] V. M. Abazov *et al.* [D0 Collaboration], “Search for CP violation in $B_s^0 \rightarrow \mu^+ D_s^- X$ decays in $p\bar{p}$ collisions at $\sqrt{s} = 1.96$ TeV,” *Phys. Rev. D* **82**, 012003 (2010) Erratum: [*Phys. Rev. D* **83**, 119901 (2011)] [arXiv:0904.3907 [hep-ex]].
- [31] M. Artuso, G. Borissov and A. Lenz, “CP Violation in the B_s^0 System,” arXiv:1511.09466 [hep-ph].
- [32] Y. Amhis *et al.* [Heavy Flavor Averaging Group (HFAG) Collaboration], “Averages of b -hadron, c -hadron, and τ -lepton properties as of summer 2014,” arXiv:1412.7515 [hep-ex]. and online updates at <http://www.slac.stanford.edu/xorg/hfag/>
- [33] R. Aaij *et al.* [LHCb Collaboration], “Measurements of CP violation in the three-body phase space of charmless B^\pm decays,” *Phys. Rev. D* **90**, no. 11, 112004 (2014) [arXiv:1408.5373 [hep-ex]].
- [34] B. Aubert *et al.* [BaBar Collaboration], “Measurement of Time-Dependent CP Asymmetry in $B_0 \rightarrow c\bar{c}K^{*0}$ Decays,” *Phys. Rev. D* **79**, 072009 (2009) [arXiv:0902.1708 [hep-ex]].
- [35] I. Adachi *et al.*, “Precise measurement of the CP violation parameter $\sin(2\phi_1)$ in $B_0 \rightarrow (c\bar{c})K_0$ decays,” *Phys. Rev. Lett.* **108**, 171802 (2012) [arXiv:1201.4643 [hep-ex]].
- [36] R. Aaij *et al.* [LHCb Collaboration], “Measurement of CP violation in $B^0 \rightarrow J/\psi K_S^0$ decays,” *Phys. Rev. Lett.* **115**, no. 3, 031601 (2015) [arXiv:1503.07089 [hep-ex]].
- [37] R. Fleischer, “CP violation in the B system and relations to $K \rightarrow \pi\nu\bar{\nu}$ decays,” *Phys. Rept.* **370**, 537 (2002) [hep-ph/0207108].
- [38] G. Isidori, Y. Nir and G. Perez, “Flavor Physics Constraints for Physics Beyond the Standard Model,” *Ann. Rev. Nucl. Part. Sci.* **60**, 355 (2010) [arXiv:1002.0900 [hep-ph]].
- [39] G. Isidori, “Flavor physics and CP violation,” arXiv:1302.0661 [hep-ph].
- [40] R. S. Chivukula and H. Georgi, “Composite Technicolor Standard Model,” *Phys. Lett. B* **188**, 99 (1987).
- [41] L. J. Hall and L. Randall, “Weak scale effective supersymmetry,” *Phys. Rev. Lett.* **65**, 2939 (1990).

- [42] A. J. Buras, P. Gambino, M. Gorbahn, S. Jager and L. Silvestrini, “Universal unitarity triangle and physics beyond the standard model,” *Phys. Lett. B* **500**, 161 (2001) [hep-ph/0007085].
- [43] G. D’Ambrosio, G. F. Giudice, G. Isidori and A. Strumia, “Minimal flavor violation: An Effective field theory approach,” *Nucl. Phys. B* **645**, 155 (2002) [hep-ph/0207036].
- [44] W. Altmannshofer, “The $B_s \rightarrow \mu^+ \mu^-$ and $B_d \rightarrow \mu^+ \mu^-$ Decays: Standard Model and Beyond,” *PoS Beauty* **2013**, 024 (2013) [arXiv:1306.0022 [hep-ph]].
- [45] T. Blake, G. Lanfranchi and D. M. Straub, “Rare B Decays as Tests of the Standard Model,” arXiv:1606.00916 [hep-ph].
- [46] W. Altmannshofer, A. J. Buras, S. Gori, P. Paradisi and D. M. Straub, “Anatomy and Phenomenology of FCNC and CPV Effects in SUSY Theories,” *Nucl. Phys. B* **830**, 17 (2010) [arXiv:0909.1333 [hep-ph]].
- [47] S. Aoki *et al.*, “Review of lattice results concerning low-energy particle physics,” arXiv:1607.00299 [hep-lat].
- [48] C. Bobeth, M. Gorbahn, T. Hermann, M. Misiak, E. Stamou and M. Steinhauser, “ $B_{s,d} \rightarrow l^+ l^-$ in the Standard Model with Reduced Theoretical Uncertainty,” *Phys. Rev. Lett.* **112**, 101801 (2014) [arXiv:1311.0903 [hep-ph]].
- [49] T. Aaltonen *et al.* [CDF Collaboration], “Search for $B_s^0 \rightarrow \mu^+ \mu^-$ and $B^0 \rightarrow \mu^+ \mu^-$ decays with the full CDF Run II data set,” *Phys. Rev. D* **87**, no. 7, 072003 (2013) [arXiv:1301.7048 [hep-ex]].
- [50] V. Khachatryan *et al.* [CMS and LHCb Collaborations], “Observation of the rare $B_s^0 \rightarrow \mu^+ \mu^-$ decay from the combined analysis of CMS and LHCb data,” *Nature* **522**, 68 (2015) [arXiv:1411.4413 [hep-ex]].
- [51] M. Aaboud *et al.* [ATLAS Collaboration], “Study of the rare decays of B_s^0 and B^0 into muon pairs from data collected during the LHC Run 1 with the ATLAS detector,” *Eur. Phys. J. C* **76**, no. 9, 513 (2016) [arXiv:1604.04263 [hep-ex]].
- [52] W. Altmannshofer and D. M. Straub, “Cornering New Physics in $b \rightarrow s$ Transitions,” *JHEP* **1208**, 121 (2012) [arXiv:1206.0273 [hep-ph]].
- [53] A. J. Buras, M. V. Carlucci, S. Gori and G. Isidori, “Higgs-mediated FCNCs: Natural Flavour Conservation vs. Minimal Flavour Violation,” *JHEP* **1010**, 009 (2010) [arXiv:1005.5310 [hep-ph]].
- [54] A. J. Buras, “Relations between $\Delta M(s, d)$ and $B(s, d) \rightarrow \mu \bar{\mu}$ in models with minimal flavor violation,” *Phys. Lett. B* **566**, 115 (2003) [hep-ph/0303060].
- [55] R. Aaij *et al.* [LHCb Collaboration], “Implications of LHCb measurements and future prospects,” *Eur. Phys. J. C* **73**, no. 4, 2373 (2013) [arXiv:1208.3355 [hep-ex]].
- [56] S. L. Glashow and S. Weinberg, “Natural Conservation Laws for Neutral Currents,” *Phys. Rev. D* **15**, 1958 (1977).
- [57] E. A. Paschos, “Diagonal Neutral Currents,” *Phys. Rev. D* **15**, 1966 (1977).
- [58] G. C. Branco, P. M. Ferreira, L. Lavoura, M. N. Rebelo, M. Sher and J. P. Silva, “Theory and phenomenology of two-Higgs-doublet models,” *Phys. Rept.* **516**, 1 (2012) [arXiv:1106.0034 [hep-ph]].
- [59] J. F. Gunion and H. E. Haber, “The CP conserving two Higgs doublet model: The Approach to the decoupling limit,” *Phys. Rev. D* **67**, 075019 (2003) [hep-ph/0207010].
- [60] S. Davidson and H. E. Haber, “Basis-independent methods for the two-Higgs-doublet model,” *Phys. Rev. D* **72**, 035004 (2005) Erratum: [*Phys. Rev. D* **72**, 099902 (2005)] [hep-ph/0504050].
- [61] P. M. Ferreira, L. Lavoura and J. P. Silva, “Renormalization-group constraints on Yukawa alignment in multi-Higgs-doublet models,” *Phys. Lett. B* **688**, 341 (2010) [arXiv:1001.2561 [hep-ph]].
- [62] A. Pich and P. Tuzon, “Yukawa Alignment in the Two-Higgs-Doublet Model,” *Phys. Rev. D* **80**, 091702 (2009) [arXiv:0908.1554 [hep-ph]].
- [63] S. Gori, H. E. Haber and E. Santos, “High scale flavor alignment in the two-Higgs doublet model

- and its phenomenology", in preparation.
- [64] W. Altmannshofer, S. Gori and G. D. Kribs, "A Minimal Flavor Violating 2HDM at the LHC," *Phys. Rev. D* **86**, 115009 (2012) [arXiv:1210.2465 [hep-ph]].
 - [65] A. L. Kagan, G. Perez, T. Volansky and J. Zupan, "General Minimal Flavor Violation," *Phys. Rev. D* **80**, 076002 (2009) [arXiv:0903.1794 [hep-ph]].
 - [66] A. J. Buras, S. Jager and J. Urban, "Master formulae for $\Delta F = 2$ NLO QCD factors in the standard model and beyond," *Nucl. Phys. B* **605**, 600 (2001) [hep-ph/0102316].
 - [67] W. Altmannshofer, M. Carena, N. R. Shah and F. Yu, "Indirect Probes of the MSSM after the Higgs Discovery," *JHEP* **1301**, 160 (2013) [arXiv:1211.1976 [hep-ph]].
 - [68] M. Aaboud *et al.* [ATLAS Collaboration], "Search for Minimal Supersymmetric Standard Model Higgs bosons H/A and for a Z' boson in the $\tau\tau$ final state produced in pp collisions at $\sqrt{s} = 13$ TeV with the ATLAS Detector," arXiv:1608.00890 [hep-ex].
 - [69] CMS Collaboration, "Search for a neutral MSSM Higgs boson decaying into $\tau\tau$ at 13 TeV," CMS-PAS-HIG-16-006.
 - [70] W. Altmannshofer, R. Harnik and J. Zupan, "Low Energy Probes of PeV Scale Sfermions," *JHEP* **1311**, 202 (2013) [arXiv:1308.3653 [hep-ph]].
 - [71] G. F. Giudice and R. Rattazzi, "Theories with gauge mediated supersymmetry breaking," *Phys. Rept.* **322**, 419 (1999) [hep-ph/9801271].
 - [72] N. Arkani-Hamed and S. Dimopoulos, "Supersymmetric unification without low energy supersymmetry and signatures for fine-tuning at the LHC," *JHEP* **0506**, 073 (2005) [hep-th/0405159].
 - [73] G. F. Giudice and A. Romanino, "Split supersymmetry," *Nucl. Phys. B* **699**, 65 (2004) Erratum: [*Nucl. Phys. B* **706**, 487 (2005)] [hep-ph/0406088].
 - [74] N. Arkani-Hamed, S. Dimopoulos, G. F. Giudice and A. Romanino, "Aspects of split supersymmetry," *Nucl. Phys. B* **709**, 3 (2005) [hep-ph/0409232].
 - [75] L. J. Hall and Y. Nomura, "Spread Supersymmetry," *JHEP* **1201**, 082 (2012) [arXiv:1111.4519 [hep-ph]].
 - [76] A. Arvanitaki, N. Craig, S. Dimopoulos and G. Villadoro, "Mini-Split," *JHEP* **1302**, 126 (2013) [arXiv:1210.0555 [hep-ph]].
 - [77] N. Arkani-Hamed, A. Gupta, D. E. Kaplan, N. Weiner and T. Zorawski, "Simply Unnatural Supersymmetry," arXiv:1212.6971 [hep-ph].
 - [78] Y. Nir and N. Seiberg, "Should squarks be degenerate?," *Phys. Lett. B* **309**, 337 (1993) [hep-ph/9304307].
 - [79] L. J. Hall, V. A. Kostelecky and S. Raby, "New Flavor Violations in Supergravity Models," *Nucl. Phys. B* **267**, 415 (1986).
 - [80] W. Altmannshofer, A. J. Buras and D. Guadagnoli, "The MFV limit of the MSSM for low $\tan(\beta)$: Meson mixings revisited," *JHEP* **0711**, 065 (2007) [hep-ph/0703200].
 - [81] CMS Collaboration, "Search for top quark decays via Higgs-boson-mediated flavor changing neutral currents in pp collisions at $\sqrt{s} = 8$ TeV," CMS-PAS-TOP-13-017.
 - [82] G. Aad *et al.* [ATLAS Collaboration], "Search for flavour-changing neutral current top quark decays $t \rightarrow Hq$ in pp collisions at $\sqrt{s} = 8$ TeV with the ATLAS detector," *JHEP* **1512**, 061 (2015) [arXiv:1509.06047 [hep-ex]].
 - [83] CMS Collaboration, "Search for the Flavor-Changing Neutral Current Decay $t \rightarrow qH$ Where the Higgs Decays to $b\bar{b}$ Pairs at $\sqrt{s} = 8$ TeV," CMS-PAS-TOP-14-020.
 - [84] CMS Collaboration, "Search for top quark decays $t \rightarrow qH$ with $H \rightarrow \gamma\gamma$ in pp collisions at $\sqrt{s} = 8$ TeV," CMS-PAS-TOP-14-019.
 - [85] G. Aad *et al.* [ATLAS Collaboration], "Search for single top-quark production via flavour-changing neutral currents at 8 TeV with the ATLAS detector," *Eur. Phys. J. C* **76**, no. 2, 55 (2016)

- [arXiv:1509.00294 [hep-ex]].
- [86] G. Aad *et al.* [ATLAS Collaboration], “Search for flavour-changing neutral current top-quark decays to qZ in pp collision data collected with the ATLAS detector at $\sqrt{s} = 8$ TeV,” *Eur. Phys. J. C* **76**, no. 1, 12 (2016) [arXiv:1508.05796 [hep-ex]].
- [87] S. Chatrchyan *et al.* [CMS Collaboration], “Search for Flavor-Changing Neutral Currents in Top-Quark Decays $t \rightarrow Zq$ in pp Collisions at $\sqrt{s} = 8$ TeV,” *Phys. Rev. Lett.* **112**, no. 17, 171802 (2014) [arXiv:1312.4194 [hep-ex]].
- [88] CMS Collaboration, “Search for associated production of a Z boson with a single top quark and for tZ flavour-changing interactions in pp collisions at $\sqrt{s} = 8$ TeV,” CMS-PAS-TOP-12-039.
- [89] V. Khachatryan *et al.* [CMS Collaboration], “Search for anomalous single top quark production in association with a photon in pp collisions at $\sqrt{s} = 8$ TeV,” *JHEP* **1604**, 035 (2016) [arXiv:1511.03951 [hep-ex]].
- [90] J. A. Aguilar-Saavedra, “Top flavor-changing neutral interactions: Theoretical expectations and experimental detection,” *Acta Phys. Polon. B* **35**, 2695 (2004) [hep-ph/0409342].
- [91] K. Agashe *et al.* [Top Quark Working Group Collaboration], “Working Group Report: Top Quark,” arXiv:1311.2028 [hep-ph].
- [92] L. Randall and R. Sundrum, “A Large mass hierarchy from a small extra dimension,” *Phys. Rev. Lett.* **83**, 3370 (1999) [hep-ph/9905221].
- [93] D. Atwood, L. Reina and A. Soni, “Phenomenology of two Higgs doublet models with flavor changing neutral currents,” *Phys. Rev. D* **55**, 3156 (1997) [hep-ph/9609279].
- [94] K. Agashe, G. Perez and A. Soni, “Collider Signals of Top Quark Flavor Violation from a Warped Extra Dimension,” *Phys. Rev. D* **75**, 015002 (2007) [hep-ph/0606293].
- [95] G. Blankenburg, J. Ellis and G. Isidori, “Flavour-Changing Decays of a 125 GeV Higgs-like Particle,” *Phys. Lett. B* **712**, 386 (2012) [arXiv:1202.5704 [hep-ph]].
- [96] R. Harnik, J. Kopp and J. Zupan, “Flavor Violating Higgs Decays,” *JHEP* **1303**, 026 (2013) [arXiv:1209.1397 [hep-ph]].
- [97] W. Altmannshofer, S. Gori, A. L. Kagan, L. Silvestrini and J. Zupan, “Uncovering Mass Generation Through Higgs Flavor Violation,” *Phys. Rev. D* **93**, no. 3, 031301 (2016) [arXiv:1507.07927 [hep-ph]].
- [98] V. Khachatryan *et al.* [CMS Collaboration], “Search for Lepton-Flavour-Violating Decays of the Higgs Boson,” *Phys. Lett. B* **749**, 337 (2015) [arXiv:1502.07400 [hep-ex]].
- [99] V. Khachatryan *et al.* [CMS Collaboration], “Search for lepton flavour violating decays of the Higgs boson to $e\tau$ and $e\mu$ in proton-proton collisions at $\sqrt{s} = 8$ TeV,” [arXiv:1607.03561 [hep-ex]].
- [100] CMS Collaboration, “Search for Lepton Flavour Violating Decays of the Higgs Boson in the $\mu - \tau$ final state at 13 TeV,” CMS-PAS-HIG-16-005.
- [101] CMS Collaboration, “Search for lepton-flavour-violating decays of the Higgs boson to $e\tau$ and $e\mu$ at $\sqrt{s} = 8$ TeV,” CMS-PAS-HIG-14-040.
- [102] G. Aad *et al.* [ATLAS Collaboration], “Search for lepton-flavour-violating $H \rightarrow \mu\tau$ decays of the Higgs boson with the ATLAS detector,” *JHEP* **1511**, 211 (2015) [arXiv:1508.03372 [hep-ex]].

Behind the Standard Model

A. Wulzer

University of Padova and INFN, Padova, Italy

Abstract

These lectures provide a concise introduction to the so-called “Beyond the Standard Model” physics, with particular emphasis on the problem of the microscopic origin of the Higgs mass term and of the Electro-Weak symmetry breaking scale in connection with Naturalness. The standard scenarios of Supersymmetry and Composite Higgs are shortly reviewed. An attempt is made to summarise the implications of the LHC run-1 results on what we expect to lie beyond (or behind) the Standard Model.

Keywords

Lectures; beyond the standard model; supersymmetry; composite higgs; naturalness.

1 BSM: What For?

Physics is the continuous effort towards a deeper understanding of the laws of Nature. The Standard Model (SM) theory summarises the state-of-the-art of this understanding, providing the correct description of all known fundamental particles and interactions (including Gravity) at the energy scales we have been capable to explore experimentally so far. “Beyond the SM” (BSM) physics aims to the next step of this understanding, namely to unveil the microscopic origin of the SM itself, of its field content, Lagrangian and parameters. From this viewpoint, the acronym “BSM” should better be read as “Behind” rather than “Beyond” the SM, from which the unconventional title (see however [1]) I gave to these lectures. The main focus is indeed not on new physics (beyond what predicted by the SM) per se, but on the solution of some of the mysteries associated with the microscopic theory that lie behind the SM itself. In this respect, a lack of discovery, namely a non-trivial confirmation of the SM that closes the door to BSM physics potentially associated with one of these mysteries, might be as informative as the observation of new physics.

The one described above is only one of the possible approaches to forefront research in fundamental physics. A valid alternative is to start from observations rather than from theory, in particular from those observations that cannot be accounted for by the SM, signalling the existence of new physics. What I have in mind are of course neutrino masses and oscillations and evidences of Dark Matter, Inflation and Baryogenesis. Dedicated lectures were given at this School on these topics [2] [3]. Even within the context of high-energy physics research, where no BSM discovery crossed our horizon yet ¹, new physics searches driven by data rather than by theory are highly desirable and complementary to the study of specific signal topologies dictated by theoretical BSM scenarios. Also, we should not discard the possibility of performing theory-unbiased new physics searches in final states that appear promising because of their simplicity, of their low SM background and/or of their experimental purity. Notice however that a fully “unbiased” approach to new physics searches is virtually impossible. A certain degree of theory bias is unavoidably needed in order to limit the infinite variety of possible channels (or of experiments) one could search in. Even the very fact that TeV-scale reactions at the LHC are promising places to look at is in itself a theory bias, though dictated by extremely general and robust BSM considerations. Theory-unbiased or theory-driven new physics searches thus just correspond to a different gradation of BSM bias we decide to apply.

¹Still, the ongoing LHC program makes the direct exploration of the energy frontier the most promising tool of investigation we currently have to our disposal. Also, one should not forget the strong impact of Flavour physics [4], because of its capability of indirectly exploring very high-energy scales, on BSM physics.

1.1 No-Lose Theorems

Sometimes, the quest for the microscopic origin of known particles and interactions has extremely powerful implications, leading to absolute *guarantees* of new physics discoveries. A mathematical argument based on currently established laws of Nature, which ensures future discoveries provided the experimental conditions become favourable enough (i.e., high enough energy in the examples that follow), is what we call a “No-Lose Theorem”. Though exceptional in the long history of science, several No-Lose Theorem could be formulated (and exploited, resulting in a number of discoveries) in the context of fundamental interaction physics over the last several decades. So many No-Lose Theorem existed, and for so long, that we got used to them, somehow forgetting their importance and their absolutely exceptional nature. They deserve a review now, after the discovery of the Higgs which prevents the formulation of new No-Lose Theorems marking the end of the age of guaranteed discoveries.

The simplest No-Lose Theorem is the one that guarantees the existence of new physics beyond (and behind) the Fermi Theory of Weak interactions. To appreciate the value of this theorem we must go back to the times when the Fermi Theory was the only experimentally established, potentially “fundamental”, description of Weak interactions. At that times, our knowledge of the Weak force was entirely encapsulated in a four-fermions operator of energy dimension $d = 6$, the Fermi interaction, with its $d = -2$ coefficient, the Fermi constant G_F .² The question of whether the Fermi theory can be truly fundamental or not, and correspondingly whether or not G_F can be a fundamental constant of Nature, has a very sharp negative answer, schematically summarised below

$$\sim G_F E^2 \simeq E^2/v^2 < 16\pi^2 \implies m_W < 4\pi v$$

The point is that the four-fermions scattering amplitude grows with the square of the center-of-mass energy “ E ” of the reaction, a fact that trivially follows from dimensional analysis (since the amplitude is dimensionless and proportional to the $d = -2$ coupling constant G_F) and is intrinsically linked with the non-renormalizable nature of the Fermi Theory. But the Weak scattering amplitude becoming too large, overcoming the critical value of $16\pi^2$, means that the Weak force gets too strong to be treated as a small perturbation of the free-fields dynamics and the perturbative treatment of the theory breaks down. Of course there is nothing conceptually wrong in the Weak force entering a non-perturbative regime, the problem is that this regime cannot be described by the Fermi Theory, which is intrinsically defined in perturbation theory. Namely, the Fermi Theory does not give trustable predictions and becomes internally inconsistent as soon as the non-perturbative regime is approached. Therefore a new theory, i.e. new physics, is absolutely needed. Either in order to modify the energy behaviour of the amplitude before it reaches the non-perturbative threshold, keeping the Weak force perturbative, or to describe the new non-perturbative regime. In all cases this new, more fundamental, theory will account for the microscopic origin of the Fermi interaction and of its coupling strength G_F as a low-energy effective description of the Weak force. According to the theorem, the microscopic theory must show up at an energy scale below $4\pi/\sqrt{G_F} \simeq 4\pi v$, having expressed $G_F = 1/\sqrt{2}v^2$ in terms of the ElectroWeak Symmetry Breaking (EWSB) scale $v \simeq 246$ GeV. We now know that the new physics beyond the Fermi Theory is the Intermediate Vector Boson (IVB) theory, which was confirmed by discovering the W boson at the scale $m_W \simeq 80$ GeV, far below $4\pi v$ compatibly with the theorem.

As everyone knows, well before the discovery of the W discovery we already had strong indirect indications on the validity of the IVB theory and a rather precise estimate of the W boson mass. These indications came from fortunate theoretical speculations and from the measurement of the Weak angle through neutrino scattering processes, and are completely unrelated with the No-Lose Theorem outlined above. Indeed, the theorem makes no assumption on, and gives no indication about, the details of the

²Of course the Cabibbo angle was also needed in order to describe hadronic Weak processes.

microscopic physics that lies behind the Fermi Theory. Namely, the theorem guarantees that something would have been discovered in fermion-fermion scattering, possibly not the W and possibly not at a scale as low as m_W , even if all the theoretical speculations about the IVB theory had turned out to be radically wrong. This means in particular that if the UA1 and UA2 experiments at the CERN SPS collider had not discovered the W , we would have for sure continued searching for it, or for whatever new physics lies behind the Fermi theory, by the construction of higher energy machines.

A situation like the one described above was indeed encountered in the search for the top quark, which according to a widespread belief was expected to be much lighter than $m_t \simeq 173$ GeV, where it was eventually observed. Consequently, the top discovery was expected at several lower-energy colliders, constructed before the Tevatron, which instead produced a number of negative results. However we never got discouraged and we never even considered the possibility of giving up searching for the top quark, or for some other new physics related with the bottom quark, because of a second No-Loose Theorem:

$$\begin{array}{c}
 b \\
 \nearrow \\
 \gamma/Z \\
 \nwarrow \\
 \bar{b}
 \end{array}
 +
 \begin{array}{c}
 W_L \\
 \nearrow \\
 t \\
 \nwarrow \\
 W_L
 \end{array}
 \sim g_W^2 E^2 / m_W^2 < 16\pi^2 \longrightarrow m_t < 4\pi v$$

The theorem relies on the validity of the IVB theory and on the existence of the bottom quark with its neutral current interactions, which we consider here as experimentally established facts at the times when the top was not yet found. The observation is that the amplitude for longitudinally polarised W bosons production from a $b \bar{b}$ pair grows quadratically with the energy if the top quark is absent or if it is too heavy to be relevant. It is indeed the t-channel contribution from the top exchange that makes the amplitude constant at high energies in the complete SM. Perturbativity thus requires new physics at a scale below $4\pi m_W / g_W \simeq 4\pi v$, having used the relation $m_W = g_W v / 2$. When interpreted in the SM, the upper bound on the new physics scale translates in the familiar perturbativity bound on the top mass, however the Theorem does not rely on the SM and on the existence of the top quark. It states that the top, or something else, must exist beyond the bottom quark in order to moderate the growth with the energy of the scattering amplitude. More physically, the Theorem says that the microscopic origin of the bottom quark (e.g., the fact that its left-handed component lives in a doublet together with the top) must reveal itself below $4\pi v$.

Another particle whose discovery was significantly “delayed” with respect to the expectations is the Higgs boson, which also comes with its own No-Loose Theorem:

$$\begin{array}{c}
 W_L \\
 \nearrow \\
 H \\
 \nwarrow \\
 W_L
 \end{array}
 + \dots \sim g_W^2 E^2 / m_W^2 < 16\pi^2 \longrightarrow m_H < 4\pi v$$

The growth with the energy of the longitudinally polarised W bosons scattering amplitude in the IVB theory requires the presence of new particles and/or interactions, once again below the critical threshold of $4\pi v \sim 3$ TeV. Given that the TeV scale is within the reach of the LHC collider, the Theorem above offered absolute guarantee of new physics discoveries at the LHC and was heavily used to motivate its construction. Now the Higgs has been found, with couplings compatible with the SM expectations, we know that it is indeed the Higgs particle the agent responsible for cancelling (at least partially, given the limited accuracy of the Higgs couplings measurements) the quadratic term in the scattering amplitude. This leaves us, as I will better explain below, with no No-Loose Theorem and thus with no guaranteed discovery to organise our future efforts in the investigation of fundamental interactions.

Each of the No-Lose theorems discussed above emerges because of the anomalous power-like growth with the energy of some scattering amplitude, a behaviour which unmistakably signals that a non-renormalizable interaction operator of energy dimension $d > 4$ is present in the theory. This being the case is completely obvious for the Fermi theory, a bit less so in the two other examples. In the latter

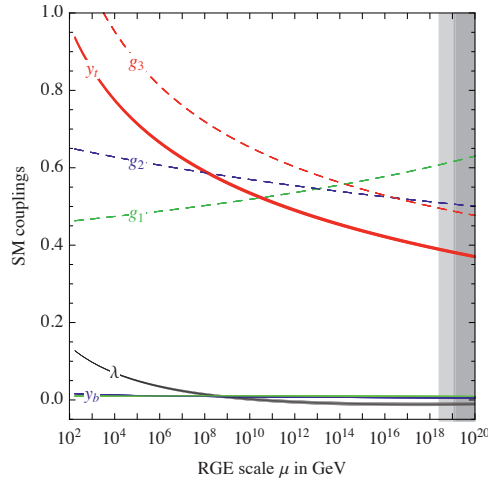


Fig. 1: The RG running of the most relevant couplings of the SM, namely the three gauge couplings $g_{1,2,3}$, the top and bottom Yukawa’s $y_{t,b}$ and the Higgs quartic coupling λ . See Ref. [6] and references therein for more details.

cases it requires, to be understood, somewhat technical considerations related with the Goldstone boson Equivalence Theorem [5] which go beyond the purpose of the present lectures. It suffices here to say that one given $d = 6$ non-renormalizable operator, responsible for the E^2 growth of the scattering amplitude, can be identified for each of the 3 No-Lose theorems above. When each theorem was “exploited” by discovering the associated new physics we “got rid” of the corresponding operator by replacing it with a more fundamental theory that explains its origin as a low-energy effective description. Having exploited all the theorems, we got rid of all the non-renormalizable operators and we are left, for the first time, with an experimentally verified renormalizable theory of electroweak and strong interactions. No new No-Lose theorems can be thus formulated in this theory, at least not as simple and powerful ones as the ones listed above.

However the SM is not only a theory of electroweak and strong interactions. It can be (and it must be, to account for observations) extended to incorporate Gravity and the only sensible way to do so is by introducing and quantising the Einstein-Hilbert action. This produces a number of non-renormalizable interaction operators involving gravitons, giving rise to another well-known No-Lose theorem

$$\begin{array}{ccc}
 \text{grav.} & & \text{grav.} \\
 \diagdown & & / \\
 & \sim G_N E^2 \simeq E^2 / M_P^2 < 16\pi^2 & \longrightarrow \Lambda_{\text{SM}} < M_P \\
 / & & \diagdown \\
 \text{grav.} & & \text{grav.}
 \end{array}$$

where $M_P \simeq 10^{19}$ GeV is the Planck scale. What the theorem says is that the SM is for sure not the “final theory” of Nature, because it does not provide a complete description of Gravity at the quantum level. It does incorporate a description of quantum gravity that is valid and predictive at low energy but breaks down at a finite scale Λ_{SM} , which we call the “SM cutoff”. BSM particles and interactions are present at that scale, which however can be as high as 10^{19} GeV. Given our technical inability to test such an enormous scale, it is unlikely that we might ever exploit this last No-Lose Theorem as a guide towards a concrete new physics discovery.

The second aspect to be discussed is that even in a renormalizable theory the scattering amplitudes can actually grow with the energy. Not with a power-law, but logarithmically, through the Renormalisation Group (RG) running of the dimensionless coupling constants of the theory. The RG evolution can make some of the couplings grow with the energy until they violate the perturbativity bound, producing a new No-Lose Theorem. Obviously this No-Lose Theorem would most likely be not as powerful as those obtainable in non-renormalizable theories because the RG evolution is logarithmically slow and

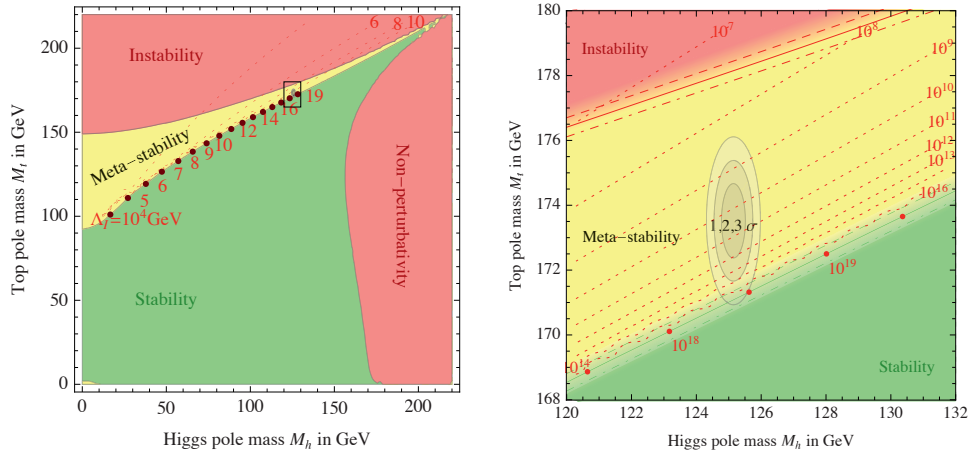


Fig. 2: Stability, instability, metastability and non-perturbativity regions for the SM in the plane of the Higgs and top masses. A zoom on the experimentally viable region is displayed in the right plot, with the 1, 2 and 3 σ regions allowed by m_H and m_t uncertainties. From Ref. [6].

thus the perturbativity violation scale is exponentially high, but still it is interesting to ask if one such a theorem exists for the SM and at which scale it points to. The answer is that perturbativity violation does not occur in the SM below the Planck mass scale, at which new physics is anyhow needed to account for gravity, as shown in fig. 1. The only coupling that grows significantly with the energy is the one associated with the $U(1)_Y$ gauge group, g_1 , which however is still well below the perturbativity bound at the Planck scale. Notice that the result crucially depends on the initial conditions of the running, namely on the values of the SM parameters measured at the 100 GeV scale. The result would have been different, and an additional No-Lose Theorem would have been produced, if that values were radically different than what we actually observed.

The vacuum stability problem [7] is yet another potential source of high-energy inconsistencies (and thus of No-Lose Theorems) in renormalizable theories that display, like the SM, a non-trivial structure of the vacuum state. The problem is again due to RG evolution effects, which modify the form of the Higgs potential at very high values of the Higgs field and potentially make it develop a second minimum. If the energy of this second minimum is lower than the first one, transitions can occur via quantum tunnelling from the ordinary EWSB vacuum where $v \simeq 246$ GeV to an inhospitable minimum characterised by a very large vacuum expectation value (VEV) of the Higgs field. Whether this actually happens or not depends, once again, on the measured value of the SM parameters and in particular on the Higgs boson and top quark masses as displayed in fig. 2. We see that our vacuum is not stable and thus it is fated to decay provided we wait long enough. However it falls in the “meta-stability” region of the diagram, which is where the vacuum lifetime is longer than the age of the Universe. Therefore the decay of our vacuum might not have had enough time to occur. Some people find disturbing that we live in a meta-stable vacuum. Some others [6] find intriguing the fact that we live close (see the right panel of fig. 2) to the boundary between the stability and meta-stability regions and suggest that we should measure m_t better in order to be sure of how close we actually are. Anyhow what is sure (and what matters for our discussion) is that the analysis of the vacuum stability does not reveal any concrete inconsistency of the SM at high energy. Consequently, no new No-Lose Theorem is found.

1.2 The “SM-only” Option

Two extremely important (and in some sense contradictory) facts emerge from the previous considerations. On one hand, we know that BSM physics exists at a finite energy scale Λ_{SM} . This makes that the SM is necessarily an approximate low-energy description of a more fundamental theory, i.e. an Effective

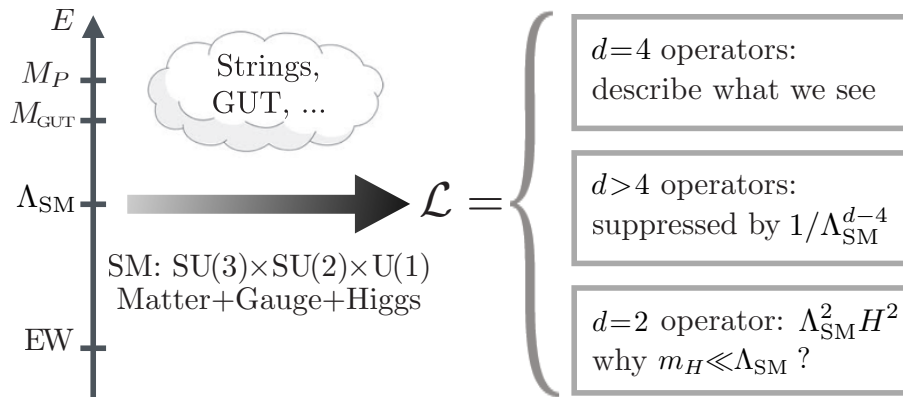


Fig. 3: Pictorial view of the SM as an effective field theory, with its Lagrangian generated at the scale Λ_{SM} .

Field Theory (EFT) with a finite cutoff Λ_{SM} . On the other hand, the only upper bound on the cutoff scale is provided by the Planck mass, which is to a very good approximation equal to infinity compared with the much lower scales we are able to explore experimentally today and in any foreseeable future. We are thus led to consider the “SM-only” option for high-energy physics. Namely the possibility that the SM cutoff Λ_{SM} (i.e., the scale of new physics) is extremely high, much above the TeV as depicted in fig. 3. Values as high as $\Lambda_{\text{SM}} \sim M_{\text{P}}$ and $\Lambda_{\text{SM}} \sim 10^{15} \text{ GeV} \equiv M_{\text{GUT}}$ can be considered.

The SM-only option is not just a logical possibility. On the contrary, it is a predictive and phenomenologically successful scenario for high-energy physics. To appreciate its value, we look again at fig. 3, starting from the high energy (UV) region and we ask ourselves how the SM theory emerges in the IR. As pictorially represented in the figure, we have no idea of how the theory in the UV looks like. It might be a string theory, a GUT model (for a review, see for instance Refs. [8, 9]), or something completely different we have not yet thought about. All what we know about the UV theory is that, by assumption, its particle content reduces to the one of the SM at Λ_{SM} , all BSM particles being at or above that scale.³ Below Λ_{SM} the UV theory thus necessarily reduces, after integrating out the heavy states, to a low-energy EFT which only describes the light SM degrees of freedom. A technically consistent description of the force carriers (gluon and EW bosons) requires invariance under the $\text{SU}(3)_c \times \text{SU}(2)_L \times \text{U}(1)_Y$ gauge group, but apart from being gauge (and Lorentz) invariant there is not much we can tell a priori on how the SM effective Lagrangian will look like. It will consist of an infinite series of local gauge- and Lorentz-invariant operators with arbitrary energy dimension “ d ”, constructed with the SM Matter, Gauge and Higgs fields as in fig. 3. The coefficient of the operators must be proportional to $1/\Lambda_{\text{SM}}^{d-4}$ by dimensional analysis, given that $[\mathcal{L}] = E^4$ and Λ_{SM} is the only relevant scale. This simple observation lies at the heart of the phenomenological virtues of the SM-only scenario but also, as we will see, of its main limitation.

We now classify the SM effective operators by their energy dimension and discuss their implications, starting from those with $d = 4$. They describe almost all what we have seen in Nature, namely EW and strong interactions, quarks and charged leptons masses. They define a renormalizable theory and thus, together with the $d = 2$ operator we will introduce later, they are present in the textbook SM Lagrangian formulated in the old times when renormalizability was taken as a fundamental principle.

Several books have been written (see for instance Refs. [10–12]) on the extraordinary phenomenological success of the renormalizable SM Lagrangian in describing the enormous set of experimental data [13] collected in the past decades. In a nutshell, as emphasized in Ref. [14], most of this success is due to symmetries, namely to “accidental” symmetries. We call “accidental” a symmetry that arises by accident at a given order in the operator classification, without being imposed as a principle in the

³The presence of light feebly coupled BSM particles would not affect the considerations that follow.

construction of the theory. The renormalizable ($d \leq 4$) SM Lagrangian enjoys exact (or perturbatively exact) accidental symmetries, namely baryon and lepton family number, and approximate ones such as the flavour group and custodial symmetry. For brevity, we focus here on the former symmetries, which have the most striking implications. Baryon number makes the proton absolutely stable, in accordance with the experimental limit $\Gamma_p/m_p \lesssim 10^{-64}$ on the proton width over mass ratio. It is hard to imagine how we could have accounted for the proton being such a narrow resonance in the absence of a symmetry. Similarly lepton family number forbids exotic lepton decays such as $\mu \rightarrow e\gamma$, whose branching ratio is experimentally bounded at the 10^{-12} level. From neutrino oscillations we know that the lepton family number is actually violated, in a way that however nicely fits in the SM picture as we will see below. Clearly this is connected with the neutrino masses, which exactly vanish at $d = 4$ because of the absence, in what we call here “the SM”, of right-handed neutrino fields.

We now turn to non-renormalizable operators with $d > 4$. Their coefficient is proportional to $1/\Lambda_{\text{SM}}^n$, with $n = d - 4 > 0$, thus their contribution to low-energy observables is suppressed by $(E/\Lambda_{\text{SM}})^n$ with respect to renormalizable terms. Given that current observations are at and below the EW scale, $E \lesssim m_{\text{EW}} \simeq 100$ GeV, their effect is extremely suppressed in the SM-only scenario where $\Lambda_{\text{SM}} \gg \text{TeV}$. This could be the reason why Nature is so well described by a renormalizable theory, without renormalizability being a principle.

Non-renormalizable operators violate the $d = 4$ accidental symmetries. Lepton number stops being accidental already at $d = 5$ because of the Weinberg operator [15]

$$\frac{c}{\Lambda_{\text{SM}}} (\bar{\ell}_L H^c)(\ell_L^c H^c), \quad (1)$$

where ℓ_L denotes the lepton doublet, ℓ_L^c its charge conjugate, while H is the Higgs doublet and $H^c = i\sigma^2 H^*$. The $\text{SU}(2)_L$ indices are contracted within the parentheses and the spinor index between the two terms. A generic lepton flavour structure of the coefficient, leading to the breaking of lepton family number, is understood. Surprisingly enough, the Weinberg operator is the unique $d = 5$ term in the SM Lagrangian. When the Higgs is set to its VEV, the Weinberg operator reduces to a Majorana mass term for the neutrinos, $m_\nu \sim c v^2/\Lambda_{\text{SM}}$. For $\Lambda_{\text{SM}} \simeq 10^{14}$ GeV and order one coefficient “ c ” it generates neutrino masses of the correct magnitude ($m_\nu \sim 0.1$ eV) and neutrino mixings that can perfectly account for all observed neutrino oscillation phenomena. Baryon number is instead still accidental at $d = 5$ and its violation is postponed to $d = 6$. We thus perfectly understand, qualitatively, why lepton family violation effects are “larger”, thus easier to discover, while baryon number violation like proton decay is still unobserved. At a more quantitative level we should actually remark that the bounds on proton decay from the $d = 6$ operators, with order one numerical coefficients, set a limit $\Lambda_{\text{SM}} \gtrsim 10^{15}$ GeV that is in slight tension with what required by neutrino masses. However few orders of magnitude are not a concern here, given that there is no reason why the operator coefficient should be of order one. A suppression of the proton decay operators is actually even expected because they involve the first family quarks and leptons, whose couplings are reduced already at the renormalizable level. Namely, it is plausible that the same mechanism that makes the first-family Yukawa couplings small also reduces proton decay, while less suppression is expected in the third family entries of the Weinberg operator coefficient that might drive the generation of the heaviest neutrino mass.

The considerations above make the SM-only option a plausible picture, which becomes particularly appealing if we set $\Lambda_{\text{SM}} \sim M_{\text{GUT}}$. This choice happens to coincide with the gauge coupling unification scale, but this doesn’t mean that the new physics at the cutoff is necessarily a Grand Unified Theory. On the contrary, the physics at the cutoff can be very generic in this picture, the compatibility with low-energy observations being ensured by the large value of the Λ_{SM} scale and not by the details of the UV theory. New physics is virtually impossible to discover directly in this scenario, but this doesn’t make it completely untestable. Purely Majorana neutrino masses would be a strong indication of its validity while observing a large Dirac component would make it less appealing.

Having discussed the virtues of the SM-only scenario, we turn now to its limitations. One of those,

which was already mentioned, is the hierarchy among the Yukawa couplings of the various quark and lepton flavours, which span few orders of magnitude. This tells us that the new physics at Λ_{SM} cannot actually be completely generic, given that it must be capable of generating such a hierarchy in its prediction for the Yukawa's. This limits the set of theories allowed at the cutoff but is definitely not a strong constraint. Whatever mechanism we might imagine to generate flavour hierarchies at $\Lambda_{\text{SM}} \sim M_{\text{GUT}}$, it will typically not be in contrast with observations given that the bounds on generic flavour-violating operators are “just” at the 10^8 GeV scale. Incorporating dark matter also requires some modification of the SM-only picture, but there are several ways in which this could be done without changing the situation dramatically. Perhaps the most appealing solution from this viewpoint is “minimal dark matter” [16], a theory in which all the symmetries that are needed for phenomenological consistence are accidental. This includes not only the SM accidental symmetries, but also the additional \mathbb{Z}_2 symmetry needed to keep the dark matter particle cosmologically stable. Similar considerations hold for the strong CP problem, for inflation and all other cosmological shortcomings of the SM. The latter could be addressed by light and extremely weakly-coupled new particles or by very heavy ones above the cutoff. In conclusion, none of the above-mentioned issues is powerful enough to put the basic idea of very heavy new physics scale in troubles. The only one that is capable to do so is the Naturalness (or Hierarchy) problem discussed below.⁴

We have not yet encountered the Naturalness problem in our discussion merely because we voluntarily ignored, in our classification, the operators with $d < 4$. The only such operator in the SM is the Higgs mass term, with $d = 2$.⁵ When studying the $d > 4$ operators we concluded that their coefficient is suppressed by $1/\Lambda_{\text{SM}}^{d-4}$. Now we have $d = 2$ and we are obliged to conclude that the operator is *enhanced* by Λ_{SM}^2 , *i.e.* that the Higgs mass term reads

$$c \Lambda_{\text{SM}}^2 H^\dagger H, \quad (2)$$

with “ c ” a numerical coefficient. In the SM the Higgs mass term sets the scale of EWSB and it directly controls the Higgs boson mass. Today we know that $m_H = 125$ GeV and thus the mass term is $\mu^2 = m_H^2/2 = (89 \text{ GeV})^2$. But if $\Lambda_{\text{SM}} \sim M_{\text{GUT}}$, what is the reason for this enormous hierarchy? Namely

$$\text{why } \frac{\mu^2}{\Lambda_{\text{SM}}^2} \sim 10^{-28} \lll 1 \text{ ?}$$

This is the essence of the Naturalness problem.

Further considerations on the Naturalness problem and implications are postponed to the next section. However, we can already appreciate here how radically it changes our expectations on high energy physics. The SM-only picture gets sharply contradicted by the Naturalness argument since the problem is based on the same logic (*i.e.*, dimensional analysis) by which its phenomenological virtues (*i.e.*, the suppression of $d > 4$ operators) were established. The new picture is that Λ_{SM} is low, in the 100 GeV to few TeV range, such that a light enough Higgs is obtained “Naturally”, *i.e.* in accordance with the estimate in eq. (2). The new physics at the cutoff must now be highly non-generic, given that it cannot rely any longer on a large scale suppression of the BSM effects. To start with, baryon and lepton family number violating operators must come with a highly suppressed coefficient, which in turn requires baryon and lepton number being imposed as symmetries rather than emerging by accident. In concrete, the BSM sector must now respect these symmetries. This can occur either because it inherits them from an even more fundamental theory or because they are accidental in the BSM theory itself. Similarly, if $\Lambda_{\text{SM}} \sim \text{TeV}$ flavour violation cannot be generic. Some special structure must be advocated on the BSM theory, Minimal flavour Violation (MFV) [22, 23] being one popular and plausible option. The limits from EW Precision Tests (EWPT) come next; they also need to be carefully addressed for

⁴See Refs. [17] and [18] for recent essays on the Naturalness problem. The problem was first formulated in Refs. [19] and [20, 21], however according to the latter references it was K.Wilson who first raised the issue.

⁵There is also the cosmological constant term, of $d = 0$. It poses another Naturalness problem that I will mention later.

TeV scale new physics. On one hand this makes Natural new physics at the TeV scale very constrained. On the other hand it gives us plenty of indications on how it should, or it should not, look like.

1.3 The Naturalness Argument

The reader might be unsatisfied with the formulation of the Naturalness problem we gave so far. All what eq. (2) tells us is that the numerical coefficient “ c ” that controls the actual value of the mass term beyond dimensional analysis should be extremely small, namely $c \sim 10^{-28}$ for GUT scale new physics. Rather than pushing Λ_{SM} down to the TeV scale, where all the above-mentioned constraints apply, one could consider keeping Λ_{SM} high and try to invent some mechanism to explain why c is small. After all, we saw that there are other coefficients that require a suppression in the SM Lagrangian, namely the light flavours Yukawa couplings. One might argue that it is hard to find a sensible theory where c is small, while this is much simpler for the Yukawa’s. Or that 28 orders of magnitude are by far much more than the reduction needed in the Yukawa sector. But this would not be fully convincing and would not make full justice to the importance of the Naturalness problem.

In order to better understand Naturalness we go back to the essential message of the previous section. The SM is a low-energy effective field theory and thus the coefficients of its operators, which we regard today as fundamental input parameters, should actually be derived phenomenological parameters, to be computed one day in a more fundamental BSM theory. Things should work just like for the Fermi theory of weak interactions, where the Fermi constant G_F is a fundamental input parameter that sets the strength of the weak force. We know however that the true microscopic description of the weak interactions is the IVB theory. The reason why we are sure about this is that it allows us to predict G_F in terms of its microscopic parameters g_W and m_W , in a way that agrees with the low-energy determination. What we have in mind here is merely the standard textbook formula

$$G_F = \frac{g_W^2}{4\sqrt{2}m_W^2}, \quad (3)$$

that allows us to carry on, operatively, the following program. Measure the microscopic parameters g_W and m_W at high energy; compute G_F ; compare it with low-energy observations.⁶ Since this program succeeds we can claim that the microscopic origin of weak interaction is well-understood in terms of the IVB theory. We will now see that the Naturalness problem is an obstruction to repeating the same program for the Higgs mass and in turn for the EWSB scale.

Imagine knowing the fundamental, “true” theory of EWSB. It will predict the Higgs mass term μ^2 or, which is the same, the physical Higgs mass $m_H^2 = 2\mu^2$, in terms of its own input parameters “ p_{true} ”, by a formula that in full generality reads

$$m_H^2 = \int_0^\infty dE \frac{dm_H^2}{dE}(E; p_{\text{true}}). \quad (4)$$

The integral over energy stands for the contributions to m_H^2 from all the energy scales and it extends up to infinity, or up to the very high cutoff of the “true” theory itself. The integrand could be localized around some specific scale or even sharply localized by a delta-function at the mass of some specific particle, corresponding to a tree-level contribution to m_H^2 . Examples of theories with tree-level contributions are GUT [8, 9] and Supersymmetric (SUSY) models, where m_H emerges from the mass terms of extended scalar sectors. The formula straightforwardly takes into account radiative contributions, which are the only ones present in the composite Higgs scenario (see sect. 2). Also in SUSY, as discussed in sect. 3, radiative terms have a significant impact given that the bounds on the scalar (SUSY and soft) masses that contribute at the tree-level are much milder than those on the coloured stops and gluinos that contribute

⁶Actually G_F is taken as an input parameter in actual calculations because it is better measured than g_W and m_W , but this doesn’t affect the conceptual point we are making.

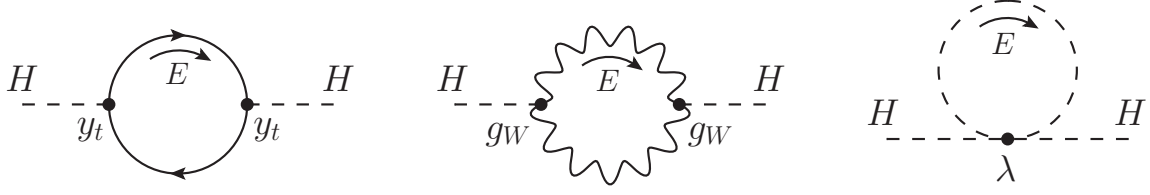


Fig. 4: Some representative top, gauge and Higgs boson loop diagrams that contribute to the Higgs mass.

radiatively. In the language of old-fashioned perturbation theory [24], “ E ” should be regarded as the energy of the virtual particles that run into the diagrams through which m_H^2 is computed.

Consider now splitting the integral in two regions defined by an intermediate scale that we take just a bit below the SM cutoff. We have

$$\begin{aligned} m_H^2 &= \int_0^{\lesssim \Lambda_{\text{SM}}} dE \frac{dm_H^2}{dE}(E; p_{\text{true}}) + \int_{\gtrsim \Lambda_{\text{SM}}}^{\infty} dE \frac{dm_H^2}{dE}(E; p_{\text{true}}) \\ &= \delta_{\text{SM}} m_H^2 + \delta_{\text{BSM}} m_H^2, \end{aligned} \quad (5)$$

where $\delta_{\text{BSM}} m_H^2$ is a completely unknown contribution, resulting from energies at and above Λ_{SM} , while $\delta_{\text{SM}} m_H^2$ comes from virtual quanta below the cutoff, whose dynamics is by assumption well described by the SM. While there is nothing we can tell about $\delta_{\text{BSM}} m_H^2$ before we know what the BSM theory is, we can easily estimate $\delta_{\text{SM}} m_H^2$ by the diagrams in Figure 4, obtaining

$$\delta_{\text{SM}} m_H^2 = \frac{3y_t^2}{4\pi^2} \Lambda_{\text{SM}}^2 - \frac{3g_W^2}{8\pi^2} \left(\frac{1}{4} + \frac{1}{8 \cos^2 \theta_W} \right) \Lambda_{\text{SM}}^2 - \frac{3\lambda}{8\pi^2} \Lambda_{\text{SM}}^2, \quad (6)$$

from, respectively, the top quark, EW bosons and Higgs loops. The idea is that we know that the BSM theory must reduce to the SM for $E < \Lambda_{\text{SM}}$. Therefore no matter what the physics at Λ_{SM} is, its prediction for m_H^2 must contain the diagrams in fig 4 and thus the terms in eq. (6). These terms are obtained by computing dm_H^2/dE from the SM diagrams and integrating it up to Λ_{SM} , which effectively acts as a hard momentum cutoff. The most relevant contributions come from the quadratic divergences of the diagrams, thus eq. (6) can be poorly viewed as the “calculation” of quadratic divergences. Obviously quadratic divergences are unphysical in quantum field theory. They are canceled by renormalization and they are even absent in certain regularizations schemes such as dimensional regularization. However the calculation makes sense, in the spirit above, as an estimate of the low-energy contributions to m_H^2 .

The true nature of the Naturalness problem starts now to show up. The full finite formula for m_H^2 obtained in the “true” theory receives two contributions that are completely unrelated since they emerge from separate energy scales. At least one of those, $\delta_{\text{SM}} m_H^2$, is for sure very large if Λ_{SM} is large. The other one is thus obliged to be large as well, almost equal and with opposite sign in order to reproduce the light Higgs mass we observe. A cancellation is taking place between the two terms, which we quantify by a fine-tuning Δ of at least

$$\Delta \geq \frac{\delta_{\text{SM}} m_H^2}{m_H^2} = \frac{3y_t^2}{4\pi^2} \left(\frac{\Lambda_{\text{SM}}}{m_H} \right)^2 \simeq \left(\frac{\Lambda_{\text{SM}}}{450 \text{ GeV}} \right)^2. \quad (7)$$

Only the top loop term in eq. (6) has been retained for the estimate since the top dominates because of its large Yukawa coupling and because of color multiplicity. Notice that the one above is just a lower bound on the total amount of cancellation Δ needed to adjust m_H in the true theory. The high energy contribution $\delta_{\text{BSM}} m_H^2$, on which we have no control, might itself be the result of a cancellation, needed to arrange for $\delta_{\text{BSM}} m_H^2 \simeq -\delta_{\text{SM}} m_H^2$. Examples of this situation exist both in SUSY and in composite Higgs.

The problem is now clear. Even if we were able to write down a theory that formally predicts the Higgs mass, and even if this theory turned out to be correct we will never be able to really predict m_H if Λ_{SM} is much above the TeV scale, because of the cancellation. For $\Lambda_{\text{SM}} = M_{\text{GUT}}$, for instance, we have $\Delta \gtrsim 10^{24}$. This means that in the “true” theory formula for m_H a 24 digits cancellation is taking place between two a priori unrelated terms. Each of these terms must thus be known with at least 24 digits accuracy even if we content ourselves with an order one estimate of m_H . We will never achieve such an accuracy, neither in the experimental determination of the p_{true} “true” theory parameters m_H depends on, nor in the theoretical calculation of the Higgs mass formula. Therefore, we will never be able to repeat for m_H the program we carried on for G_F and we will never be able to claim we understand its microscopic origin and in turn the microscopic origin of the EWSB scale. A BSM theory with $\Lambda_{\text{SM}} = M_{\text{GUT}}$ has, in practice, the same predictive power on m_H as the SM itself, where eq. (4) is replaced by the much simpler formula

$$m_H^2 = m_H^2. \quad (8)$$

Namely if such an high-scale BSM theory was realized in Nature m_H will remain forever an input parameter like in the SM. The microscopic origin of m_H , if any, must necessarily come from new physics at the TeV scale, for which the fine-tuning Δ in eq. (7) can be reasonably small.

The Higgs mass term is the only parameter of the SM for which such an argument can be made. Consider for instance writing down the analog of eq. (4) for the Yukawa couplings and splitting the integral as in eq. (5). The SM contribution to the Yukawa’s is small even for $\Lambda_{\text{SM}} = M_{\text{GUT}}$, because of two reasons. First, the Yukawa’s are dimensionless and thus, given that there are no couplings in the SM with negative energy dimension, they do not receive quadratically divergent contributions. The quadratic divergence is replaced by a logarithmic one, with a much milder dependence on Λ_{SM} . Second, the Yukawa’s break the flavour group of the SM. Therefore there exist selection rules (namely those of MFV) that make radiative corrections proportional to the Yukawa matrix itself. The Yukawa’s, and the hierarchies among them, are thus “radiatively stable” in the SM (see sect. 3.2 for more details). This marks the essential difference with the Higgs mass term and implies that their microscopic origin and the prediction of their values could come at any scale, even at a very high one. The same holds for all the SM parameters apart from m_H .

The formulation in terms of fine-tuning (7) turns the Naturalness problem from a vague aesthetic issue to a concrete semiquantitative question. Depending on the actual value of Δ the Higgs mass can be operatively harder or easier to predict, making the problem more or less severe. If for instance $\Delta \sim 10$, we will not have much troubles in overcoming a one digit cancellation once we will know and we will have experimental access to the “true” theory. After some work, sufficiently accurate predictions and measurements will become available and the program of predicting m_H will succeed. The occurrence of a one digit cancellation will at most be reported as a curiosity in next generation particle physics books and we will eventually forget about it. A larger tuning $\Delta = 1000$ will instead be impossible to overcome. The experimental exploration of the high energy frontier will tell us, through eq. (7), what to expect about Δ . Either by discovering new physics that addresses the Naturalness problem or by pushing Λ_{SM} higher and higher until no hope is left to understand the origin of the EWSB scale in the sense specified above. One way or another, a fundamental result will be obtained.

1.4 What if Un-Natural?

I argued above that searching for Naturalness at the LHC is relevant regardless of the actual outcome of the experiment. Such a bold statement needs to be more extensively defended. The case of a discovery is so easy that it would not even be worth discussing. If new particles are found at the TeV scale, with properties that resemble what predicted by a Natural BSM theory such as the ones described in the following sections, Naturalness would have guided us towards the discovery of new physics. Moreover, it will provide the theoretical framework for the interpretation of the discoveries, by which the new particles will eventually find their place in a concrete BSM model. If instead nothing related with Naturalness will

be found, strong limits will be set on Δ and we will be pushed towards the idea that the m_H^2 parameter does not have a canonical “microscopic” origin as previously explained. This would still qualify as a discovery: the discovery of “Un-Naturalness”.⁷ The profound implications of this potential discovery are discussed below.

If Un-Naturalness will be discovered, other options will have to be considered to explain the origin of the Higgs mass term. The two known possibilities are that m_H^2 has an “environmental” or a “dynamical” origin rather than a “microscopic” one, as previously assumed. A well-known parameter with environmental origin is the Gravity of Earth $g = 9.8 \text{ m/s}^2$. It is the input parameter of Ballistics, a theory of great historical relevance which in Galileo’s times might have been conceivably thought to be a fundamental theory of Nature. The origin of g is obviously dictated by the environment in which the theory is formulated, namely by the fact that Ballistics applies to processes that occur close to the surface of Earth. Its value depends on the Earth’s mass and radius and it cannot be inferred just based on the knowledge of the “truly fundamental” theory of Gravity (Newton’s law) and of its parameters (Newton’s constant). This is not the case for those parameters, such as G_F , with a purely microscopic origin. The dependence on the environment can help explaining the size of an environmental parameter by the so-called “Anthropic” argument. In fact, the value of $g = 9.8 \text{ m/s}^2$ is rather peculiar. It is much larger than the one we would observe in interstellar space and much smaller than the one on the surface of a neutron star, very much like m_H is much smaller than M_P or M_{GUT} . However we do perfectly understand the magnitude of g , for the very simple reason that no ancient physicist might have lived in empty space or on a neutron star. The magnitude of g must be compatible with what is needed for the development of intelligent life, otherwise no physicist would have existed and nobody would have measured it.

The Weinberg prediction of the cosmological constant [25] proceeds along similar lines. The cosmological constant operator suffers of exactly the same Naturalness problem as the Higgs mass. Provided we claim we understand gravity well enough to estimate them, radiative corrections push the cosmological constant to very high values, tens of orders of magnitude above what we knew it had to be (and was subsequently observed) in order for galaxies being able to form in the early universe. Weinberg pointed out that the most plausible value for the cosmological constant should thus be close to the maximal allowed value for the formation of galaxies because galaxies are essential for the development of intelligent life. The idea is that if many ground state configurations (a landscape of vacua) are possible in the fundamental theory, typically characterised by a very large cosmological constant but with a tail in the distribution that extends up to zero, the largest possible value compatible with galaxies formation, and thus with the very existence of the observer, will be actually observed. A similar argument can be made for the Higgs mass (see for instance Ref. [26]), however it is harder in the SM to identify sharply the boundary of the anthropically allowed region of the parameter space.

I tried here to vulgarise the mechanism of anthropic vacua selection by the example of Gravity of Earth, however the analogy is imperfect under several respects. Perhaps the most important difference is that the landscape of vacua cannot be viewed as a set of physical regions (like the interstellar space or the neutron star) separated in space, where m_H or the cosmological constant assume different values. Or at least, since the other vacua live in space-time regions that are causally disconnected from us, it will be impossible to have access to them and check directly that the mechanism works.

The possibility of a “dynamical” origin of the Higgs mass term is quite new [27] and not much studied.⁸ The idea, first proposed in [28] as an unsuccessful attempt to solve the cosmological constant problem, is that m_H might be set by the expectation value of a new scalar field, whose value evolves

⁷Deciding whether or not negative LHC results will have the last word on Naturalness is a matter of taste, to some extent, since it is unclear how much tuning we can tolerate. It also depends on how good we will be in searching for Natural new physics and consequently how strong and robust the limit on Δ will actually be. It is nevertheless undoubtable that negative LHC results will put the idea of Naturalness in serious troubles.

⁸The word “dynamical” is used here in its proper sense, related with evolution in the course of time. It has nothing to do with the generation of energy scales (e.g., the QCD confinement scale) induced by an underlying strongly-coupled theory, which is also said to be a “dynamical” generation mechanism.

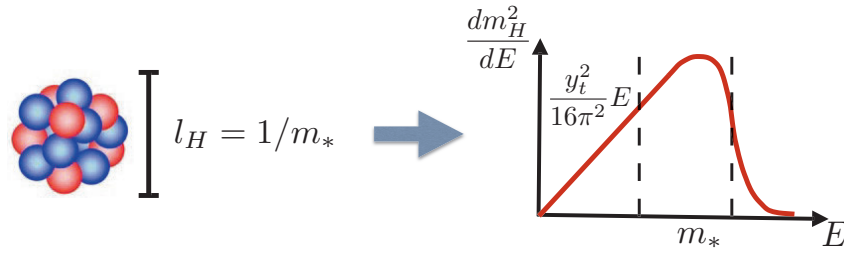


Fig. 5: Pictorial representation of the Composite Higgs solution to the Naturalness problem.

during cosmological Inflation. This field is called “relaxion” in [27] because it is similar to the QCD axion needed to address the strong-CP problem and because it sets the value of m_H by a dynamical relaxation mechanism. At the beginning of Inflation, the relaxion VEV is such that the Higgs mass term is large and positive, but it evolves in the course of time making the Higgs mass term decrease and eventually cross zero so that EWSB can take place. The structure of the theory is such that once a non-vanishing Higgs VEV is generated, a barrier develops in the relaxion potential and makes it stop evolving. The Higgs mass term gets thus frozen to the value which is just sufficient for an high enough barrier to form. If the theory is special enough (but not necessarily complicate), this value can be small and the Hierarchy problem can be solved.

You might find these speculations extremely interesting. Or you might believe that they have no chance to be true. Anyhow, their very existence demonstrates how radically the discovery of Un-Naturalness would change our perspective on the physics of fundamental interactions. They show the capital importance of searching for Naturalness or Un-Naturalness at the LHC and, perhaps, at future colliders.

2 Composite Higgs

One aspect of the Naturalness problem which has not yet emerged is the fact that addressing it requires BSM physics of rather specific nature at $\Lambda_{SM} \lesssim \text{TeV}$. Namely, it is true that any BSM scenario that Naturally explains the origin of m_H is obliged to show up at the TeV by eq. (7), but this does not mean that the presence of generic new particles at the TeV scale would solve the Naturalness problem. Conversely, it is not true that any BSM particle we might happen not to discover at the TeV scale would signal that the theory is fine-tuned as a naive application of eq. (7) would suggest. Natural BSM physics would show up through new particles (and/or, indirect effects on SM processes) of specific nature and it is only the non-discovery of these particles the one that matters for the tuning Δ . Addressing this point requires studying concrete BSM solutions to the Naturalness problem.

Among the various scenarios which have been proposed to address the Naturalness problem I decided to focus on two of them: Supersymmetry and Composite Higgs. The reason for this choice is that they are representative of the only two known mechanisms which truly address the problem of the microscopic origin of m_H by a well-defined high-energy picture. Alternative Natural models are often reformulations or deformations of these basic scenarios, or a combination of the two.⁹ You are referred to Ref. [29] for a comprehensive overview.

2.1 The Basic Idea

The composite Higgs scenario offers a simple solution to the problem of Naturalness. Suppose that the Higgs, rather than being a point-like particle as in the SM, is instead an extended object with a finite geometric size l_H . We will make it so by assuming that it is the bound state of a new strong force characterised by a confinement scale $m_* = 1/l_H$ of TeV order. In this new theory the dm_H^2/dE integrand in the Higgs mass formula (4), which stands for the contribution of virtual quanta with a given energy, behaves as shown in fig. 5. Low energy quanta have too a large wavelength to resolve the Higgs size l_H . Therefore the Higgs behaves like an elementary particle and the integrand grows linearly with E like in the SM, resulting in a quadratic sensitivity to the upper integration limit. However this growth gets canceled by the finite size effects that start becoming visible when E approaches and eventually overcomes m_* . Exactly like the proton when hit by a virtual photon of wavelength below the proton radius, the composite Higgs is transparent to high-energy quanta and the integrand decreases. The linear SM behaviour is thus replaced by a peak at $E \sim m_*$ followed by a steep fall. The Higgs mass generation phenomenon gets localised at $m_* = 1/l_H$ and m_H is insensitive to much higher energies. This latter fact is also obvious from the fact that no Higgs particle is present much above m_* . Therefore there exist no Higgs field and no $d = 2$ Higgs mass term to worry about.

Implementing this idea in practice requires a theory with the structure in fig. 6. The three basic elements are a ‘‘Composite Sector’’ (CS), an ‘‘Elementary Sector’’ (ES) and a set of interactions ‘‘ \mathcal{L}_{int} ’’ connecting the two. The Composite Sector contains the new particles and interactions that form the Higgs as a bound state and it should be viewed as analogous to the QCD theory of quarks and gluons. The CS plays the main role for the composite Higgs solution to the Naturalness problem as it gives physical origin to the Higgs compositeness scale m_* . In the analogy with QCD, m_* corresponds to the QCD confinement scale Λ_{QCD} and it is generated, again like in QCD, by the mechanism of dimensional transmutation. Thanks to this mechanism it is insensitive to other much larger scales which are present in the problem. For instance the microscopic origin of the CS itself might well be placed at $\Lambda_{\text{UV}} \sim M_{\text{GUT}}$, but still m_* could be Naturally of TeV order, very much like $\Lambda_{\text{QCD}} \sim 300 \text{ MeV} \ll m_{\text{EW}}$ is perfectly Natural within the SM.

The Elementary Sector contains all the particles we know, by phenomenology, cannot be composite at the TeV scale.¹⁰ Those are basically all the SM gauge and fermion fields with the possible exception of the right-handed component of the top quark. The most relevant operators in the ES Lagrangian, namely those that are not suppressed by $1/\Lambda_{\text{UV}}^n$, are thus just the ordinary $d = 4$ SM gauge and fermion kinetic terms and gauge interactions. Since there is no Higgs, no dangerous $d = 2$ operator is present in the ES and thus the theory is perfectly Natural. Obviously the lack of a Higgs also forbids Yukawa couplings and a different mechanism will have to be in place to generate fermion masses and mixings.

The Elementary-Composite interactions \mathcal{L}_{int} consist of two classes of terms: those involving the elementary gauge fields and those involving the elementary fermionic field. The latter are responsible for fermion masses and will be discussed later. The former are instead sharply dictated by gauge invariance and read

$$\mathcal{L}_{\text{int}}^{\text{gauge}} = \sum_{i=1,2,3} g_i A_i^\mu J_\mu^i, \quad (9)$$

where i runs over the three $\text{SU}(3)_c \times \text{SU}(2)_L \times \text{U}(1)_Y$ irreducible factors of the SM gauge group and g_i denotes the corresponding gauge coupling. In the equation, J_μ^i represents the global current operators of

⁹For instance, certain Randall-Sundrum models are reformulations of the Composite Higgs scenario with or without the Higgs being a pseudo-Nambu-Goldstone Boson (pNGB). Little Higgs (see [30, 31] for a review) is a pNGB Higgs endowed with a special mechanism which could make it more Natural. Twin Higgs [32] is an additional protection for m_H which postpones the emergence of coloured particles in the spectrum. It can be applied both to the Composite Higgs and to the SUSY scenario.

¹⁰Those particles might be ‘‘partially composite’’, a concept that we will introduce below.

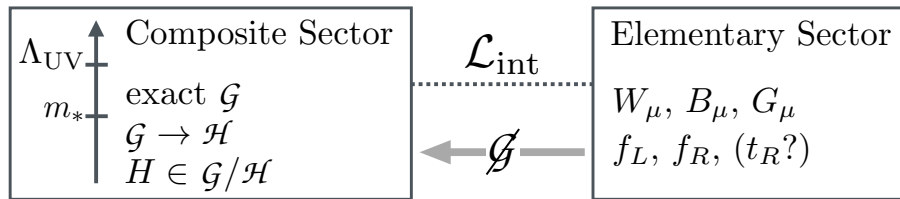


Fig. 6: The basic structure of the composite Higgs scenario.

the Composite Sector, namely the Noether currents associate with each of the three irreducible factors of the SM group. Notice that for this to make sense the CS must be invariant under the SM symmetries, therefore the complete global symmetry group of the CS, denoted by “ \mathcal{G} ” in fig. 6, must at least contain the SM one as a subgroup. Good reasons to make \mathcal{G} larger will be discussed shortly. Pushing forward the analogy with low-energy QCD and hadron physics, the ES sector is analogous to the photon plus light leptons system, whose coupling to the CS proceed through the electromagnetic gauge interaction precisely as in eq. (9).

The generic framework described until now has an important pitfall, which is overcome in what we nowadays properly call the “Composite Higgs” scenario¹¹ by the fact that the Higgs is a pseudo Nambu–Goldstone Boson (pNGB). The pitfall is that if the Higgs is a generic bound state of the CS dynamics one generically expects its mass to be of the order of the CS confinement scale m_* , namely $m_H \sim m_*$. In a sense, the point is that the mechanism of fig. 5 does indeed solve the Naturalness problem by making the shape of dm_H^2/dE localised at m_* but tells us nothing about the normalisation of the dm_H^2/dE function. In the absence of a special mechanism one can estimate $dm_H^2/dE \sim m_*$ at $E \sim m_*$ and the result of the integral is $m_H^2 \sim m_*^2$. One can reach the same conclusion heuristically by exploiting the analogy with QCD and browsing one of the many PDG [13] summary tables devoted to the properties of hadrons. By picking one generic (random) hadron in the list one would find that its mass is around the QCD confinement scale Λ_{QCD} and that it is surrounded by many other hadrons (a bit heavier or lighter) with similar properties. The Higgs particle is instead alone in the spectrum, or at least we are pretty sure that we would have seen (directly and/or indirectly) at least some of the other particles that would come with it if m_* was around $m_H \sim 100$ GeV. Therefore m_* must be of the TeV or multi-TeV order and some mechanism must be in place to explain why $m_H \ll m_*$. The problem is actually even more severe than that because the Higgs, on top of being light, is a narrow weakly coupled particle and furthermore its couplings are measured to agree with what predicted by the SM at the 10 or 20% level.¹² The existence of a CS resonance obeying these non-trivial properties by accident for no special underlying reason, appears extremely unlikely. The explanation of all these facts might be that the Higgs is a pNGB, namely a special CS hadron associated with the spontaneous breaking of the CS’s global symmetry group \mathcal{G} . The Higgs is said a “pseudo” NGB (pNGB) because \mathcal{G} is not an exact but an approximate symmetry. This is precisely what happens in QCD, where the π mesons are light because they are pNGB’s associated with the spontaneous breaking of the chiral group. The Higgs might be analogous to a pion, rather than to a random hadron in the PDG list.

The theory of Nambu–Goldstone Bosons works as follows. If the CS is endowed by the global group of symmetry \mathcal{G} , it is generically expected that this group will be broken spontaneously to a subgroup $\mathcal{H} \subset \mathcal{G}$ by CS confinement. If this happens, the Goldstone Theorem guarantees that a set of scalar particles, exactly massless as long as \mathcal{G} is an exact symmetry, are present in the spectrum. The theorem says that one such massless NGB particle arises for each of the symmetry generators that are broken in the $\mathcal{G} \rightarrow \mathcal{H}$ pattern, namely one for each generator in \mathcal{G} which is not part of the unbroken \mathcal{H} . The broken

¹¹See [33–35] for earlier references and [36, 37] for more recent ones.

¹²We nowadays know this directly from the LHC Higgs couplings determinations. Indirect evidences of SM-like couplings for the Higgs boson could however already be extracted from precision LEP data.

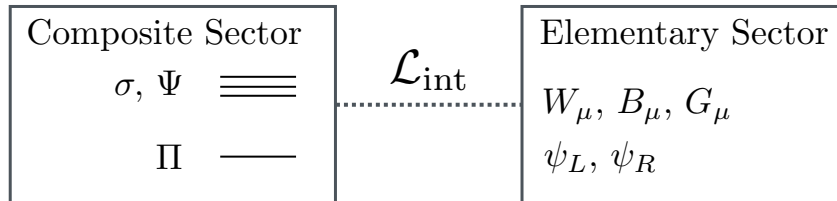


Fig. 7: The composite Higgs setup. The elementary SM gauge fields are the three W 's, the hypercharge boson B and the eight QCD gluons. The elementary fermionic quark and lepton fields are collectively denoted as ψ_L and ψ_R . The Higgs is labeled as “ Π ” (see the main text) and σ, Ψ represent Composite Sector resonances.

generators and the corresponding NGB's are collected in what is called the “ \mathcal{G}/\mathcal{H} coset”. If the Higgs emerges as one of those particle, which we can achieve by a judicious choices of the coset as discussed in the next section, it will be Naturally light given that its mass cannot be generated from the CS alone, which is exactly invariant under \mathcal{G} . A non-vanishing Higgs mass requires the interplay with the ES that breaks the \mathcal{G} symmetry and communicates the breaking to the CS trough \mathcal{L}_{int} as in fig. 6. Given that the Elementary/Composite interactions are weak and perturbative, such as the gauge couplings in eq. (9), a considerable gap between m_H and m_* is Naturally expected.

It is important to remark that the pNGB nature of the Higgs can also explain why its couplings are close to the SM expectations. This comes from a general mechanism called “vacuum misalignment” discovered in Refs. [33–35]. I will illustrate how it works in the next section through an example. The picture according to which the Higgs might be the lightest state of the CS, and thus the first one in being discovered, because it is a pNGB, turns out to be rather plausible.

2.2 The Minimal Composite Higgs Couplings

A rigorous and complete description of the Composite Higgs (CH) scenario goes beyond the purpose of these lectures, the interested reader is referred to the extensive reviews in [38, 39]. However most of the relevant features of CH can be illustrated by performing a specific calculation in a specific CH model, namely by computing the couplings of the Higgs to SM particles in the so-called Minimal CH Model (MCHM). Studying Higgs couplings and their possible departures from the SM expectations is one of the ways in which CH models have been and are being searched for at the LHC. Therefore the relevance of the calculation goes beyond its pedagogical value.

The MCHM [36] is based on the choice $\mathcal{G} = \text{SO}(5)$ and $\mathcal{H} = \text{SO}(4)$, which delivers NGB's in the so-called “minimal coset” $\text{SO}(5)/\text{SO}(4)$. According to the Goldstone theorem, the number of real NGB scalar fields in this theory is $4 = 10 - 6$, equal to the number of generators in $\text{SO}(5)$ minus those in $\text{SO}(4)$. Four real scalars are just sufficient to account for the two complex components of one Higgs doublet. Therefore the $\text{SO}(5)/\text{SO}(4)$ coset delivers a single doublet, rather than an extended Higgs sector as it would be the case if larger \mathcal{G} and \mathcal{H} groups are considered. This is why it is called the minimal coset. The Goldstones, i.e. the Higgs, are the lightest particles of the CS, as shown in fig. 7. Therefore they can be studied independently of the other hadrons of the CS (called “resonances”) at all energies below the resonance mass scale $m_* \sim \text{TeV}$. On-shell Higgs couplings are low-energy observables in this context, thus they can be computed independently of the detailed knowledge of the resonance dynamics.

A simple model for Goldstone bosons is defined as follows. Be $\vec{\Phi}$ a five-components vector of real fields, on which the $\text{SO}(5)$ group acts as rotations in five dimensions, and impose on it the condition

$$\vec{\Phi}^T \cdot \vec{\Phi} = f^2. \quad (10)$$

The constant parameter f is called the “Higgs decay constant” because it plays in CH the same role of the pion decay constant f_π in the low-energy theory of QCD pions. It has the dimensionality of energy

and it represents the scale of $\mathcal{G} \rightarrow \mathcal{H}$ spontaneous breaking. The 4 Goldstone bosons Π_i , $i = 1, \dots, 4$ are introduced as the fields that parameterise the solutions to the constraint (10), namely

$$\vec{\Phi} = f \begin{bmatrix} \sin \frac{\Pi}{f} \vec{\Pi} \\ \cos \frac{\Pi}{f} \end{bmatrix}, \quad (11)$$

where $\Pi = \sqrt{\vec{\Pi}^T \cdot \vec{\Pi}}$. Geometrically (see fig. 8), $\vec{\Phi}$ lives on a sphere in the five-dimensional space and $\vec{\Pi}$ are the four angular variables which are needed to parametrise the sphere. Notice that the constraint (10) is invariant under $\text{SO}(5)$ rotations of $\vec{\Phi}$, therefore the theory of Goldstone Bosons we will construct out of it will respect the $\text{SO}(5)$ symmetry. A controlled and perturbative breaking of the symmetry will emerge from the coupling with SM gauge fields and fermions.

The four Π 's are the Higgs, but this is not yet apparent because the Higgs field is typically represented as a two-components complex doublet $H = (h_u, h_d)^T$ rather than a real quadruplet. The conversion between the two notations is provided by

$$\vec{\Pi} = \begin{bmatrix} \Pi_1 \\ \Pi_2 \\ \Pi_3 \\ \Pi_4 \end{bmatrix} = \frac{1}{\sqrt{2}} \begin{bmatrix} -i(h_u - h_u^\dagger) \\ h_u + h_u^\dagger \\ i(h_d - h_d^\dagger) \\ h_d + h_d^\dagger \end{bmatrix}. \quad (12)$$

The deep meaning of this equation is that the unbroken group $\text{SO}(4)$ is actually equivalent to the product of two groups, $\text{SU}(2)_L \times \text{SU}(2)_R$, where $\text{SU}(2)_L$ is the habitual SM one and $\text{SU}(2)_R$ is a generalisation of the SM Hypercharge $\text{U}(1)_Y$.¹³ Namely, $\text{SU}(2)_R$ contains the Hypercharge, which is identified with its third generator, $Y = T_R^3$. The Higgs quadruplet $\vec{\Pi}$ is a 4 of $\text{SO}(4)$, or equivalently a $(\mathbf{2}, \mathbf{2})$ of $\text{SU}(2)_L \times \text{SU}(2)_R$. The $(\mathbf{2}, \mathbf{2})$ transforms as a $\mathbf{2}_{1/2}$ Higgs doublet under the SM $\text{SU}(2)_L \times \text{U}(1)_Y$ subgroup. The conversion formula in eq. (12) does depend on the convention chosen for the $\text{SO}(4)$ generators. I thus report them for completeness

$$T_{L/R}^\alpha = \begin{bmatrix} t_{L/R}^\alpha & 0 \\ 0 & 0 \end{bmatrix}, \quad (t_{L/R}^\alpha)_{ij} = -\frac{i}{2} \left[\varepsilon_{\alpha\beta\gamma} \delta_i^\beta \delta_j^\gamma \pm (\delta_i^\alpha \delta_j^4 - \delta_j^\alpha \delta_i^4) \right]. \quad (13)$$

In the equation, capital $T_{L/R}^\alpha$ ($\alpha = 1, 2, 3$) denote the 5×5 generators of $\text{SO}(4)$ seen as a subgroup of $\text{SO}(5)$, small $t_{L/R}^\alpha$ are the habitual generators written as 4×4 matrices.

The Lagrangian for $\vec{\Phi}$, out of which the one of the Goldstones will be straightforwardly extracted, simply reads

$$\mathcal{L} = \frac{1}{2} D_\mu \vec{\Phi}^T \cdot D^\mu \vec{\Phi}, \quad \text{where } D_\mu \vec{\Phi} = (\partial_\mu - i g W_\mu^\alpha T_L^\alpha - i g' B_\mu T_R^3) \vec{\Phi}. \quad (14)$$

Notice that the couplings with the SM gauge fields W^α and B come from the covariant derivative and they are completely determined by the requirement of gauge invariance. This is exactly what happens when we construct the SM through the habitual gauging procedure and follows from the fact that we decided, in eq. (9), to introduce the SM W and B as gauge fields. As a result of this fact, a very sharp prediction will be obtained for the Higgs couplings to the SM vector bosons. To compute the couplings of the physical Higgs we go to the unitary gauge

$$H = \begin{bmatrix} 0 \\ \frac{V+h(x)}{\sqrt{2}} \end{bmatrix}, \quad (15)$$

¹³This group is also called the ‘‘custodial’’ $\text{SO}(4)_c$. It plays a major role in BSM physics as it suppresses certain BSM effects constrained by LEP and often helps the compatibility of BSM models with data.

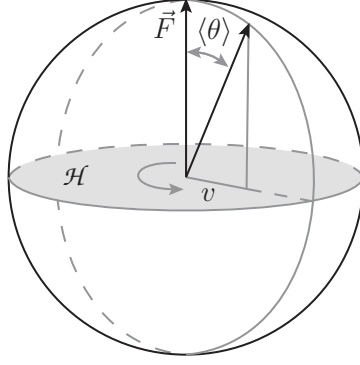


Fig. 8: A geometrical illustration of EWSB through vacuum misalignment, in the case of the spatial rotations group $\mathcal{G} = \text{SO}(3)$ with $\mathcal{H} = \text{SO}(2)$. The $\text{SO}(2)$ breaking from vacuum misalignment is proportional to the projection of \vec{F} on the $\text{SO}(2)$ plane, $v = f \sin\langle\theta\rangle$.

and eq. (14) becomes

$$\mathcal{L} = \frac{1}{2} (\partial_\mu h)^2 + \frac{g^2}{4} f^2 \sin^2 \frac{V+h}{f} \left(|W|^2 + \frac{1}{2c_w^2} Z^2 \right), \quad (16)$$

where W and Z denote the ordinary SM mass and charge eigenstate fields, c_w is the cosine of the weak mixing angle defined as usual by $\tan \theta_w = g'/g$. The parameter V denotes the VEV of the Higgs field, induced by a yet unspecified potential.

We can learn a lot on CH by looking at eq. (16). First of all, we can read the mass of the SM vector bosons

$$m_W = c_w m_Z = \frac{1}{2} g f \sin \frac{V}{f} \equiv \frac{1}{2} g v, \quad (17)$$

and, by comparing with the corresponding SM formulas, extract the definition of the physical EWSB scale $v \simeq 246$ GeV. We see that v , unlike in the SM, is not directly provided by the composite Higgs VEV, but rather it is given by

$$v = f \sin \frac{V}{f}. \quad (18)$$

The geometrical reason for this equation is illustrated in fig. 8. According to eq. (11), the vacuum configuration assumed by $\vec{\Phi}$ when the Higgs takes a VEV, call it $\langle\vec{\Phi}\rangle$, is a vector of norm f that forms an angle $\langle\theta\rangle = \langle\Pi\rangle/f = V/f$ with the reference vector $\vec{F} = (0, 0, 0, f)^T$. The reference vector is the vacuum configuration $\vec{\Phi}$ would assume if the Higgs had vanishing VEV and the angle $\langle\theta\rangle$ measures how far the true VEV is from the reference vector. If $\langle\vec{\Phi}\rangle = \vec{F}$, the vacuum would be invariant under $\text{SO}(4)$, and thus in particular under the SM group which is part of $\text{SO}(4)$. The amount of breaking of the EW symmetry is thus measured by the transverse component of $\langle\vec{\Phi}\rangle$ with respect to \vec{F} because it is only this component the one that makes the vacuum configuration non-invariant under the SM group. From this observation, eq. (18) follows. An important property of eq. (17) that I should not forget to outline is that the W and Z boson masses are related by the familiar SM tree-level condition $m_W = c_w m_Z$, which is accurately established experimentally. This property is due to the unbroken $\text{SO}(4)$ group and it furnishes one example of the ability of this ‘‘custodial’’ symmetry to suppress BSM effects as mentioned in footnote 13.

Next, we can Taylor-expand eq. (16) in powers of the physical Higgs field $h(x)$ and notice that it provides an infinite set of local interactions involving two gauge and an arbitrary number of Higgs fields. The first few terms in the expansion are

$$\frac{g^2 v^2}{4} \left(|W|^2 + \frac{1}{2c_w^2} Z^2 \right) \left[2\sqrt{1-\xi} \frac{h}{v} + (1-2\xi) \frac{h^2}{v^2} - \frac{4}{3}\xi\sqrt{1-\xi} \frac{h^3}{v^3} + \dots \right], \quad (19)$$

where we traded the parameters V and f for the physical EWSB scale v and for the parameter

$$\xi = \frac{v^2}{f^2} = \sin^2 \frac{V}{f} \leq 1. \quad (20)$$

ξ measures how smaller the scale of EWSB scale is with respect to the scale of $\text{SO}(5) \rightarrow \text{SO}(4)$ breaking or, equivalently, the magnitude of the misalignment angle $\langle \theta \rangle$. The capital importance of the ξ parameter in CH models will become apparent by the discussion that follows. Eq. (19) contains single- and double-Higgs vertices similar to those which arise in the SM, but with modified couplings

$$k_V \equiv \frac{g_{hVV}^{\text{CH}}}{g_{hVV}^{\text{SM}}} = \sqrt{1 - \xi}, \quad \frac{g_{hhVV}^{\text{CH}}}{g_{hhVV}^{\text{SM}}} = 1 - 2\xi. \quad (21)$$

Also, it contains higher-dimensional vertices with more Higgs field insertions which are absent for the SM Higgs. By measuring Higgs couplings and/or (if possible) by searching for these higher-dimensional vertices we can thus test experimentally the possible composite nature of the Higgs boson.

One peculiarity of eq. (21) that you might have noticed already is that both formulas approach 1 in the limit $\xi \rightarrow 0$, meaning that both the hVV and the $hhVV$ couplings reduce to the values predicted by the SM in this limit. Moreover the coupling strength of the higher-dimensional vertices in eq. (19) are proportional to ξ so that they disappear for $\xi \rightarrow 0$ and the same happens to all other interactions of even higher order in the Taylor series. In summary, the complete Lagrangian for the Higgs and the EW boson collapses to the one of the SM for $\xi \rightarrow 0$ so that the Composite Higgs becomes effectively indistinguishable from the elementary SM Higgs in this limit. The reason for this is that the $\xi \rightarrow 0$ limit is taken at fixed v by sending $f \rightarrow \infty$, and f is related with the typical energy scale of the Composite Sector. For $f \gg v$ the CS decouples from the EWSB scale while the Higgs stays light because it is a NGB. The only way in which the theory can account for this large scale separation is by turning itself, spontaneously, into the SM. Of course ξ is not zero, but provided it is sufficiently small this phenomenon explains why the measured couplings of the Higgs boson are close to the SM predictions, which is a priori not trivial at all as discussed in section 2.1. The very existence of the parameter ξ and the possibility of adjusting it in order to mimic the SM predictions with arbitrary accuracy marks the essential difference between the modern CH construction and the old idea of Technicolor [21, 40, 41] (see Ref. [42] for a review). Not only in Technicolor, unlike in CH, there is no structural reason to expect the presence of a light Higgs boson. There is not even a reason why this scalar, if accidentally present in the spectrum, should have couplings which are similar to the SM ones. Notice however that taking ξ very small, as we will be obliged to do if the agreement with the SM will survive more precise measurement, does not come for free in CH models. I will come back to this point in the next section.

Let us now turn to the calculation of the Higgs couplings to fermions. In order to proceed we first need to specify the structure of the fermionic part of the interaction that connects the elementary and the composite sector as in fig. 7. This is taken to be similar to the gauge part in eq. (9), namely

$$\mathcal{L}_{\text{int}}^{\text{fermion}} \sim \lambda \bar{\psi} \mathcal{O}, \quad (22)$$

where ψ is one of the SM fermion fields in the elementary sector, \mathcal{O} is a composite sector local operator and λ is a free parameter that sets the strength of the interaction. One such operator is present for each of the SM chiral fermions, each with its own coupling strength λ . Below we will mostly focus on the top quark sector, in which case the relevant SM fields are the $\psi = q_L$ doublet and the $\psi = t_R$ singlet. The similarity with eq. (9) consists in the fact that ψ is an elementary sector field just like A_μ , which is coupled linearly to an operator \mathcal{O} made of composite sector constituents very much like A_μ couples to the composite sector current operator J_μ . Linear fermion couplings of the type (22) were first introduced in Ref. [43] and are said to have the ‘‘Partial Compositeness’’ structure for a reason that I will explain in the next section.

	Top	Bottom
$\mathbf{5} \oplus \mathbf{5}$	$k_t = \frac{1-2\xi}{\sqrt{1-\xi}} \quad c_2 = -2\xi$	$k_b = \frac{1-2\xi}{\sqrt{1-\xi}}$
$\mathbf{4} \oplus \mathbf{4}$	$k_t = \sqrt{1-\xi} \quad c_2 = -\frac{\xi}{2}$	$k_b = \sqrt{1-\xi}$
$\mathbf{14} \oplus \mathbf{1}$	$k_t = \frac{1-2\xi}{\sqrt{1-\xi}} \quad c_2 = -2\xi$	$k_b = \frac{1-2\xi}{\sqrt{1-\xi}}$

Table 1: Kappa factor and anomalous c_2 coupling predictions in the top and bottom quark sector for different choices of the fermionic operators representations under the $\text{SO}(5)$ group.

An important difference between gauge (9) and fermion (22) interactions is that in the former case we do know perfectly what the CS operator J is, while in the latter one we have to deal with an operator \mathcal{O} of yet unspecified properties. What we know is that \mathcal{O} must be a spin 1/2 fermionic operator in order for equation (22) to comply with Lorentz invariance and that it must be a triplet of QCD colour to respect the $\text{SU}(3)_c$ symmetry. This latter property will have important phenomenological implications in that it obliges the CS to carry QCD colour and thus to produce coloured resonances which are easy to produce at the LHC. We also know that \mathcal{O} must be in some multiplet of the CS global group \mathcal{G} but we don't know in which one. The only constraint is that the representation in which \mathcal{O} lives must contain the SM $\text{SU}(2)_L \times \text{U}(1)_Y$ group representation of the corresponding ψ fermion, in order for eq. (22) not to break the EW group. Few options (focussing on reasonably small multiplets) exist to solve this constraint and for each option the calculation of Higgs couplings might produce a different result. Unlike those with gauge bosons, Higgs couplings to fermions are thus not uniquely predicted in terms of ξ .

One simple option is to make \mathcal{O} be in the $\mathbf{5}$, in which case eq. (22) becomes

$$\mathcal{L}_{\text{int}}^{\text{fermion}} = \lambda_L (\bar{Q}_L)^I \mathcal{O}_I + \lambda_R (\bar{T}_R)^I \mathcal{O}_I. \quad (23)$$

The index I runs from 1 to 5 and it transforms in the $\mathbf{5}$ of $\mathcal{G} = \text{SO}(5)$. The capital Q and T fields are two quintuplets that contain the elementary $q_L = (t_L, b_L)$ and t_R fermions. Explicitly, they are

$$\vec{Q}_L = \frac{1}{\sqrt{2}}(-i b_L, -b_L, -i t_L, t_L, 0)^T, \quad \vec{T}_R = (0, 0, 0, 0, t_R)^T. \quad (24)$$

Their form is chosen in such a way that (t_L, b_L) and t_R appear precisely in those components of the Q_L and T_R quintuplets that display the transformation properties of a $\mathbf{2}_{1/6}$ and of a $\mathbf{1}_{2/3}$ of the SM $\text{SU}(2)_L \times \text{U}(1)_Y$ subgroup. In short, the form of the embeddings is fixed by the requirement that eq. (23) must respect the SM gauge symmetry.¹⁴

Once the representation is chosen, Higgs couplings are determined by symmetries. There is indeed a unique \mathcal{G} -invariant operator we can form with $\vec{\Phi}$ (i.e., the Higgs), the embeddings and no derivatives. Furthermore the coefficient of this operator is fixed by the fact that the correct top mass must be reproduced when the Higgs is set to its VEV. The operator is

$$\begin{aligned} \mathcal{L}_{\text{Yukawa}}^t &= -\frac{\sqrt{2}m_t}{\sqrt{\xi(1-\xi)}} \Phi_I \bar{Q}_L^I T_R = -\frac{m_t}{2} \frac{1}{\sqrt{\xi(1-\xi)}} \sin \frac{2(V+h)}{f} \bar{t}t \\ &= -m_t \bar{t}t - k_t \frac{m_t}{v} h \bar{t}t - c_2 \frac{m_t}{v^2} h^2 \bar{t}t + \dots \end{aligned} \quad (25)$$

¹⁴I'm being quite sloppy here. In order to make the thing work one needs to enlarge the global group of the CS promoting it to $\mathcal{G} = \text{SO}(5) \times \text{U}(1)_X$ and to change the definition of the SM Hypercharge into $Y = T_R^3 + X$, with X the charge under the newly introduced $\text{U}(1)_X$ group. It is only by giving an X charge of 2/3 to \mathcal{O} and to Q_L and T_R that one finds a $\mathbf{2}_{1/6}$ and of a $\mathbf{1}_{2/3}$ in the decomposition and eq. (23) truly complies with gauge invariance.

It produces the top quark mass plus, after Taylor-expanding, a set of interactions of the physical Higgs with $t\bar{t}$. The first interaction is an $h-t\bar{t}$ vertex like the one we have in the SM. The second one is an exotic $hh-t\bar{t}$ coupling which is absent in the SM and could be tested in the double-Higgs production process [44, 45]. The modified single-Higgs coupling and the double-Higgs vertex read

$$k_t^{\mathbf{5}} \equiv \frac{g_{htt}^{\text{comp}}}{g_{htt}^{\text{SM}}} = \frac{1 - 2\xi}{\sqrt{1 - \xi}}, \quad c_2^{\mathbf{5}} = -2\xi, \quad (26)$$

where the $\mathbf{5}$ superscript reminds us that the prediction depends on the choice of the representation (the $\mathbf{5}$) for the fermionic operator \mathcal{O} .

One proceeds in exactly the same way to generate the mass and the Yukawa coupling for the bottom quark, obtaining the bottom coupling modification k_b and an anomalous $hh-b\bar{b}$ vertex, which however is weighted by the bottom mass and thus it is too small to be phenomenologically relevant. Also for the bottom, the $\mathbf{5}$ could be a valid representation for the corresponding \mathcal{O} operator. Other choices like the $\mathbf{4}$ could be considered both for the bottom and for the top, with the results reported in table 1. In the table, the notation “ $\mathbf{5} \oplus \mathbf{5}$ ” means that the fermionic operators that couples to the left-handed doublet q_L and the one that couples to the right-handed singlet (t_R or b_R) are in the same representation, i.e. the $\mathbf{5}$, while they are both in the $\mathbf{4}$ in the “ $\mathbf{4} \oplus \mathbf{4}$ ” case. However the two representations might be different, in spite of the fact that a single name was given for shortness to the two \mathcal{O} operators in eq. (23). A reasonable option is to take the doublet mixed with a $\mathbf{14}$ and the singlet mixed with a singlet operator. This is denoted as the “ $\mathbf{14} \oplus \mathbf{1}$ ” case in the table. Up to caveats which is not worth discussing here, table 1 exhausts what are considered to be the “most reasonable” options for the fermionic operator representations and the corresponding predictions of Higgs couplings. Other patterns which could be worth studying are in Appendix B of Ref. [46].

2.3 Composite Higgs Signatures

Now that the basic structure of the CH scenario has been introduced, I can start illustrating its phenomenology. Additional structural aspects that were left out from the previous discussion will be introduced when needed. The signatures of CH that have been searched for at the 8 TeV LHC run (run-1) and we will keep studying at run-2 and possibly at future colliders are Higgs couplings modifications, vector resonances and top partners.

Higgs Couplings Modifications

The current status of our field is that we are not sure of which kind of new physics we are looking for. This is much different from what it used to be the case when the Higgs still had to be discovered. In searching for the Higgs one could rely on one single full-fledged model (the SM) with only one at that time unknown parameter (the Higgs mass). Searching for the Higgs boson was basically equivalent to searching for the SM theory, which was capable to provide detailed and specific predictions for the expected signal to be searched for in the data. We are not anymore in this situation. Even if we focus on one given BSM hypothesis (CH, in the present case, but the same applies to SUSY, WIMP DM or whatever else), this hypothesis is not at all equivalent to a single specific model. This is why in BSM searches so much importance is given to model-independence. Namely to the fact that we should not organise our efforts around specific signatures of specific benchmark models, but rather on generic model-independent features of the scenario we aim to investigate, ideally on those features that are unmistakably present in all the models that provide specific realisations of the generic scenario.

Model-independence is the first reason to be interested in coupling modifications in CH, given that we saw in the previous section how Higgs couplings can be universally predicted as a function of ξ . This prediction is independent of the detailed dynamics of the Composite Sector resonances, for which many different explicit models (with plenty of free parameters) can be written down (see e.g. [36, 47]). The

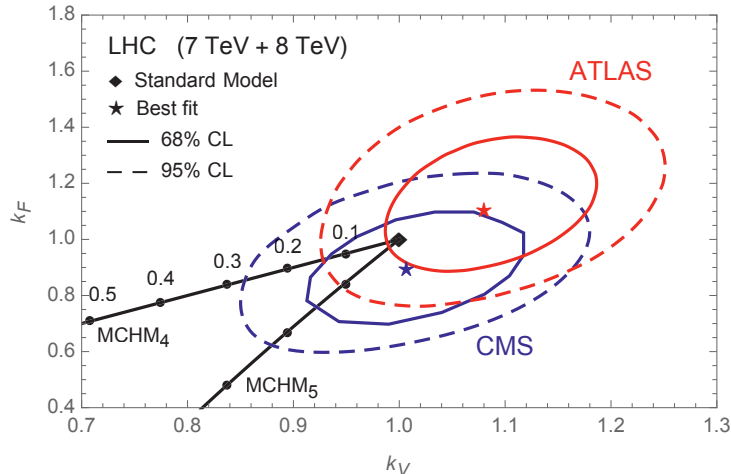


Fig. 9: Fit of the Higgs coupling strength to the gauge bosons (k_V) and fermions (k_F) obtained by the ATLAS (red contours) and CMS collaborations (blue contours) from the combination of the 7 and 8 TeV LHC data. Solid black lines show the CH predictions, depending on the fermionic operators representation, at different values of ξ .

Higgs couplings predictions in all these models are always (up to small corrections) those in eq. (21) and in table 1. Higgs couplings have been measured at the LHC run-1 both by ATLAS [48] and CMS [49], with the result reported in fig. 9 in the k_V - k_F plane. k_F is a common rescaling factor for the SM coupling to fermions, therefore the plot assumes $k_t = k_b = k_F$. The CH predictions are also reported on the plot for different values of ξ . The curve labeled “MCHM₄” follows the trajectory in the second line of table 1, while the “MCHM₅” one represents the first and the third lines. The resulting limit quoted by ATLAS in Ref. [50] is $\xi < 0.12$ in the MCHM₄ and $\xi < 0.10$ in the MCHM₅ at 95% CL. ATLAS limit is stronger than the CMS one because the ATLAS central value is slightly away from the SM in the opposite direction than the one predicted by CH. The resulting limit is thus stronger than the expected one. Because of this stringent bound, it is unlikely that much progress will be made with the next runs of the LHC, given that the expected limit with the full luminosity of 300 fb^{-1} is of around $\xi < 0.1$ [51–53], very close to the present one. Of course if the central value will not sit on the SM the limit could improve, but we can definitely exclude the occurrence of the discovery of a non-vanishing ξ .

We saw that ATLAS and CMS are doing a rather good job in studying Higgs couplings modifications due to compositeness. The study is however not fully complete, and it could be generalised in three directions. First, one can easily construct models where $\kappa_t \neq \kappa_b$. It is sufficient for instance to place the fermionic operators associated with the top quark in the 5 representation while assigning those for the bottom to a 4. In this case k_t will follow the prediction in the first line of table 1, while k_b will follow the second line. Studying this case is straightforward even if it requires going beyond the k_V - k_F plane. No much improvement is however expected in the compatibility of the model since k_V is still the one in eq. (21) and the ATLAS preference for $k_V > 1$, independently of the fermion couplings, is already sufficient to produce a limit on ξ not much above 0.1. A second direction of improvement is to study not only the modification of the Higgs vertices that exist already in the SM, but also anomalous couplings such as hh - $t\bar{t}$ in eq. (25). The latter might be visible in double-Higgs production when enough luminosity will be collected. However existing studies (see e.g. [54]) suggest that even with the high-luminosity stage of the LHC (HL-LHC) it might be hard to reach a competitive accuracy. A third direction of improvement would be to generalise the analysis to non-minimal cosets, namely to go beyond the minimal $\text{SO}(5)/\text{SO}(4)$ example we discussed here. The problem is that non-minimal cosets produce an extended Higgs sector and thus the modification of the Higgs couplings emerge from the pile-up of two effects. One has the modifications due to compositeness, which are analogous to those in eq. (21) and table 1, plus further modifications due to the mixing of the Higgs boson with extra light scalar states. The former

effect is easy to compute, while the latter one is hard to parametrise with a sufficient degree of generality as it depends on the properties of the extra scalars that mix with the Higgs. Furthermore, all this should be studied in correlation with the direct searches for extra scalars. A detailed phenomenological analysis of extended cosets is missing in the literature, in spite of the fact that extended cosets are not at all implausible from the view-point of model-building. The original CH model [33], for instance, was based on an $SU(5)/SO(5)$ coset, which delivers one complex and one real scalar triplet, plus one singlet, on top of the ordinary Higgs doublet.

The second reason to be interested in Higgs couplings modification is the (almost) direct connection between the parameter ξ , which couplings measurements are capable to probe, and the level of fine-tuning Δ of the theory. We discussed in the previous section that for $\xi \rightarrow 0$ CH models reduce to the SM, which is an eminently Un-Natural theory. It is thus expected that taking ξ small might be dangerous in terms of fine-tuning. In order to illustrate how this works, let us write down the structure of the Higgs potential, as it emerges in a certain class of models and under certain approximations.¹⁵ It reads

$$V[H] \simeq -\alpha f^2 \sin^2 \frac{H}{f} + \beta f^2 \sin^4 \frac{H}{f}, \quad (27)$$

where the coefficients α and β can be computed within explicit models (see ...) and depend on some of their free parameters. By adjusting the free parameters one can set α and β in such a way that the VEV V of the Higgs field (i.e., the minimum of the potential) produces our favorite value of ξ through eq. (20) and also to reproduce the observed Higgs boson mass. These two constraints read, respectively

$$\begin{aligned} \alpha &= 2\xi\beta, \\ m_H^2 &= 8\xi(1-\xi)\beta. \end{aligned} \quad (28)$$

Both conditions might cost fine-tuning, let us however momentarily focus only on the first one. It tells us that the “expected” value of ξ is proportional to $(\alpha)_{\text{expected}}/(\beta)_{\text{expected}}$, where by “expected” I mean the size of the α and β coefficients that are generically encountered in the parameter space of the model. In all existing CH models, the expected magnitudes of α and β either are comparable, or α is larger than β , making that having $\xi \ll 1$ is never an expected structural feature of the model. In this situation, enforcing $\xi \ll 1$ requires fine-tuning. Namely, a cancellation must take place in the prediction for α , obtained by finely adjusting the parameters of the underlying model. This tuning is at least of order

$$\Delta = \frac{(\alpha/\beta)_{\text{expected}}}{\alpha/\beta} \geq \frac{1}{2\xi}. \quad (29)$$

The above equation displays the anticipated connection between ξ and the level of Un-Naturalness of the theory. The current bound $\xi < 0.1$ corresponds to a not fully Natural (but still acceptably so) theory with a level of tuning $\Delta > 5$.

Actually, we are not sure of the connection between ξ and Δ in a fully model-independent way. In principle, it would be sufficient to find a model where α is structurally smaller than β in order to avoid the tuning in the Higgs VEV and to have ξ Naturally small. The problem, as mentioned above, is that no such model currently exists, but this does not mean that one could not be invented in the future. Engineer a Naturally small ξ is the purpose of the Little Higgs constructions [30, 31], however as of now I’m not aware of any convincing and realistic model of this class.

Vector Resonances

Searching for modified couplings of the Higgs boson is not the only way to test Higgs compositeness experimentally. Direct searches for new particles also play an important role, which will become the

¹⁵The one that follows is an approximate formula for the Higgs potential in models where the fermionic operators in the top quark sector are in the $\mathbf{5} \oplus \mathbf{5}$ or in the $\mathbf{14} \oplus \mathbf{1}$ configurations. The connection between the Higgs potential and the top quark sector will be explained later. Further details can be found in Chapter 3 of Ref. [39].

leading role at the LHC run-2 thanks to the improved collider energy. The new particles to be searched for are the resonances that emerge, together with the Higgs, from the Composite Sector of the theory (see fig. 7). Resonances at a scale $m_* \sim \text{TeV}$ are unmistakably present in CH, they are the “hadrons” of the new strong force we are obliged to postulate if we want the Higgs to be a composite object. If we are lucky and the CH scenario is realised in Nature, plenty of such resonances exist and a sort of new “Subatomic Zoo” is waiting to be discovered at the TeV scale.

Predicting the quantum numbers and the properties of the CS resonances is not completely straightforward. However a valid rule of thumb is that resonances are associated with the operators of the CS. Namely, for each resonance it should be possible to identify at least one CS operator that is capable to excite it from the vacuum. The first set of operators we encountered are the global currents “ J ” in eq. (9), associated to a set of resonances “ ρ ” through the equation

$$\langle \rho | J | 0 \rangle \neq 0. \quad (30)$$

The currents are bosonic operators that transform as vectors of the Lorentz group, therefore we expect ρ to be a spin-1 vector particle in order for eq. (30) to comply with Lorentz symmetry.¹⁶ The analogous hadrons in QCD are the ρ mesons, the ω and the a_1 , each associated with one of the global currents of the chiral group. Eq. (30) also tells us the quantum numbers of ρ under the SM group. If for instance $\mathcal{G} = \text{SO}(5)$, the global current J is in the Adjoint **10** representation of the group, which decomposes in a **3**₀, plus a **1**₀, plus a **1**₁ and a **2**_{1/2} of the SM $\text{SU}(2)_L \times \text{U}(1)_Y$ subgroup (i.e., a $(\mathbf{3}, \mathbf{1}) \oplus (\mathbf{1}, \mathbf{3}) \oplus (\mathbf{2}, \mathbf{2})$ of $\text{SO}(4)$). ρ particles in all these representations are thus expected, plus one further **1**₀ because $\mathcal{G} = \text{SO}(5)$ actually needs to be enlarged to $\text{SO}(5) \times \text{U}(1)_X$ (see Footnote 14) in order to incorporate SM fermion masses into the theory. The existence of vectors with these quantum numbers is confirmed by explicit models. A first study of their phenomenology in the context of holographic realisations of the CH scenario was performed in Ref.s [55–57]. Other interesting particles of this class are coloured spin-1 vectors, the so-called “KK-gluons” [58]. KK-gluons emerge because the CS (see section 2.2) needs to carry QCD colour and thus it contains an extra $\text{SU}(3)_c$ group of symmetry on top of the “electroweak” $\text{SO}(5) \times \text{U}(1)_X$ factors. This produces extra global current operators and their corresponding particles in the octet of the QCD group.

All particles above are worth searching for, however here I will focus, for definiteness, on vector resonances in the **3**₀ triplet, the so-called Heavy Vector Triplet (HVT) [59]. The reason for this choice is that HVT’s display a quite simple phenomenology, still varied enough and promising in terms of mass-reach. Furthermore, the **3**₀ vectors are associated with the global currents of the SM $\text{SU}(2)_L$ subgroup of the CS symmetry group. The existence of such subgroup is absolutely unavoidable in CH models, independently of whether or not we stick to the minimal coset or even of whether the Higgs is a pNGB or not. HVT’s thus unmistakably emerge in all models where a strong dynamics is involved in the mechanism responsible for EWSB. This includes old-fashioned Technicolor, in which these particles are also present and are known as “techni-rho” mesons.

Characterising the HVT phenomenology requires a little digression on how we do expect, in general, Composite Sector particles to be coupled among themselves and with the gauge and fermionic fields in the Elementary Sector. This expectation can be encapsulated (see Ref. [37] and Ch. 3 of [39]) in a “power-counting rule”, namely a formula that tells us the expected size of the interaction vertices or, which is the same, of the interaction operators in the Lagrangian. The rule is based on the idea that the CS is characterised by one typical mass scale m_* (the confinement scale) and by one typical coupling strength parameter “ g_* ”. It is thus said to be a “1 Scale 1 Coupling” (1S1C) power-counting. The parameter g_* represent the typical magnitude of the interaction vertices involving CS particles, among which

¹⁶ ρ cannot have spin greater than 1 because a Lorentz vector operator cannot have a non-vanishing matrix element between the vacuum and a high-spin particle. Massless scalars can instead be excited from the vacuum by a conserved current if it is associated with a spontaneously broken generator. These scalars are nothing but the NGB’s of the theory we already discussed extensively.

the Higgs. It can thus be expressed in terms of the Higgs decay constant f and defined as

$$g_* = \frac{m_*}{f}. \quad (31)$$

The coupling g_* can easily be very large, close to the absolute maximal value $g_* \sim 4\pi$ a coupling strength parameter can assume. It is for instance very large in real-world QCD, where it can be identified with the ρ meson coupling $g_\rho \simeq 6$. It can however be smaller if the underlying strongly-interacting theory is characterised by a large number of colours N_c . For instance, $g_* \sim 4\pi/\sqrt{N_c} \rightarrow 0$ in the large- N_c limit of QCD. We are thus entitled to consider values of g_* anywhere from 0 to 4π , however basic phenomenological consistency of the CH scenario requires it to be above around $y_t \simeq 1$. Therefore in what follows we will take $g_* \in [1, 4\pi]$.

On top of g_* , the other couplings that are present in the theory are the SM gauge couplings “ g ” in eq. (9) and the fermionic interactions “ λ ” in eq. (23). They control the strength of those interactions of the Elementary Sector fields (gauge and fermions, respectively) that are generated by the CS dynamics, such as for instance their couplings with the Higgs and with the CS resonances. The complete power-counting formula, which takes care both of CS particles self-couplings and of Elementary/Composite interactions, reads

$$\mathcal{L} = \frac{m_*^4}{g_*^2} \widehat{\mathcal{L}} \left[\frac{\partial}{m_*}, \frac{g_* H}{m_*}, \frac{g_* \sigma}{m_*}, \frac{g_* \Psi}{m_*^{3/2}}, \frac{g \cdot A_\mu}{m_*}, \frac{\lambda \cdot \psi}{m_*^{3/2}} \right], \quad (32)$$

where $\widehat{\mathcal{L}}$ is a dimensionless polynomial function with order one coefficients. In the equation, σ represents a bosonic CS resonance, such as a spin-1 particle like the ρ 's we aim to study, while Ψ denotes a fermionic resonance such as the Top Partners we will discuss in the next section. The different power of m_* in the denominator simply follows from the different energy dimensionality (1 and 3/2) of bosonic and fermionic fields. The fields A_μ and ψ collectively denote the ES sector gauge and fermions, each entering in the power-counting formula with its own “ g ” and “ λ ” coupling. For instance $A_\mu = W_\mu^\alpha$ couples through the weak coupling g while the QCD gluons, $A_\mu = G_\mu^a$, couples through the strong coupling g_S . Similarly the third family q_L doublet couples through the λ_L parameter in eq. (23) and t_R couples with strength λ_R . Notice that light generation quarks and leptons couple with their own strengths, which are typically much smaller than λ_L and λ_R because their role in the theory is to generate the light fermions Yukawa's rather than the large top Yukawa coupling. An estimate of light generation couplings is postponed to the next section, since they will turn out to be very small we are entitled to neglect them in what follows.

Let us now turn to HVT phenomenology. Since g_* is the largest coupling in the theory, the strongest vertices of ρ are those that only involve CS particles and no ES degrees of freedom. Among those we have a coupling with the Higgs field

$$g_* c_H \rho_\mu^a i H^\dagger \tau^a \overleftrightarrow{D}^\mu H, \quad (33)$$

where $\rho_\mu^{a=1,2,3}$ denotes the components of the triplet, $\tau^a = \sigma^a/2$ are the $SU(2)_L$ generators and the double arrow denotes the covariant derivative acting on the right minus the one acting on the left. The coefficient of the operator has been estimated with eq. (32) up to an unknown order one parameter c_H . The one in eq. (33) is the unique gauge-invariant operator involving the ρ and two Higgs fields that cannot be eliminated by the equations of motions. It produces couplings of ρ with all the four real components of the Higgs doublet which correspond to the physical Higgs boson plus the three longitudinal polarisation components of the SM W^\pm and Z massive vector bosons.¹⁷ The operator thus mediates the decay of ρ

¹⁷The correspondence between longitudinally polarised vector bosons and the so-called “unphysical” components of the Higgs field (i.e., the charged h_u and the imaginary part of the neutral h_d component of the doublet) is ensured by the Equivalence Theorem [5]. It holds at energies much above the vector boson masses, which is an excellent approximation for our purposes. In practice the theorem says that the Feynman amplitudes with longitudinal vector bosons on the external legs can be equivalently be computed as the amplitude for the corresponding scalar fields.

to different combinations of vector bosons and Higgs final states, with decay widths

$$\Gamma_{\rho_0 \rightarrow W^+W^-} \simeq \Gamma_{\rho_0 \rightarrow Zh} \simeq \Gamma_{\rho_{\pm} \rightarrow W^{\pm}Z} \simeq \Gamma_{\rho_{\pm} \rightarrow W^{\pm}h} \simeq \frac{g_*^2 c_H^2 m_{\rho}}{192\pi}. \quad (34)$$

With obvious notation, ρ_0 and ρ_{\pm} respectively denote the electrically neutral and charged ρ 's, obtained as linear combinations of the ρ^a triplet components. Neutral and charged resonances are approximately degenerate in mass because of the $SU(2)_L$ symmetry. Their common mass is denoted as m_{ρ} .

The second term to be considered is the one responsible for the interaction of ρ with light quarks and leptons. Notice that such an interaction cannot occur directly with an operator involving light elementary fermionic fields because we argued above that the insertion of such fields in the Lagrangian (32) costs very small λ 's that make the resulting vertices negligible. However what we can do is to write, compatibly with gauge invariance, an operator that mixes ρ with the elementary W boson field. Since the W couples to quarks and leptons just like in the SM, this ρ - W mixing eventually generates the interaction we are looking for. In accordance with the power-counting (32), the mixing and the resulting interaction reads

$$\frac{g}{g_*} c_F W_{\mu\nu}^a D^{\mu} \rho_a^{\nu}, \implies \frac{g^2}{g_*} c_F \rho_a^{\mu} J_{\mu}^a, \quad (35)$$

with c_F an unknown order one parameter. In the equation, $J_{\mu}^a = \bar{f}_L \gamma_{\mu} \tau^a f_L$ denotes the ordinary $SU(2)_L$ current, namely the one to which W_{μ}^a couples in the SM. Since the interaction emerges from the mixing with the W , this is precisely the structure we should have expected for the ρ coupling. The scaling of the coefficient is also easily understood. The power-counting formula predicts a g/g_* for the ρ mixing with W , while the W coupling with fermions gives an extra power of g . The result is the rather peculiar g^2/g_* factor, which makes that the ρ coupling with fermions decreases when g_* increases and the CS becomes more and more strongly coupled. The opposite behaviour is observed for the coupling to bosons in eq. (33). The translation between the mixing and the interaction operator reported in eq. (35) is obtained by performing by a field redefinition, namely by shifting the W field by an amount proportional to ρ in such a way that the mixing cancels and the interaction is generated. However this technicality should not obscure the fact that the coupling physically emerges from the mixing with the W .

The mixing in eq. (35) is responsible for ρ decays to quarks and to leptons. Leptonic decays are particularly important because searches in l^+l^- and $l\nu$ final states (with $l = e, \mu$) are extremely sensitive to the presence of resonances. These decays are controlled by one parameter only, c_F , therefore the processes $\rho_{\pm} \rightarrow l^{\pm}\nu$ and $\rho_0 \rightarrow l^+l^-$ (and the decays to quarks as well) are universally related very much like we saw for the bosonic channels in eq. (34). The widths are

$$\Gamma_{\rho_{\pm} \rightarrow l^{\pm}\nu} \simeq 2 \Gamma_{\rho_0 \rightarrow l^+l^-} \simeq \left(\frac{g^2 c_F}{g_*} \right)^2 \frac{m_{\rho}}{48\pi}. \quad (36)$$

Notice the presence of g_*^2 in the denominator. Together with the g_*^2 factor in the numerator of the bosonic decay widths (34), it makes the relative branching fraction between leptons and bosons scales like $1/g_*^4$, which is a strong suppression in the large g_* limit. In this limit, leptonic final states are suppressed and the ρ is better seen in diboson channels in spite of the fact that they reach in terms of cross-section is much better for the leptonic than for the diboson searches. Eq. (35) is also responsible for ρ Drell-Yan production from a quark anti-quark pair.¹⁸ The relative magnitude of the ρ_{\pm} and ρ_0 couplings to quarks are fixed and thus the ρ_{\pm} and ρ_0 relative production rate is entirely determined by the parton luminosities. For $m_{\rho} \sim \text{TeV}$, $\sigma(\rho_{\pm}) \simeq 2 \sigma(\rho_0)$ at the LHC. The absolute normalisation of the cross section is of course also easily computed, depending on the parameter c_F . Together with the partial widths (34) and (36) (plus the analogous formula for the decay to quarks), and assuming that no other

¹⁸The ρ can also be produced in vector boson fusion (VBF) through the c_H operator (33), however the VBF rate is too small to be relevant, at least at the current stage of the LHC.

decay channel is present, cross sections times branching ratios can be computed for all the channels of interest in terms of two free parameters only, c_H and c_F .¹⁹ Or better, if not willing to assume a fixed g_* , in terms of the parameter combinations $c_H g_*$ and $c_F g^2/g_*$, which are those that appear in the vertices. This provides a synthetic approximate description of the HVT phenomenology which allows for a comprehensive experimental investigation of the HVT signal [59]. Notice that the production rate scales like $1/g_*^2$, again due to the $1/g_*$ suppression of the vertex (35), and the HVT's become more and more elusive in the strong coupling regime.

The left panel of figure 10 gives an idea of current limits on HVT from the negative searches performed at the LHC run-1. The figure assumes $c_H = c_F = 1$, which leaves g_* as the only free parameter. The bound is thus simply reported as an excluded region in the mass versus coupling plane. The yellow region is excluded by resonance searches in leptonic final states (specifically, $l\nu$) while two diboson searches are reported in blue (see [59] for details). The behaviour is the expected one. Namely, the mass reach deteriorates at large g_* because of the suppression of the production rate and the one in the leptonic channel deteriorates much faster than the diboson ones because of the suppression of the leptonic branching ratio. Diboson searches thus become competitive and overcome the leptonic sensitivity for $g_* \gtrsim 3$. This behaviour is peculiar of HVT's with a composite origin, as apparent from the right panel of the figure where the bounds are shown for an ‘‘elementary’’ HVT such as those encountered in W' models. Elementary HVT's are massive vector bosons emerging from an underlying gauge theory, therefore all their couplings emerge as gauge interactions and thus there is no way in which the coupling to vector bosons can scale differently with g_* than the one to fermions. The branching ratios to leptons and bosons thus remain comparable even at large g_* and the diboson channels never win in terms of mass-reach. Overall, we see that current limits are rather poor in the composite case. Resonance as low as 2 or 3 TeV, perfectly compatible with Naturalness and with EWPT limits (reported in black in the figure), are still allowed for a reasonable g_* of order 3. A priori g_* could be even larger than that, making composite HVT's virtually invisible, however a moderate value is suggested by other kind of considerations. The left panel of figure 11 shows how much the next runs of the LHC could improve the limits, both in the high mass and in the high coupling directions. The plot is based on an approximate extrapolation of current bounds to the 14 TeV LHC [63] and assumes a total luminosity of 300 fb^{-1} . The HL-LHC reach, with 3 ab^{-1} , is also reported, and the exercise is repeated in the right panel of the figure for an hypothetical future 100 TeV collider. The dashed straight lines in the plot represent indirect limits from the Higgs coupling measurements described in the previous section. The logic is that the resonance mass m_ρ is expectedly comparable with the CS confinement scale m_* . If we take them exactly equal we can use eq. (31) to compute f , and in turn ξ (20), on the (m_ρ, g_*) plane. Lines are shown for $\xi = 0.1$, $\xi = 0.08$, $\xi = 0.01$ and $\xi = 0.004$, corresponding to the reach of the LHC, of the HL-LHC, of ILC and TLEP/CLIC future colliders (see references in [63]). This shows the complementarity of direct and indirect searches of the Composite Higgs scenario.

Top Partners

Top partners are the Composite Sector resonances associated with the fermionic operator \mathcal{O} introduced in eq. (22) to couple the third family $q_L = (t_L, b_L)$ doublet and the singlet t_R with the CS. Similarly to what we saw for vectors in eq. (30), top partners quantum numbers can be extracted from the relation

$$\langle \Psi | \mathcal{O} | 0 \rangle \neq 0. \quad (37)$$

Since \mathcal{O} is a Lorentz Dirac spinor, Ψ must be a spin 1/2 particle in order to be excited by \mathcal{O} from the vacuum. Also, \mathcal{O} is in the triplet of the QCD colour group and thus Ψ must also be coloured as I

¹⁹This is not necessarily accurate for the channels involving third family quarks. The large λ coupling of the third family produced extra contribution to the vertex that can easily overcome the one from the mixing in eq. (35). This enhances $\rho_0 \rightarrow tt$ and $\rho_\pm \rightarrow tb$ making them promising search channels [60]. Composite HVT's might also dominantly decay to other composite sector particles like the fermionic top partners [61], if kinematically allowed. These decays can also be searched for.

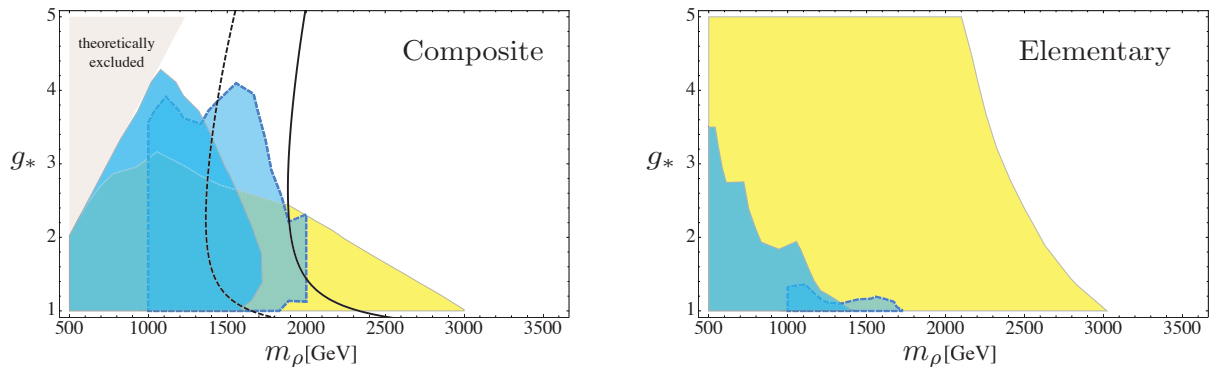


Fig. 10: Run-1 limits on HVT's from leptonic (yellow) and bosonic (blue) searches. HVT's of the “composite” type, namely with properties that comply with the expectations of the CH scenario, are shown on the left panel. The case of an “elementary” model, namely the W' of Ref. [62] is displayed on the right. Black curves are limits from EWPT. See [59] for details.

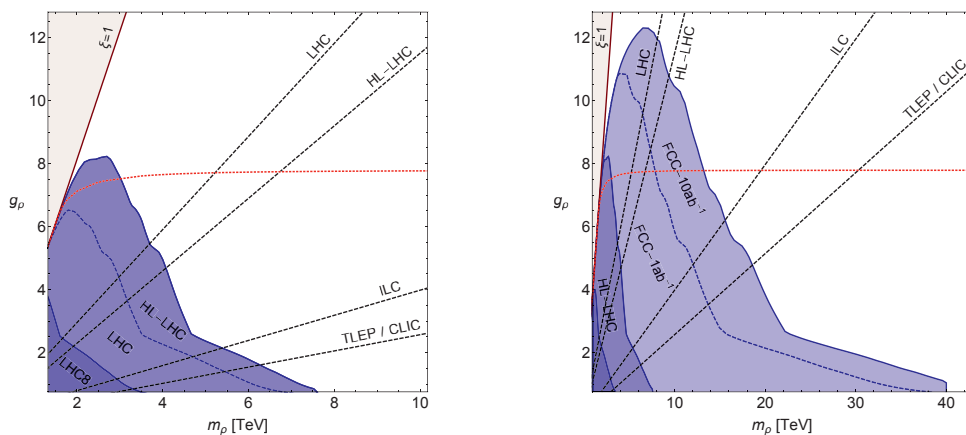


Fig. 11: Expected exclusion limits on composite HVT's compared with indirect constraints from Higgs coupling measurements. From Ref. [63].

anticipated in section 2.2. Finally, top partners are CS resonances and as such their mass must be large, of order $m_* \sim \text{TeV}$, barring special suppression mechanisms which we have no reason to expect a priori. The large top partners mass comes directly from the CS and it is unrelated with the occurrence of EWSB. Unlike quarks and leptons, top partners masses would be present in the theory even if the EW gauge symmetry was unbroken, meaning that top partners must be endowed with a perfectly gauge-invariant Dirac mass term. This requires top partners to be “vector-like” fermions, i.e. to come as complete Dirac fields with their left- and the right-handed components transforming in the same way under the gauge group. Coloured particles of this sort are said to be Vector-Like Quarks (VLQ's). Top partners are VLQ's of specific type and with specific properties.²⁰

Top partners gauge quantum numbers can also be extracted from eq. (37). The result depends on the representation of \mathcal{O} under the CS global group $\text{SO}(5)$, which is a priori ambiguous as I explained in section 2.2. However any valid representation of $\text{SO}(5)$, or actually any valid representation of any CS group \mathcal{G} we might decide to deal with, going beyond the minimal choice $\mathcal{G} = \text{SO}(5)$, must contain

²⁰VLQ's are somehow similar to a fourth family of quarks, but they are also radically different in that their vector-like mass allows them to be at the TeV scale without need of huge Yukawa couplings. Unlike a fourth family, VLQ's are not excluded by the measurement of the Higgs production rate from gluons. See [64] for an analysis of the (moderate) impact of CH top partners on Higgs physics.

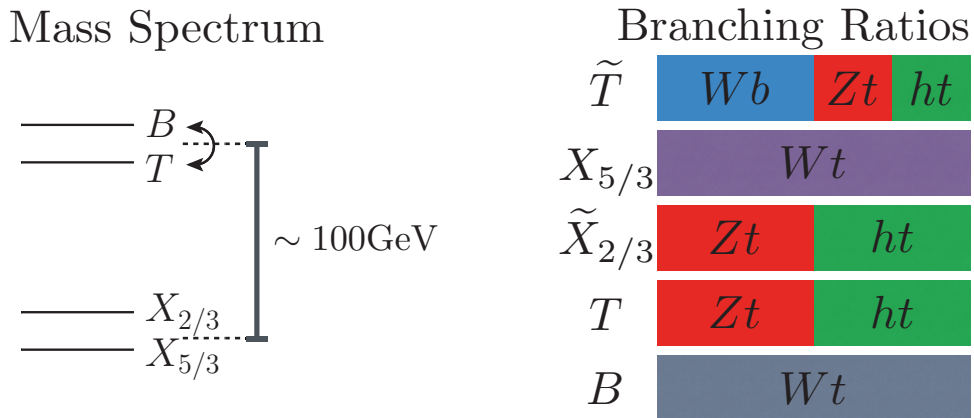


Fig. 12: Typical top partners mass spectrum and decay branching ratios.

at least one SM doublet with $1/6$ Hypercharge and one singlet with Hypercharge $2/3$. The reason is of course that eq. (22) must comply with gauge invariance and thus some of the components of \mathcal{O} must have the same gauge quantum numbers as those of the SM q_L and t_R fields. Top partners are thus at least one (T, B) doublet and one \tilde{T} singlet, plus extra states that possibly emerge from the decomposition of \mathcal{O} . Among those, one extra doublet with exotic Hypercharge of $7/6$ is often present, producing one additional top partners doublet $(X_{2/3}, X_{5/3})$ with electric charge $2/3$ and $5/3$, respectively. It is possible to show that all choices of the \mathcal{O} representation for which the extra doublet is absent, such as the **4** we mentioned in section 2.2, are typically in serious phenomenological troubles because of unacceptably large modifications of the $Zb\bar{b}$ coupling [65, 66]. We thus have good reasons to expect the presence of the extra top partners doublet and thus good reasons to search for it.

Similarly to what we saw above for vector resonances, top partners phenomenology can be characterised by employing symmetry, which constrain the structure of their interactions, and power-counting (32), which sets the expected strengths of the different couplings. The characterisation is slightly more complicated than the one for vectors, mainly because the whole symmetry structure of the theory must be taken into account and not just the SM gauge group. This includes the $SO(4)$ unbroken group of the CS and even the full non-linearly realised $SO(5)$ which takes care of the pNGB nature of the Higgs. The analysis produces relatively sharp predictions [67, 68] of the top partners mass spectrum, decay and production processes. As shown in figure 12, particles within the two doublets are essentially degenerate, but also the two doublets are quite close in mass, with a splitting between them of around 100 GeV. The exotic Hypercharge doublet is always the lightest of the two. This spectrum is due to the fact that the two doublets emerge as a single $SO(4)$ quadruplet and by the peculiar way in which the $SO(4)$ symmetry is broken by the pNGB Higgs VEV. The \tilde{T} singlet can have any mass, significantly below or above (or close to) the two doublets. The top partners decay branching ratios are approximately universal, as shown in the right panel of the figure. This feature is not peculiar of top partners, it holds for any VLQ with a mass much above the EW scale and follows from considerations related with the Equivalence Theorem similar to those that led us to eq. (34) for vector resonances.

Top partners are colour triplets, thus they are produced in pair by QCD interactions at a fixed and predictable rate as a function of their mass. Since the branching ratios are also known, negative searches for top partners pair production allow to set sharp mass limits, of around 800 or 900 GeV at the LHC run-1. The run-2 reach in terms of exclusions is around 1.2 or 1.5 TeV, and it is unlikely it will ever overcome 1.7 TeV even when the full luminosity of the HL-LHC will be available in many years from now (see [69, 70] and references therein). The reach could however be extended up to around 2 TeV by exploiting another sizeable production mechanism top partners are found to possess, namely single production (see figure 13) in association with a top or with a bottom plus a forward jet from the splitting

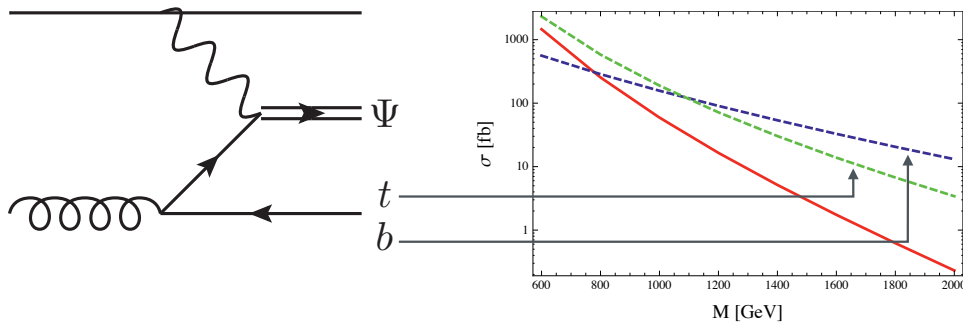


Fig. 13: Top partners production cross-section for typical values of the single-production coupling at the 14 TeV LHC. Pair production is shown as a continuous red line.

of an EW boson out of a quark line. Single production emerges from a vertex with schematic form

$$\mathcal{L}_{\text{single}} \sim \lambda_{L/R} \bar{\Psi} H q_{L/R}, \quad (38)$$

with $q = t$ or $q = b$. The vertex couples top partners with third family quarks and the Higgs, and its power-counting estimate (32) is rather sizeable because it is controlled by third family $\lambda_{L/R}$ couplings. The Equivalence Theorem relates as usual the Higgs field components to longitudinally polarised EW bosons (see Footnote 17), therefore the operator produces single-production vertices like the one in figure 13. These vertices are of course also responsible for Top Partners decays. Single production cross-section, as the figure shows, is favoured at high mass by the steeply falling parton luminosities and readily starts to dominate over pair production. The mass-limit one can set for single production is not as sharp as the one from pair production because the reach crucially depends on the magnitude of the interaction vertex (38), which is not fully predicted. The above-mentioned expected reach (~ 2 TeV [69, 70]) is based on a conservative estimate of the single production coupling strength.

Top partners are arguably the most important CH signatures to be searched for in the forthcoming LHC runs, in spite of the fact that the mass-reach is not great if compared with the one on vectors that can easily overcome 3 TeV by exploiting the complementarity between direct and indirect searches as in figure 11. The point is that a 3 or even 5 TeV bound on vectors would not be as problematic for the CH scenario as a 2 TeV bound on top partners. Conversely, we don't have a strong theoretical preference for vectors below 3 or 5 TeV, or at least not such a strong one as we have for top partners below 2 TeV. Of course all resonance masses are set by the same scale, m_* , therefore we expect them to be comparable but a factor of two hierarchy between vectors and top partners is perfectly conceivable. What makes top partners special is that it is their mass the one that actually enters in the fine-tuning formula in eq. (7), not the mass of vectors or of other CS resonances. Namely, the statement which I will now justify is that the generic estimate of fine-tuning in eq. (7) specialises, in the case of the CH scenario, to $\Lambda_{\text{SM}} = M_{\Psi}$. Top partners at 2 TeV would thus cost a tuning well above ten.

The connection between top partners and fine-tuning is due to the fact that top quark loops (see section 4 and in particular figure 1.3) are the dominant term in the low-energy contribution to the Higgs mass which is at the origin of the fine-tuning problem, and top partners are strongly coupled with the top quark. An example of such coupling is the single production operator in eq. (38). Another relevant interaction is the top/top partners mixing of the form ²¹

$$\mathcal{L}_{\text{mix}} \sim \frac{\lambda_L}{g_*} m_* \bar{T} t_L + \frac{\lambda_R}{g_*} m_* \bar{\tilde{T}} t_R, \quad (39)$$

and analogously for the b_L mixing with the B . In explicit model it is only the mixing term above which is actually generated (in the appropriate field basis) and all the other quarks interactions such as those in

²¹Order one coefficients, which of course are predicted by the power-counting formula (32), are understood in both terms.

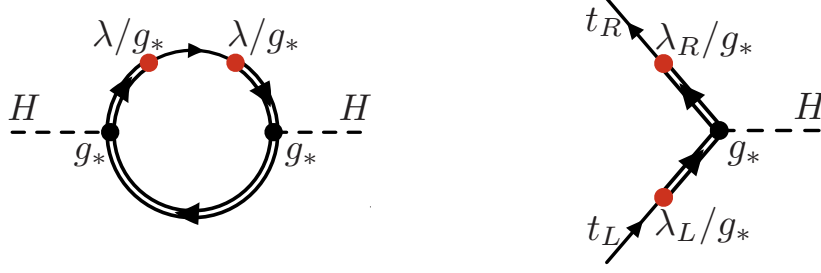


Fig. 14: Left panel: one representative diagram contributing to the Higgs mass. The Higgs-top partners vertex is a purely CS interaction and thus it has been estimated as g_* . The insertion of the mixing weights as in eq. (39). Right panel: the generation of the top Yukawa coupling through mixing.

eq. (38) emerge after diagonalization. The mixing can be used to construct loop diagrams like the one in the left panel of figure 14, involving the exchange of a virtual top and a top partner. These diagrams generate a mass for the Higgs, of order

$$m_H^2 \sim a_L \frac{\lambda_L^2}{16\pi^2} M_\Psi^2 + a_R \frac{\lambda_R^2}{16\pi^2} M_\Psi^2, \quad (40)$$

where the two terms stand respectively for the exchange of a virtual t_L and t_R . The order one numerical coefficients a_L and a_R are calculable in explicit CH models (see e.g. [67]) and, depending on the model's microscopic parameters, can assume any sign. The estimate of m_H has been performed by counting the powers of λ and g_* , reported in figure 14, multiplying by the loop factor $1/16\pi^2$ and by two powers of the top partners mass M_Ψ because of dimensionality. This is quite right in spite of the fact that the diagram is still logarithmically divergent because the log only produces order one numerical coefficients which is not worth retaining in our rough estimate.²²

Eq. (40) requires some clarification. As I explained at length in the previous sections, the fact that the Higgs is a NGB prevents the generation of its mass as long as the Goldstone symmetry, i.e. the group \mathcal{G} , is an exact symmetry of the theory. Since the CS is exactly invariant under \mathcal{G} , no contribution to m_H can come from the CS alone. In our language this contribution would be a tree-level Higgs mass-term, and the fact that it is absent is the reason why to estimate m_H we had to go at the loop level as in figure 1.3. The diagrams in the figure have the chance to produce a mass because they do feel \mathcal{G} breaking through the insertion of the top/top partner mixing. Remember that are indeed the Composite/Elementary Sector interactions the ones responsible for \mathcal{G} breaking (see figure 6) in our construction, and the mixing is one of those interaction. Moreover the mixing is the largest of those interaction because it is associated with the generation of the largest coupling of the Higgs boson, namely the top quark Yukawa y_t . Other Elementary/Composite interaction such as the gauge couplings also contribute to m_H , producing however only small corrections to eq. (40). This is the reason why it is the top partners mass scale M_Ψ , and not for instance the mass of spin one resonances, the one that controls the size of the Higgs mass.

Mixed top/top partners loops generate not only a mass-term, but a full potential for the Higgs field. The potential has the form of eq. (27), with an α parameter

$$\alpha \sim a_L \lambda_L^2 \frac{N_c M_\Psi^2}{16\pi^2} + a_R \lambda_R^2 \frac{N_c M_\Psi^2}{16\pi^2}. \quad (41)$$

This estimate is slightly more accurate than the one in eq. (40), in particular it takes into account the number of colours $N_c = 3$, but it scales in the same way with the parameters. The physical mass of the

²²This would not be the case if a parametrically large separation was present between M_Ψ and the confinement scale m_* at which the loop is naturally cut off. We assume a factor of a few separation at most, which does not qualifies as parametrically large and thus the estimate is correct.

Higgs boson, obtained by combining the two lines of eq. (28), thus reads

$$m_H^2 = 4(1 - \xi)\alpha \sim a_L \lambda_L^2 \frac{N_c M_\Psi^2}{4\pi^2} + a_R \lambda_R^2 \frac{N_c M_\Psi^2}{4\pi^2}. \quad (42)$$

If M_Ψ is large, obtaining the correct Higgs mass $m_H = 125$ GeV requires a cancellation between the two terms, obtained by choosing the fundamental parameters of the models such that a_L is almost equal and opposite to a_R . This means a fine-tuning

$$\Delta = \frac{3\lambda^2}{4\pi^2} \left(\frac{M_\Psi}{m_H} \right)^2 \simeq \lambda^2 \left(\frac{M_\Psi}{450 \text{ GeV}} \right)^2, \quad (43)$$

having assumed $\lambda_L \simeq \lambda_R \equiv \lambda$, which is the configuration that minimises the required amount of tuning. The equation clearly illustrates that light top partners are needed for a Natural (low-tuning) CH model.

Our estimate closely resembles the general formula (7) with $\Lambda_{\text{SM}} = M_\Psi$, apart from the prefactor λ^2 that is replaced by y_t^2 in eq. (7). In order to see that the two formulas match we should relate λ with the top Yukawa coupling, by proceeding as follows. The top/top partners mass-mixing (39) makes that the two chirality components of the physical top quark, which is massless before EWSB is taken into account, are a quantum mechanical superimposition of Elementary and Composite degrees of freedom

$$\begin{aligned} |t_L^{\text{phys.}}\rangle &= \cos \phi_L |t_L^{\text{Elem.}}\rangle + \sin \phi_L |T_L^{\text{Comp.}}\rangle, \\ |t_R^{\text{phys.}}\rangle &= \cos \phi_R |t_R^{\text{Elem.}}\rangle + \sin \phi_R |\tilde{T}_R^{\text{Comp.}}\rangle, \end{aligned} \quad (44)$$

with $\sin \phi_L \simeq \lambda_L/g_*$ and $\sin \phi_R \simeq \lambda_R/g_*$. A similar formula holds for the b_L . This comes from diagonalising the mass-matrix of the top/top partners system, which consists of the mass-mixing (39) plus the vector-like mass-term M_Ψ for the partners. For the estimate we took $m_* = M_\Psi$ in eq. (39), consistently with what implicitly done in the estimate of the m_H . Eq. (44) shows, in the first place, why we call ‘‘Partial Compositeness’’ [43] the mechanism (22) we are using to couple ES fermions with the CS: it is because it produces physical particles that are partially made of Composite degrees of freedom. Second, the formula allows us to estimate the top Yukawa generated by mixing as in the right panel of figure 14, obtaining

$$y_t = \sin \phi_L \sin \phi_R g_*, \quad \xrightarrow{\lambda_L = \lambda_R = \lambda} \quad \lambda = \sqrt{y_t g_*}. \quad (45)$$

But we said that g_* has to be large, at least above $y_t \simeq 1$, therefore the above equation tells us $\lambda > y_t$ and eq. (43) can be turned into a lower bound

$$\Delta > \frac{3y_t^2}{4\pi^2} \left(\frac{M_\Psi}{m_H} \right)^2 \simeq \left(\frac{M_\Psi}{450 \text{ GeV}} \right)^2, \quad (46)$$

identical to eq. (7).

Notice that the estimate of the Yukawa couplings can be carried on for the light quarks (including the bottom) and leptons in exactly the same way as for the top, producing expressions for the corresponding λ parameters which are identical to eq. (45) aside from the fact that the light quarks and leptons Yukawas, rather than y_t , are involved. Light generation λ 's are thus very suppressed and this is why we could systematically ignore them. Correspondingly, light fermions compositeness fraction $\sin \phi \sim \lambda/g_*$ are very small. Light fermions are thus almost entirely elementary particles, with a tiny composite component which is however essential to generate their Yukawa's and masses.²³

²³There are however exceptions to this rule. On one hand, it is possible to make largely composite one of the light quarks chirality components recovering the small Yukawa by giving very very small compositeness to the other one. This helps in evading flavour constraints [71, 72] and produces interesting LHC signatures related with the fermionic partners of the light quarks [73, 74]. On the other hand, it is possible to avoid partial compositeness altogether for the light fermions [75, 76] and obtain their mass by bilinear interactions.

In summary, the importance of top partners stems from their connection with tuning in eq. (46). Not finding them at the LHC below 2 TeV would cost more tuning than what negative searches of Higgs couplings modifications (whose reach is $\xi < 0.1$) would imply through eq. (29).²⁴ Vector resonances are mildly connected with tuning, therefore even a multi-TeV bound on their mass would not be competitive in terms of fine-tuning reach. Top partners searches are so important because their capable to put the very idea of Naturalness in serious troubles, at least in the Composite Higgs framework. We will see in the next chapter that a similar role is played in Supersymmetry by the stops. It is also important to keep in mind that top partners might very well be discovered at the LHC run-2. Current bounds are below 1 TeV and thus their impact on tuning is modest, well below ten and comparable with the one from coupling measurements. The interesting mass region is the one from 1 to 2 TeV in which we are about to enter.

3 Supersymmetry

Supersymmetry (SUSY) is probably the most intensively studied theoretical subject of the last 30 or 40 years. Its applications range from string theory and supergravity down to collider phenomenology, with digressions on AdS/CFT correspondence and holography, dualities and scattering amplitude properties. I mention this to outline that the scope of SUSY is much broader than phenomenology and to explain why theorists care about SUSY a priori, independently of its applicability to the real world on a short timescale. Plenty of excellent reviews [77–81], lecture notes²⁵ and books [82, 83] have been written about SUSY, just to mention some of those that are relevant in the (relatively narrow, as I mentioned) context of SUSY phenomenology. With all this literature available, it makes no sense trying to condense a self-contained introduction to SUSY in these few pages. I will thus keep introductory material to the minimum, focusing only on few basic concepts and results that are absolutely needed for the discussion. Next, in sections 3.2 and 3.3, I will describe SUSY phenomenology building around two specific questions which I find particularly important to address in this particular moment.

3.1 Basics of SUSY

Symmetries are so much important in particle physics that Coleman and Mandula in ‘67 found interesting to ask themselves what is the largest symmetry content a relativistic theory of interacting particles can possess [84]. Their answer was that the largest global symmetry group is Poincaré, generated by the 6 $M^{\mu\nu}$ Lorentz generators plus the 4 P^μ ’s associated with space-time translations, times a generic Lie group of symmetries generated by a set of charges \vec{Q}_B . Here “times” means direct product, namely their result was that all the internal symmetry generators have to commute with those of the Poincaré group

$$\left[P^\mu, \vec{Q}_B \right] = 0, \quad \left[M^{\mu\nu}, \vec{Q}_B \right] = 0. \quad (47)$$

Remember that commutators are the way in which the symmetry generators act on the other operators. The first equation thus means that the \vec{Q}_B ’s are invariant under translations and the second one means that the \vec{Q}_B ’s are Lorentz scalars, namely that they stay the same in any reference frame. With a modern terminology we would say that what Coleman and Mandula had in mind were “bosonic” generators, this is why I labeled them with the subscript “B”. Concretely what they had in mind are generators that obey ordinary commutation relations among them, of the form $[Q_B^i, Q_B^j] = i f^{ijk} Q_B^k$.

However Gol’fand and Likhtman proved that Coleman and Mandula were wrong, and in so doing they discovered SUSY [85]. They pointed out that a set of 2 symmetry generators Q_α ($\alpha = 1, 2$) exist which do not obey eq. (47), but instead

$$[P^\mu, Q_\alpha] = 0, \quad [M^{\mu\nu}, Q_\alpha] = -(\sigma^{\mu\nu})_\alpha^\beta Q_\beta. \quad (48)$$

²⁴Eq. (46) does not supersede eq. (29). The two equations estimate tuning from different sources, namely the one from the Higgs VEV and from the Higgs mass, respectively. Therefore the maximum of the two expressions should be taken for a complete estimate of Δ .

²⁵At least 22 of them, counting only those produced by the CERN ESHEP school founded in 1993.

The Q 's are still invariant under translations, and in particular under time translations (which is of course obvious if they are conserved), but they are not anymore invariant under Lorentz transformations. Under Lorentz, i.e. under commutation with $M^{\mu\nu}$, the Q 's transform with the matrix $\sigma^{\mu\nu}$ which is a 2×2 representation of the Lorentz group called the (left-handed) Weyl representation. Therefore we will say that the SUSY generators (or charges) Q_α form a two-components Weyl spinor under the Lorentz group.

The reader unfamiliar with the formalism of Weyl spinors is referred to standard textbooks or to Ref. [78] (section 4.1 and Appendix A and B) for a concise introduction. The essential point is that Weyl spinor fields are the ‘‘building’’ blocks of the habitual Dirac fermions we normally employ to describe spin-1/2 particles. Namely, one four-components Dirac spinor Ψ can be decomposed as

$$\Psi = \begin{bmatrix} (\psi_1)_\alpha \\ (\bar{\psi}_2)^{\dot{\alpha}} \end{bmatrix} \begin{array}{l} \xrightarrow{(m=0)} f \uparrow \downarrow + \bar{f} \uparrow \uparrow \\ \xrightarrow{(m=0)} f \uparrow \uparrow + \bar{f} \uparrow \downarrow \end{array} \quad (49)$$

in terms of two two-components spinors $(\psi_1)_\alpha$ and $(\psi_2)_\alpha$ called ‘‘left-handed’’ Weyl spinors.²⁶ As anticipated, the Lorentz generators acting on these objects are the $\sigma^{\mu\nu}$ matrices. Namely, under an infinitesimal Lorentz transformation

$$(\delta\psi_{1,2})_\alpha = -\frac{i}{2}\omega_{\mu\nu}(\sigma^{\mu\nu})_\alpha{}^\beta, \quad \sigma^{\mu\nu} = \frac{i}{4}(\sigma^\mu\bar{\sigma}^\nu - \sigma^\nu\bar{\sigma}^\mu), \quad (50)$$

where $\sigma^\mu = (\mathbb{1}, \vec{\sigma})$ and $\bar{\sigma}^\mu = (\mathbb{1}, -\vec{\sigma})$, with $\vec{\sigma}$ the Pauli matrices. Notice that unlike ψ_1 , ψ_2 does not enter the decomposition formula directly, but rather through the object $(\bar{\psi}_2)^{\dot{\alpha}}$ which is related to ψ_2 by complex conjugation. Namely

$$(\bar{\psi}_2)^{\dot{\alpha}} = \varepsilon^{\dot{\alpha}\beta}[(\psi_2)_\beta]^*, \quad (51)$$

where ε is the antisymmetric Levi-Civita tensor in two dimensions and the sum over $\beta = 1, 2$ is understood. We sometimes call $(\bar{\psi}_2)^{\dot{\alpha}}$ a ‘‘right-handed’’ Weyl spinor, however the previous formula shows that there is no actual distinction between left- and right-handed spinors because one can be turned into the other by complex conjugation. What is normally done in the SUSY literature is to use only left-handed spinors to describe fermions, an habit which can be confusing for beginners. For instance, because of this convention the SM right-handed top quark is represented by a left-handed spinor with electric charge equal to $-2/3$ rather than $+2/3$ because the correspondence between left and right spinors involves complex conjugation.

If the Dirac spinor Ψ is massless, the two Weyl components are endowed with a very simple physical interpretation, pictorially reported in eq. (49). ψ_1 corresponds to a massless fermion f with helicity $h = -1/2$ plus its anti-particle \bar{f} with $h = +1/2$, while ψ_2 is an $h = +1/2$ fermion plus an $h = -1/2$ anti-fermion. If instead the Dirac spinor is massive, namely if it is endowed with a Dirac mass term, there is no direct correspondence between Weyl spinors and physical particles because the Dirac mass mixes the two Weyl components and produces physical particles which are combinations of the two components. Still, a Weyl spinor can be in direct correspondence with a massive fermion, but only if it is a completely neutral particle, not endowed with any conserved charge or quantum number. In this case there is no way to distinguish particle from anti-particle, namely $f = \bar{f}$, and the two helicity states of each Weyl can be interpreted as the two helicity (or spin) eigenstates of a single massive fermion. A mass term given to a single Weyl spinor, which unlike the Dirac mass does not mix the two Weyl components, is called a ‘‘Majorana’’ mass. One Weyl 2-component spinor can be equivalently representations as a 4-component spinor called a ‘‘Majorana spinor’’. There is no physical distinction between the two representations, thus a Weyl fermion with Majorana mass is often called a Majorana fermion.

²⁶This assumes that the Weyl basis is chosen for the γ matrices, otherwise the decomposition is more complicate.

After this interlude on Weyl spinors, we return to our historical introduction to SUSY. Gol’fand and Likhtman could find a counterexample to the Coleman–Mandula theorem because Coleman and Mandula made too restrictive assumptions in their proof. Namely they assumed bosonic internal symmetry generators, characterised by ordinary commutation relations as previously mentioned. The Gol’fand–Likhtman SUSY charges are instead fermionic generators, characterised by anti-commutation relations

$$\{Q_\alpha, Q_\beta\} = 0, \quad \{Q_\alpha, \bar{Q}_{\dot{\beta}}\} = 2(\sigma^\mu)_{\alpha\dot{\beta}} P_\mu, \quad (52)$$

where \bar{Q} is the conjugate of the SUSY charge ²⁷

$$\bar{Q}_{\dot{\alpha}} = [Q_\alpha]^*. \quad (53)$$

SUSY charges are thus very different from the ordinary generators of internal symmetries like baryon and lepton number, isospin, etc. Unlike the latter, they do not form an algebra, specified by commutation relations, but rather what is called a “super-algebra”, specified by relations that involve the anti-commutators. Moreover, and perhaps more importantly, SUSY generators do not commute with $M^{\mu\nu}$ (48) unlike the ordinary bosonic charges (47). The story ends with Haag, Lopuszański and Sohnius, who had the final word on the maximal symmetry content of a relativistic theory (with massive particles) [86]. They found that it consists of the Poincaré generators, plus bosonic bosonic charges, plus a set of replicas, Q_α^i with $i = 1, \dots, N$, of Gol’fand–Likhtman’s SUSY generators. Actually they also found other symmetries related with SUSY, called “ R -charges”. Extended SUSY, namely $N \neq 1$, does not play an important role in phenomenology, therefore in what follows we will stick to the minimal case $N = 1$. A similar consideration holds for the continuous R -symmetry group, aside from a discrete subgroup of it called “ R -parity” which is instead very relevant and will be discussed in the next section.

SUSY-invariant theories display a number of remarkable properties, some of which can be summarised by the famous rule

$$\text{Bosons} \stackrel{\text{SUSY}}{=} \text{Fermions}. \quad (54)$$

The rule has several meanings, the simplest one being that SUSY requires bosonic and fermionic particles with the same mass. In order to see why it is so, consider the state $|h, p\rangle$ describing a single particle with helicity h and four-momentum p . For definiteness, we will take the particle moving along the z -axis so that the helicity operator coincides with the third component of the angular momentum, i.e. the $1 - 2$ component of the Lorentz generator, $S_3 = M^{12}$. Let us now act on the state with one of the SUSY charges, Q_α . This produces a new single-particle state, $Q_\alpha|h, p\rangle$, with the following properties

$$\begin{aligned} P^\mu|h, p\rangle = p^\mu|h, p\rangle &\Rightarrow P^\mu(Q_\alpha|h, p\rangle) = (Q_\alpha P^\mu + [P^\mu, Q_\alpha])|h, p\rangle = p^\mu(Q_\alpha|h, p\rangle), \\ M^{12}|h, p\rangle = h|h, p\rangle &\Rightarrow M^{12}(Q_\alpha|h, p\rangle) = (Q_\alpha M^{12} + [M^{12}, Q_\alpha])|h, p\rangle = (h \mp 1/2)(Q_\alpha|h, p\rangle), \end{aligned} \quad (55)$$

where the $-1/2$ is for $\alpha = 1$ and the $+1/2$ for $\alpha = 2$. The first equation tells us that the new particle has the same four-momentum as the original one, and thus in particular the same mass. It follows from the first relation in eq. (48), which states that the SUSY charges commute with the P^μ operator. This first result is of course not at all surprising. Any symmetry generator commutes with P^μ and connects among each other particles with the same mass. The second relation in eq. (55) is instead peculiar of SUSY. Ordinary generators commute with M^{12} and as such they connect particles with the same spin and the same helicity. The commutator of SUSY charges with M^{12} is instead $[M^{12}, Q_\alpha] = -1/2(\sigma^3)_\alpha^\beta Q_\beta$, as dictated by eq. (48), so that SUSY connects particles with helicity h to particles with helicity $h \mp 1/2$ as in eq. (55). Given that it shifts the helicity by a semi-integer amount, SUSY relates bosons with fermions and thus it requires the existence of mass-degenerate multiplets containing at the same time bosonic and fermionic particles.

²⁷Weyl spinor indices can be raised or lowered by acting with $\varepsilon^{\alpha\beta} = \varepsilon^{\dot{\alpha}\dot{\beta}} = -\varepsilon_{\alpha\beta} = -\varepsilon_{\dot{\alpha}\dot{\beta}}$. With this convention the definition of $\bar{Q}_{\dot{\alpha}}$ reported below matches with eq. (51).

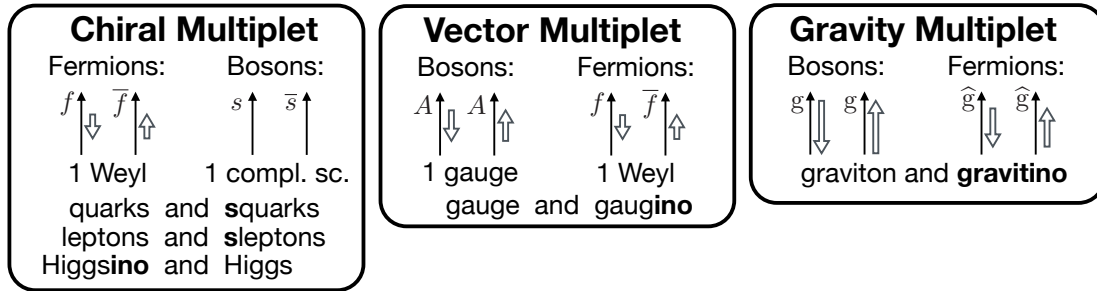


Fig. 15: The $N = 1$ SUSY multiplets that are relevant for phenomenology.

By proceeding along these lines, i.e. by repeatedly acting with Q and \bar{Q} , one can classify the irreducible representations of $N = 1$ SUSY. The relevant ones are those that contain particles of spin two at most, i.e. the chiral, vector and gravity multiplets, schematically represented in fig. 15. When constructing supersymmetric extensions of the SM, chiral multiplets are used to describe the SM chiral fermions (quarks and leptons), plus the corresponding SUSY particles (squarks and sleptons). The latter are complex scalars with the same quantum numbers of the corresponding SM fermions under the SM gauge group. A chiral multiplet (actually, two of them, as we will see) also describes the SM Higgs field, plus the “higgsinos” superpartners, which are 2-components fermions. Vector multiplets describe the SM gauge field (photon, gluons, W and Z) with their partners, which are again 2-components fermions called photino, gluinos, wino and zino. Clearly the vector multiplets describe the W and Z bosons, plus their super-partners, before the breaking of the EW symmetry, when they are massless. The gauge fields becoming massive require extra components taken from the Higgs multiplet, like in the SM. The graviton is part of the gravity multiplet, together with a particle of spin $3/2$, the gravitino. A proper description of the gravity multiplet and thus of the gravitino requires a supersymmetric theory of gravity, i.e. a Supergravity model. This goes far beyond the purpose of the present lectures, we will thus not consider the gravity multiplet anymore in what follows.

Notice that each of the multiplets in fig. 15 contains the exact same number (2) of bosonic and of fermionic degrees of freedom.²⁸ If we combine them to form a SUSY theory we will thus obtain a model with the same number of bosonic and of fermionic degrees of freedom, in accordance with the general rule “bosons = fermions” in eq. (54). Notice that if SUSY is spontaneously broken, bosons and fermions will not anymore form mass-degenerate multiplets according to fig. 15, but still the total number of bosonic and of fermionic degrees of freedom in the theory will remain the same. It is interesting to remark that the validity of the “bosons = fermions” rule crucially relies on the fact that the trivial representation, i.e. the singlet, does not exist in SUSY, unlike any other ordinary symmetry group. If it existed, it would be possible to add “SUSY-singlet” states (bosonic or fermionic) to the theory, violating in this way the equality of the number of bosonic and fermionic degrees of freedom. No SUSY-singlet particle exists because a singlet would be a state that is invariant under SUSY, which means that it must be annihilated both by Q and by \bar{Q} . But since $\{Q, \bar{Q}\} \propto P_\mu$, this hypothetical SUSY singlet would be also annihilated by P_μ and thus it would have vanishing four-momentum and could not be interpreted as a particle. The only state with such properties, i.e. the only SUSY-singlet state, is a (SUSY-invariant) vacuum configuration.

Let us now turn to the problem of writing down SUSY-invariant theories. If SUSY was an ordinary (bosonic) global symmetry, this would be a trivial step to take, once the single-particle state multiplets are known. One would just introduce one field for each particle and construct a multiplet of fields that transform under the symmetry in the exact same way as the corresponding particle multiplets. Symmetric Lagrangians will eventually be obtained by constructing invariant combinations of the field multiplets. The situation is more complicate in SUSY. Constructing invariant Lagrangians requires the concept of

²⁸By “degree of freedom” we mean single-particles states of given helicity and quantum numbers.

“auxiliary fields” and the one of “super-fields”. The issue comes from the “bosons = fermions” rule in eq. (54), which happens to hold not only for the states, but also for the fields. Namely, any set of fields that form a representation of SUSY must contain the same number of bosonic and of fermionic fields components. Consider for instance the chiral multiplet of particles. We describe its scalar degrees of freedom by one complex scalar field $\phi(x)$, which has 2 real bosonic components, while to describe the 2-components fermion we must use a Weyl spinor $\psi_\alpha(x)$, which amounts to 4 real (2 complex) fermionic components. Purely in terms of fields, i.e. before we impose the Equations Of Motion (EOM) that reduce the number of fermionic degrees of freedom to 2, there is a mismatch between the number of bosonic and fermionic components. This mismatch means that a SUSY multiplet cannot just contain the $\{\psi, \phi\}$ fields. One additional complex scalar field, the auxiliary field $F(x)$, is needed to match bosonic and fermionic components. The chiral multiplet is thus made of the set of fields $\{\psi, \phi, F\}$. The exact way in which the SUSY symmetry acts on this multiplet is not worth reporting here. What matters is that a consistent SUSY transformation exists and thus the problem of writing down a SUSY-invariant theory boils down, from this point on, to the one of combining these fields in order to form a SUSY-invariant Lagrangian. The super-field formalism turns out to be extremely effective for this purpose.

Before discussing super-fields, it is important to clarify the role of the auxiliary fields in the construction of SUSY theories. They are introduced in order to comply with the “bosons = fermions” rule applied to the fields, but of course their presence cannot invalidate the rule at the particle level. Namely, auxiliary fields cannot produce extra propagating degrees of freedom, and for this being the case their Lagrangian must not contain a kinetic term. The simplest SUSY-invariant Lagrangian for a chiral multiplet indeed reads

$$\mathcal{L} = i\bar{\psi}\bar{\sigma}^\mu\partial_\mu\psi - \frac{m}{2}(\psi\psi + \bar{\psi}\bar{\psi}) + \partial_\mu\phi^\dagger\partial^\mu\phi - m(\phi F + \phi^\dagger F^\dagger) + F^\dagger F, \quad (56)$$

and it is such that the dependency on the auxiliary field F is purely polynomial. Consequently, the EOM for F is polynomial and can be solved exactly, leading to

$$F = m\phi^\dagger. \quad (57)$$

A field whose EOM can be uniquely solved in terms of the other fields in the theory produces no physical particles, and furthermore it can be eliminated (or, “integrated out”) from the theory by plugging the solution into the Lagrangian. Auxiliary fields thus will not enter in the final expressions for our SUSY-invariant Lagrangian, in spite of the fact that their presence was needed in order to construct it (in the super-field formalism, at least). In the case of eq. (56) we obtain

$$\mathcal{L} = i\bar{\psi}\bar{\sigma}^\mu\partial_\mu\psi - \frac{m}{2}(\psi\psi + \bar{\psi}\bar{\psi}) + \partial_\mu\phi^\dagger\partial^\mu\phi - m^2\phi^\dagger\phi, \quad (58)$$

which is simply the Lagrangian of a free complex scalar, with mass m , plus a Majorana fermion (i.e., a neutral Weyl spinor endowed with a Majorana mass-term) with the same mass.

All fields (including the auxiliary ones) in a SUSY multiplet can be collected in a single object, called a super-field. Super-fields can be thought as fields in an extended coordinate space (the super-space), which contains four additional “fermionic” coordinates θ^α and $\bar{\theta}_{\dot{\alpha}}$ on top of the ordinary “bosonic” space-time coordinates x^μ . The idea is to treat SUSY charges in analogy with the P_μ momentum operator, which acts on ordinary fields $\mathcal{F}(x)$ as a shift $x \rightarrow x + \delta x$ of the coordinates. A super-field is a function $\mathcal{F}(x, \theta, \bar{\theta})$ and the SUSY charges Q and \bar{Q} act on it (almost) as translations $\theta \rightarrow \theta + \delta\theta$ and $\bar{\theta} \rightarrow \bar{\theta} + \delta\bar{\theta}$. A SUSY invariant Lagrangian²⁹ is thus constructed as a functional of the super-field that is translational-invariant in the super-space. The θ and $\bar{\theta}$ coordinates are however very different from the ordinary space-time ones. Rather than real numbers, they are “Grassmann variables”, namely the product of two of them anti-commutes rather than commuting. This has several bizarre implications,

²⁹More precisely, an invariant Action since SUSY Lagrangian are often only invariant up to total derivatives

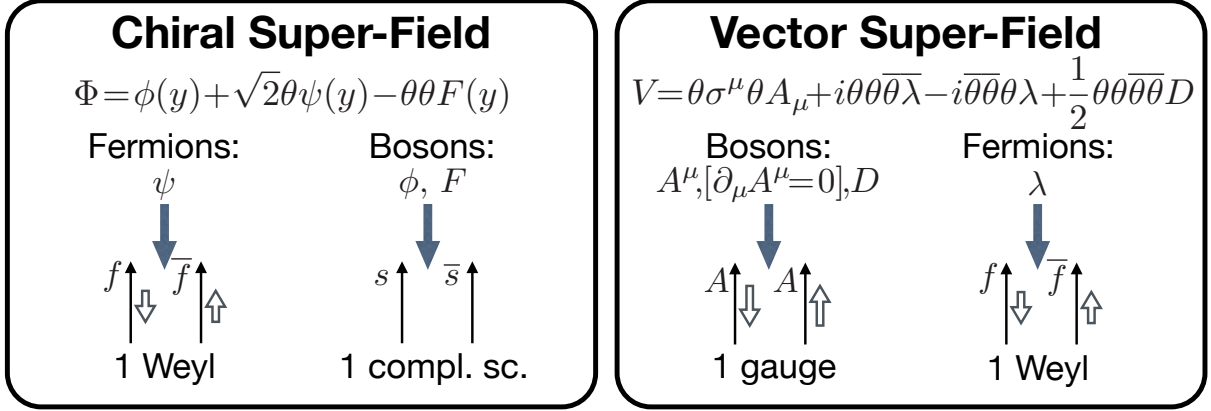


Fig. 16: The chiral and vector superfields, together with the physical degrees of freedom they produce after the EOM are applied to get rid of the auxiliary fields F and D . The variable y that appears in the chiral super-field is defined as $y^\mu = x^\mu - i\theta\sigma^\mu\bar{\theta}$.

among which the fact that the square of one of the θ or $\bar{\theta}$ components just vanishes. The most general super-field thus is not an arbitrary function of θ and $\bar{\theta}$, but just a fourth order (corresponding to the total number of independent components) polynomial in θ and $\bar{\theta}$, whose coefficients are ordinary fields in the x space. Namely

$$\mathcal{F}(x, \theta, \bar{\theta}) = a(x) + b(x)\theta + c(x)\bar{\theta} + d(x)\theta\theta + e(x)\bar{\theta}\bar{\theta} + f_\mu(x)\theta\sigma^\mu\bar{\theta} + g(x)\theta\theta\bar{\theta} + h(x)\bar{\theta}\bar{\theta}\theta + i(x)\bar{\theta}\bar{\theta}\theta\theta. \quad (59)$$

The super-field is taken to be a bosonic object, therefore the fields in the decomposition that accompany even powers of θ and $\bar{\theta}$ (i.e., a, d, e, f_μ and i) are bosonic while the ones that come with odd powers (b, c, g and h) are fermionic Weyl fields.

The generic super-field in eq. (59) (or, which is the same, the fields a, \dots, i it is made of) is a representation of the SUSY algebra, but it is a reducible one. Irreducible representations, corresponding to the chiral and to the vector multiplets, are restricted versions of the general super-field reported in fig. 16. We already discussed the auxiliary field F appearing in the chiral field multiplet, we now see that it corresponds to the $\theta\theta$ component of the chiral super-field. This component is thus sometimes dubbed the “ F -component”. A real auxiliary field D is present in the vector multiplet, together with the gauge field A_μ and the Weyl gaugino fields λ_α . The auxiliary D is needed because the A_μ field is taken to be in the Feynman gauge, i.e. it is subject to the condition $\partial_\mu A^\mu = 0$ that reduces to three its independent components. One extra real field is thus required in order to match the 4 real components of the gaugino field. The D field is the $\theta\theta\bar{\theta}\bar{\theta}$ component of the vector super-field, which is thus called “ D -component”.

The rules to construct SUSY-invariant Lagrangians out of super-fields are rather simple. The first one is that (generic) super-fields, like ordinary fields, can be summed, multiplied and conjugated to produce other super-fields. Super-fields can also be derived with respect to the ordinary x^μ coordinates and also with respect to the SUSY coordinates θ and $\bar{\theta}$, by defining certain differential operators called “SUSY covariant derivatives”. I will not define SUSY covariant derivatives here, the reader is referred to the literature. Chiral super-fields can also be summed and multiplied producing other chiral super-fields, but they cannot be conjugated. The conjugate of a chiral super-field is still a super-field, but not a chiral one (it is called “anti-chiral”). The product of a chiral super-field with its conjugate is instead neither chiral nor anti-chiral. An important composite chiral super-field, which we will readily use to construct our SUSY Lagrangian, is the super-potential

$$W(\Phi) = a\Phi + \frac{1}{2}m\Phi^2 + \frac{1}{3}\lambda\Phi^3. \quad (60)$$

It is a cubic polynomial in the chiral super-field Φ , with an obvious generalisation to the case in which

several super-fields Φ_i are present. The super-potential is the SUSY generalisation of the ordinary scalar potential. However unlike the latter it cannot contain the conjugate of the chiral field, Φ^\dagger , otherwise it would not be a chiral super-field as previously explained. A super-potential can actually contain higher power of Φ . I stopped at the third order because higher term would produce non-renormalizable interactions in the Lagrangian.

The last set of rules tells us how to extract invariant Lagrangians out of functionals (sums, products and derivatives) of super-fields. All SUSY invariants happen to be either the D component (i.e., $\theta\theta\bar{\theta}\bar{\theta}$) of a generic super-field or the F component (i.e., $\theta\theta$) of a chiral super-field. The most general SUSY-invariant Lagrangian for a chiral super-field (with obvious generalisation to several super-fields) is thus

$$\begin{aligned} \left[\Phi^\dagger \Phi \right]_F &= i\bar{\psi}\bar{\sigma}^\mu\partial_\mu\psi + \partial_\mu\phi^\dagger\partial^\mu\phi + F^\dagger F, \\ [W(\Phi)]_D + \text{h.c.} &= \left. \frac{\partial W}{\partial\Phi} \right|_\phi F - \frac{1}{2} \left. \frac{\partial^2 W}{\partial\Phi\partial\Phi} \right|_\phi \psi\psi + \text{h.c.} . \end{aligned} \quad (61)$$

We see that the simple SUSY-invariant Lagrangian in eq. (56) is recovered for $a = \lambda = 0$ in the super-potential. Also notice that even in the more general Lagrangian in eq. (61) the auxiliary field F does not possess a kinetic term and it can be integrated out by solving its EOM, which is just $F^\dagger = -\partial W/\partial\Phi$. This results in a potential for the scalar component ϕ of the chiral super-field

$$V_F(\phi) = \left| \left. \frac{\partial W}{\partial\Phi} \right|_\phi \right|^2 = |a + m\phi + \lambda\phi^2|^2, \quad (62)$$

which is called “ F -term potential”.

Similarly, one can write down the Lagrangian for the vector super-field and the interactions between the vector super-field and the chiral one. The vector super-field is the SUSY generalisation of the A_μ gauge field, therefore its interactions are dictated by gauge-invariance (plus SUSY), very much like the interaction of an ordinary gauge field. For a single vector super-field, corresponding to a $U(1)$ gauge symmetry (the generalisation to non-abelian groups like the ones of the SM is rather straightforward) and a single chiral super-field with charge q under the group, the Lagrangian consists of the two following terms

$$\begin{aligned} \frac{1}{4} [\mathcal{W}^\alpha\mathcal{W}_\alpha]_F + \text{h.c.} &= -\frac{1}{4} A_{\mu\nu}A^{\mu\nu} + i\bar{\lambda}\bar{\sigma}^\mu\partial_\mu\lambda + \frac{1}{2} D^2, \\ \left[\Phi^\dagger e^{2qgV} \Phi \right]_D &= D_\mu\phi^\dagger D^\mu\phi + i\bar{\psi}\bar{\sigma}^\mu D_\mu\psi + F^\dagger F - i\sqrt{2}qg\phi\bar{\psi}\lambda + i\sqrt{2}qg\phi^\dagger\psi\lambda - qq\phi^\dagger\phi D. \end{aligned} \quad (63)$$

The first one is simply the kinetic term for the gauge and for the gaugino fields, plus a quadratic (non-derivative, as it should) term for the auxiliary D .³⁰ The second contains the kinetic terms of the scalar and Weyl fields in the chiral multiplet, with “ D_μ ” denoting the ordinary covariant derivative with with charge q and gauge coupling g , which produces the habitual gauge interactions. Interestingly enough, Yukawa couplings are also present involving ϕ , ψ and the gaugino λ . These are supersymmetric generalisations of the A_μ gauge interactions with ψ and with ϕ and they emerge with a coupling strength, $\sqrt{2}qg$, which is completely fixed by gauge invariance. Also notice that the auxiliary field can, as usual, easily be integrated out producing another contribution to the scalar potential called “ D -term potential”. It reads

$$V_D(\phi) = \frac{1}{2} q^2 g^2 |\phi|^2. \quad (64)$$

Once again, like the Yukawa’s previously mentioned, its coefficient is completely specified in terms of the representation of the gauge group in which the field lives (i.e., the charge q in our example) and by the gauge coupling g of the theory.

³⁰The chiral super-fields \mathcal{W}_α are a SUSY generalisation of the field-strength in ordinary gauge theories. Their definition is not worth reporting here.

3.2 Why SUSY is Great: a Tale from the 80's

The possibility of SUSY being the right tool to construct realistic extensions of the SM below or at the TeV scale (and not “just” a tool to build string theories of quantum gravity and to study deep theoretical aspects of Quantum Field Theory) is supported by a number of surprising phenomenological properties SUSY theories happen to possess (see [79, 80] for a complete discussion). These properties were discovered in the early 80's and produced enormous excitement in the theory community. The virtues of SUSY, which I will describe in the present section, of course are still there today. However they are now accompanied by a set of issues, related with negative searches of super-particles at different experimental facilities and with the determination of the Higgs boson mass, as I will explain in sect. 3.3. None of these experimental issues were of course known in the 80's, and thus the great excitement about SUSY was fully justified. The situation is different now. SUSY might still be waiting to be discovered at the TeV scale, but apparently not in the simple “vanilla” form theorists imagined in the 80's.

The main reason why SUSY should be relevant for TeV scale physics is that SUSY models can solve the Naturalness Problem, as first pointed out by several authors in '81, among which S. Dimopoulos, H. Georgi and E. Witten. In order to see how this works, let us recall the Naturalness Argument, as formulated in sect. 1.3, for the Higgs mass parameter m_H^2 . The problem has to do with a contribution that comes (in whatever new physics model is ultimately responsible for the microscopic origin of the Higgs mass) from low-energies, below the SM cutoff Λ_{SM} , i.e. at energies where physics is known and is provided by the SM. We focus on the largest contribution, the one from the top quark loop in eq. (6)

$$\delta_{\text{SM}} m_H^2 = \frac{3y_t^2}{4\pi^2} \Lambda_{\text{SM}}^2. \quad (65)$$

It can be interpreted, poorly speaking, as a divergent contribution to the Higgs mass. The Naturalness Problem is that this term becomes much larger than the actual value of m_H^2 , obliging us to a cancellation, if Λ_{SM} is much above the TeV, as eq. (7) shows.

The problem emerges because the Higgs mass has two properties, which have to be simultaneously verified for the Naturalness Problem to arise. These are the fact that the Higgs mass term is a parameter with positive energy dimension and the fact that it is not protected by any symmetry, namely no new symmetry emerges in the SM Lagrangian if m_H^2 is taken to vanish. Parameters that violate both conditions are instead, for instance, the SM Yukawa couplings. Take for simplicity one single fermion, with its Yukawa coupling y_f to the Higgs field, and repeat for y_f the considerations that led us to the Naturalness Problem in sect. 1.3. We can still split the integral expression for it as in eq. (5), but now if we compute the $E < \Lambda_{\text{SM}}$ contribution we find

$$\delta_{\text{SM}} y_f \sim \frac{y_f g^2}{16\pi^2} \log(\Lambda_{\text{SM}}/M_{\text{EW}}). \quad (66)$$

In the expression, M_{EW} denotes the EW scale and g is one SM coupling which, depending on the diagram, could be either y_f itself or one of the gauge couplings. The result contains no power-like divergence, for the very simple reasons is that all the SM couplings are dimensionless. It is thus impossible to have a polynomial divergence on a dimensionless quantity, only logarithmic divergencies are allowed. Clearly a logarithm is much less dangerous. Even for $\Lambda_{\text{SM}} = M_P$, the log is around 40 and hardly compensates the $g^2/16\pi^2$ loop factor. The contribution to y_f is thus of order y_f or smaller and no cancellation is required. The fact that $\delta_{\text{SM}} y_f$ contains at least one power of y_f is instead less trivial and has to do with the fact that a symmetry (chiral symmetry, i.e. two independent phase transformations acting on the two chirality components) is recovered at $y_f = 0$. Then if y_f was really vanishing, loop corrections could not generate it. A diagram contributing to it must thus contain at least one insertion of the y_f vertex. As mentioned in sect. 1.3, this symmetry argument can be extended in order to deal with all the three SM families, ensuring that the correction of each Yukawa coupling is proportional to itself. This avoids, for instance, relatively large contribution to the Yukawa coupling of the up induced by the much larger coupling of the top quark.

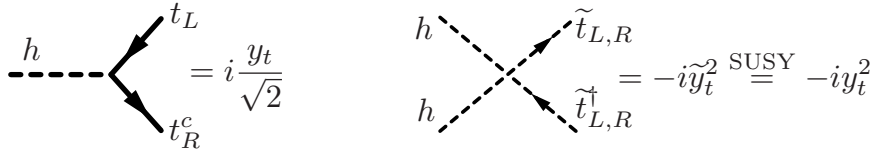


Fig. 17: The ordinary Yukawa coupling (left) with its SUSY counterpart (right).

A less simple case is the one of a massive fermion. Of course we don't have one in the SM since no fermion masses (but only Yukawa's) are present in the SM above the EW scale. Consider however a toy model in which a massive fermion is included in the theory, coupled through a set of dimensionless couplings “ g ” to the SM fields. Its mass m_F has of course positive energy dimension like m_H , but still the low-energy contribution to it is only logarithmically divergent³¹

$$\delta_{\text{IR}} m_F \sim \frac{g^2}{16\pi^2} m_F \log(\Lambda/M_{\text{IR}}). \quad (67)$$

Unlike the Yukawa's, m_F has positive dimension but, exactly like the Yukawa's, it is protected by the chiral symmetry which is recovered in the theory if $m_F = 0$. Thus loop corrections are proportional to m_F itself and are not large. As such, m_F does not suffer of a Naturalness Problem.

We just discovered that a fermion, unlike a scalar boson, can be “Naturally” light, even if the cutoff Λ of the theory it is part of is extremely large. It is thus now clear why SUSY, which obliges the mass of the scalar Higgs boson to be equal to the one of its fermionic higgsino partner, can help us with the Naturalness Problem. If the former is “Naturally” light, the latter must be “Natural” as well in a SUSY model. In order to illustrate how this works, let us only consider the Higgs boson, the top quark and the Yukawa interaction between them, which is responsible for the largest contribution to m_H^2 in eq. (65). I will even ignore the bottom quark, as well as the other components of the Higgs doublet, and I will just focus on the neutral Higgs field component h coupled to t_L and t_R through the Yukawa coupling. In order to construct a supersymmetric version of this theory, three chiral super-fields need to be introduced: Φ_h , Φ_{t_L} and Φ_{t_R} . After integrating out the auxiliary fields, they lead respectively to the fields $\{h, \tilde{h}\}$, $\{t_L, \tilde{t}_L\}$ and $\{t_R^c, \tilde{t}_R^\dagger\}$, where \tilde{h} is the higgsino, \tilde{t}_L is the left-handed stop and \tilde{t}_R is the right-handed stop. Notice that what appears in Φ_{t_R} is the conjugate of the right-handed top, t_R^c , which is a left-handed field and as such can appear in the chiral super-field. Correspondingly, the right-handed stop is defined with a conjugate such that it has the same quantum numbers of the (not conjugate) SM t_R . Introducing the SM Yukawa in the theory requires us to put a trilinear term in the super-potential

$$W = \frac{y_t}{\sqrt{2}} \Phi_h \Phi_{t_L} \Phi_{t_R} \longrightarrow \begin{cases} \text{SM Yukawa (from eq. (61)):} & -\frac{y_t}{\sqrt{2}} h \bar{t} t_R, \\ F\text{-term potential (from eq. (62)):} & -\frac{y_t^2}{2} h^2 [|\tilde{t}_L|^2 + |\tilde{t}_R|^2]. \end{cases} \quad (68)$$

Therefore in SUSY the Yukawa coupling, diagrammatically represented on the left panel of fig. 17, is necessarily associated with a quartic $h^2 \tilde{t}_{L,R}^2$ vertex with the stops, reported on the right. Both couplings must be included in the calculation of $\delta_{\text{IR}} m_H^2$, and the stop loop cancel exactly the one of the top

$$\begin{aligned} \delta_{\text{IR}} m_H^2 &= \int_0^{\lesssim \Lambda} dE \left[\text{---} \bigcirc \text{---} + \text{---} \bigcirc \text{---} \right] \\ &= \frac{3}{8\pi^2} \Lambda^2 [y_t^2 - \tilde{y}_t^2] \stackrel{\text{SUSY}}{=} 0 \end{aligned}$$

The result is that the Naturalness Problem is solved, as expected, in a supersymmetric theory.

³¹From now on, since the low-energy (IR) theory we are considering to compute the low energy contribution is not anymore the SM, I will substitute “ δ_{SM} ” with “ δ_{IR} ” and “ Λ_{SM} ” with Λ , representing the cutoff scale of the IR theory.

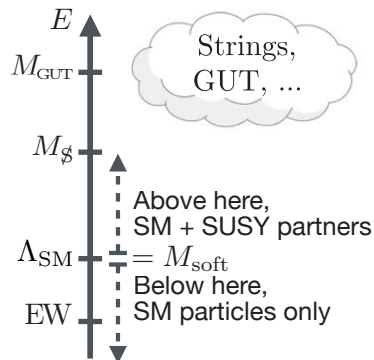


Fig. 18: The SUSY picture of high-energy physics.

Obviously in order to exploit the solution to the Naturalness Problem offered by supersymmetry we cannot just replace the SM with its SUSY version. This would be in sharp contrast with observations given that the particles we know about, their spectrum and interactions, do not respect SUSY. What one has to do is to first extend the SM to its (possibly minimal, but not necessarily so) SUSY version, and then include extra terms in the Lagrangian that break supersymmetry and reconcile the model with observations. Very importantly, it turns out that it is possible to do this without spoiling the SUSY solution to the Naturalness Problem, by introducing a special set of SUSY-breaking terms called “soft terms”. Equally importantly, explicit microscopic models exist where SUSY is exact at very high scale, gets spontaneously broken and produces only soft breaking terms at low energy. Soft SUSY-breaking terms, namely terms that break SUSY but preserve Naturalness, include (see e.g. [79, 80]) mass, bilinear and trilinear terms for the scalar fields and gaugino mass terms. Including them in the Lagrangian happens to be sufficient to make all the SUSY partners of the SM particles heavy, explaining why we have not yet seen them. SUSY models addressing the Naturalness Problem can thus be made fully realistic, as a result of a fortunate series of “coincidences” related with a bunch of non-trivial properties of SUSY.

The SUSY picture of high-energy physics is thus the one of fig. 18. Starting from above, the theory is exactly supersymmetric at very high energies, until the scale M_g where SUSY is broken producing a set of soft terms. The typical mass-scale M_{soft} of the soft terms generated by the breaking, among which we have the mass of the supersymmetric particles, needs however not to be of the order of M_g . It can be of that size in specific SUSY breaking scenarios, but it can also easily be much smaller than that, $M_{\text{soft}} \ll M_g$, as in the framework of “gravity-mediated” SUSY breaking (which used to be very popular in the 80’s). Below M_g , the theory reduces to a supersymmetric extensions of the SM containing both the SM particles and the SUSY partners as propagating degrees of freedom, the latter ones with a mass of order M_{soft} , larger than the EW scale. Below M_{soft} , SUSY partners decouple from the theory and one is left with the SM. Seen from below, M_{soft} is the scale at which BSM particles appear and thus it provides the SM cutoff Λ_{SM} .

In view of the identification $M_{\text{soft}} \sim \Lambda_{\text{SM}}$, it is clear that the SUSY partners cannot be arbitrarily heavy if we really want to solve the Naturalness Problem, because of eq. (65). This is readily checked by giving a mass $M_{\tilde{t}} \simeq M_{\text{soft}}$ to the stops and repeating the calculation of $\delta_{\text{IR}} m_H^2$. It is rather obvious by dimensional analysis that we are going to obtain

$$\delta_{\text{IR}} m_H^2 = \frac{3y_t^2}{8\pi^2} M_{\tilde{t}} \log(M_g/M_{\tilde{t}}). \quad (69)$$

Up to the log, which can just worsen the situation, we get the same expression as in eq. (65) with Λ_{SM} replaced by $M_{\tilde{t}} \simeq M_{\text{soft}}$. Consequently we get a large fine-tuning Δ , as in eq. (7), if SUSY particles are not at the TeV scale or below.

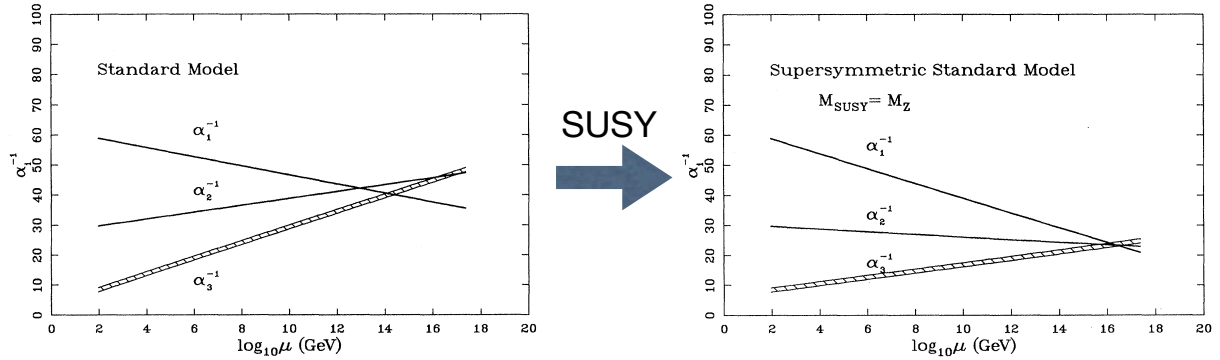


Fig. 19: The SU(3), SU(2) and U(1) inverse structure constant ($\alpha_i^{-1} = 4\pi/g_i^2$) renormalisation group running in the SM (left) and in its minimal supersymmetric extension, the MSSM (right).

SUSY having to show up before the TeV was of course not at all an issue in the 80', when this scale was far to be directly probed experimentally. It was actually a reason for excitement having all these new particles close enough to be discovered in the future. More reasons for excitement came from two more arguments, seemingly unrelated with SUSY: coupling unification and Dark Matter. Coupling unification (see [8, 9] for a review) is the idea that the three SM gauge forces might have a common origin at very high scales, where they are all described by a single simple unified gauge group (e.g., SU(5) or SO(10)), characterised by a single gauge coupling. This is supported, in the first place, by the fact that the SM matter fermion content fills, for no obvious reason, complete multiplets of the unified group (see [29] for a concise discussion). These multiplets contain at the same time quarks and leptons. GUT models are also supported by the fact that the running of the three SM gauge couplings makes them approach each other at high scale. As shown in fig. 19, this more or less happens (but not very accurately) in the SM at a scale $M_{\text{GUT}} \sim 10^{14}$ GeV. At this scale, the full unified theory should show up. In particular, new massive gauge bosons should appear, with interactions connecting leptons and quarks that sit in the same GUT multiplets as previously mentioned. These interactions make the proton decay at an unacceptably large rate if $M_{\text{GUT}} \sim 10^{14}$ GeV. The situation is much better in supersymmetric extensions of the SM, as shown in the right panel of fig. 19. First, the couplings unify more accurately, simply due to the effect of the super-partners on the running, which happen to go in the right direction for no obvious reason. Second, unification is postponed to $M_{\text{GUT}} \sim 10^{16}$ GeV and proton decay experiments are not sensitive to such a high suppression scale. All this of course happens only provided M_{soft} is small enough for the super-partners starting to contribute to the running early enough, $M_{\text{soft}} \sim 100$ GeV is assumed in the plot. Clearly the running is logarithmically slow, so that $M_{\text{soft}} = 10$ TeV or even more would not change the situation radically. However it is clear that also coupling unification, as well as the Naturalness Argument, point towards low-energy supersymmetry. The positive interplay between low-energy SUSY and unification is a very strong argument in favour of SUSY and of unification as well.

The interplay between SUSY and DM is equally impressive. It originates from a serious phenomenological problem of SUSY and of its solution, which consists in imposing a discrete symmetry called “ R -parity”. I stressed in sect. 1.2 the phenomenological importance of Baryon and Lepton number as accidental symmetry in the SM and how much non-trivial it is that these symmetries emerge at $d = 4$ without being imposed in the construction of the theory. I also argued that BSM scenarios will in general not possess accidental Baryon and Lepton number and that those symmetries will have to be imposed in some way. This is the case also in SUSY. Indeed, when trying to construct the minimal supersymmetric extension of the SM (the Minimal Supersymmetric Standard Model, MSSM), one immediately encounters terms in the super-potential, allowed by the gauge symmetries, that violate both the Baryon and the Lepton number. For instance, Baryon number is violated by (see e.g. [80] for more details)

$$\Delta W_{\Delta B=1} = \lambda'' \varepsilon_{\alpha\beta\gamma} \Phi_{u_R}^\alpha \Phi_{d_R}^\beta \Phi_{d_R}^\gamma, \quad (70)$$

where α, β, γ are QCD color indices while the flavour indices are understood. Adding those terms in the super-potential produces SUSY-invariant $d = 4$ interactions that violate Baryon and Lepton number, in sharp contrast with observations. However all these dangerous terms, and all the soft SUSY-breaking ones which also violate Baryon and Lepton number, are avoided by imposing only one discrete symmetry, R -parity. R -parity consists in the sign-flip $\theta \rightarrow -\theta$ and $\bar{\theta} \rightarrow -\bar{\theta}$ of the super-space coordinates, times an additional overall minus sign for all the matter fermions (quarks and leptons) super-fields. A quick look at fig. 16 immediately reveals that with this assignment all the SM fields (quarks, leptons, gauge and Higgs) are even and all the super-partners (or s-particles) are odd. The super-potential in eq. (70) is obviously odd under R -parity and it is thus forbidden, together with all the other Baryon and Lepton number-violating terms, if R -parity is imposed as a symmetry of the MSSM.

Since they are odd under R -parity, s-particles cannot decay to SM particles only, at least one s-particle must be present in the final state. In particular this means that the lightest of the s-particles (the LSP) cannot decay at all and it is absolutely stable. If it happens to be electrically and QCD neutral, it is potentially a viable DM candidate. Moreover, the LSP mass will be of the order of M_{soft} , which we argued above to be likely of the 100 GeV to TeV order. Furthermore, the LSP will typically couple to SM through EW gauge interactions. A particle with these properties is called a Weakly-Interacting Massive Particle (WIMP) and it can perfectly account for the observed DM component of the Universe through the mechanism of thermal freeze-out (see [3] for a review). This is the so-called “WIMP miracle”, which automatically emerges as a byproduct of SUSY model-building.

3.3 SUSY after LEP, Tevatron and LHC run-1

Naturalness, coupling unification and Dark Matter are extremely strong arguments in favour of low-scale SUSY, and all the enthusiasm they triggered towards SUSY is perfectly justified. However this enthusiasm cooled considerably after 30 years of negative experimental s-particle searches. LEP was the collider at which SUSY had its first chance to be discovered, in spite of the fact that LEP energy was far below 450 GeV (see eq. (7)), which is what we nowadays consider to be threshold for “Natural” BSM physics. This is because in the fine-tuning estimate we should not forget the logarithmic term we found in eq. (69), and we should remember that a high SUSY-breaking scale was expected in the 80’s. With this expectation, taking for definiteness $M_g = 10^{15}$ GeV, the log is around 30 and the Naturalness threshold moves down to $450/\sqrt{30} = 82$ GeV. Even taking into account that s-particles must be produced in pairs because of R -parity, the LEP collider (in the LEP-II stage) could have had enough energy to produce them. Of course M_g needs not to be that high, viable SUSY-breaking scenarios exist where M_g is not far from the TeV scale and the log is small. Still, negative LEP search were the first evidence against the “vanilla” SUSY picture described in the previous section.

The search for s-particles continued at Tevatron and at the LHC run-1, with negative results.³² Current limits on certain SUSY particles (light squarks and gluinos) are as high as 1.7 TeV signalling, if taken at face value, that SUSY is a quite “Un-Natural” theory. One should however be more careful, because the s-particles needs not to be all degenerate and a bound on few of them cannot be directly translated into a bound on M_{soft} . Furthermore, not all the s-particles are equally important as far as fine-tuning is concerned because the way in which they contribute to the Higgs mass is very different. For instance, the stops are those that give the largest radiative contribution, in eq. (69), because their coupling to the Higgs is the largest one. The 450 GeV threshold only applies to the stops, and the limit on their mass is only 700 GeV or less, still compatible with Naturalness.³³ The strong limit on the light squarks is instead irrelevant for Naturalness, given that the squark contribution to m_H^2 is extremely suppressed by the small Yukawa couplings. The partners of the EW gauge bosons (EWinos) give the second largest radiative contribution (see eq. (6)), which is proportional to the Weak coupling square rather than to y_t .

³²And at the LHC run-2, however here I stick to the run-1 results, the only ones that were available when I gave the lectures.

³³Tree-level contributions to m_H^2 emerge from higgsinos, and thus the Naturalness threshold on these particles is extremely low. However there no tension with the experimental bounds, which are too weak.

The Naturalness threshold for the EWinos is thus around the TeV, much above the limits. The gluinos are also relevant for Naturalness. In spite of the fact that their contribution to m_H^2 arises at two loops, the strong QCD coupling and certain color multiplicity factors produce a Naturalness threshold for gluinos around the TeV, which is comparable with the run-1 limit. The overall picture that emerges from this kind of considerations (the so-called “Natural SUSY” approach) is that the LHC run-1 started probing the “Natural” parameter space of SUSY, but no conclusive statement can be made. For an extensive presentation of this viewpoint and a quantitative discussion of run-1 searches the reader is referred to the lecture notes in Ref. [87].

The very last topic of these lectures is the structure of the Higgs potential in supersymmetry. This topic is relevant by itself, as it constitutes the starting point for SUSY Higgs phenomenology, extensively discussed in [88]. However it is also relevant in order to assess the current status of SUSY because it will allow us to understand and to qualify the often-heard statement that the LEP bound on the Higgs mass (and its measurement at the LHC) is problematic for SUSY. The first important point is that any SUSY extension of the SM requires us to introduce at least two Higgs chiral super-fields: Φ_u and Φ_d . This follows from the fact in order to generate the Yukawa couplings in the up and in the down sector two Higgs doublets are needed, with respectively Hypercharge equal to $1/2$ and $-1/2$. Only one doublet is introduced in the SM because the other one can be obtained by complex conjugation, but this is impossible in SUSY since the conjugate of a chiral super-field cannot appear in the super-potential. Two chiral super-fields are thus needed,³⁴ with super-potential terms

$$W_u = y_u \Phi_{qL} \Phi_u \Phi_{uR}, \quad W_d = y_d \Phi_{qL} \Phi_d \Phi_{dR}. \quad (71)$$

Therefore two scalar Higgs doublets H_u and H_d are present in SUSY, coupled to up- and down-type quarks respectively. After EWSB, three of these 8 real degrees of freedom are eaten by the EW bosons becoming massive, one provides the neutral SM Higgs boson and the remain four are extra scalars which are absent in the SM. The extra scalars in SUSY are one heavy neutral CP-even state H_0 , one charged H_{\pm} and a neutral CP-odd A . Searching for these particles directly, or indirectly by studying their effects (through mixing) on the couplings of the SM-like Higgs, is one way to test supersymmetry.

The scalar potential for the H_u and H_d doublets consists of three terms³⁵

$$\begin{aligned} V(H_u, H_d) &= \mu^2 (|H_u|^2 + |H_d|^2) \\ &+ \frac{g^2 + g'^2}{8} (|H_u|^2 - |H_d|^2)^2 + \frac{g^2}{2} |H_u^\dagger H_d|^2 \\ &+ m_u^2 |H_u|^2 + m_d^2 |H_d|^2 + B(H_u H_d + H_u^* H_d^*). \end{aligned} \quad (72)$$

The one on the first line is an F -term, originating from the μ -term $\mu \Phi_u \Phi_d$ in the super-potential. The one on the second line is a D -term, dictated by the gauge quantum numbers of the Higgs doublets. Notice that it is the only one that contains quartic couplings, which are thus completely fixed in terms of the SM gauge couplings g and g' . The soft SUSY-breaking terms are displayed in the last line. The potential in eq. (72) allows, with the appropriate choice of its parameters, EWSB to occur. Also, it allows (or better, generically requires) both doublets to get a VEV

$$\langle |H_u|^2 \rangle = \frac{v_u^2}{2}, \quad \langle |H_d|^2 \rangle = \frac{v_d^2}{2}. \quad (73)$$

The sum of the square of the two VEVs is fixed to $v_u^2 + v_d^2 = v^2$, where $v \simeq 246$ GeV, but the ratio between them is a free parameter, which is typically traded for the tangent of the “ β ” angle

$$\tan \beta \equiv \frac{v_u}{v_d}. \quad (74)$$

³⁴The cancellation of gauge anomalies also requires two Higgs super-fields.

³⁵The contraction with the ε_{ij} tensor is understood in last term of the equation that follows.

Notice that both Higgses taking VEV is necessary in order to generate quark masses since, as we discussed, the up- and down-type Yukawa couplings are only present for H_u and for H_d , respectively.

With the knowledge of the 80's, the potential in eq. (72) is quite successful. It produces realistic EWSB and fermion masses, and an extended Higgs sector which was perfectly plausible at that times, in which almost no experimental information was available on Higgs physics. After LEP could not discover the Higgs boson and set a lower bound $m_H > 115$ GeV, the potential (72) started being in tension with observations. Indeed, it is possible to show that the structure of the potential is such that the Higgs mass is unavoidably smaller than the one of the Z boson. More precisely, it turns out that for any choice of the free parameters one has

$$m_H \leq |\cos 2\beta| m_Z \leq m_Z. \quad (75)$$

The relation follows from the fact that the quartic terms in the potential are not free parameters, but instead they are uniquely dictated, through supersymmetry, by the gauge coupling. In order to see how this works, consider a simplified limit, the so-called ‘‘decoupling limit’’, in which the soft mass of the H_d , m_d^2 , is taken to be large. In the limit, H_d decouples and it can be just ignored (i.e., set to zero) in eq. (72), obtaining a SM-like potential

$$V = \mu_{\text{SM}}^2 |H_u|^2 + \lambda_{\text{SM}} |H_u|^4, \quad (76)$$

with $\mu_{\text{SM}}^2 = \mu^2 + m_u^2$ and $\lambda_{\text{SM}} = (g^2 + g'^2)/8$. The habitual SM formula $m_H = \sqrt{2\lambda}v$ thus tells us that $m_H = m_Z$ in the decoupling limit. This matches eq. (75) because in the decoupling limit one finds that $\tan \beta \rightarrow \infty$, i.e. $\beta \rightarrow \pi/2$.

Since the mass relation in eq. (75) is violated experimentally, we might wonder if it excludes SUSY as a realistic theory of Nature. Of course it does not, because of two reasons, but it has important implications. The first point is that eq. (75) is only valid at the tree-level order, radiative corrections violate it. For instance top and stop loops contribute to the quartic by an amount

$$\delta\lambda \sim \frac{3y_t^2}{8\pi^2} \log \frac{M_{\tilde{t}}}{m_t}, \quad (77)$$

so that by making stops heavy one can get a large enough quartic and a large enough Higgs mass. Working in the decoupling limit for simplicity (and because it is the most favourable one), the shift we need on λ is

$$\delta\lambda = \frac{m_H^2 - m_Z^2}{2v^2} \simeq 0.06, \quad \Rightarrow \quad M_{\tilde{t}} \simeq 1.3 \text{ TeV}. \quad (78)$$

That heavy stops cost quite a lot of fine-tuning, definitely above ten. More refined estimates [89], taking into account the need of a separation between M_g and the weak scale (i.e., of some log enhancement in the tuning), reveal that the tuning needed to accomodate the 125 GeV Higgs mass is at least 100.

The second reason why eq. (75) cannot disprove supersymmetry is that it only holds in the MSSM, thus it is not a robust property of SUSY models. It can be violated in SUSY scenarios like λ SUSY [90] (A.K.A. NMSSM), in which an extra singlet chiral super-field Φ_S is added to the theory with a $\lambda\Phi_S\Phi_u\Phi_d$ term in the super-potential. This contributes to the quartic Higgs coupling and leads to a heavy enough Higgs boson if λ is sufficiently large. The main drawback of this construction is that λ needs to be relatively big, therefore its RG-running is very fast and reaches a Landau pole not much above the 10 TeV scale. The alternative to a fine-tuned scenario seems thus to be a model which cannot be extended far above the TeV scale. This clearly seems very different from the basic SUSY picture we had in mind in fig. 18. However there might be caveats, new model-building ways out, or space for a ‘‘partially Un-Natural’’, but still true, SUSY model at the TeV scale. Let us wait and see, the LHC run-2 will tell us more about SUSY.

4 Conclusions and Outlook

My purpose, when giving these lectures, was to outline that BSM physics is not (only) a collection of models, but rather a set of structural questions on fundamental physics and of possible answers to be checked against data. The microscopic origin of the Higgs mass, in connection with Naturalness (or Un-Naturalness), is only one of such questions. However it is the one about which decisive experimental progress will be made at the LHC, this is why I built the lectures around it. Several other relevant questions and ideas were encountered during the lectures, among which GUT, DM, neutrino masses and vacuum stability, each of which deserves a separate course. Some of these courses were given at this School [2, 3]. For what is missing, the lectures in Ref. [29] are a valid starting point. The course aimed at providing a pedagogical introduction to BSM physics, for this reason basic material was presented and many recent developments were left out from the discussion. This should not obscure the fact that “Natural” BSM model-building is an active research area. Approaches related with the “Twin Higgs” mechanism [32] are worth mentioning in this context.

Concerning the future of BSM physics, there is not much I can add to what discussed in sect. 1. There is not guarantee that the ongoing LHC program will produce a new physics discovery, but it is sure that it will improve our comprehension of fundamental interactions. This is more than enough to work on LHC physics to the best of our abilities. On a longer timescale, the future is impossible to predict. We will definitely keep asking structural questions on fundamental physics, however it is unclear if high-energy collider experiments will continue being the optimal investigation tools to search for answers. My viewpoint is well summarised by a famous sentence

*“Learn from yesterday, live for today, hope for tomorrow.
The important thing is not to stop questioning.”*

– Albert Einstein

References

- [1] R. Rattazzi, EPFL Lectures, link.
- [2] S. Petcov, “Neutrino Physics”, these proceedings.
- [3] A. De Simone, “Cosmology”, these proceedings.
- [4] S. Gori, “Flavour Physics and CP violation”, these proceedings.
- [5] For a pedagogical introduction to the Equivalence Theorem, see J. Horejsi, Czech. J. Phys. **47** (1997) 951 [hep-ph/9603321].
- [6] D. Buttazzo, G. Degrassi, P. P. Giardino, G. F. Giudice, F. Sala, A. Salvio and A. Strumia, JHEP **1312** (2013) 089 [arXiv:1307.3536].
- [7] I. V. Krive and A. D. Linde, Nucl. Phys. B **117** (1976) 265.
- [8] P. Langacker, Phys. Rept. **72** (1981) 185.
- [9] S. Raby, “Grand Unified Theories,” hep-ph/0608183.
- [10] L. B. Okun, *Leptons and Quarks*. North Holland, 1982.
- [11] T. Cheng and L. Li, *Gauge theory of elementary particle physics*. Oxford University Press, 1984.
- [12] M. D. Schwartz, *Quantum Field Theory and the Standard Model*. Cambridge University Press, 2013.
- [13] K. A. Olive *et al.* [Particle Data Group Collaboration], Chin. Phys. C **38** (2014) 090001.
- [14] R. Barbieri, Pisa, Italy: Sc. Norm. Sup. (2007) 84 p [arXiv:0706.0684].
- [15] S. Weinberg, Phys. Rev. Lett. **43** (1979) 1566.
- [16] M. Cirelli, N. Fornengo and A. Strumia, Nucl. Phys. B **753** (2006) 178 [hep-ph/0512090].

- [17] R. Barbieri, Phys. Scripta T **158** (2013) 014006 [arXiv:1309.3473].
- [18] G. F. Giudice, In *Kane, Gordon (ed.), Pierce, Aaron (ed.): Perspectives on LHC physics* 155-178 [arXiv:0801.2562].
- [19] G. 't Hooft, Proceedings of the 1979 Cargese Institute on Recent Developments in Gauge Theories, Plenum Press, New York (1980) 135.
- [20] S. Dimopoulos and L. Susskind, Nucl. Phys. B **155** (1979) 237.
- [21] L. Susskind, Phys. Rev. D **20** (1979) 2619.
- [22] S. L. Glashow and S. Weinberg, Phys. Rev. D **15** (1977) 1958.
- [23] G. D'Ambrosio, G. F. Giudice, G. Isidori and A. Strumia, Nucl. Phys. B **645** (2002) 155 [hep-ph/0207036].
- [24] S. Weinberg, *The quantum theory of fields. Vol. 1: Foundations.* Cambridge University Press, 1995.
- [25] S. Weinberg, Phys. Rev. Lett. **59** (1987) 2607.
- [26] L. J. Hall and Y. Nomura, Phys. Rev. D **78** (2008) 035001 [arXiv:0712.2454].
- [27] P. W. Graham, D. E. Kaplan and S. Rajendran, Phys. Rev. Lett. **115** (2015) no.22, 221801 [arXiv:1504.07551].
- [28] L. F. Abbott, Phys. Lett. B **150** (1985) 427.
- [29] A. Pomarol, "Beyond the Standard Model," arXiv:1202.1391.
- [30] M. Schmaltz and D. Tucker-Smith, Ann. Rev. Nucl. Part. Sci. **55** (2005) 229 [hep-ph/0502182].
- [31] M. Perelstein, Prog. Part. Nucl. Phys. **58** (2007) 247 [hep-ph/0512128].
- [32] Z. Chacko, H. S. Goh and R. Harnik, Phys. Rev. Lett. **96** (2006) 231802 [hep-ph/0506256].
- [33] D. B. Kaplan and H. Georgi, Phys. Lett. **136B** (1984) 183.
- [34] D. B. Kaplan, H. Georgi and S. Dimopoulos, Phys. Lett. **136B** (1984) 187.
- [35] M. J. Dugan, H. Georgi and D. B. Kaplan, Nucl. Phys. B **254** (1985) 299.
- [36] K. Agashe, R. Contino and A. Pomarol, Nucl. Phys. B **719** (2005) 165 [hep-ph/0412089].
- [37] G. F. Giudice, C. Grojean, A. Pomarol and R. Rattazzi, JHEP **0706** (2007) 045 [hep-ph/0703164].
- [38] R. Contino, "The Higgs as a Composite Nambu-Goldstone Boson," arXiv:1005.4269.
- [39] G. Panico and A. Wulzer, Lect. Notes Phys. **913** (2016) pp.1 [arXiv:1506.01961].
- [40] S. Weinberg, Phys. Rev. D **13** (1976) 974.
- [41] S. Weinberg, Phys. Rev. D **19** (1979) 1277.
- [42] K. Lane, "Two lectures on technicolor," hep-ph/0202255.
- [43] D. B. Kaplan, Nucl. Phys. B **365** (1991) 259.
- [44] R. Grober and M. Muhlleitner, JHEP **1106** (2011) 020 [arXiv:1012.1562].
- [45] R. Contino, M. Ghezzi, M. Moretti, G. Panico, F. Piccinini and A. Wulzer, JHEP **1208** (2012) 154 [arXiv:1205.5444].
- [46] A. Pomarol and F. Riva, JHEP **1208** (2012) 135 [arXiv:1205.6434].
- [47] G. Panico and A. Wulzer, JHEP **1109** (2011) 135 [arXiv:1106.2719].
- [48] ATLAS Collaboration, Eur. Phys. J. C **76** (2016) no.1, 6 [arXiv:1507.04548 [hep-ex]].
- [49] CMS Collaboration, Eur. Phys. J. C **75** (2015) no.5, 212 [arXiv:1412.8662 [hep-ex]].
- [50] ATLAS Collaboration, JHEP **1511** (2015) 206 [arXiv:1509.00672 [hep-ex]].
- [51] CMS Collaboration, [CMS-NOTE-2012-006].
- [52] ATLAS Collaboration, [ATL-PHYS-PUB-2013-014].
- [53] S. Dawson *et al.*, "Working Group Report: Higgs Boson," arXiv:1310.8361 [hep-ex].
- [54] A. Azatov, R. Contino, G. Panico and M. Son, Phys. Rev. D **92** (2015) no.3, 035001

- [arXiv:1502.00539].
- [55] K. Agashe, H. Davoudiasl, S. Gopalakrishna, T. Han, G. Y. Huang, G. Perez, Z. G. Si and A. Soni, *Phys. Rev. D* **76** (2007) 115015 [arXiv:0709.0007].
- [56] K. Agashe, S. Gopalakrishna, T. Han, G. Y. Huang and A. Soni, *Phys. Rev. D* **80** (2009) 075007 [arXiv:0810.1497].
- [57] K. Agashe, A. Azatov, T. Han, Y. Li, Z. G. Si and L. Zhu, *Phys. Rev. D* **81** (2010) 096002 [arXiv:0911.0059].
- [58] K. Agashe, A. Belyaev, T. Krupovnickas, G. Perez and J. Virzi, *Phys. Rev. D* **77** (2008) 015003 [hep-ph/0612015].
- [59] D. Pappadopulo, A. Thamm, R. Torre and A. Wulzer, *JHEP* **1409** (2014) 060 [arXiv:1402.4431].
- [60] D. Liu and R. Mahbubani, *JHEP* **1604** (2016) 116 [arXiv:1511.09452].
- [61] C. Bini, R. Contino and N. Vignaroli, *JHEP* **1201** (2012) 157 [arXiv:1110.6058].
- [62] V. D. Barger, W. Y. Keung and E. Ma, *Phys. Rev. D* **22** (1980) 727.
- [63] A. Thamm, R. Torre and A. Wulzer, *JHEP* **1507** (2015) 100 [arXiv:1502.01701].
- [64] A. Azatov and J. Galloway, *Phys. Rev. D* **85** (2012) 055013 [arXiv:1110.5646].
- [65] R. Contino, L. Da Rold and A. Pomarol, *Phys. Rev. D* **75** (2007) 055014 [hep-ph/0612048].
- [66] K. Agashe, R. Contino, L. Da Rold and A. Pomarol, *Phys. Lett. B* **641** (2006) 62 [hep-ph/0605341].
- [67] O. Matsedonskyi, G. Panico and A. Wulzer, *JHEP* **1301** (2013) 164 [arXiv:1204.6333].
- [68] A. De Simone, O. Matsedonskyi, R. Rattazzi and A. Wulzer, *JHEP* **1304** (2013) 004 [arXiv:1211.5663].
- [69] O. Matsedonskyi, G. Panico and A. Wulzer, *JHEP* **1412** (2014) 097 [arXiv:1409.0100].
- [70] O. Matsedonskyi, G. Panico and A. Wulzer, *JHEP* **1604** (2016) 003 [arXiv:1512.04356].
- [71] M. Redi and A. Weiler, *JHEP* **1111** (2011) 108 [arXiv:1106.6357].
- [72] R. Barbieri, D. Buttazzo, F. Sala and D. M. Straub, *JHEP* **1207** (2012) 181 [arXiv:1203.4218].
- [73] M. Redi, V. Sanz, M. de Vries and A. Weiler, *JHEP* **1308** (2013) 008 [arXiv:1305.3818].
- [74] C. Delaunay, T. Flacke, J. Gonzalez-Fraile, S. J. Lee, G. Panico and G. Perez, *JHEP* **1402** (2014) 055 [arXiv:1311.2072].
- [75] O. Matsedonskyi, *JHEP* **1502** (2015) 154 [arXiv:1411.4638].
- [76] G. Panico and A. Pomarol, arXiv:1603.06609.
- [77] M. F. Sohnius, "Introducing Supersymmetry," *Phys. Rept.* **128** (1985) 39.
- [78] J. P. Derendinger, "Lecture notes on globally supersymmetric theories in four-dimensions and two-dimensions," In *Corfu 1989, Elementary particle physics* 111-243
- [79] M. Drees, "An Introduction to supersymmetry," hep-ph/9611409.
- [80] S. P. Martin, *Adv. Ser. Direct. High Energy Phys.* **21** (2010) 1 [hep-ph/9709356].
- [81] M. E. Peskin, "Supersymmetry in Elementary Particle Physics," arXiv:0801.1928.
- [82] J. Wess and J. Bagger, *Supersymmetry and Supergravity*.
Princeton series in physics. Princeton University Press, New Jersey, 1992.
- [83] S. Weinberg, *The quantum theory of fields. Vol. 3: Supersymmetry*.
Cambridge University Press, 2000.
- [84] S. R. Coleman and J. Mandula, *Phys. Rev.* **159** (1967) 1251.
- [85] Y. A. Golfand and E. P. Likhtman, *JETP Lett.* **13** (1971) 323
- [86] R. Haag, J. T. Lopuszański and M. Sohnius, *Nucl. Phys. B* **88** (1975) 257.
- [87] N. Craig, arXiv:1309.0528.
- [88] A. Djouadi, *Phys. Rept.* **459** (2008) 1 [hep-ph/0503173].
- [89] L. J. Hall, D. Pinner and J. T. Ruderman, *JHEP* **1204** (2012) 131 [arXiv:1112.2703].

- [90] R. Barbieri, L. J. Hall, Y. Nomura and V. S. Rychkov, Phys. Rev. D **75** (2007) 035007 [hep-ph/0607332].

A very brief Introduction to Heavy Ion Physics

*S. Floerchinger**

Institut für Theoretische Physik, Universität Heidelberg, Heidelberg, Germany

Abstract

Relativistic heavy ion collisions provide a possibility to investigate a fundamental quantum field theory (QCD) in a regime away from the conventional vacuum, namely at non-zero temperature and density. I will discuss why this is important, give a brief overview over what is known already and also mention currently still open questions.

Keywords

Lectures; ESHEP; Heavy ion collisions; Quark-gluon plasma.

1 Motivation and introduction

Why should one be interested in heavy ion collisions? There are several reasons. An experimentalist may argue: Heavy ion collisions at high energy provide a possibility to experimentally address questions like: What happens with Quantum Chromodynamics (QCD) at large density or temperature? Is there, for example, a phase transition at the Hagedorn temperature?

From a more theoretical point of view one may say: Quantum field theory is so important for the description of the phenomena in our world that it should be studied and understood not only in the regime of a few particles or excitations around the conventional vacuum but also at non-vanishing temperature and density. This is also important for many questions in cosmology and in condensed matter theory. Heavy ion collisions allow to study one of the fundamental building blocks of the standard model (namely QCD) at non-zero temperature and density. This is particularly interesting due to the asymptotic freedom property of QCD. For very large momenta or at very small distances, the theory is theoretically very well understood. Once the Lagrangian of QCD is fixed in terms of the fundamental parameters (the strong coupling constant α_s and the quark masses) everything else is in principle determined, as well, including the thermal equilibrium properties and even the non-equilibrium dynamics. It is a formidable challenge to understand this in detail and to solve the corresponding equations in practice.

From a cosmologists perspective one may argue that the quark gluon plasma is interesting because it has filled the universe from about 10^{-12} to 10^{-6} seconds after the big bang. Heavy ion collisions allow to learn something about this state of matter from laboratory experiments.

Finally, heavy ion physics is a very active field of research. A large experimental program is ongoing at the Large Hadron Collider (LHC) at CERN, Geneva, Switzerland, with experimental research being performed by the collaborations ALICE, ATLAS, CMS and LHCb. Another large program is ongoing at the Relativistic Heavy Ion Collider (RHIC) at Brookhaven National Laboratory (BNL) in Brookhaven, USA, with experimental collaborations Phenix and STAR. Future experiments are planned at the Facility for Antiproton and Ion Research (FAIR) in Darmstadt, Germany, and at the Nuclotron-based Ion Collider Facility (NICA) at JINR, Dubna, Russia.

We end this introductory section with a brief overview on the different regimes following a heavy ion collision event. The initial state directly after the collision is determined in principle by the wave function of the colliding nuclei. However, the latter is unfortunately not understood from first principles yet. (The problem is of considerable complexity already for protons.) Directly after the collision there must be a regime of strong dynamics driving an approximate thermalization (or at least

*Previous affiliation: CERN, Geneva, Switzerland

pre-thermalization sometimes also called “hydrodynamization” such that the energy-momentum tensor approaches the form of relativistic fluid dynamics). The concrete dynamics is not yet known in all details but it is very plausible that strong color fields play an important role as well as possibly different plasma instabilities.

Afterwards there is a phase with (approximate) local thermal and chemical equilibrium that can be described by relativistic fluid dynamics. The strong microscopic dynamics that leads to short equilibration times is now responsible for rather small dissipative transport coefficients (such as shear viscosity and corresponding relaxation times, see discussions below). The main characteristic of the fluid dynamic phase is a rapid expansion both in longitudinal and transverse direction and an associated dilution and cool down of the fluid.

Together with the dilution comes a change in the relevant microscopic degrees of freedom. While these are gluons and quarks at high temperatures, mesons and baryons dominate the low temperature and density phase. As long as the densities are still rather large, there are many inelastic (and elastic) collisions such that chemical and kinetic equilibrium are maintained. When the density drops, the rate of inelastic collisions decreases and at some point becomes too small to maintain chemical equilibrium. This process is called chemical freeze-out. After this point the total particle yields do not change substantially any more (except by some resonance decays that are ongoing). One can still use an (approximate) fluid dynamic description in the phase that follows, but now with a chemical potential for each (separately) conserved particle number.

Finally, when the densities drop even further, also elastic collisions become more and more rare such that also kinetic equilibrium is no longer maintained. After this point also the momenta of particles do not change substantially any more (again with the exception of resonance decays) and they are “free streaming” towards the detector. This process is described as kinetic freeze-out. More details about both chemical and kinetic freeze-out will be discussed below.

There are some very good reviews and monographs on heavy ion physics which are much more detailed than I can possibly be in these introductory lectures, for example refs. [1–6]. A very helpful source of information are also the collected proceedings of the “Quark Matter” conferences.

For these lecture notes I will mainly employ relativistic natural units with $c = \hbar = k_B = 1$.

2 Basic quantum chromodynamics

We now continue with a very basic reminder about the microscopic properties of QCD as a quantum field theory. The Lagrangian is

$$\mathcal{L} = -\frac{1}{2} \text{tr} \mathbf{F}_{\mu\nu} \mathbf{F}^{\mu\nu} - \sum_f \bar{\psi}_f (i\gamma^\mu \mathbf{D}_\mu - m_f) \psi_f \quad (1)$$

with matrix valued field strength tensor $\mathbf{F}_{\mu\nu} = \partial_\mu \mathbf{A}_\nu - \partial_\nu \mathbf{A}_\mu - ig[\mathbf{A}_\mu, \mathbf{A}_\nu]$ and covariant derivative $\mathbf{D}_\mu = \partial_\mu - ig\mathbf{A}_\mu$. In the high energy regime, where perturbation theory is valid, the particle content of the theory are $N_c^2 - 1 = 8$ real massless vector bosons, the gluons, and $N_c \times N_f$ massive Dirac fermions, the quarks. From the quark masses (Up 2.3 MeV, Down 4.8 MeV, Strange 95 MeV, Charm 1275 MeV, Bottom 4180 MeV and Top 173 GeV) one can see that for typical temperatures in the regime of a few 100 MeV mainly the Up, Down and Strange quarks play a role as thermalized particles while Charm and Bottom can be considered as heavy. Top quarks can be counted as very heavy.

An important feature of QCD is asymptotic freedom. The coupling constant $\alpha_s = g^2/(4\pi)$ has a renormalization group running such that the effective interaction strength is small for processes with large momentum transfer or at high energy scales. On the other side, the effective interaction strength becomes large for soft processes or at small energy scales. An illustration of this is given by Fig. 1.

From this one concludes generically that at high-temperatures QCD should have the properties of a weakly coupled field theory while it becomes effectively strongly coupled at small temperatures. This

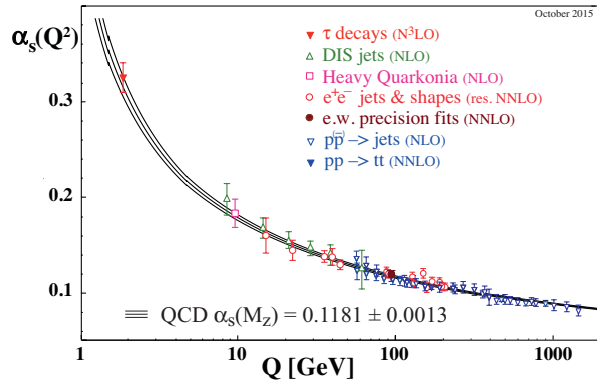


Fig. 1: Summary of measurements of α_s as a function of the energy scale Q as compiled by the Particle Data Group in 2015. Figure taken from ref. [7].

is so for a description in terms of the elementary degrees of freedom (quarks and gluons). In terms of the composite degrees of freedom that dominate at low temperatures (mesons and baryons) the situation is different and in particular the low temperature regime permits a description which resembles in many aspects a weakly coupled theory.

This brings us to the next important property of QCD: confinement. For low temperatures, quarks and gluons are confined to hadrons. In contrast, the large temperature behavior is dominated by deconfined quarks and gluons. Lattice QCD calculations have shown that the intermediate regime does not show a sharp (first or second order) phase transition but rather a continuous crossover.

3 Particle production in heavy ion collisions

When heavy ions are colliding at large center of mass energy, many particles are being produced. Consider for example the first heavy ion run at the LHC. The total collision energy for the Pb-Pb system is $\sqrt{s} = 2 \times 574$ TeV. The fully ionized nuclei ^{208}Pb consist of $82+126=208$ nucleons. This implies a collision energy per nucleon of $\sqrt{s_{\text{NN}}} = \frac{574}{208}$ TeV = 2.76 TeV.

Lower energy experiments performed at the Alternating Gradient Synchrotron (AGS) operating at BNL since the mid 1980's reached typical values $\sqrt{s_{\text{NN}}} \approx 2 - 5$ GeV. For the fixed target experiments at the Super Proton Synchrotron (SPS) at CERN since 1994 the energies are in the range $\sqrt{s_{\text{NN}}} < 17$ GeV. Finally the Relativistic Heavy Ion Collider (RHIC) in operation at BNL since 2000 reaches energies $\sqrt{s_{\text{NN}}} \leq 200$ GeV.

The number of charged particles found in the detector varies with the longitudinal angle with respect to the beam axis. Usually this angle is parametrized by the pseudo-rapidity $\eta = -\ln(\tan(\theta/2))$. Depending on the coverage of the detector one can access $dN_{\text{ch}}/d\eta$ in the range of a few units around mid-rapidity $\eta = 0$. Integration of this function (or an interpolation thereof) gives total number of charged particles N_{ch} . A typical number is $N_{\text{ch}} = 5060 \pm 250$ at upper RHIC energies. One should keep in mind that not all particles are charged and one can estimate the total number of hadrons as $1.6 \times 5060 \approx 8000$ hadrons in total. The number of produced particles grows with the collision energy and at the LHC one can estimate $N_{\text{ch}} = 25000$ corresponding to about 40000 hadrons in total.

Using modern detector technology one can also identify the produced particles and determine the yields or multiplicities for each species separately. Some results are shown in Fig. 2 together with fits based on the so-called statistical or thermal model. The thermal model describes the particle yields in terms of a non-interacting hadron resonance gas in thermal and chemical equilibrium. Essentially all hadrons and resonances listed by the particle data group are included. Fit parameters are the temperature T , volume V and chemical potentials for the conserved baryon number μ_b and similar for isospin,

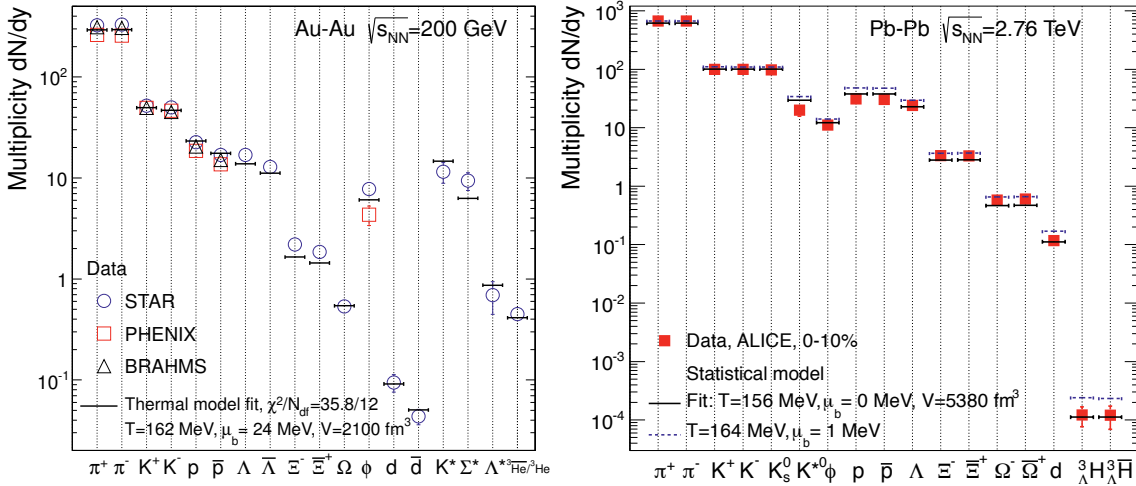


Fig. 2: Comparison of hadron yields as measured at RHIC (left panel) and by ALICE at the LHC (right panel) and fits using the thermal hadronization model. The first figure is taken from ref. [8], the second from ref. [9].

strangeness and charm.

The thermal model works so surprisingly well that a number of questions arise. First of all, why does it actually work so well? Why should all the particle yields be determined by one and the same temperature? One should keep in mind that hadronization is governed by non-perturbative QCD processes that are not completely understood yet. One interpretation is in terms of a sudden chemical freeze-out. The picture is based on a close-to-equilibrium expansion and cool-down of the fluid. Number changing processes are fast when the densities are high and keep up the chemical equilibrium. At lower temperatures these processes become too slow to keep up with the expansion and particle numbers get frozen in. The freeze-out process itself is not describable in a close-to-equilibrium picture but if it happens quickly enough, it is nevertheless possible that the particle yields are frozen in to their thermal values on the “surface of last inelastic scattering”. In order to explain the fact that a single temperature accounts for all particle yields, rates of inelastic collisions have to drop rather quickly. It has been argued that this is the case very close to the chiral crossover [10] and indeed, the chemical freeze-out temperatures as determined from the thermal model fits and the crossover temperatures as calculated by lattice QCD seem to be in reasonable agreement for the high energy experiments where the net baryon chemical potential is small. On the other side, this picture seems to be too simple for the experiments at lower energies corresponding to higher baryon number chemical potentials at freeze-out [11]. In Fig. 3 an overview over the chemical freeze-out points in the plane of temperature and baryon chemical potential is given for experiments at various energies together with lattice QCD results about the chiral crossover line.

4 Thermodynamics and fluid dynamics

We now turn to the thermodynamic and fluid dynamic description of the QCD matter that is produced by relativistic heavy ion collisions. As a warm-up let us recapitulate the Stefan-Boltzmann law for the pressure of a gas of N_B species of real, massless bosonic degrees of freedom and N_F real, massless fermionic degrees of freedom

$$p(T) = \frac{\pi^2}{90} \left(N_B + \frac{7}{8} N_F \right) T^4. \quad (2)$$

For QCD at high temperatures one has $N_c^2 - 1$ gluons in two helicity states where $N_c = 3$ is the number of colors, i. e. $N_B = 2 \times (N_c^2 - 1) = 16$. In addition, in the temperature regime of relevance, there are $N_f =$

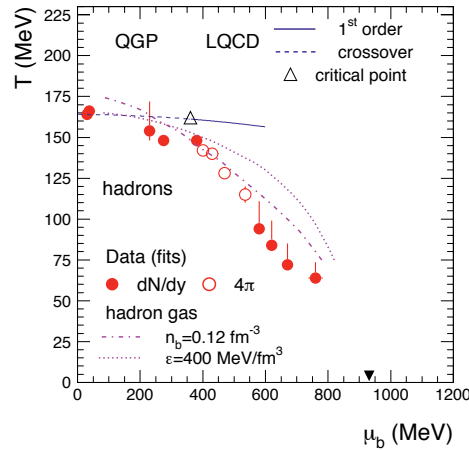


Fig. 3: Values for temperature T and baryon chemical potential μ_b as obtained from thermal fits. The Lattice QCD results are from ref. [12]. The full triangle indicates the location of first order phase transition of normal nuclear matter. The figure is taken from ref. [13].

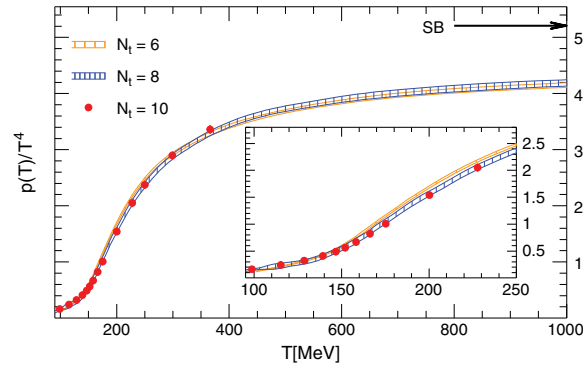


Fig. 4: The “thermodynamic equation of state” or pressure $p(T)$ (divided by T^4) as a function of temperature T as calculated from Lattice QCD. Figure taken from ref. [14].

3 quark flavors that are effectively massless with $N_c = 3$ colors and 2 helicity states. Moreover, quarks are complex fermions corresponding to 2 real degrees of freedom. That gives $N_F = 4 \times N_c \times N_f = 30$.

Corrections to the pressure in eq. (2) arise from the non-vanishing quark masses as well as from interactions. For small temperatures there are fewer effective degrees of freedom. For example, for $M_\pi < T < M_\rho$ one has approximately $N_B = 3$ massless pions and no massless fermions, $N_F = 0$. More general, at low temperature, $p(T)$ can be calculated approximately from a hadron resonance gas. For the transition region between large and small temperatures one needs a non-perturbative calculation of $p(T)$ as it is given by lattice QCD. Fig. 4 shows the result of a lattice QCD simulation at vanishing chemical potentials, which is the regime most relevant for heavy ion collisions at high energies. By the formula of thermodynamics, other quantities such as energy density $\epsilon(T)$, entropy density $s(T)$ and so on can be calculated from the pressure $p(T)$ in terms of the appropriate derivatives and Legendre transforms.

Let us now come to fluid dynamics. Quite generally, if one considers large enough time and length scales and if the interaction effects that drive local thermalization are strong enough, quantum fields form a fluid. A fluid dynamic description is always an approximation which does not describe all particles or degrees of freedom individually, but it is an approximate description that works rather well for many

aspects of heavy ion physics. Fluid dynamics is a rather general framework that allows to describe many different physical phenomena within a common setup and with similar equations. This ranges from conventional liquids such as water to superfluid helium, strongly interacting cold atomic gases, the quark gluon plasma or the cosmological fluid.

However, fluid dynamics it is not a closed theory. It needs input from calculations at a more microscopic level (or corresponding measurements) in terms of some macroscopic material properties. These are first of all the thermodynamic equation of state, i. e. information such as the function $p(T)$ from which one can derive also other thermodynamic quantities. In addition one needs information about transport properties such as the shear viscosity $\eta(T)$, the bulk viscosity $\zeta(T)$, heat conductivity $\kappa(T)$ and at least if one is interested in finer details, one also needs corresponding relaxation times $\tau_{\text{shear}}(T)$, $\tau_{\text{bulk}}(T)$ and other related quantities.

As a theoretical framework, fluid dynamics is organized as an expansion in derivatives. The lowest order is ideal fluid dynamics which we discuss first. The starting point is the energy-momentum tensor of a fluid in *global* thermal equilibrium,

$$T^{\mu\nu} = \epsilon u^\mu u^\nu + p (g^{\mu\nu} + u^\mu u^\nu) \quad (3)$$

with (inverse) metric $g^{\mu\nu}$ and fluid velocity u^μ . In Minkowski space and in cartesian coordinates, the metric is a diagonal matrix with entries $-1, +1, +1, +1$ in our conventions. The fluid velocity is $u^\mu = (1, 0, 0, 0)$ in the reference frame where the fluid is at rest but deviates from this in other frames. It is normalized by $g_{\mu\nu} u^\mu u^\nu = -1$. The pressure p is related to the energy density ϵ by a thermodynamic equation of state, $p = p(\epsilon)$.

Now let us go from *global* thermal equilibrium to *local* equilibrium. The ideal fluid approximation assumes that $T^{\mu\nu}$ is of the form in (3) but now with space and time dependent energy density $\epsilon = \epsilon(x)$ and fluid velocity $u^\mu = u^\mu(x)$. From the conservation law $\nabla_\mu T^{\mu\nu} = 0$ one can obtain evolution equations for $\epsilon(x)$ and $u^\mu(x)$ in ideal fluid dynamics,

$$\begin{aligned} u^\mu \partial_\mu \epsilon + (\epsilon + p) \nabla_\mu u^\mu &= 0, \\ (\epsilon + p) u^\mu \nabla_\mu u^\nu + (g^{\nu\mu} + u^\nu u^\mu) \partial_\mu p &= 0. \end{aligned} \quad (4)$$

In these equations, no dissipative effects and in particular no viscosities have been taken into account. This is remedied at the next level of the derivative expansion.

One can decompose a general symmetric energy-momentum tensor as

$$T^{\mu\nu} = \epsilon u^\mu u^\nu + (p + \pi_{\text{bulk}}) \Delta^{\mu\nu} + \pi^{\mu\nu} \quad (5)$$

where the shear stress $\pi^{\mu\nu}$ is symmetric, transverse to the fluid velocity, $u_\mu \pi^{\mu\nu} = 0$, and traceless, $\pi^\mu{}_\mu = 0$. The bulk viscous pressure π_{bulk} and shear stress $\pi^{\mu\nu}$ parametrize deviations from ideal fluid dynamics. To first order in derivatives of the fluid velocity one has

$$\begin{aligned} \pi_{\text{bulk}} &= -\zeta \nabla_\mu u^\mu + \dots, \\ \pi^{\mu\nu} &= -2\eta \left(\frac{1}{2} \Delta^{\mu\alpha} \Delta^{\nu\beta} + \frac{1}{2} \Delta^{\mu\beta} \Delta^{\nu\alpha} - \frac{1}{3} \Delta^{\mu\nu} \Delta^{\alpha\beta} \right) \nabla_\alpha u_\beta + \dots, \end{aligned} \quad (6)$$

with bulk viscosity $\zeta = \zeta(\epsilon)$ and shear viscosity $\eta = \eta(\epsilon)$. At second order also the relaxation times $\tau_{\text{shear}}(\epsilon)$ and $\tau_{\text{bulk}}(\epsilon)$ enter, as well as other terms.

Let us now discuss in a little more detail the equations of relativistic viscous fluid dynamics. The evolution equation for energy density becomes for the viscous theory

$$u^\mu \partial_\mu \epsilon + (\epsilon + p + \pi_{\text{bulk}}) \nabla_\mu u^\mu + \pi^{\mu\nu} \nabla_\mu u_\nu = 0. \quad (7)$$

The non-relativistic limit $\vec{v}^2 \ll c^2$ gives for the first order approximation

$$\partial_t \epsilon + \vec{v} \cdot \vec{\nabla} \epsilon + (\epsilon + p) \vec{\nabla} \cdot \vec{v} = \zeta \left(\vec{\nabla} \cdot \vec{v} \right)^2 + 2\eta \sigma_{ij} \sigma_{ij}, \quad (8)$$

with $\sigma_{ij} = \frac{1}{2}\partial_i v_j + \frac{1}{2}\partial_j v_i - \frac{1}{3}\delta_{ij}(\vec{\nabla} \cdot \vec{v})$. The left hand side of this equation describes the change in the fluid's internal energy ϵ by thermodynamic work due to expansion or contraction of the fluid. The right hand side describes the dissipation of the fluid's macroscopic kinetic energy to thermal energy. Using the thermodynamic relations $\epsilon + p = sT$ and $d\epsilon = Tds$ where s is the entropy density, leads to an equation for entropy production

$$\partial_t s + \vec{\nabla} \cdot (s\vec{v}) = \frac{\zeta}{T} (\vec{\nabla} \cdot \vec{v})^2 + \frac{2\eta}{T} \sigma_{ij} \sigma_{ij}. \quad (9)$$

A local form of the second law of thermodynamics says that the entropy can never decrease. Accordingly, the right hand side of eq. (9) must be positive semi-definite. This implies in particular $\zeta \geq 0$ and $\eta \geq 0$.

The evolution equation for the fluid velocity becomes for the viscous theory

$$(\epsilon + p + \pi_{\text{bulk}}) u^\mu \nabla_\mu u^\nu + \Delta^{\nu\mu} \partial_\mu (p + \pi_{\text{bulk}}) + \Delta^\nu{}_\alpha \nabla_\mu \pi^{\mu\alpha} = 0. \quad (10)$$

The non-relativistic limit of this equation gives for the first order approximation the non-relativistic Navier-Stokes equation (ρ is the mass density which is well defined for a non-relativistic fluid)

$$\rho \left[\partial_t v_j + \vec{v} \cdot \vec{\nabla} v_j \right] + \partial_j p = \partial_j (\zeta \vec{\nabla} \cdot \vec{v}) + \partial_m (2\eta \sigma_{jm}). \quad (11)$$

In this equation, the second term on the left hand side describes acceleration by pressure gradients. The terms on right hand side describe damping by viscosity. More general than the first order approximation, the equations for ϵ and u^μ which follow from the conservation law $\nabla_\mu T^{\mu\nu} = 0$, get closed by relations for π_{bulk} and $\pi^{\mu\nu}$, the so called constitutive relations.

Let us now discuss the transport properties that enter fluid dynamics. For a fluid without any conserved charges besides energy and momentum, such as the quark gluon plasma at negligible net baryon number density, the most relevant transport properties are shear and bulk viscosity. The physical mechanism underlying viscosity is the microscopic transport of momentum. Typically, the momentum is transported out of a local fluid cell by diffusive processes which involve particles, radiation or more general quasi-particles. The strength of shear viscosity can be quantified in terms of the ratio η/s . In order for this ratio to become large, momentum must be transported efficiently over distances $s^{-1/3}$ by well defined quasiparticles. On the other side, theories with small η/s have no well defined quasiparticles.

In general, transport properties like shear viscosity, bulk viscosity, heat conductivity, relaxation times, etc. are difficult to determine from quantum field theory. Lattice QCD calculations in Euclidean space cannot determine them directly and the analytic continuation from Euclidean to Minkowski space is numerically very difficult. Concrete expressions can be obtained for very weakly interacting theories from perturbation theory (or from a mapping to kinetic theory) or for strongly interacting theories with gravity dual via the AdS/CFT correspondence. For theories that are neither very weakly nor very strongly interacting, the determination of transport properties is essentially an open problem.

An example, where the viscosities are known, is a dilute simple non-relativistic gas with elastic two-to-two collisions. Here one can obtain from kinetic theory

$$\eta = \tau_f n T, \quad (12)$$

with particle density n , temperature T , and mean free time

$$\tau_f = \frac{1}{\sigma_{\text{tot}} \bar{v} n}. \quad (13)$$

In the last equation, σ_{tot} is the total elastic cross section and \bar{v} the mean square velocity of the particles with respect to the fluid velocity. Using $T = \frac{1}{3} m \bar{v}^2$ gives

$$\eta = \frac{m \bar{v}}{3 \sigma_{\text{tot}}}. \quad (14)$$

Interestingly, the shear viscosity becomes large for small cross-section! The bulk viscosity vanishes for the simple non-relativistic gas, $\zeta = 0$.

For QCD, the transport properties can be determined at very high temperature where QCD becomes weakly coupled, $g \ll 1$. The shear viscosity at leading logarithmic accuracy is [15]

$$\eta(T) = k(N_f) \frac{T^3}{g^4 \ln(1/g)}. \quad (15)$$

The bulk viscosity is related to this via the velocity of sound c_s [16]

$$\zeta(T) \approx 15\eta(T) \left(\frac{1}{3} - c_s^2(T) \right)^2. \quad (16)$$

For very high temperature $c_s^2 \rightarrow 1/3$ and $\zeta \rightarrow 0$.

One can also determine the transport properties for a class of strongly interacting field theories which have a gravitational dual in the sense of the AdS/CFT correspondence. It was found that for conformal theories with gravitational dual one has $\eta(T) = s(T)/(4\pi)$ [17]. This was later conjectured to be a universal lower bound for any fluid [18],

$$\frac{\eta}{s} \geq \frac{\hbar}{4\pi k_B}. \quad (17)$$

(We have restored units \hbar and k_B to make the quantum nature of this conjectured bound apparent.) Meanwhile, theoretical counterexamples have been found but experimentally, no system seems to violate the bound so far.

For some theories with deviations from conformal symmetry it was found that the bulk viscosity is related to the shear viscosity by $\zeta(T) = 2\eta(T) \left(\frac{1}{3} - c_s^2(T) \right)$ [19] but this does not seem to be a universal relation.

Ultimately, one would like to gain a theoretical understanding of the shear and bulk viscosity (and related relaxation times) of QCD for the whole range of temperatures. It is possible to write down formal expressions (so called Kubo relations) which express the transport coefficients in terms of correlation functions that can in principle be determined in terms of functional integral expressions. However, it is in practice rather difficult to solve the corresponding equations. Nevertheless, some theoretical attempts in this direction are currently ongoing, using for example the analytic continuation of lattice QCD results [20, 21] or functional renormalization group calculations [22, 23].

5 Fluid dynamics of the fireball for more and more realistic initial conditions

In this section we will discuss the actual solution of relativistic viscous fluid dynamics for the fireball created by two colliding heavy ions. It is obvious that these solutions depend on the initial conditions as they are specified at some early time where the fluid dynamic description is initialized. It would be great to know these initial conditions in detail, for example from first principle calculations in QCD. This is however a very difficult problem by itself. So for the time being, the detailed initial conditions are not known but some of their properties are.

Generically, solutions of partial differential equations as the ones of fluid dynamics are easier to find when the initial conditions are more symmetric. We will therefore start our discussion with particularly symmetric and therefore simple situations although they are not fully realistic. We will then increase the complexity step by step and thereby become more and more realistic.

We start by considering the fluid velocity in the longitudinal direction z , i. e. in the direction parallel to the beam axis. What should be the fluid velocity in that direction as a function of time and space coordinates? It was first argued by Bjorken that a good guess should be $v_z = z/t$ where

the longitudinal position z and the time t are defined such that the actual collision took place at the coordinate origin, i. e. at $z = t = 0$. Note that due to the high energy, the ions are strongly Lorentz contracted in the longitudinal direction such that to good approximation one can speak of a collision at a single instance in time and longitudinal space direction, indeed. In a coordinate system consisting of the longitudinal proper time $\tau = \sqrt{t^2 - z^2}$, the transverse coordinates x, y , and rapidity $\eta = \text{arctanh}(z/t)$, the fluid velocity is of the form $u^\mu = (u^\tau, u^x, u^y, 0)$, i. e. the fluid velocity in the rapidity direction vanishes. If scalar functions like energy density depend on t and z only in terms of the proper time, $\epsilon = \epsilon(\tau, x, y)$ an invariance under boosts in the longitudinal direction $\eta \rightarrow \eta + \Delta\eta$ arises (so called Bjorken boost invariance). The remaining initial value problem to be solved is then effectively only 2+1 dimensional. This is a substantial simplification. Bjorken boost symmetry is an idealization but it is reasonably accurate close to mid-rapidity $\eta \approx 0$.

Based on the above considerations one can construct a toy model that can almost be solved analytically. Consider initial conditions at $\tau = \tau_0$ of the form $\epsilon = \epsilon(\tau_0)$, $u^\mu = (1, 0, 0, 0)$. This describes an initial energy density that is extended over the whole transverse plane. Although this is of course not realistic for the whole fireball it constitutes a simplified model for inner region at early times after a central collision. In addition to Bjorken boost invariance $\eta \rightarrow \eta + \Delta\eta$, the initial conditions are now also symmetric with respect to translations and rotations in the transverse plane. Together, these symmetries imply that $u^\mu = (1, 0, 0, 0)$ for all times τ and that $\epsilon = \epsilon(\tau)$ is independent of x, y and η . It remains to solve a single, 0+1 dimensional differential equation to determine $\epsilon(\tau)$. In the first order formalism of viscous relativistic fluid dynamics, this equation reads

$$\partial_\tau \epsilon + (\epsilon + p) \frac{1}{\tau} - \left(\frac{4}{3}\eta + \zeta\right) \frac{1}{\tau^2} = 0. \quad (18)$$

The solution depends on the thermodynamic equation of state $p(\epsilon)$ and the viscosities $\eta(\epsilon)$ and $\zeta(\epsilon)$.

For example, assuming $p \sim \epsilon \sim T^4$ leads to

$$\partial_\tau T + \frac{T}{3\tau} \left(1 - \frac{4\eta/3 + \zeta}{sT\tau}\right) = 0. \quad (19)$$

The solution for $\eta/s = \text{const}$ and $\zeta = 0$ is

$$T(\tau) = T(\tau_0) \left(\frac{\tau_0}{\tau}\right)^{1/3} \left[1 + \frac{2}{3\tau_0 T(\tau_0)} \frac{\eta}{s} \left(1 - \left(\frac{\tau_0}{\tau}\right)^{2/3}\right)\right]. \quad (20)$$

For an ideal fluid where $\eta/s = 0$, or more general at late times, the temperature simply decays like $T \sim \tau^{-1/3}$. This is due to the dilution of the fluid by the longitudinal expansion. For $\eta/s > 0$ and at early times there is in addition a small heating effect due to shear viscosity. Fig. 5 illustrates the solution in eq. (20) for different values of η/s .

Let us now increase the level of complexity by one step and study an initial energy density with somewhat more realistic dependence on the transverse coordinates. For an azimuthally symmetric, central collision event, the energy density is of the form $\epsilon = \epsilon(\tau, r)$ where $r = \sqrt{x^2 + y^2}$. Connected with the initial energy distribution is a pressure gradient in radial direction which leads after a short time to a positive fluid velocity in radial direction, $u^r > 0$, the so-called radial flow. To determine $\epsilon(\tau, r)$ or $T(\tau, r)$ and the fluid velocity $u^r(\tau, r)$ one needs to solve a system of 1+1 dimensional, coupled differential equations, which is still rather easy to do numerically. A solution for $T(\tau, r)$ obtained for a realistic initial temperature profile, as well as equation of state and viscosities, is shown in Fig. 6. The effects of the longitudinal as well as radial expansion are clearly visible.

Before we continue our endeavor of solving viscous relativistic fluid dynamics for more and more realistic initial conditions, let us pause for a moment and consider the process of kinetic freeze-out.

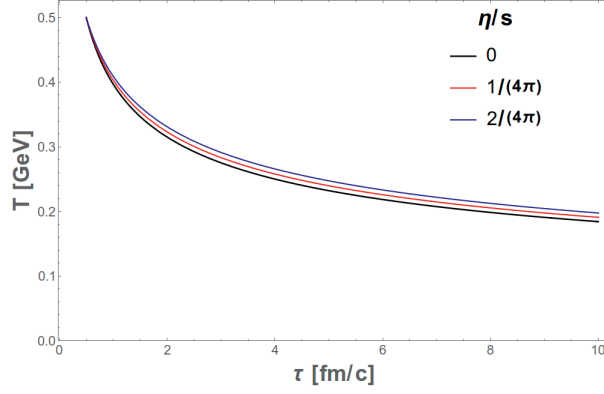


Fig. 5: Bjorken flow solution for temperature T as a function of proper time τ for different values of the ratio of shear viscosity to entropy density η/s . Figure taken from ref. [24].

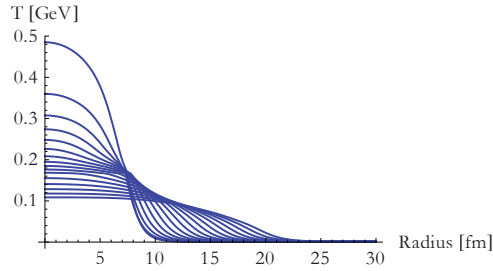


Fig. 6: Temperature profile $T(\tau, r)$ as a function of radius r for different times τ . The equation of state, shear viscosity and initial values are chosen as described in ref. [25].

Although we can in principle follow the dynamics of the expansion and the associated dilution and cool-down of the fluid as described by fluid dynamics down to very small temperatures, there is in reality a point where the fluid dynamic description breaks down. Indeed, after the transition from quarks and gluons to hadronic degrees of freedom and when the temperature and densities drop further, collisions become less and less frequent. At some point, hadrons stop interacting and occupation numbers in momentum space do not change any more. This is the process of kinetic freeze-out.

Just before the freeze-out one might assume local close-to-equilibrium occupation numbers of hadrons in each fluid element

$$\frac{dN_i}{d^3p d^3x} = f_i(p^\mu; T(x), u^\mu(x), \pi^{\mu\nu}(x), \pi_{\text{bulk}}(x)). \quad (21)$$

The occupation numbers for each particle species as a function of the thermodynamic variables, the fluid velocity and the dissipative shear stress and bulk viscous pressure can in principle be determined from microscopic calculations. For example, neglecting the effect of $\pi^{\mu\nu}$ and π_{bulk} and assuming an ideal gas with Boltzmann statistics gives

$$f_i = c_i e^{\frac{u_\mu(x)p^\mu}{T(x)}} \rightarrow c_i e^{-\frac{E_{\vec{p}} - \vec{v}(x) \cdot \vec{p}}{T(x)}} \quad (\vec{v}^2 \ll c^2). \quad (22)$$

In the last expression we have taken the non-relativistic limit for illustration. The factor c_i accounts for the degeneracy due to spin. Summing up the contribution of all fluid cells in terms of an integral over the three-dimensional freeze-out hyper-surface (or hyper-surface of last scattering) Σ_f yields particle spectra in momentum space as they can actually be measured in the particle detector [26],

$$E \frac{dN_i}{d^3p} = -\frac{1}{(2\pi)^3} p^\mu \int_{\Sigma_f} d\Sigma_\mu f_i. \quad (23)$$

The freeze-out surface is in principle determined by the dynamics of expansion and the scattering processes. In practice it is often assumed for simplicity that it corresponds to a surface of constant temperature T_{fo} in the region around 100 MeV.

The particle spectra $E \frac{dN_i}{d^3p}$ are usually written in terms of the momentum rapidity $y = \text{arctanh}(p^z/E)$, the transverse momentum p_T and the momentum azimuthal angle ϕ as $dN_i/(dyd\phi p_T dp_T)$. They inherit some symmetry properties from the fluid dynamic fields. For example, when the fluid dynamic fields are independent of position-space rapidity η , the spectrum is independent of momentum space rapidity y . Similarly, the spectrum originating from an azimuthally symmetric solution of fluid dynamics is independent of the momentum-space azimuthal angle ϕ .

In order to reliably calculate the particle spectrum $dN_i/(dyd\phi p_T dp_T)$ one has to solve the relativistic fluid dynamic equations. There is, however, also a shortcut that is often used to study some aspects of the resulting particle spectrum, the so-called blast-wave models. For these, the particle spectra are not determined from realistic solutions of fluid dynamics but rather for a simplified ansatz and a simple parametrization of the kinetic freeze-out surface. For example, one might assume for simplicity that freeze-out takes place at constant time τ_f and in a transverse area with radius $r < r_{\max}$. If one also assumes constant temperature T and radial flow velocity v_r , as well as the Boltzmann occupation numbers as in equation (22), one can solve the integrals in eq. (23) and one obtains the analytic expression

$$\frac{dN_i}{dyd^2p_T} = \frac{c_i}{4\pi^2} \tau_f r_{\max}^2 \sqrt{p_T^2 + m_i^2} K_1 \left(\frac{\sqrt{p_T^2 + m_i^2}}{T\sqrt{1-v_r^2}} \right) I_0 \left(\frac{p_T v_r}{T\sqrt{1-v_r^2}} \right), \quad (24)$$

where $K_1(\cdot)$ and $I_0(\cdot)$ are Bessel functions. Many variants of such simple blast-wave models have been studied. They capture some qualitative features of full fluid dynamics solutions. Generically, particle spectra following from integrals over thermal occupation numbers are close to exponential shape. The radial flow velocity, so-called radial flow, leads to a ‘‘blue shift’’ of the particle spectrum. Another generic observation is that particle spectra become steeper for smaller particle mass m_i .

An experimental result for the spectrum of charged particle as a function of p_T is shown in Fig. 7. For the 0-5% most central collisions and small p_T , the spectrum has an almost exponential form indeed, with the slope determined by freeze-out temperature and radial flow velocity. In contrast, for peripheral collisions, the spectrum measured in heavy ion collisions is of a form similar to the proton-proton reference.

Let us now come to non-central collisions. The overlap region of two nuclei, illustrated in Fig. 8, is approximately ‘‘almond shaped’’. Correspondingly, the initial energy density at the point where a fluid dynamic description becomes valid, has this shape, as well. The pressure gradients are larger in the reaction plane which leads after some time of fluid dynamic evolution to a larger fluid velocity in this direction. The freeze-out formula in eq. (23) implies then that more particles fly in this direction after freeze-out than in the transverse direction orthogonal to this. This asymmetry is quantified in terms of the elliptic flow coefficient v_2 .

Quite general, an azimuthal particle distribution can be expanded like

$$\frac{dN}{d\phi} = \frac{N}{2\pi} \left[1 + 2 \sum_m v_m \cos(m(\phi - \psi_m)) \right] \quad (25)$$

where the coefficients v_m are called harmonic flow coefficients and the ψ_m are corresponding angles (obviously the ψ_m are defined modulo $2\pi/m$). If the particle asymmetry originates solely from the orientation of the reaction plane, the angles should all be the same, $\psi_m = \psi_R$ (up to terms π/m which determine the sign of v_m). Moreover, the symmetry with respect to $\phi \rightarrow \phi + \pi$ of the configuration in Fig. 8 would imply $v_1 = v_3 = v_5 = \dots = 0$.

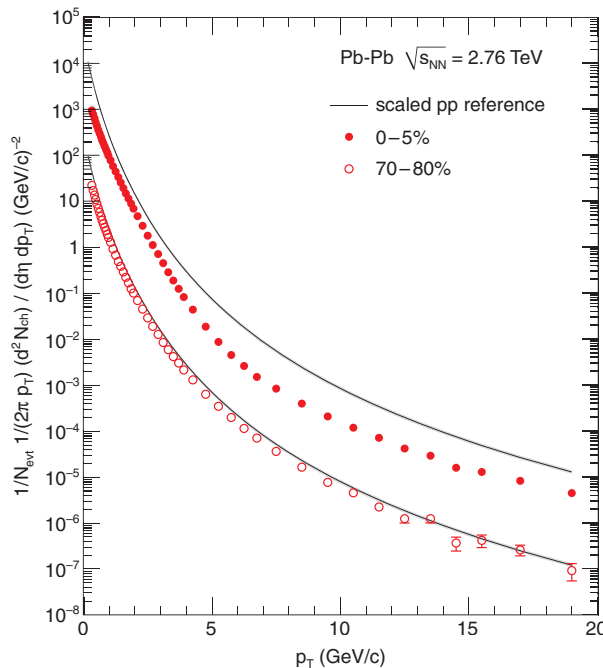


Fig. 7: Charged particle spectrum as a function of the transverse momentum in central (0 - 5%) and peripheral (70 - 80%) heavy ion collisions as measured by the ALICE collaboration. Figure taken from ref. [27].

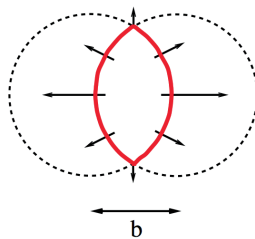


Fig. 8: Illustration of a non-central heavy ion collision. The dashed lines mark the density of the two colliding nuclei in the transverse plane, the red line marks the overlap region. The arrows illustrate the elliptic flow which results from the initial pressure gradients. Figure taken from ref. [2].

At this point, some remarks on experimental techniques are in order. The impact parameter of a heavy ion collisions is of course random. It can neither be adjusted nor be measured precisely. There is, however, a statistical method to say something about impact parameters. The underlying principle is that very central collisions produce more charged particles, in contrast to more peripheral collisions. One can order the full set of events recorded during some measurement campaign according to the multiplicity and divide them into classes - so called centrality classes. An histogram-type diagram with the corresponding centrality classes is shown in Fig. 9. Using further elements of modeling - for example based on the so-called Glauber model - one can associate impact parameters, or ranges of impact parameters, to these centrality classes with the highest multiplicity class corresponding to the smallest impact parameters. The harmonic flow coefficients v_m can also be measured as a function of transverse momentum p_T . An example for elliptic flow is shown in Fig. 10 for different centrality classes in a comparison between early results from the LHC and similar measurements at RHIC.

A very interesting observable is also a two-particle correlation function defined by a ratio of the expectation value of particle distributions at two angles ϕ_1 and ϕ_2 by two separate expectation values of

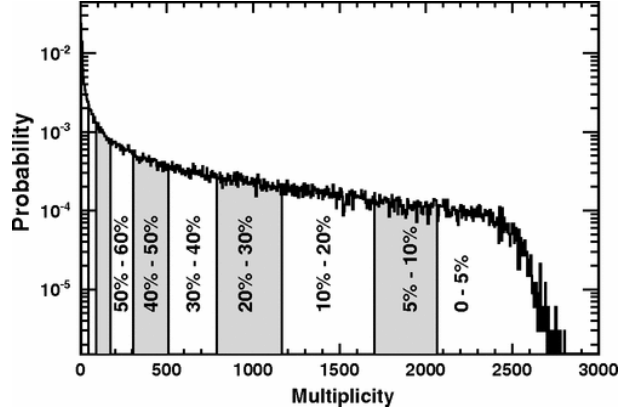


Fig. 9: Centrality classes as determined via the multiplicity in the Time Projection Chamber (TPC) by the ALICE collaboration. Figure taken from ref. [28].

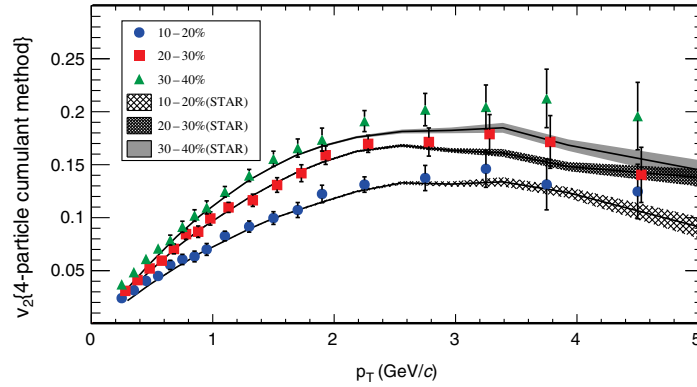


Fig. 10: Elliptic flow v_2 as a function of transverse momentum for different centrality classes as measured by the ALICE collaboration at the LHC (symbols) and by the STAR collaboration at RHIC (shaded regions). Figure taken from ref. [28].

this type,

$$C(\phi_1, \phi_2) = \frac{\langle \frac{dN}{d\phi_1} \frac{dN}{d\phi_2} \rangle_{\text{events}}}{\langle \frac{dN}{d\phi_1} \rangle_{\text{events}} \langle \frac{dN}{d\phi_2} \rangle_{\text{events}}} = 1 + 2 \sum_m v_m^2 \cos(m(\phi_1 - \phi_2)). \quad (26)$$

A priori, this depends on the two angles ϕ_1 and ϕ_2 but due to the statistical azimuthal rotation symmetry it is a function of the difference $\phi_1 - \phi_2$, only. Experimentally, the correlation function is typically measured with a rapidity gap $\Delta\eta$ imposed between the two particles whose correlation in azimuthal angle is studied. The last equation in (26) is the prediction for this correlation function in a fluid dynamic model. It shows that one can obtain the squares of the harmonic flow coefficients v_m^2 by performing a Fourier decomposition of the correlation function $C(\phi_1 - \phi_2)$. Now, surprisingly, if one does the corresponding analysis for a set of events with very high multiplicity corresponding to the centrality class with the lowest impact parameters as shown in Fig. 11, one finds that the flow coefficients v_2 , v_3 , v_4 , v_5 and v_6 are actually all non-zero! At the same time, the full correlation function is actually very nicely represented by the superposition of these harmonic modes.

This result is surprising for two reasons. First, the symmetry with respect to $\phi \rightarrow \phi + \pi$ discussed below eq. (25) would imply that the odd flow coefficients v_3 , v_5 etc. should vanish. Moreover, for very central collisions, the elliptic flow coefficient v_2 as well as higher order even coefficients v_4 , v_6 etc. should actually vanish, as well, if they simply measure the effect of a non-vanishing impact parameter. The fact that this is not the case shows that additional effects not discussed so far must play a role here.

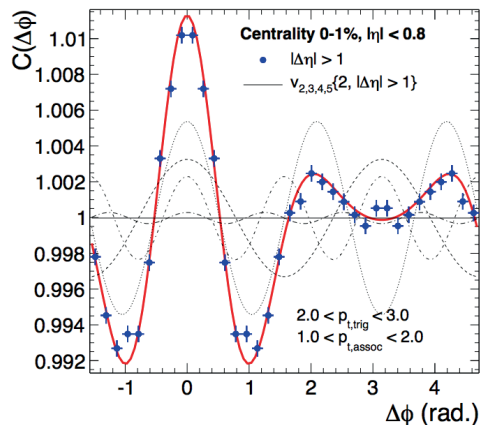


Fig. 11: Two-particle azimuthal correlation for the 0-1% centrality class as measured by the ALICE collaboration. The solid red line shows the sum of the contributions from anisotropic flow coefficients v_2 , v_3 , v_4 and v_5 (dashed lines). Figure taken from ref. [30].

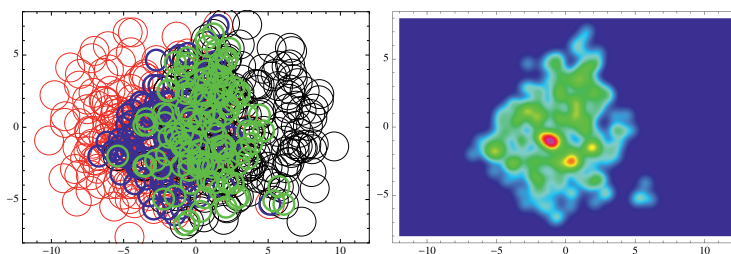


Fig. 12: Transverse energy density from a Monte-Carlo Glauber model. See text for further explanations. Figure taken from ref. [31].

In fact, what we have not discussed so far, are event-by-event fluctuations in the initial energy density distribution. We have based our arguments, for example for $v_3 = v_5 = 0$, on smooth and symmetric energy densities corresponding to expectation values. For a single event, the energy densities can deviate from this simple picture, however. This is actually predicted by realistic models of the initial state. Consider for example the Glauber model. The nuclei are here modeled as a combination of nucleons which have a statistical distribution in the form of a Woods-Saxon profile. A heavy ion collision is modeled by a superposition of individual collisions between nucleons. We will not discuss the details of this model here but illustrate the resulting energy density in Fig. 12. On the left hand side, the transverse positions of the nucleons in the two nuclei are marked by the red and black rings. The size corresponds to the nuclear cross section. Those nucleons that overlap with nucleons from the other nucleus are marked in addition by blue and green rings. The right hand side of fig. 12 shows the energy density that results if one associates a certain Gaussian-shaped contribution to each individual nucleon-nucleon collision.

Because of the fluctuations in the initial energy density, sizable flow coefficients v_m can be generated by the fluid dynamic expansion, even for central collisions. Beyond the energy density, also the other fluid dynamic fields such as fluid velocity, shear stress, bulk viscous pressure or baryon number density may actually have fluctuating initial configurations. It is currently an interesting direction of research to understand this better, both from analyzing experimental data and from theoretical investigations.

At this point, a few remarks on theoretical simulations of heavy ion collisions based on relativistic fluid dynamics might be in order. Specialized numerical codes have been developed for this purpose and typically they solve a variant of second order relativistic fluid dynamics for given initial conditions

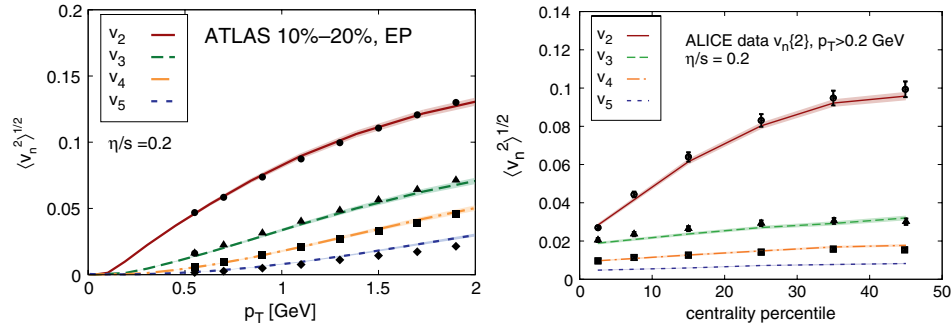


Fig. 13: Root-mean-square anisotropic flow coefficients $\langle v_n^2 \rangle^{1/2}$ as a function of transverse momentum (left panel) and centrality (right panel) as calculated by numerical fluid dynamic simulations [32], compared to experimental data by the ATLAS [29] and ALICE collaborations [30]. Figures taken from ref. [32].

and also include a description of the kinetic freeze-out and in some cases a subsequent phase of hadron resonance decays and further scatterings described by kinetic theory. The codes use the thermodynamic equation of state as calculated from lattice QCD and initial conditions which fluctuate from event-to-event and are calculated from the Monte-Carlo Glauber or related models. The transport properties such as η/s are usually varied with the goal of determining the experimentally favored value. A result of such a comparison is shown exemplarily in Fig. 13. Typical values for η/s that are favored by such comparisons between theory and experiment are in the range of a few times $1/(4\pi) \approx 0.08$. This suggests that the fluid dynamics in the relevant phase might be dominated by strongly coupled degrees of freedom. More realistically, η/s should not be constant but vary with temperature T and it will be one of the challenges for the coming years to see how one can constrain this dependence from the experimental data.

6 Initial state fluctuations and their fluid dynamic propagation

Because fluctuations in fluid dynamic fields have played such an interesting role in heavy ion phenomenology in the recent years, and will probably continue to do so in the coming years, we will discuss them here in a little more detail.

Interesting are in particular initial fluid perturbations which are event-by-event fluctuations around a background or average of fluid fields at the (proper) time τ_0 where the fluid dynamic description is initialized. Examples for fluid dynamic fields are the energy density ϵ , the fluid velocity w^μ , the shear stress $\pi^{\mu\nu}$ or the bulk viscous pressure π_{bulk} . Although they can usually be neglected, there are questions for which also other variables like the baryon number density n_B , the electric charge density, electromagnetic fields or others have to be taken into account. Fluctuations in fluid fields are particularly interesting because they are governed by universal evolution equations and because they can be used to constrain the thermodynamic and transport properties of a QCD fluid. Moreover, they contain interesting information from early times and can be taken as a measure for deviations from complete thermal equilibrium.

In some respects, the situation is similar as for the cosmic microwave background and the large scale structure which are studied in cosmology. Also there, the fluctuation spectrum contains very interesting information from early times and from the history of the dynamical expansion. Much can be learned because many numbers can be measured and compared to theory. This in turn has led cosmologists to a detailed understanding of the evolution history and the properties of our universe. A similar development may eventually trigger something like a precision era in heavy ion physics.

What would one have to do to understand initial fluid fluctuations in detail? Here is a program: First, one would have to characterize initial state fluctuations in a suitable and ideally complete way. Second, these fluctuations or perturbations need to be propagated through the fluid dynamic regime. Third, one has to determine their influence on particle spectra and harmonic flow coefficients. Finally,

one should take also perturbations from non-hydro sources, as for example jets, into account.

One possibility to implement the above program is in terms of numerical simulations, or more specific, event-by-event viscous relativistic hydrodynamic simulations (see e.g. ref. [33] for a recent overview). However, one can also make progress by (semi) analytic methods which are closer to the theoretical methods used to in cosmology. This shows the parallels between the big bang and the little bangs in the laboratory in more detail.

The theoretical approach called “Mode-by-mode fluid dynamics” or “Fluid dynamic perturbation theory for heavy ions” works in analogy to the Cosmological perturbation theory [25]. For that, one first solves the fluid equations of motion for a smooth background corresponding essentially to an averaged initial condition and afterwards order-by-order in perturbations around that configuration. The convergence properties of this expansion have been investigated and seem favorable [34]. The background solution can be taken symmetric with respect to azimuthal rotations and Bjorken boosts in the longitudinal direction while the perturbations can break these (statistical) symmetries.

For mode-by-mode fluid dynamics, a characterization of initial conditions in terms of a Bessel-Fourier expansion is particularly favorable. To that end one writes a transverse density distribution, say for the enthalpy density $w = \epsilon + p$ in the following form [25, 35, 36],

$$w(r, \phi) = w_{\text{BG}}(r) + w_{\text{BG}}(r) \sum_{m,l} w_l^{(m)} e^{im\phi} J_m \left(z_l^{(m)} \rho(r) \right). \quad (27)$$

The function $w_{\text{BG}}(r)$ parametrizes the azimuthally symmetric background configuration. The argument of the Bessel functions J_m is given by the numbers $z_l^{(m)}$ which correspond to the l 'th zero crossing of the function $J_m(z)$, and the function $\rho(r)$ which maps the relevant range of transverse radii r to the interval $[0,1]$. A particularly useful choice is discussed in ref. [36].

The expansion coefficients $w_l^{(m)}$ are dimensionless and have a discrete azimuthal wavenumber m as well as a radial wavenumber l . Higher values of m and l correspond to finer spatial resolution. The coefficients $w_l^{(m)}$ can also be related to the so-called eccentricities, another popular way to characterize initial transverse density distributions. While the expansion in (27) can be used for scalar quantities such as enthalpy density, a similar expansion can be used for vectors (such as the fluid velocity) and tensors (such as the shear stress). Observe that when all the coefficients $w_l^{(m)}$ vanish, one is left with the background configuration, only. The configuration in (27) is independent of rapidity η but it is straight forward to extend the scheme in that direction.

Quite generically, one can now solve the fluid equations of motion by the following perturbative scheme. One writes the hydrodynamic fields $h = (w, u^\mu, \pi^{\mu\nu}, \pi_{\text{Bulk}}, \dots)$ at initial time τ_0 as $h = h_0 + \epsilon h_1$ with the background configuration h_0 and the fluctuation part ϵh_1 . We have introduced here a formal expansion parameter ϵ . At later times $\tau > \tau_0$ one can write the fluid fields as $h = h_0 + \epsilon h_1 + \epsilon^2 h_2 + \epsilon^3 h_3 + \dots$. Solving for the time evolution in this scheme implies to determine h_0 as the solution of full, non-linear fluid equations but in a particularly symmetric situation with azimuthal rotation and Bjorken boost invariance. The linear term h_1 is a solution of the linearized fluid equations where the linearization is done around the background configuration h_0 . This solution can be determined mode-by-mode, i. e. for each mode with one azimuthal wavenumber m and radial wavenumber l in the expansion (27). The quadratic term h_2 can be obtained from an iterative solution involving quadratic interactions between modes and so on.

In order to find the linear solution h_1 , it is advantageous to use again a Fourier expansion in the azimuthal direction and with respect to rapidity. In that way, one can effectively reduce the numerical problem from a 3+1 dimensional partial differential equation to a 1+1 dimensional one. The latter is rather easy to solve numerically. This reduction of the complexity helps also to find the quadratic and higher order terms.

The perturbative scheme can also be used at freeze-out. For that purpose one propagates both

the background and the perturbations until the freeze-out surface has been reached. In the perturbative scheme, the latter is determined by the background solution alone and can correspond for example to constant background temperature. (In general, there is no precise understanding of where the freeze-out surface is positioned exactly.) The freeze-out surface is then as symmetric as the background configuration. Also the particle spectrum due to the background inherits these symmetries. However, the corrections due to the perturbations are not symmetric. In contrast, at linear order, they inherit the transformation behavior of the initial modes. At quadratic and higher orders this is a little more involved but straight forward to determine directly or by simple group theoretic methods.

One can expand the resulting particle spectrum for a single event to linear order in initial state perturbations like [37]

$$\ln \left(\frac{dN^{\text{single event}}}{p_T dp_T d\phi dy} \right) = \underbrace{\ln S_0(p_T)}_{\text{from background}} + \underbrace{\sum_{m,l} w_l^{(m)} e^{im\phi} \theta_l^{(m)}(p_T)}_{\text{from fluctuations}} + \dots \quad (28)$$

Note that each mode comes with an angle, $w_l^{(m)} = |w_l^{(m)}| e^{-im\psi_l^{(m)}}$ and the contribution of each mode has different p_T -dependence, $\theta_l^{(m)}(p_T)$. At quadratic order, the expression in (28) is supplemented by a term of the form

$$\sum_{m_1, m_2, l_1, l_2} w_{l_1}^{(m_1)} w_{l_2}^{(m_2)} e^{i(m_1+m_2)\phi} \kappa_{l_1, l_2}^{(m_1, m_2)}(p_T). \quad (29)$$

The non-linearities parametrized by the function $\kappa_{l_1, l_2}^{(m_1, m_2)}(p_T)$ arise both from the non-linear terms in the fluid dynamic evolution and from non-linear terms at freeze-out.

One can also determine the harmonic flow coefficients defined in eq. (25) within this scheme. For a single event one has

$$\begin{aligned} V_m^* &= v_m e^{-im\psi_m} \\ &= \sum_l S_{(m)l} w_l^{(m)} + \sum_{\substack{m_1, m_2, \\ l_1, l_2}} S_{(m_1, m_2)l_1, l_2} w_{l_1}^{(m_1)} w_{l_2}^{(m_2)} \delta_{m, m_1+m_2} + \dots \end{aligned}$$

The function $S_{(m)l}$ is here the linear dynamic response function and $S_{(m_1, m_2)l_1, l_2}$ may be called a quadratic dynamic response function and so on. The symmetries of the problem imply a conservation of azimuthal wavenumber. The response functions can be determined and they depend on the thermodynamic and transport properties of the fluid formed by the quark gluon plasma, in particular viscosity. One of the challenges for the coming years will be to understand these dependencies in detail and to use the experimental knowledge about the response functions in order to constrain the thermodynamic and transport properties of QCD from experimental data.

7 Jet quenching

We will now leave the fluid dynamic considerations aside and concentrate for the remaining time on processes at higher energies. More specific, consider again the transverse momentum distribution of charged particles in Fig. 7. At small transverse momenta and for central collisions, the particle spectra are determined by the decay products of a thermalized medium. This is reflected in a close-to-exponential shape, which shows up as a straight line on the logarithmic scale of Fig. 7. In contrast, the physics of high energetic particles and partons is different: they are not thermalized but can nevertheless be influenced by the medium. More specific, they can loose energy and momentum to the medium when they fly through it.

To understand this in a little more detail, let us first recapitulate some elements of the description of high energetic processes in conventional hadron collisions (for example proton - proton or proton -

antiproton collisions). An important theoretical concept is the one of *factorization*. According to this principle, processes at high energy are governed by a convolution of

- Process-independent *parton distribution functions* which parametrize the probability to find partons with given momentum in the incident hadron.
- Process-dependent *hard scattering cross sections* which determine the probability that initial partons scatter to final state partons with given momenta.
- Process-independent *parton fragmentation functions* which describe the probability that final state partons fragments into a jet with certain hadron content.

A very detailed theoretical and experimental understanding of high energetic processes in hadron collisions using perturbative QCD has been gained over the years with the help of the factorization principle. This constitutes a solid foundation to measure changes occurring in heavy ion collisions. A very short summary of these changes is as follows. Nuclear parton distribution functions differ from proton parton distribution functions but may be measured by proton-nucleus collisions, electron-nucleus collisions etc. Hard scattering cross sections are not modified by the medium if the momentum transfer is high enough. The key modification in a heavy ion context compared to hadron collisions is: After production, high energetic partons must propagate through the hot and dense medium produced in heavy ion collisions. By interactions with the (soft) gluons and quarks in the medium, high energetic partons loose part of their energy and momentum. Because parton production rates are steeply falling with energy, energy loss leads to a reduction of the number of partons with large energy. This can be clearly seen in Fig. 7.

The energy loss of highly energetic partons in a heavy ion collision can also be seen on the level of reconstructed jets. One prominent observable in this context is the so-called dijet asymmetry which is defined as

$$A_J = \frac{p_{T,1} - p_{T,2}}{p_{T,1} + p_{T,2}} \quad (30)$$

where $p_{T,1}$ and $p_{T,2}$ are the transverse momenta of a leading and a sub-leading jet, respectively. Event distributions of this observable are shown in Fig. 14 for different centrality classes, as measured by the CMS collaboration. Also shown there are results of simulations based on the Monte-Carlo code PYTHIA, which does not take any jet energy loss into account. For peripheral collisions, the distribution is also compared to proton-proton collisions. As one can see clearly, the measured asymmetries in heavy ion collisions have the tendency to be larger than in the simulations for central collisions, which illustrates that a significant fraction of transverse momentum gets transported outside the jet cone by interactions with the medium.

We do not have the space here to discuss the theory of jet energy loss in detail. Very briefly, the main parton energy loss mechanism in QCD is medium induced gluon radiation [39, 40]. This is in some aspects analogous to bremsstrahlung in QED. While in vacuum QCD, there are essentially only small angle (colinear) splittings of gluons and quarks, in the context of a heavy ion collisions, additional kicks from scattering with the medium lead to larger angles. In a statistical description, this leads to a broadening of the transverse momentum k_{\perp} (orthogonal to the main parton momentum) by a diffusion or random walk type process,

$$\frac{d}{dt} \langle k_{\perp}^2 \rangle = \hat{q}. \quad (31)$$

Here, \hat{q} is the so-called jet quenching parameter. Based on this principle, a detailed theoretical description can be formulated. In addition to transverse momentum broadening, interactions with the medium also induce color decoherence. Jet energy loss models have been implemented also in Monte-Carlo codes, for example JEWEL [41, 42].

In addition to calorimetric jet observables, a traditional measure of energy loss is the so called

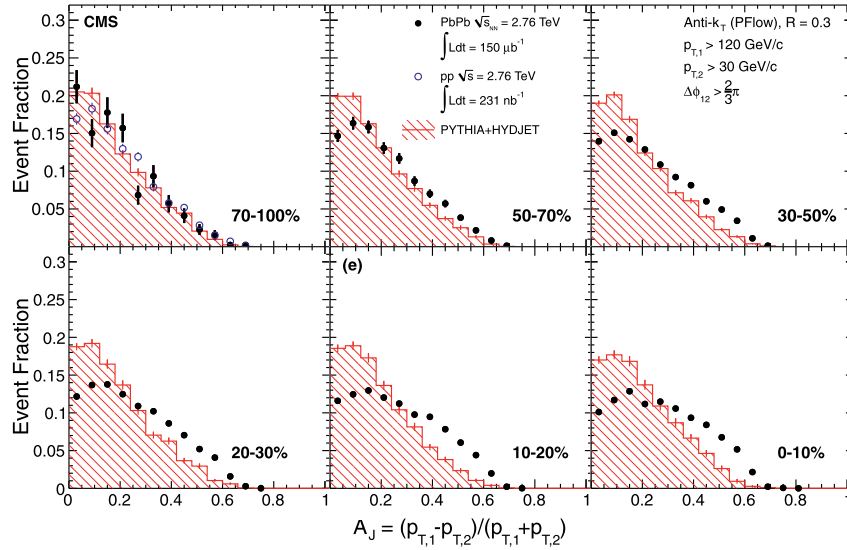


Fig. 14: Dijet asymmetry ratio A_J for leading jets of $p_{T,1} > 120$ GeV and sub-leading jets of $p_{T,2} > 30$ GeV, with a selection of $\Delta\phi_{1,2} > 2\pi/3$ between the two jets, for different centrality classes. Experimental results (points) are compared to simulations (histograms) based on PYTHIA and HYDJET (without any parton energy loss). Figure taken from ref. [38].

nuclear modification factor,

$$R_{AA}^h(p_T, \eta, \text{centrality}) = \frac{\frac{dN_{\text{medium}}^{AA \rightarrow h}}{dp_T d\eta}}{\langle N_{\text{coll}}^{AA} \rangle \frac{dN_{\text{vacuum}}^{pp \rightarrow h}}{dp_T d\eta}}. \quad (32)$$

This ratio of production cross sections for a particle h in heavy ion (AA) collisions and the scaled proton-proton (pp) reference can be defined for many different processes. It depends in general on transverse momentum p_T , rapidity η and centrality but some of these variables are sometimes integrated over. Nuclear modification factors have been measured for many different particles h . Note that this variable depends also sensitively on the proton-proton reference. This can sometimes be a problem, in particular when no measurements exist for a given collision energy and one therefore has to rely on interpolations. In a similar way to R_{AA} , one defines also the modification factor R_{pA} for proton - ion collisions or R_{CP} as a ratio between cross sections for central and peripheral collisions.

A compilation of various nuclear modification factors by the CMS collaboration is shown in Fig. 15. One observes that unidentified charged particles and b-quarks are quenched, while photons, W- and Z-bosons are not quenched, i.e. they have $R_{AA} = 1$ within the experimental uncertainties. This is of course expected because these particles are color-neutral.

8 Quarkonia in hot matter

For the last part of these introductory lectures we will be concerned with quarkonia, which are bound states of heavy quark - antiquark pairs in the context of heavy ion collisions. This is a traditional field of study in the context of the quark gluon plasma for the following reasons.

Some interesting and important questions concerning the quark gluon plasma are: How can one test deconfinement of quarks and gluons at large temperature? Or related: What prevents the formation of a meson in a quark-gluon plasma? The attractive force between a quark and an antiquark is actually screened within a plasma at non-vanishing temperature when the two are separated by more than the typical distance between free color charges in the medium. This effect can be seen nicely in lattice QCD

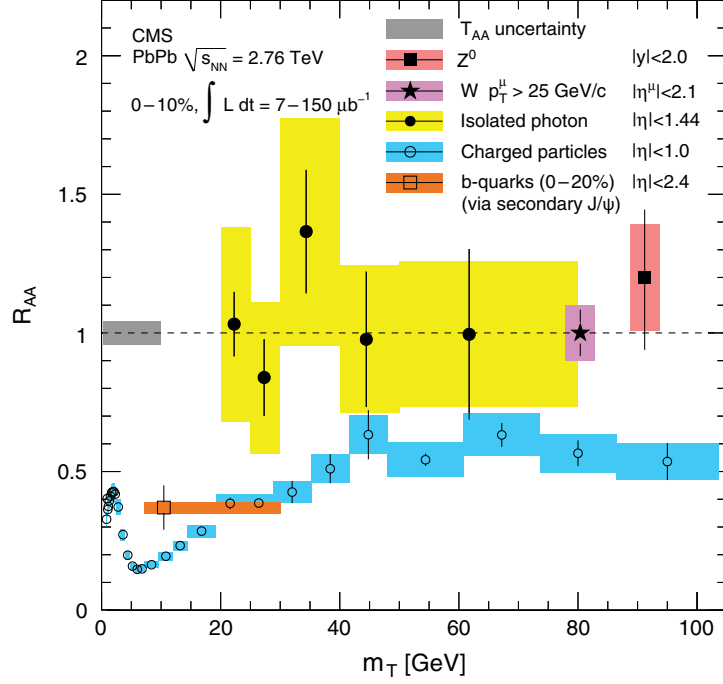


Fig. 15: Nuclear modification factor R_{AA} for different particles as a function of the transverse mass $m_T = \sqrt{m^2 + p_T^2}$ as measured and compiled by the CMS collaboration. Figure taken from ref. [43].

simulations.

One can ask more quantitatively: How close do quark and anti-quark have to be in order for their interaction not to be screened? And how does this depend on temperature? It was suggested to investigate these questions for bound states of heavy quark-antiquark pairs (quarkonia) by Matsui and Satz in 1986 [44].

A few examples of charmonium states ($c\bar{c}$ bound states) are the $J/\psi(1S)$ with a mass of 3.09 GeV, the $\psi(2S)$ with a mass of 3.69 GeV, the $\chi_{c1}(1P)$ with mass 3.51 GeV or the $\chi_{c2}(1P)$ with a mass of 3.56 GeV. Some bottomonium states ($b\bar{b}$ bound states) are the $\Upsilon(1S)$ with mass 9.46 GeV and its excited states, the $\Upsilon(2S)$ with a mass of 10.02 GeV and the $\Upsilon(3S)$ with a mass of 10.36 GeV.

The traditional picture of what should happen to these bound states at non-vanishing temperature is the one of sequential suppression. Qualitatively, when the temperature is increased, larger mesons or bound states are hindered from binding first while smaller bound states can survive up to higher temperature. (The typical distance between free color charges becomes smaller at higher temperature.) An heuristic Schrödinger equation approach using screened static quark potentials [45] suggests for example that the $J/\psi(1S)$ dissociates at $T_d \approx 2.1 T_c$. The $\psi(2S)$ is larger and dissociates at $T_d \approx 1.1 T_c$. The bottomonium state $\Upsilon(1S)$ dissociates at $T_d \approx 4 T_c$ while $\Upsilon(2S)$ is larger and dissociates already at $T_d \approx 1.6 T_c$ and $\Upsilon(3S)$ is even larger and dissociates at $T_d \approx 1.2 T_c$. While this picture gives some guidance, the use of static potentials to describe bound states in a QCD medium is somewhat questionable.

While there is little doubt that the qualitative picture sketched above is qualitatively correct, there are also some confounding effects that must be taken into account to properly understand quarkonia in the context of heavy ion collisions. Some of them are:

- Cold nuclear matter effects (which are already present for pA collisions) must be understood.
- The collective dynamics of heavy ion collisions plays a role, i. e. the expansion, fluid dynamic flow etc.

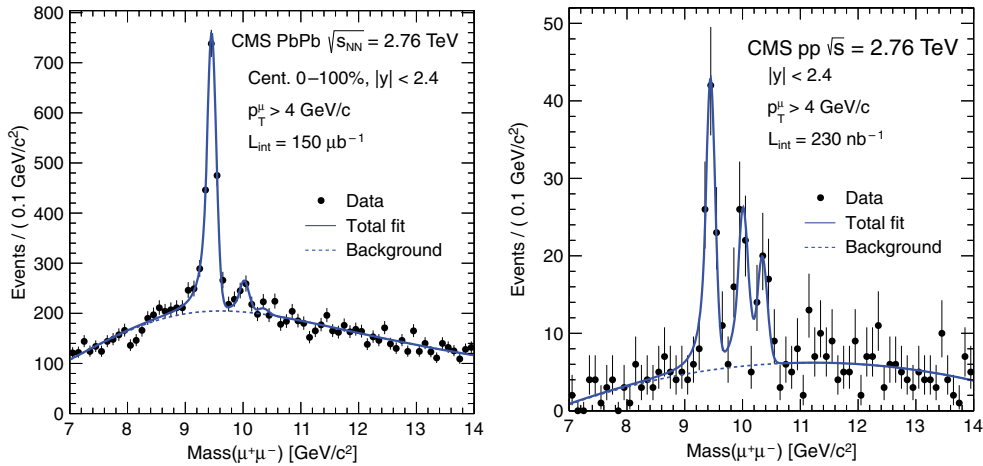


Fig. 16: Invariant mass spectrum of di-muons in heavy ion (left panel) and proton-proton (right panel) collisions. See text for further discussion. Figures taken from ref. [46].

- Quarkonia are in general not at rest with respect to the medium.
- The formation of quarkonium bound states is purely understood but should also takes some time. What is the influence of the medium for that process?
- Quarkonia can also be formed by recombination of open heavy quarks at hadronization / chemical freeze-out.

At present there is no clear picture about the quantitative importance and the interplay of all these effects, yet. However, experimental and theoretical efforts to improve the understanding of quarkonia in the context of heavy ion collisions are ongoing.

As a particularly clear example for the suppression effects that can arise due to a hot medium, consider the number of $\mu^+ \mu^-$ pairs as a function of their center of mass energy as measured by CMS. Fig. 16 shows this for Pb-Pb collisions in the left panel and for comparison the corresponding curve for proton-proton collisions in the right panel. One can see directly that the excited states of Υ are clearly suppressed in heavy ion collisions compared to pp collisions at the equivalent collision energy. It is a more difficult question, however, whether this already proves sequential suppression according to the Matsui & Satz picture.

9 Conclusions

To conclude these introductory lectures one may say that we are on the way of understanding the properties of QCD at high temperature and density with the help of relativistic heavy ion collision experiments.

Many experimental results for particles at small transverse momentum can be understood in terms of relativistic fluid dynamics. As it turns out, heavy ion collisions at RHIC and LHC energies produce a rather strongly coupled liquid with a small ratio of shear viscosity to entropy density η/s . New data with improved statistics will provide more insights and better constraints in the coming years.

High momentum partons loose energy when traversing the dense QCD medium. A more detailed understanding of this effect is currently gained from reconstructed jets and more detailed data on nuclear modification factors.

Modifications of heavy quark bound state spectra in heavy ion collisions have been observed both for charm and bottom quarks. A more detailed quantitative understanding of this physics is work in progress.

Finally, other topics such as initial state physics, photons & di-leptons, the results from the low

energy run at RHIC and many more had to be skipped here for a lack of time but that does not make them less interesting in any way.

References

- [1] E. V. Shuryak, “The QCD Vacuum, Hadrons and Superdense Matter”, World Scientific, 2003.
- [2] U. W. Heinz, “Concepts of heavy ion physics,” hep-ph/0407360.
- [3] J. I. Kapusta and C. Gale, “Finite-Temperature Field Theory”, Cambridge University Press 2006.
- [4] R. Vogt, “Ultrarelativistic Heavy-Ion Collisions”, Elsevier 2007.
- [5] W. Florkowski, “Phenomenology or Ultra-Relativistic Heavy-Ion Collisions”, World Scientific, 2010.
- [6] J. Casalderrey-Solana, H. Liu, D. Mateos, K. Rajagopal and U. A. Wiedemann, “Gauge/String Duality, Hot QCD and Heavy Ion Collisions,” Cambridge University Press, Cambridge 2014.
- [7] K. A. Olive *et al.* [Particle Data Group Collaboration], “Review of Particle Physics,” Chin. Phys. C **38**, 090001 (2014). doi:10.1088/1674-1137/38/9/090001 and 2015 update.
- [8] A. Andronic, P. Braun-Munzinger, K. Redlich and J. Stachel, “The statistical model in Pb-Pb collisions at the LHC,” Nucl. Phys. A **904-905**, 535c (2013) doi:10.1016/j.nuclphysa.2013.02.070 [arXiv:1210.7724 [nucl-th]].
- [9] J. Stachel, A. Andronic, P. Braun-Munzinger and K. Redlich, “Confronting LHC data with the statistical hadronization model,” J. Phys. Conf. Ser. **509**, 012019 (2014) doi:10.1088/1742-6596/509/1/012019 [arXiv:1311.4662 [nucl-th]].
- [10] P. Braun-Munzinger, J. Stachel and C. Wetterich, “Chemical freezeout and the QCD phase transition temperature,” Phys. Lett. B **596**, 61 (2004) doi:10.1016/j.physletb.2004.05.081 [nucl-th/0311005].
- [11] S. Floerchinger and C. Wetterich, “Chemical freeze-out in heavy ion collisions at large baryon densities,” Nucl. Phys. A **890-891**, 11 (2012) doi:10.1016/j.nuclphysa.2012.07.009 [arXiv:1202.1671 [nucl-th]].
- [12] Z. Fodor and S. D. Katz, “Critical point of QCD at finite T and mu, lattice results for physical quark masses,” JHEP **0404**, 050 (2004) doi:10.1088/1126-6708/2004/04/050 [hep-lat/0402006].
- [13] A. Andronic, P. Braun-Munzinger and J. Stachel, “The Horn, the hadron mass spectrum and the QCD phase diagram: The Statistical model of hadron production in central nucleus-nucleus collisions,” Nucl. Phys. A **834**, 237C (2010) doi:10.1016/j.nuclphysa.2009.12.048 [arXiv:0911.4931 [nucl-th]].
- [14] S. Borsanyi, G. Endrodi, Z. Fodor, A. Jakovac, S. D. Katz, S. Krieg, C. Ratti and K. K. Szabo, “The QCD equation of state with dynamical quarks,” JHEP **1011**, 077 (2010) doi:10.1007/JHEP11(2010)077 [arXiv:1007.2580 [hep-lat]].
- [15] P. B. Arnold, G. D. Moore and L. G. Yaffe, “Transport coefficients in high temperature gauge theories. 1. Leading log results,” JHEP **0011**, 001 (2000) doi:10.1088/1126-6708/2000/11/001 [hep-ph/0010177].
- [16] P. B. Arnold, C. Dogan and G. D. Moore, “The Bulk Viscosity of High-Temperature QCD,” Phys. Rev. D **74**, 085021 (2006) doi:10.1103/PhysRevD.74.085021 [hep-ph/0608012].
- [17] G. Policastro, D. T. Son and A. O. Starinets, “The Shear viscosity of strongly coupled N=4 supersymmetric Yang-Mills plasma,” Phys. Rev. Lett. **87**, 081601 (2001) doi:10.1103/PhysRevLett.87.081601 [hep-th/0104066].
- [18] P. Kovtun, D. T. Son and A. O. Starinets, “Viscosity in strongly interacting quantum field theories from black hole physics,” Phys. Rev. Lett. **94**, 111601 (2005) doi:10.1103/PhysRevLett.94.111601 [hep-th/0405231].

- [19] A. Buchel, “Transport properties of cascading gauge theories,” *Phys. Rev. D* **72**, 106002 (2005) doi:10.1103/PhysRevD.72.106002 [hep-th/0509083].
- [20] H. B. Meyer, “A Calculation of the shear viscosity in SU(3) gluodynamics,” *Phys. Rev. D* **76**, 101701 (2007) doi:10.1103/PhysRevD.76.101701 [arXiv:0704.1801 [hep-lat]].
- [21] H. B. Meyer, “Transport properties of the quark-gluon plasma from lattice QCD,” *Nucl. Phys. A* **830**, 641C (2009) doi:10.1016/j.nuclphysa.2009.09.053 [arXiv:0907.4095 [hep-lat]].
- [22] N. Christiansen, M. Haas, J. M. Pawłowski and N. Strodthoff, “Transport Coefficients in Yang–Mills Theory and QCD,” *Phys. Rev. Lett.* **115**, no. 11, 112002 (2015) doi:10.1103/PhysRevLett.115.112002 [arXiv:1411.7986 [hep-ph]].
- [23] M. Haas, L. Fister and J. M. Pawłowski, “Gluon spectral functions and transport coefficients in Yang–Mills theory,” *Phys. Rev. D* **90**, 091501 (2014) doi:10.1103/PhysRevD.90.091501 [arXiv:1308.4960 [hep-ph]].
- [24] S. Floerchinger and M. Martinez, “Fluid dynamic propagation of initial baryon number perturbations on a Bjorken flow background,” *Phys. Rev. C* **92**, no. 6, 064906 (2015) doi:10.1103/PhysRevC.92.064906 [arXiv:1507.05569 [nucl-th]].
- [25] S. Floerchinger and U. A. Wiedemann, “Mode-by-mode fluid dynamics for relativistic heavy ion collisions,” *Phys. Lett. B* **728**, 407 (2014) doi:10.1016/j.physletb.2013.12.025 [arXiv:1307.3453 [hep-ph]].
- [26] F. Cooper and G. Frye, “Comment on the Single Particle Distribution in the Hydrodynamic and Statistical Thermodynamic Models of Multiparticle Production,” *Phys. Rev. D* **10**, 186 (1974). doi:10.1103/PhysRevD.10.186
- [27] K. Aamodt *et al.* [ALICE Collaboration], “Suppression of Charged Particle Production at Large Transverse Momentum in Central Pb-Pb Collisions at $\sqrt{s_{NN}} = 2.76$ TeV,” *Phys. Lett. B* **696**, 30 (2011) doi:10.1016/j.physletb.2010.12.020 [arXiv:1012.1004 [nucl-ex]].
- [28] K. Aamodt *et al.* [ALICE Collaboration], “Elliptic flow of charged particles in Pb-Pb collisions at 2.76 TeV,” *Phys. Rev. Lett.* **105**, 252302 (2010) doi:10.1103/PhysRevLett.105.252302 [arXiv:1011.3914 [nucl-ex]].
- [29] G. Aad *et al.* [ATLAS Collaboration], “Measurement of the azimuthal anisotropy for charged particle production in $\sqrt{s_{NN}} = 2.76$ TeV lead-lead collisions with the ATLAS detector,” *Phys. Rev. C* **86**, 014907 (2012) doi:10.1103/PhysRevC.86.014907 [arXiv:1203.3087 [hep-ex]].
- [30] K. Aamodt *et al.* [ALICE Collaboration], “Higher harmonic anisotropic flow measurements of charged particles in Pb-Pb collisions at $\sqrt{s_{NN}}=2.76$ TeV,” *Phys. Rev. Lett.* **107**, 032301 (2011) doi:10.1103/PhysRevLett.107.032301 [arXiv:1105.3865 [nucl-ex]].
- [31] S. Floerchinger and U. A. Wiedemann, “Fluctuations around Bjorken Flow and the onset of turbulent phenomena,” *JHEP* **1111**, 100 (2011) doi:10.1007/JHEP11(2011)100 [arXiv:1108.5535 [nucl-th]].
- [32] C. Gale, S. Jeon, B. Schenke, P. Tribedy and R. Venugopalan, “Event-by-event anisotropic flow in heavy-ion collisions from combined Yang-Mills and viscous fluid dynamics,” *Phys. Rev. Lett.* **110**, no. 1, 012302 (2013) doi:10.1103/PhysRevLett.110.012302 [arXiv:1209.6330 [nucl-th]].
- [33] U. Heinz and R. Snellings, “Collective flow and viscosity in relativistic heavy-ion collisions,” *Ann. Rev. Nucl. Part. Sci.* **63**, 123 (2013) doi:10.1146/annurev-nucl-102212-170540 [arXiv:1301.2826 [nucl-th]].
- [34] S. Floerchinger, U. A. Wiedemann, A. Beraudo, L. Del Zanna, G. Inghirami and V. Rolando, “How (non-)linear is the hydrodynamics of heavy ion collisions?,” *Phys. Lett. B* **735**, 305 (2014) doi:10.1016/j.physletb.2014.06.049 [arXiv:1312.5482 [hep-ph]].
- [35] C. E. Coleman-Smith, H. Petersen and R. L. Wolpert, “Classification of initial state granularity via 2d Fourier Expansion,” *J. Phys. G* **40**, 095103 (2013) doi:10.1088/0954-3899/40/9/095103 [arXiv:1204.5774 [hep-ph]].

- [36] S. Floerchinger and U. A. Wiedemann, “Statistics of initial density perturbations in heavy ion collisions and their fluid dynamic response,” JHEP **1408**, 005 (2014) doi:10.1007/JHEP08(2014)005 [arXiv:1405.4393 [hep-ph]].
- [37] S. Floerchinger and U. A. Wiedemann, “Kinetic freeze-out, particle spectra and harmonic flow coefficients from mode-by-mode hydrodynamics,” Phys. Rev. C **89**, no. 3, 034914 (2014) doi:10.1103/PhysRevC.89.034914 [arXiv:1311.7613 [hep-ph]].
- [38] S. Chatrchyan *et al.* [CMS Collaboration], “Jet momentum dependence of jet quenching in PbPb collisions at $\sqrt{s_{NN}} = 2.76$ TeV,” Phys. Lett. B **712**, 176 (2012) doi:10.1016/j.physletb.2012.04.058 [arXiv:1202.5022 [nucl-ex]].
- [39] R. Baier, Y. L. Dokshitzer, A. H. Mueller, S. Peigne and D. Schiff, “Radiative energy loss of high-energy quarks and gluons in a finite volume quark - gluon plasma,” Nucl. Phys. B **483**, 291 (1997) doi:10.1016/S0550-3213(96)00553-6 [hep-ph/9607355].
- [40] B. G. Zakharov, “Fully quantum treatment of the Landau-Pomeranchuk-Migdal effect in QED and QCD,” JETP Lett. **63**, 952 (1996) doi:10.1134/1.567126 [hep-ph/9607440].
- [41] K. C. Zapp, F. Krauss and U. A. Wiedemann, “A perturbative framework for jet quenching,” JHEP **1303**, 080 (2013) doi:10.1007/JHEP03(2013)080 [arXiv:1212.1599 [hep-ph]].
- [42] K. C. Zapp, “JEWEL 2.0.0: directions for use,” Eur. Phys. J. C **74**, no. 2, 2762 (2014) doi:10.1140/epjc/s10052-014-2762-1 [arXiv:1311.0048 [hep-ph]].
- [43] T. Dahms [CMS Collaboration], “Quarkonia and heavy-flavour production in CMS,” Nucl. Phys. A **910-911**, 91 (2013) doi:10.1016/j.nuclphysa.2012.12.017 [arXiv:1209.3661 [nucl-ex]].
- [44] T. Matsui and H. Satz, “ J/ψ Suppression by Quark-Gluon Plasma Formation,” Phys. Lett. B **178**, 416 (1986). doi:10.1016/0370-2693(86)91404-8
- [45] H. Satz, “Colour deconfinement and quarkonium binding,” J. Phys. G **32**, R25 (2006) doi:10.1088/0954-3899/32/3/R01 [hep-ph/0512217].
- [46] S. Chatrchyan *et al.* [CMS Collaboration], “Observation of sequential Upsilon suppression in PbPb collisions,” Phys. Rev. Lett. **109**, 222301 (2012) doi:10.1103/PhysRevLett.109.222301 [arXiv:1208.2826 [nucl-ex]].

Practical Statistics for High Energy Physics

E. Gross

Weizmann Institute of Science, Rehovot, Israel

Abstract

In these lecture notes the frequentist methods used in the Higgs search, discovery and measurement are reviewed. The idea is that the reader will be able to understand what lies beneath the surface of the results and the plots shown in the experiments publications. Though the results shown are mainly from ATLAS and CMS, the methods and the lessons can be propagated to other fields such as Astro-Particles and fixed target experiments.

Keywords

CERN report; ESHEP; statistics; data analysis.

1 Introduction

These lecture notes are based on statistics lectures I gave in the European CERN school for High Energy Physics, 2015. They contain material published mainly in the following two papers: "Asymptotic formulae for likelihood-based tests of new physics" by Cowan, Cranmer, Gross and Vitells [1] and "Trial factors or the look elsewhere effect in high energy physics" by Gross and Vitells [2]. The frequentist approach used in the Higgs search, discovery and measurement are reviewed. Examples from real data analysis are given to clarify the methods.

2 The Search for the Higgs Boson

From Wikipedia: On 4 July 2012, the discovery of a new particle with a mass between 125 and 127 GeV/c² was announced; physicists suspected that it was the Higgs boson. Since then, the particle has been shown to behave, interact, and decay in many of the ways predicted by the Standard Model.

High Energy Physicists (HEP) rely on a hypothesis: The Standard Model. This model relies on the existence of the 2012 discovery of the Higgs Boson. The minimal content of the Standard Model includes the Higgs Boson, the Quarks, the Leptons and the force mediating Bosons including the photons, gluons, W and Z . However, the Standard Model suffers from some problems, e.g. the hierarchy and naturalness problems that are solved by various extensions of the Model and include other particles that are yet to be discovered. The challenge of HEP is to generate tons of data and to develop powerful analyses to tell if the data indeed contains evidence for new particles. Once the new particle, such as the 2012 scalar, has been discovered, the next step would have been to measure its mass, and confirm that it has the expected properties of the Higgs Boson (Spin, CP). Perhaps it is not the expected Standard Model Higgs Boson, but a member of a family of Scalar Bosons, the rest, yet to be discovered.

The statistical challenge is obvious: to tell in the most powerful way, and to the best of our current scientific knowledge, if, in our data, there is new physics, beyond what is already known. In that sense, what is already known is the background to what we search, which is treated as the signal. The complexity of the apparatus and the physics (both signal and background) suffer from large systematic errors that should be taken care of in a correct statistical way.

Though the Higgs Boson has been already discovered, in these lecture notes, for pedagogic reasons, it is assumed, that, the so-called Standard Model, contains no Higgs Boson, serve as the background to the signal, which is the Higgs Boson. The Higgs Boson cannot exist without the Standard Model, so there are two nested hypotheses tested against each other. The Standard Model (denoted by b for background) and the Standard Model containing a Higgs Boson with a mass m_H , i.e. the signal+background, denoted by $s(m_H) + b$.

3 Essential Terminology

3.1 A Tale of Two Hypotheses

From Wikipedia: A hypothesis (plural hypotheses) is a proposed explanation for a phenomenon. For a hypothesis to be a scientific hypothesis, the scientific method requires that one can test it. Scientists generally base scientific hypotheses on previous observations that cannot satisfactorily be explained with the available scientific theories.

The expected signal and background are determined by the corresponding cross sections, luminosity delivered by the accelerator and the detectors response (efficiency and geometrical acceptance). $s(m_H)$ is given by

$$s(m_H) = L \cdot \sigma_{SM}(m_H) \cdot \epsilon \cdot A. \quad (1)$$

Where L is the luminosity delivered by the accelerator, $\sigma_{SM}(m_H)$ is the Standard Model (SM) production cross section of the Higgs Boson, and ϵ and A are the efficiency and geometrical acceptance of the detector. For simplicity, let's assume a counting experiment and let n be the number of observed events, then

$$n = \mu s(m_H) + b. \quad (2)$$

b is the expected background, and μ is the signal strength given by

$$\mu = \frac{\sigma_{obs}}{\sigma_{SM}}. \quad (3)$$

There are therefore two hypotheses. One is the background only (b), and the other is the $\mu s(m_H) + b$ hypothesis, i.e., a Higgs Boson with a strength μ on top of the background. For a Standard Model Higgs Boson, we expect to measure $\mu = 1.0$. The background only hypothesis is denoted by H_0 while H_μ is the Higgs Boson hypothesis with H_1 being the SM Higgs Boson hypothesis.

3.2 Testing an Hypothesis

From Wikipedia: A statistical hypothesis test is a method of statistical inference. Commonly, two statistical data sets are compared, or a data set obtained by sampling is compared against a synthetic data set from an idealized model. A hypothesis is proposed for the statistical relationship between the two data sets, and this is compared as an alternative to an idealized null hypothesis that proposes no relationship between two data sets. The comparison is deemed statistically significant if the relationship between the data sets would be an unlikely realization of the null hypothesis according to a threshold probability; the significance level. Hypothesis tests are used in determining what outcomes of a study would lead to a rejection of the null hypothesis for a pre-specified level of significance.

The first step in any hypothesis testing is to identify and state the relevant null, H_{null} and alternative H_{alt} hypotheses. The next step is to define a test statistic, q , under the null hypothesis (the tested hypothesis). We then compute from the observations the observed value q_{obs} of the test statistic q . Finally, decide (based on q_{obs}) to either fail to reject the null hypothesis or reject it in favour of an alternative hypothesis.

3.3 Discovery and Exclusion in a Nut Shell

To establish a discovery we define the null hypothesis as the background only hypothesis, $H_{null} = H_0$, and test it. We either fail to reject it or manage to reject it in favour of the alternative hypothesis, $H_{alt} = H_\mu$. Rejection of the null H_0 hypothesis at the level of 5σ (see 3.5) is considered a discovery. Defining the null hypothesis as $H_{null} = H_\mu$ enables the exclusion of the signal. For example, if we define the null hypothesis as the Standard Model Higgs with a mass m_H , $H_{null} = H_1$, testing and rejecting this hypothesis at the 95% Confidence Level (see 3.5) is considered an exclusion of the Standard Model Higgs with a mass m_H .

3.4 A Test Statistic

As defined in Wikipedia: A hypothesis test is typically specified in terms of a test statistic, considered as a numerical summary of a data-set that reduces the data to one value that can be used to perform the hypothesis test. In general, a test statistic is selected or defined in such a way as to quantify, within observed data, behaviours that would distinguish the null from the alternative hypothesis, where such an alternative is prescribed, or that would characterise the null hypothesis if there is no explicitly stated alternative hypothesis, which often occurs when performing a measurement.

One example for using a test statistic is the discovery of the Higgs, when the data of Billions of Collisions is summarised in one number which determines if LHC rejected the background only hypothesis in favour of the Higgs Boson with a mass m_H or not.

There are many ways to define a test statistic based on the nature of the required test. Test statistics for discovery or exclusion are commonly based on Likelihood ratios.

Note that the likelihood is a function of the data, i.e.

$$L(H_0) = Prob(x|H_0) \quad (4)$$

where x is the data.

Before classifying the test statistics in a formal way, let us take a simplified approach. The two most common test statistics in High Energy Physics are the Neyman-Pearson (NP) and Profile Likelihood (PL). The NP test statistic given by

$$q^{NP} = -2\ln \frac{L(H_0)}{L(H_1)}. \quad (5)$$

$L(H_0)$ and $L(H_1)$ are the likelihoods of the null (b) and alternative ($s(m_H) + b$) hypotheses. Note that inverting the roles of the null and alternative hypotheses, simply swap the sign of the NP test statistic. The PL test statistic depends on the tested hypothesis and for a simple counting experiment (see Equation 2), when testing the b -only hypothesis, H_0 , the test statistic is given by

$$q_0 = -2\ln \frac{L(b)}{L(\hat{\mu}s(m_H) + b)}. \quad (6)$$

$\hat{\mu}$ is the Maximul Likelihood Estimators (MLE) of μ . In this simplified example b is assumed to be known. The probability distribution function (PDF) of both test statistics under the null $f(q^{NP}|b), f(q_0|b)$ and the alternative $f(q^{NP}|s(m_H) + b), f(q_0|s(m_H) + b)$ hypotheses are shown in Figure 1.

3.5 What is the p-value

As defined in Wikipedia: An important property of a test statistic is that its sampling distribution under the null hypothesis must be calculable, either exactly or approximately, which allows p -values to be calculated.

The observed p – value is a measure of the incompatibility of the data with the tested hypothesis. It is the probability, under assumption of the null hypothesis H_{null} , of finding data of equal or greater incompatibility with the predictions of H_{null} . This is clearly illustrated in Figure 1 for the PL test statistic by the light blue area (right plot). Here H_0 is the tested null hypothesis (b only) and the p – value is given by

$$p = \int_{q_{0,obs}}^{\infty} f(q_0|b) dq_0. \quad (7)$$

One can regard the hypothesis as excluded if its p -value is observed below a specified threshold (usually denoted by α).

Now, depending on the nature of the statistical test, one considers a one-sided or two-sided p -value. When performing a measurement, any deviation above or below the mean is drawing our attention

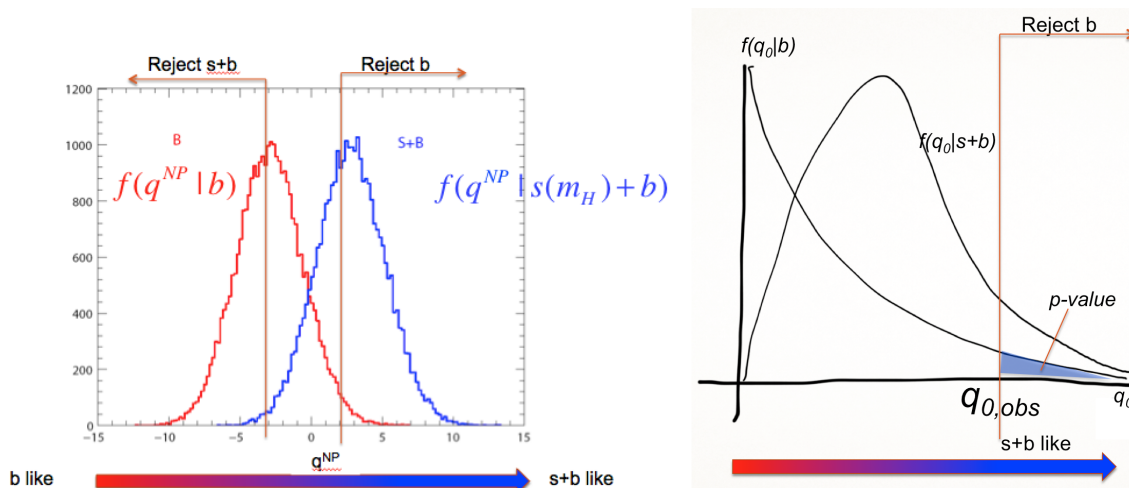


Fig. 1: The pdf of the Neyman-Pearson q^{NP} (left) and PL (Profile-Likelihood), q_0 (right) test statistics, under the null (b) and alternative ($s(m_H) + b$) hypotheses.

and might serve an indication of some anomaly or new physics. Here we consider a two sided p -value. However, when trying to reject an hypothesis while performing searches, one usually considers only one-sided tail probabilities. When the null hypothesis is the b -only hypothesis, downward fluctuations of the background, are not considered as an evidence against the background. Likewise, when deriving a limit, upward fluctuations of the hypothesised signal are not considered as an evidence against the signal. In both cases only one-sided tail probabilities are considered.

In particle physics, when performing searches, one usually converts the p -value into an equivalent significance, Z defined such that a Gaussian distributed variable, which is found Z standard deviations above its mean, has an upper-tail probability equal to p (Figure 2). That is,

$$Z = \Phi^{-1}(1 - p), \tag{8}$$

where Φ^{-1} is the quantile (inverse of the cumulative distribution) of the standard Gaussian. For a signal

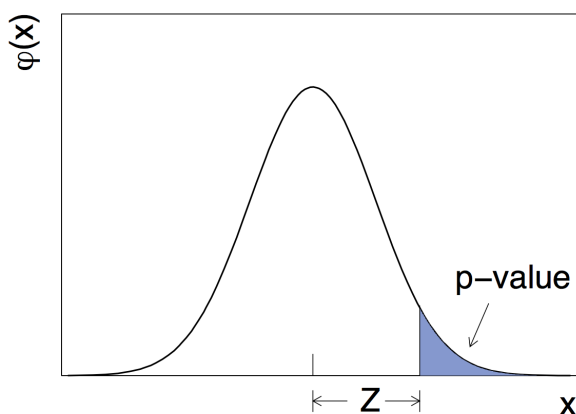


Fig. 2: The relationship between a p -value and a significance of Z sigma.

process such as the Higgs boson, the particle physics community has a tendency to regard rejection of the background hypothesis with a significance of at least $Z = 5$, as an appropriate level to constitute

a discovery. This corresponds to $p = 2.87 \times 10^{-7}$. For purposes of excluding a signal hypothesis, a threshold p -value of 0.05 (i.e., 95% confidence level) is often used, which corresponds to $Z = 1.64$. This should not be confused with a 1.96σ fluctuation of a Gaussian variable that gives 0.05 for the two-sided tail area.

Note that, for a sufficiently large data sample, one would obtain a p -value of 0.5 for data in perfect agreement with the expected background. With the definition of Z given above, this gives $Z = 0$.

3.6 Expected Significance and the Asimov Data Set

As defined in Wikipedia: The use of a single representative individual to stand in for the entire population can help in evaluating the sensitivity of a statistical method. Franchise, a science fiction short story by Isaac Asimov, was cited as the inspiration of the term "Asimov data set", where an ensemble of simulated experiments can be replaced by a single representative one.

It is often useful to quantify the sensitivity of an experiment by reporting the expected significance one would obtain with a given measurement under the assumption of various hypotheses. For example, the sensitivity to discovery of a given signal process H_1 could be characterized by the expectation value, under the assumption of H_1 , of the value of Z obtained from a test of H_0 . This would not be the same as the Z obtained using Eq. (8) with the expectation of the p -value, however, because the relation between Z and p is nonlinear. The median Z and p will, however, satisfy Eq. (8) because this is a monotonic relation. Therefore we take the term ‘expected significance’ to refer to the median.

In the Standard Model there is only one Higgs Boson with well defined couplings. To find the discovery sensitivity of an experiment, one needs to generate one ensemble of experiments containing the Higgs Boson at the tested mass. However, if one goes beyond the Standard Model, e.g., supersymmetric models, one faces a multi-dimensional parameter space where the Higgs Boson’s couplings, and hence its production cross section and decay properties (both related to the signal strength) vary as a function of the parameters. For each point in parameter space one needs to estimate the experiment’s discovery sensitivity. One faces the need to generate an enormous number of ensembles of experiments and evaluate the median sensitivity for each ensemble.

In [1] it was shown that one can replace each ensemble of the alternate-hypothesis experiments with one data set that represents the typical experiment. This “Asimov” data set delivers the desired median sensitivity. Hence, one is exempted from the need to perform an ensemble of experiments for each set of parameters.

The Asimov data set is constructed such that when one uses it to evaluate the estimators for all parameters, one obtains the true parameter values.

As intuitively used for years till proven at [1], the Asimov data set can trivially be constructed from the true parameters values. For example, in a counting experiment (see Eq. 2) the Asimov data set corresponding to the H_1 hypothesis is $n_A = s + b$. and the one correspond to the H_0 hypothesis is $n_A = b$. As strange as it reads, the Asimov data set is not necessarily an integer.

3.7 Nuisance Parameters.

From Wikipedia: In statistics, a nuisance parameter is any parameter which is not of immediate interest but which must be accounted for in the analysis of those parameters which are of interest.

A widely used procedure to establish discovery (or exclusion) in particle physics is based on a frequentist significance test using a likelihood ratio as a test statistic. In addition to parameters of interest such as the rate (cross section) of the signal process, the signal and background models will contain in general *nuisance parameters* whose values are not taken as known *a priori* but rather must be fitted from the data.

It is assumed that the parametric model is sufficiently flexible so that for some value of the param-

eters it can be regarded as true. The additional flexibility introduced to parametrise systematic effects results, as it should, in a loss in sensitivity. To the degree that the model is not able to reflect the truth accurately, an additional systematic uncertainty will be present that is not quantified by the statistical method presented here.

Here, nuisance parameters are denoted by θ . The likelihood is then a function of the parameter of interest, say, μ . Then $L = L(\mu, \theta)$. When testing H_μ , the Profile Likelihood test statistic in the presence of nuisance parameters, become

$$q_\mu = -2 \ln \frac{L(\mu, \hat{\theta}_\mu)}{L(\hat{\mu}, \hat{\theta})}. \quad (9)$$

μ is the parameter of interest, θ represent the nuisance parameters (including b). A hat stands for the MLE (Maximum Likelihood Estimator) while a double hat is the constrained MLE, i.e. the MLE of θ , fixing μ . It is common to say that θ is profiled.

3.8 Confidence Interval, Confidence Level and Coverage.

From Wikipedia: A confidence interval (CI) is a type of interval estimate of a population parameter. It is an observed interval (i.e., it is calculated from the observations), in principle different from sample to sample, that frequently includes the value of an unobservable parameter of interest if the experiment is repeated. How frequently the observed interval contains the (true) parameter is determined by the confidence level... Whereas two-sided confidence limits form a confidence interval, their one-sided counterparts are referred to as lower or upper confidence bounds.

Say, the result of a measurement is given by $\mu = 1.1 \pm 0.3$. This means that the Confidence Interval, CI, is $\mu = [0.8, 1.4]$ at the 68% Confidence Level (CL). I.e., in an ensemble of repeated experiments, each producing a CI, 68% of the Confidence Intervals contain the unknown true value of the parameter of interest μ .

There are many ways to derive a CI at a given CL. If, the method produces a CI that contains the true value of the parameter of interest (p.o.i) more than the CL (e.g. in our example, more than 68%), the method is said to over-cover, and is considered conservative. If, however, the CI contains the true value of the p.o.i. less than the claimed Confidence Level, the method is considered to under-cover, which means, one cannot trust the CL, and the true CL might be lower than the claimed one.

3.9 Upper Limits and Confidence Levels.

If one deduces that the CI of μ contains $\mu = 0$, i.e. $\mu = [0, \mu_{up}]$ at the 95% CL, then one says that $\mu < \mu_{up}$ at the 95% CL. This means that in an ensemble of experiments, 95% of the intervals contain the true value of μ including $\mu = 0$.

If $\mu < 1$ at the 95% CL, and μ is given by Eq. 3, i.e.

$$\mu = \frac{\sigma_{obs}(m_H)}{\sigma_{SM}(m_H)} < 1 \quad (10)$$

one concludes that $\sigma_{obs}(m_H) < \sigma_{SM}(m_H)$, i.e. a SM Higgs with a mass m_H is excluded at the 95% CL.

3.10 The Neyman Pearson Lemma.

Wikipedia: In statistics, the Neyman Pearson lemma, named after Jerzy Neyman and Egon Pearson, states that when performing a hypothesis test between two simple hypotheses H_{null} and H_{alt} , the likelihood-ratio test which rejects H_{null} in favour of H_{alt} is the most powerful test at (a given) significance level...

When we reject the null hypothesis H_{null} based on a very small p -value, we also take a risk. We might be wrong (this is referred to as a type I error, see section 3.11). The null hypothesis can still be true

and the p -value is a measure for this risk. The p -value can therefore be interpreted as the false-positive rate and it satisfies

$$p \leq \text{Prob}(\text{reject } H_{null} | H_{null} = \text{TRUE}) \quad (11)$$

However, if while rejecting the null hypothesis, the probability for the alternative hypothesis to be true is small.... the test statistic is probably not doing its job, i.e. it is not powerful. The power of a test is therefore related to the probability that $H_{alt} = \text{TRUE}$ while rejecting H_{null} , i.e.

$$\text{POWER} = \text{Prob}(\text{reject } H_{null} | H_{alt} = \text{TRUE}). \quad (12)$$

Neyman and Pearson showed [3], that (in the absence of nuisance parameters) the most powerful test statistic is the likelihood ratio defined in Eq. 5.

3.11 Type I & Type II Errors, the Modified Frequentist p -value, or, the CLs Technique.

Wikipedia: CLs (from Confidence Levels) is a statistical method for setting upper limits (also called exclusion limits) on model parameters, a particular form of interval estimation used for parameters that can take only non-negative values..... it differs from standard confidence intervals in that the stated confidence level of the interval is not equal to its coverage probability. The reason for this deviation is that standard upper limits based on a most powerful test necessarily produce empty intervals with some fixed probability when the parameter value is zero, and this property is considered undesirable by most physicists and statisticians.

For the sake of clarity let us define now type I and type II errors. Type I error is the probability to reject the null hypothesis, when the null hypothesis is true. This is referred to as "False Positive". It is usually denoted by α , i.e. $\alpha = \text{Prob}(\text{reject } H_{null} | H_{null} = \text{TRUE})$. Type II error, referred to as "False Negative", is when we accept the null hypothesis, when the alternative hypothesis is true. It is usually denoted by β . $\beta = \text{Prob}(\text{Accept } H_{null} | H_{null} = \text{FALSE}) = \text{Prob}(\text{Accept } H_{null} | H_{alt} = \text{TRUE})$. Quoting Birnbaum [4]: *A concept of statistical evidence is not plausible unless it finds strong evidence for H_{alt} against H_{null} , with small probability α when H_{null} is true, and with much larger probability $(1 - \beta)$ when H_{alt} is true.* $1 - \beta = \text{Prob}(\text{reject } H_{null} | H_{alt} = \text{TRUE})$ is defined as the power of the statistical test. Since rejecting H_{null} is accepting H_{alt} by definition, we find

$$\text{POWER} = 1 - \beta = \text{Prob}(\text{accept } H_{alt} | H_{alt} = \text{TRUE}) = 1 - \text{Prob}(\text{reject } H_{alt} | H_{alt} = \text{TRUE}). \quad (13)$$

Let $H_{null} = H_{s+b}$, i.e. the $s + b$ hypothesis, then, given an observation, H_{s+b} is rejected if the p -value = $p_{s+b} \leq \alpha$. At the threshold we find

$$p_{s+b} = \text{Prob}(\text{reject } H_{s+b} | H_{s+b} = \text{TRUE}). \quad (14)$$

with a power (Equation 13) of

$$\text{Power} = 1 - p_b. \quad (15)$$

A situation occurs when the power is very small and the experiment has no sensitivity to reject with high power the $s + b$ hypothesis, because it almost rejects the b -only hypothesis as well, as seen in Figure 3. A way out, was suggested by the CL_s technique [5] which is based on Birnbaum [4]. Birnbaum suggested in 1962 that the the $\{p - \text{value}\} / \{\text{power}\}$ should be used as a measure of the strength of statistical evidence provided by significance tests, rather than the $p - \text{value}$ alone. This translates into using a modified $p - \text{value}$

$$p'_{s+b} = \frac{p_{s+b}}{1 - p_b} \quad (16)$$

Equation 16 can also be interpreted as a normalised p -value, where p_{s+b} is normalised to the acceptance probability of H_b . Obviously if, while rejecting H_{s+b} one does not accept H_b , one does not have a

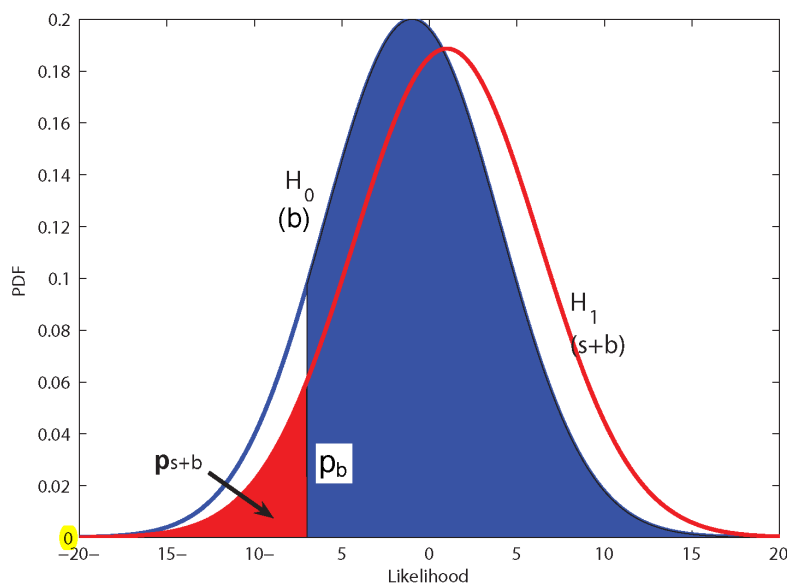


Fig. 3: An illustration showing the reasoning of the CL_s method. In this situation a signal+background hypothesis might be rejected though the experiment has no sensitivity to observe that particular signal.

sensitivity to exclude the $s + b$ hypothesis.

$$p'_{s+b} = \frac{\text{Prob}(\text{reject } H_{s+b} | H_{s+b} = \text{TRUE})}{\text{Prob}(\text{accept } H_b | H_b = \text{TRUE})} \quad (17)$$

The CL_s method lacks a frequentist coverage. However, it lacks it in places where the experiment is insensitive to the expected signal! And this is not necessarily a disadvantage from the physicists point of view! Here is what happens: One uses the Neyman-Pearson likelihood ratio as a test statistics. When the expected signal is very low the two pdf are almost overlapping (see Figure 3). The background might fluctuate down resulting in a very small p_{s+b} . As a result we are tempted to exclude the signal hypothesis. However, it is not the signal hypothesis s , that is excluded, but the signal+background hypothesis $s + b$. It is the small expected signal $s \ll s + b$ that is leading to a false exclusion. To protect against such an inference one uses the modified p -value (Eq. 16) as a criterion for taking a decision of rejecting the signal hypothesis.

As a result, for heavy Higgses with low cross section, where the experiment lacks sensitivity, the false exclusion rate is too low and the method over-covers. This is conservative because it avoids excluding when there is no sensitivity. When the signal cross section is high (light m_H), the coverage is close to full.

3.12 Feldman-Cousins: Ensuring Coverage by Neyman Construction.

Wikipedia: Neyman construction is a frequentist method to construct an interval at a confidence level $CL\%$, that if we repeat the experiment many times the interval will contain the true value a fraction $CL\%$ of the time, this way, one guarantees full coverage by construction.

As said, the Neyman construction is a method of parameter estimation that ensures coverage. One scans over all the possible true values of some parameter s and defines an acceptance interval for each s , based on the known pdf, $f(s_m | s)$, of the measured s_m given a possible true s (there is only ONE unknown true s though). The (e.g.) 68% acceptance interval $[s_l, s_h](s)$ is defined via the integration $[s_l, s_h](s) = \{s_m | \int_{s_l}^{s_h} f(s_m | s) ds_m = 68\%\}$ (Figure 4). Even in the simplest case where f is a Gaussian,

there is an ambiguity in the choice of the integration boundaries, which will lead to two-sided intervals, or one-sided integral bounded from below or above. To sort out the integration limits one needs to specify an ordering rule (i.e. which measurements should be considered within the integration boundaries and which should stay out). The construction of the acceptance intervals for all s forms a belt from which one can easily get the corresponding (e.g.) 68% confidence interval $[s_d, s_u](s_o)$, given one measurement s_o via inversion (Figure 4).

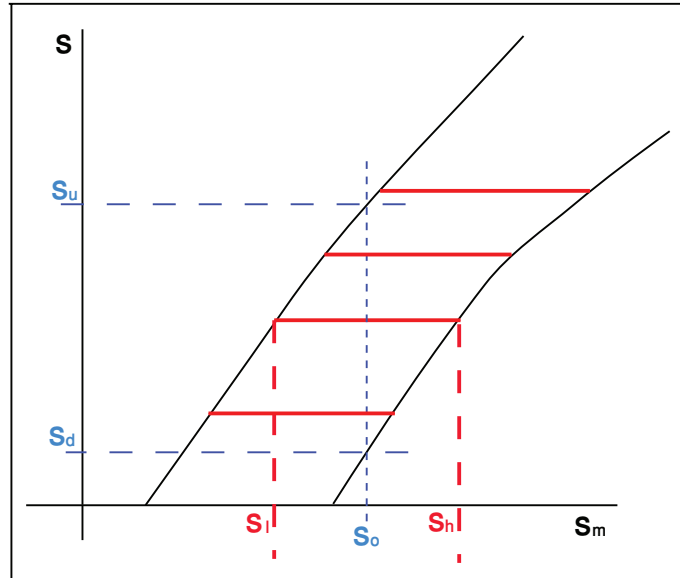


Fig. 4: An illustration showing the Neyman belt. The horizontal lines are the acceptance intervals in the measured parameter space s_m for a given possible true s , $[s_l, s_h](s)$. Given an observation s_o one can construct the confidence interval $[s_d, s_u]$ via inversion, as indicated in the Figure.

3.12.1 The Feldman-Cousins Method

The full Neyman construction was introduced to HEP by Feldman and Cousins [6]. The test statistic is the likelihood ratio $q(s) = \frac{L(s+b)}{L(\hat{s}+b)}$ where \hat{s} is the MLE of s (in $L(\hat{s} + b)$) under the constraint that s is physically allowed (i.e. positive). To construct a 68% acceptance interval in the number of observed events, $[n_1, n_2]$, one is using q as an ordering rule, i.e. $\sum_{n_1}^{n_2} p(n|s, b) \geq 68\%$ where only terms with decreasing order of $q(n)$ are included in the sum, till the sum exceeds the 68% confidence (see Fig. 4). When n_o events are observed, one is using this constructed Neyman belt to derive a confidence interval, which, depending on the observation, might be a one-sided or a two-sided interval. This method is therefore called the unified method, because it avoids a flip-flop of the inference (i.e. one decides to flip from a limit to an interval if the result is significant enough..).

One can clearly see in Fig. 4 that depending on the observation, s_o , one gets either a one sided bound, or a two sided interval.

A noted difficulty with this approach is that an experiment with higher expected background which observes no events might set a better upper limit than an experiment with lower or no expected background. This would never occur with the CL_s method.

Another difficulty is that this approach does not incorporate a treatment of nuisance parameters. However, it can either be plugged in "by hand", using the hybrid Cousins and Highland method [7] or in the LHC way, i.e. using the Profile Likelihood [1] as described above.

4 Classification of Test Statistics.

Depending on the nature of the test, one can classify the various test statistics, all based on Likelihood ratios, where the nuisance parameters are profiled (e.g. Eq. 9). The classification is based on [1] and is shown in Table 1.

Table 1: Classification of Test Statistics

Test Stat.	Purpose	Expression	LR
q_0	discovery of positive signal	$q_0 = \begin{cases} -2 \ln \lambda(0) & \hat{\mu} \geq 0 \\ 0 & \hat{\mu} < 0 \end{cases}$	$\lambda(0) = \frac{L(0, \hat{\theta})}{L(\hat{\mu}, \hat{\theta})}$
t_μ	2-sided measurement	$t_\mu = -2 \ln \lambda(\mu)$	$\lambda(\mu) = \frac{L(\mu, \hat{\theta})}{L(\hat{\mu}, \hat{\theta})}$
\tilde{t}_μ	avoid negative signal (Feldman-Cousins)	$\tilde{t}_\mu = -2 \ln \tilde{\lambda}(\mu)$	$\tilde{\lambda}(\mu) = \begin{cases} \frac{L(\mu, \hat{\theta}(\mu))}{L(\hat{\mu}, \hat{\theta})} & \hat{\mu} \geq 0 \\ \frac{L(\mu, \hat{\theta}(\mu))}{L(0, \hat{\theta}(0))} & \hat{\mu} < 0 \end{cases}$
q_μ	exclusion	$q_\mu = \begin{cases} -2 \ln \lambda(\mu) & \hat{\mu} \leq \mu \\ 0 & \hat{\mu} > \mu \end{cases}$	
\tilde{q}_μ	exclusion of positive signal	$\tilde{q}_\mu = \begin{cases} -2 \ln \frac{L(\mu, \hat{\theta}(\mu))}{L(0, \hat{\theta}(0))} & \hat{\mu} < 0, \\ -2 \ln \frac{L(\mu, \hat{\theta}(\mu))}{L(\hat{\mu}, \hat{\theta})} & 0 \leq \hat{\mu} \leq \mu \\ 0 & \hat{\mu} > \mu \end{cases}$	

5 Asymptotic Formulae

Wikipedia: In mathematics and statistics, an asymptotic distribution is a distribution that is in a sense the "limiting" distribution of a sequence of distributions. One of the main uses of the idea of an asymptotic distribution is in providing approximations to the cumulative distribution functions of statistical estimators.

The frequentist approach of statistics requires the knowledge of the probability distribution functions (PDFs) of the test statistic under the null and alternative hypotheses. These PDFs are used to find both the significance for a specific data set and the expected significance. However, obtaining these PDFs, can involve Monte Carlo generations that are computationally expensive. Ref [1] developed the asymptotic formulae based on results due to Wilks [8] and Wald [9] by which one can obtain both the significance for given data as well as the full sampling distribution of the significance under the hypothesis of different signal models, all without recourse to Monte Carlo. In this way one can find, for example, the median significance and also a measure of how much one would expect this to vary as a result of statistical fluctuations in the data. Obtaining the same things with Monte Carlo is sometimes impossible. One LHC collision might take $o(10mins)$ to generate, and one needs over 10^7 events to calculate a 5σ tail of a PDF. Moreover, the test statistics involve heavy duty fits which also take time. Combining ATLAS and CMS results in over 4000 Nuisance Parameters. Repeated fits of that many parameters result often in failure fits. Some we are not even aware of. It could be that the PDF generated by toys is subject to unknown failure of fits and is not reliable for $p - value$ calculations. In most cases, the number of events involved is satisfying the condition for the asymptotic approximation to work.

All of the asymptotic approximations of the PDFs of the test statistics shown in Table 1 have been calculated under the null and alternative hypotheses [1]. There is no point in reproducing them all here. Three common uses are for exclusion, discovery and measurement.

5.1 Exclusion

For exclusion one can either use q_μ or \tilde{q}_μ (Table 1) as a test statistic. In numerical examples we have found that the difference between the two tests is negligible, but use of q_μ leads to important simplifications. Furthermore, in the context of the asymptotic approximation, the two statistics are equivalent. That is, assuming the approximations below, q_μ can be expressed as a monotonic function of \tilde{q}_μ and thus they lead to the same results. We will therefore recommend the use of q_μ for the derivation of exclusion.

Using the asymptotic formulae of [1] we find that $f(q_\mu|\mu)$ distributes as a half-chi-square:

$$f(q_\mu|\mu) = \frac{1}{2}\delta(q_\mu) + \frac{1}{2}\frac{1}{\sqrt{2\pi}}\frac{1}{\sqrt{q_\mu}}e^{-q_\mu/2}. \quad (18)$$

It is therefore recommended to verify that $f(q_\mu|\mu) \sim \chi_1^2$. This is usually the case, in particular when combining channels.

The cumulative distribution is

$$F(q_\mu|\mu) = \Phi\left(\sqrt{q_\mu}\right). \quad (19)$$

5.1.1 The p – value

The p -value of the hypothesized μ is

$$p_\mu = 1 - F(q_\mu|\mu) = 1 - \Phi\left(\sqrt{q_\mu}\right) \quad (20)$$

and therefore the corresponding significance is

$$Z_\mu = \Phi^{-1}(1 - p_\mu) = \sqrt{q_\mu}. \quad (21)$$

If the p -value is found below a specified threshold α (often one takes $\alpha = 0.05$), then the value of μ is said to be excluded at a confidence level (CL) of $1 - \alpha$. The upper limit on μ is the largest μ with $p_\mu \leq \alpha$. Here this can be obtained simply by setting $p_\mu = \alpha$ and solving for μ . One finds

$$\mu_{\text{up}} = \hat{\mu} + \sigma\Phi^{-1}(1 - \alpha). \quad (22)$$

For example, $\alpha = 0.05$ gives $\Phi^{-1}(1 - \alpha) = 1.64$. Any point μ_0 satisfying $\mu_0 \leq \mu_{\text{up}}$ is excluded at the $100(1 - \alpha)\%$ Confidence Level. (for $\alpha = 0.05$ the 95% Confidence Interval does not contain $\mu = \mu_0$). Also as noted above, σ depends in general on the hypothesized μ . Thus in practice one may find the upper limit numerically as the value of μ for which $p_\mu = \alpha$.

5.1.2 Expected Limit and Error Bands

To find the expected limit, one should plug in the Asimov data which represents the alternative hypothesis, which in this case is the expected background (with no fluctuations). The signal strength is set to zero (in a simple counting experiment $n = b$). One then gets $q_{\mu,A}$ and the corresponding $\mu_{\text{up}}^{\text{med}}$ is given by solving $q_{\mu_{\text{up}}^{\text{med}},A} = 1.64^2$ (for $\alpha = 0.05$). The error bands are given by

$$\mu_{\text{up}+N} = \sigma(\Phi^{-1}(1 - \alpha) + N) \quad (23)$$

with

$$\sigma^2 = \frac{\mu^2}{q_{\mu,A}} \quad (24)$$

μ can be taken as μ_{up}^{med} in the calculation of σ .

5.2 Expected Limit and Error Bands a-la “(CL_s)”

To avoid setting limits when the experiment is not sensitive to the signal, one might use the modified p-value defined above, “ p'_{s+b} ”

$$p'_{s+b} = \frac{p_{s+b}}{1 - p_b} \quad (25)$$

We find

$$p'_\mu = \frac{1 - \Phi(\sqrt{q_\mu})}{\Phi(\sqrt{q_{\mu,A}} - \sqrt{q_\mu})} \quad (26)$$

The median and expected error bands will therefore be

$$\mu_{up+N} = \sigma(\Phi^{-1}(1 - \alpha\Phi(N)) + N) \quad (27)$$

with

$$\sigma^2 = \frac{\mu^2}{q_{\mu,A}} \quad (28)$$

To get the 95% expected upper limit, set $\alpha = 0.05$. μ can be taken as μ_{up}^{med} in the calculation of σ .

Note that for $N = 0$ we find the median limit

$$\mu_{up}^{med} = \sigma\Phi^{-1}(1 - 0.5\alpha) \quad (29)$$

The expected μ and the expectation for error band N is shown in Figure 5. one can clearly see the shrinkage of the error band, $\mu_{up+N\sigma} - \mu_{up+(N-1)\sigma}$, when $N \rightarrow -\infty$

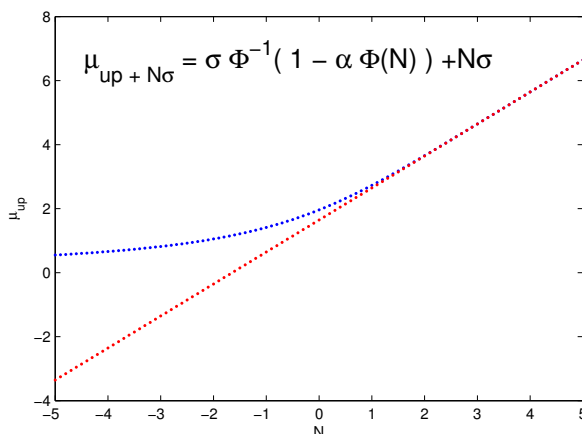


Fig. 5: $\mu_{up+N\sigma}$ as a function of N (in units of σ). Red is based on p_{s+b} blue is based on p'_{s+b} (CL_s).

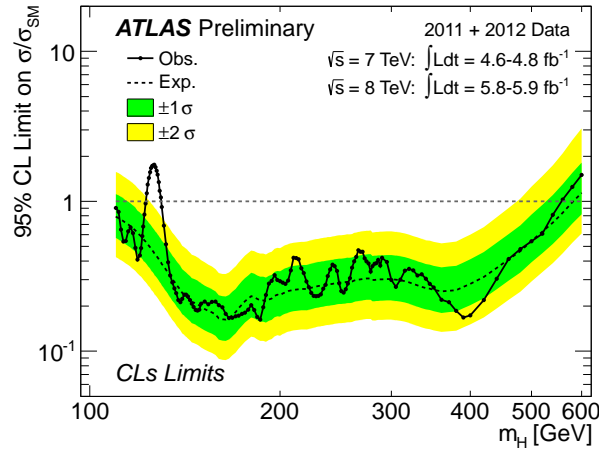


Fig. 6: The observed (full line) and expected (dashed line) 95% CL combined upper limits on the SM Higgs boson signal strength (μ_{up}) in the full mass range m_H considered in this analysis. The dashed curves show the median expected limit in the absence of a signal and the green and yellow bands indicate the corresponding 68% and 95% intervals.

5.3 Example from the Higgs Boson Search

Figure 6 taken from [10] shows μ_{up} as a function of m_H at one of the stages of the Higgs search. The mass range where $\mu_{up}(m_H) \leq 1$ is where a SM Higgs Boson with a mass m_H is excluded. Obviously one cannot exclude the Higgs around $m_H = 125$ GeV, where a real signal is being built up with luminosity $\mu_{up} > 1$. The median expected is given by the dashed line (following Equation 29 with $\alpha = 0.05$). The error bands are derived using Equation 27, with $N = \pm 1$ (Green) and $N = \pm 2$ (yellow).

Figure 7 taken from the same reference, shows p'_{s+b} (labeled in the Figure as CL_s), as a function of m_H . Mass regions where $p'_{s+b} \leq 0.05$ are excluded at, at least, the 95% CL.

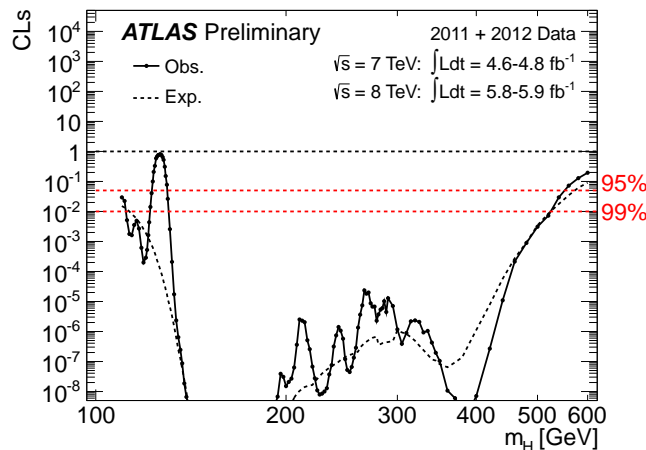


Fig. 7: The value of the combined CL_s (p'_{s+b}), testing the Standard Model Higgs boson hypothesis, as a function of m_H in the full mass range of this analysis. The expected CL_s is shown in the dashed curves. The regions with $CL_s < 0.05$ are excluded at least at 95% CL. The 95% and 99% CL values are indicated as dashed horizontal lines.

5.4 Measurement

Let the statistic be $t_\mu = -2 \ln \lambda(\mu)$ (Table 1) as the basis of the statistical test of a hypothesized value of μ . This could be a test of $\mu = 0$ for purposes of establishing existence of a signal process, or non-zero values of μ for purposes of obtaining a confidence interval. In the asymptotic regime the pdf of t_μ distributes like a χ^2 with one degree of freedom, under the H_μ hypothesis.

$$f(t_\mu|\mu) = \frac{1}{\sqrt{2\pi}} \frac{1}{\sqrt{t_\mu}} e^{-t_\mu/2} . \quad (30)$$

To measure μ , one scans the test statistics, finds $\hat{\mu}$ and σ^{up}, σ^{lo} by substituting $t_\mu = 1$. The 68% Confidence Interval of μ is then estimated to be $[\hat{\mu} - \sigma^{lo}, \hat{\mu} + \sigma^{up}]$. If one wants to estimate with how many standard deviations a specific value of μ , e.g. $\mu = 0$, is unlikely, one calculates $\sqrt{t_0}$.

To get the expected μ one repeats the above procedure, calculating t_μ with the Asimov data set, for which $\hat{\mu} = \mu$.

A formulation of the asymptotic properties of t_μ is given in [1].

5.5 Discovery

To establish a discovery one tries to reject the background only hypothesis. We use the q_0 test statistics (Table 1). Since we do not want downward fluctuations of the background to serve as an evidence against the background we define the test statistics such that $q_0 = 0$ if $\hat{\mu} < 0$. The test statistic is therefore given by (Table 1):

$$q_0 = \begin{cases} -2 \ln \frac{L(0)}{L(\hat{\mu})} & \hat{\mu} \geq 0, \\ 0 & \hat{\mu} < 0, \end{cases} \quad (31)$$

Under the background only hypothesis, H_0 , q_0 is asymptotically distributed as half a chi squared with one degree of freedom, i.e.

$$f(q_0|0) = \frac{1}{2} \delta(q_0) + \frac{1}{2} \frac{1}{\sqrt{2\pi}} \frac{1}{\sqrt{q_0}} e^{-q_0/2} . \quad (32)$$

The significance of the observation is given by

$$Z_0 = \Phi^{-1}(1 - p_0) = \sqrt{q_0} . \quad (33)$$

The p_0 value can easily be calculated using

$$p_0 = 1 - F(q_0|0) , \quad (34)$$

where

$$F(q_0|0) = \Phi(\sqrt{q_0}) . \quad (35)$$

A significance of 3σ is considered as an observation, while a significance exceeding 5σ is regarded as a discovery. The reason for using such a large number to establish a discovery is because of the Look Elsewhere Effect, discussed in section 7.

5.6 Discovery Example

In Figure 10 we show the p - value as a function of the mass, taken from the ATLAS discovery conference note [10]. Both, the p - value and its corresponding significance are indicated. One clearly sees an

upward fluctuation of the background (downward fluctuation in p -value) around a mass of 125 GeV. The fluctuation is at the level of 5σ . For other masses the p -value fluctuates around 0.5, meaning a significance of 0σ . The expected p -value is given by the dashed line. One can clearly see that only around $m_H = 125$ GeV, the expected and the observed p -value are similar, indicating a signal strength $\mu \sim 1$, as can clearly be seen in Figure 11.

5.6.1 Significance in a nut-shell.

Many people use a thumbnail formula $Z = \frac{s}{\sqrt{b}}$ to estimate the significance of an apparent signal. s represents here $n - b$, where b is the expected background, and n is the number of observed events.

Using the profile likelihood formalism we can get a much more accurate estimation for the apparent observed significance [1].

If we regard b as known, the data consist only of n and thus the likelihood function is

$$L(\mu) = \frac{(\mu s + b)^n}{n!} e^{-(\mu s + b)}, \quad (36)$$

The test statistic for discovery q_0 can be written

$$q_0 = \begin{cases} -2 \ln \frac{L(0)}{L(\hat{\mu})} & \hat{\mu} \geq 0, \\ 0 & \hat{\mu} < 0, \end{cases} \quad (37)$$

where $\hat{\mu} = n - b$. For sufficiently large b we can use the asymptotic formula [1] to obtain

$$Z_0 = \sqrt{q_0} = \begin{cases} \sqrt{2(n \ln \frac{n}{b} + b - n)} & \hat{\mu} \geq 0, \\ 0 & \hat{\mu} < 0. \end{cases} \quad (38)$$

To approximate the median significance assuming the nominal signal hypothesis ($\mu = 1$) we replace n by the Asimov value $s + b$ to obtain

$$\text{med}[Z_0|1] = \sqrt{q_{0,A}} = \sqrt{2((s + b) \ln(1 + s/b) - s)}. \quad (39)$$

Expanding the logarithm in s/b one finds

$$\text{med}[Z_0|1] = \frac{s}{\sqrt{b}} (1 + \mathcal{O}(s/b)). \quad (40)$$

Although $Z_0 \approx s/\sqrt{b}$ has been widely used for cases where $s + b$ is large, one sees here that this final approximation is strictly valid only for $s \ll b$. We therefore recommend to use Eq. 39 to estimate a significance in a nut shell. It is much more accurate.

6 Testing an hypothesis with boundaries.

In [6] Feldman and Cousins derive the test statistics with the physical condition, namely, the true value of μ must be positive, i.e. $\mu > 0$. In [1] the \tilde{t}_μ test statistic is introduced (see Table 1) in order to avoid a negative non-physical signal. As a result, depends on the observation, a two sided (measurement) or one sided (limit) Confidence Interval is obtained. This is the equivalence of the Feldman-Cousins test statistic with the advantage of taking care of the nuisance parameters. The original Feldman-Cousins test statistic is not considering systematics. In [1] the asymptotic formula of \tilde{t}_μ is derived. In a later paper [11] the same authors improve the test statistic by taking into account two sided boundaries. This

is the case, for example when one wants to measure or set limits on the measurement of a Branching Ratio, which must be $0 < BR < 1$ by definition. The revised \tilde{t}_μ is defined by

$$\tilde{t}_\mu = \begin{cases} -2 \ln \frac{L(\mu, \hat{\theta}(\mu))}{L(\mu_-, \hat{\theta}(\mu_-))} & \hat{\mu} \leq \mu_- \\ -2 \ln \frac{L(\mu, \hat{\theta}(\mu))}{L(\hat{\mu}, \hat{\theta})} & \mu_- < \hat{\mu} < \mu_+ \\ -2 \ln \frac{L(\mu, \hat{\theta}(\mu))}{L(\mu_+, \hat{\theta}(\mu_+))} & \hat{\mu} \geq \mu_+ , \end{cases} \quad (41)$$

$\hat{\theta}$ represent the nuisance parameters, $\hat{\theta}(\mu)$ is the conditional maximum likelihood estimate of θ given μ . μ_- and μ_+ are the physical boundaries. The Feldman-Cousins test statistic is retrieved for $\mu_- = 0$ and no upper boundary, μ_+ . The asymptotic formulas are derived in [11].

6.1 Pull

The pull of a nuisance parameter θ , with an expectation θ_0 is defined as:

$$pull(\theta) = \frac{\hat{\theta} - \theta_0}{\sigma_\theta} \quad (42)$$

the pull quantifies how far from its expected value we had to "pull" the parameter while finding the MLE. A healthy situation is when the pull average is zero with a standard deviation close to 1, if this is not the case, further investigation is required. The expected value of a nuisance parameter and its assumed standard deviation will be based on an auxiliary measurement or MC studies.

6.2 Impact

the impact of a nuisance parameter is defined as:

$$impact(\theta) = \Delta\mu^\pm = \hat{\mu}_{\theta_0 \pm \sigma_\theta} - \hat{\mu} \quad (43)$$

where $\hat{\mu}_{\theta_0 \pm \sigma}$ is the MLE of μ when we profile every parameter except θ , and set the value of θ to its expectation value plus or minus one standard deviation. The impact gives a measure of how much our parameter of interest varies as we change the nuisance parameter. Obviously not all nuisance parameters are equally important, so a nuisance parameter with low impact may be possibly discarded (or "pruned") to simplify the fit procedure.

6.3 Example of pull and impact

To illustrate the use of impact and pull, consider a simple counting experiment which measures n events, with $n = \mu \cdot s \cdot A \cdot \epsilon + b$, where s is the number of signal events, μ is the p.o.i and A (acceptance) ϵ (efficiency) and b (background) are nuisance parameters with gaussian distributions.

The likelihood is given by:

$$L(\mu, A, \epsilon, b) = \frac{(\mu s A \epsilon + b)^n}{n!} \exp(-(\mu s A \epsilon + b)) \exp\left(-\frac{(b - b_{obs})^2}{\sigma_b}\right) \exp\left(-\frac{(A - A_{obs})^2}{\sigma_A}\right) \exp\left(-\frac{(\epsilon - \epsilon_{obs})^2}{\sigma_\epsilon}\right) \quad (44)$$

For each nuisance parameter, there is an "observed" value which could come from some auxiliary measurement. In this simplified case all nuisance parameters are measured by their MLEs, i.e. ($\hat{\theta} = \theta_{obs}$). We assume the "true" value of the parameters are known to be θ_0 .

The pulls are calculated straightforward from equation 42. The impact is calculated with the test statistic $t_\mu(\epsilon) = -2 \ln \frac{L(\hat{\mu}, \hat{A}, \hat{\epsilon}, \hat{b})}{L(\hat{\mu}, \hat{A}, \hat{\epsilon}, \hat{b})}$ (for the nuisance parameter ϵ), with double hat indicating that the fit is constrained to ϵ , as was described above. Table 2 shows the values of the parameters used in the toy

calculation. The measured value for n , was picked from a poisson distribution with expectation value of $n_{exp} = \mu \cdot s \cdot A \cdot \epsilon + b$ (the true, Asimov, values) and ϵ_{obs} , A_{obs} and b_{obs} were picked from gaussian distributions.

Figure 8 shows a typical overlay plot of pull and impact (right plot for Asimov and left plot for some toy data set). Note the different x-axis (top for the impact, bottom for the pull). Figure 9 shows in more detail the calculation of the impact - it shows the scan of $t_\mu(\epsilon)$, $\hat{\mu}(\epsilon)$ and the procedure leading from $\hat{\epsilon} \pm \sigma_\epsilon$ points to the Impact range (right plot for Asimov and left plot for some toy data set).

Parameter	Asimov	Measured
s	90	-
n	131.5	132
μ	1	1.4
ϵ	0.5	0.465
σ_ϵ	0.05	-
A	0.7	0.487
σ_A	0.2	-
b	100	103.21
σ_b	10	-

Table 2: Parameters for toy experiment

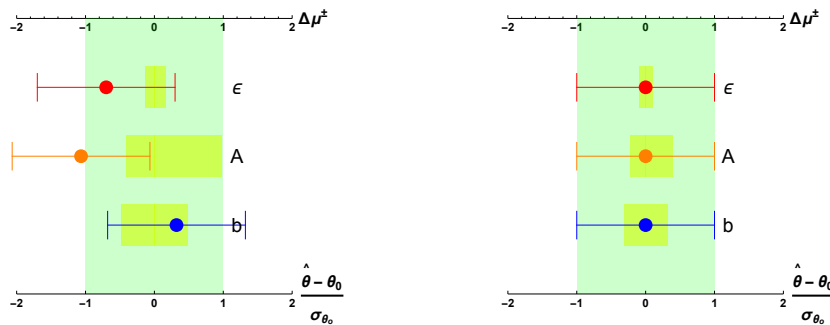


Fig. 8: Impact and pull for the three nuisance parameters (right plot for Asimov and left plot for some toy data set). The yellow rectangles show the impact range (upper x-axis) and the coloured dots show the pull (lower x-axis) with one σ error bars

7 The Look Elsewhere Effect (LEE).

Wikipedia: The look-elsewhere effect is a phenomenon in the statistical analysis of scientific experiments, particularly in complex particle physics experiments, where an apparently statistically significant observation may have actually arisen by chance because of the size of the parameter space to be searched. Once the possibility of look-elsewhere error in an analysis is acknowledged, it can be compensated for by careful application of standard mathematical techniques [2].

7.1 The LEE with one parameter (m) undefined under the null hypothesis.

When searching for a new resonance somewhere in a possible mass range, the significance of observing a local excess of events must take into account the probability of observing such an excess *anywhere* in

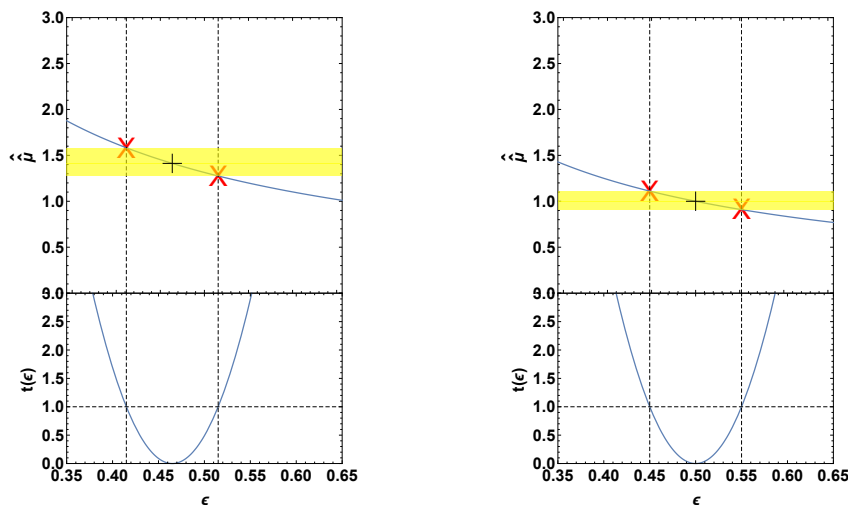


Fig. 9: Calculation of the impact of the nuisance parameter ϵ (right plot for Asimov and left plot for some toy data set). The upper plot shows the MLE of μ when profiling all parameters except ϵ (the blue curve) and the red X's show the point where $\hat{\mu}(\epsilon)$ intersects with the $\hat{\epsilon} \pm \sigma_\epsilon$ points (the dashed vertical lines), which marks the end points of the impact. The bottom plot shows the scan of the test statistic $t_\mu(\epsilon) = -2 \ln \frac{L(\hat{\mu}, \hat{A}, \hat{\epsilon}, \hat{b})}{L(\hat{\mu}, \hat{A}, \hat{\epsilon}, \hat{b})}$ and shows that the $\hat{\epsilon} \pm \sigma_\epsilon$ points correspond to $\min(t_\mu(\epsilon)) \pm 1$

the range. This is the so called “look elsewhere effect”. The effect can be quantified in terms of a trial factor, which is the ratio between the probability of observing the excess at some fixed mass point (local p -value), to the probability of observing it anywhere in the range (global p -value). The question we try to answer with a p -value is *What is the probability of observing an excess anywhere in the search range*. For years it was a common knowledge that in order to convert the local probability into a global probability one has to apply a trial factor which is simply the number of possible independent search regions, i.e. $trial \# = \frac{p_{float}}{p_{fix}} = \frac{search \ range}{mass \ resolution}$. In [2] it was shown that an important factor was missing from this rule of thumb estimation. The trial number is linearly dependent on the local significance. This can be intuitively understood by the possibility of having a look elsewhere effect within the independent search range, where the number of possibilities peak can arrange itself is proportional to the significance. The trial number is therefore asymptotically (for small p -values, i.e. large significance) given by

$$trial\# \approx 1 + \sqrt{\frac{\pi}{2}} \mathcal{N} Z_{fix} \quad (45)$$

where \mathcal{N} is the number of independent search regions.

The trial factor is thus asymptotically linear with both the effective number of independent regions, and with the fixed-mass significance.

The number of independent search region is not a trivial quantity. The resolution might not be well defined and is usually depending on the mass. We applied the formula obtained by Davies [12] for an hypothesis testing when a nuisance parameter (the mass) is known only under the alternative hypothesis. The mass is not defined under the null (background only) hypothesis.

Let $q_0(m, \theta)$ be the discovery test statistics (following Equation 31). m is undefined under the null hypothesis ($\mu = 0$). Nevertheless, there is a dependence of q_0 on the mass through the denominator.

$$q_0(m) = \begin{cases} -2 \ln \frac{L(0)}{L(\hat{\mu}, m)} & \hat{\mu} \geq 0, \\ 0 & \hat{\mu} < 0, \end{cases} \quad (46)$$

Given some data set, we scan $q_0(m)$ and find the maximal one (smallest p - value over all possible masses). We define it as

$$\hat{q}_0 \equiv \max_m [q_0(m)] = q_0(\hat{m}) \quad (47)$$

Since for any given m , $q_0(\hat{m}) \geq q_0(m)$, the global p - value, $p_{global} \geq p_{local}$. Hence, the trial number is always greater or equal to one, $Trial\# \geq 1$. We find that for high local significance (at the tail of the pdf distributions), the following relation exists between the global and local p - value:

$$P(q_0(\hat{m}) > u) \approx \frac{1}{2}P(\chi_1^2 > u) + \mathcal{N}P(\chi_2^2 > u) \quad (48)$$

where in the tail $u \rightarrow \infty$. \mathcal{N} is the number of independent search regions. To obtain this we find the average number of upcrossings at a level $u = Z^2$, n_u , i.e. $E[n_u] = \mathcal{N}e^{-u/2}$.

Since we are interested to know the global significance for high level, normally $u = Z^2 > 16$, the number of upcrossings is very small and one needs to generate expensive toys to estimate $E[n_u]$. One then renormalize the upcrossings level. Let us pick a low level u_0 where the number of upcrossings is relatively large and the statistical error on the estimation is therefore small (normally one picks $u_0 = 0$ or $u_0 = 0.5^2$). We find $E(n_{u_0}) = \mathcal{N}e^{-u_0/2}$ and therefore

$$E(n_u) = E(n_{u_0})e^{\frac{u_0-u}{2}} \quad (49)$$

Finally we find that the answer to the question: *What is the probability to have a fluctuation with a significance bigger than $Z = \sqrt{u}$ all over a given mass range?* is given by

$$P_{global}(u) \approx p_{local}(u) + E(n_{u_0})e^{\frac{u_0-u}{2}} \quad (50)$$

where u_0 is some low reference level, where the estimation of the number of upcrossings $E(n_{u_0})$ is easy and fast.

To illustrate it let us look at a real example from the Higgs Boson search and discovery. In the following Figures we show the p_0 (Figure 10) and the signal strength μ (Figure 11) as a function of the Higgs mass. The plots are taken from the ATLAS discovery conference note [10]. $Z = 0$ corresponds

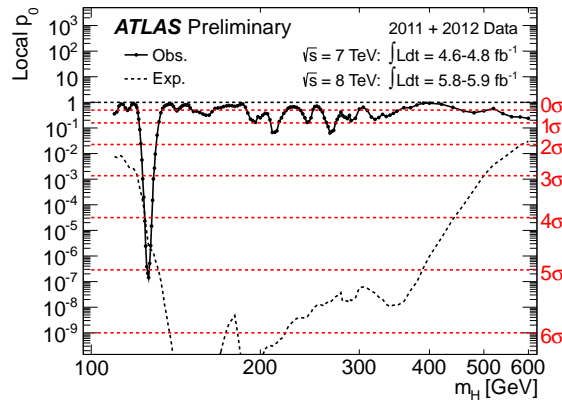


Fig. 10: The local probability p_0 for a background-only experiment to be more signal-like than the observation in the full mass range of this analysis as a function of m_H . The dashed curves show the median expected local p_0 under the hypothesis of a Standard Model Higgs boson production signal at that mass. The horizontal dashed lines indicate the p -values corresponding to significances of 1σ to 6σ .

to either $p_0 = 0.5$ or $\hat{\mu} = 0$. So we have to count the number of up-crossings at 0σ . We should have performed a few Monte Carlo experiments and count the average number of up-crossings at $u = 0$. But

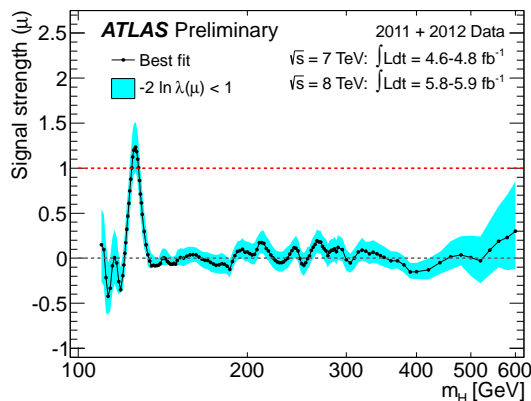


Fig. 11: The combined best-fit signal strength $\hat{\mu}$ as a function of the Higgs boson mass hypothesis in the full mass range of this analysis

this seems to be not practical when we combine all the channels. Instead we could simply take the data itself and count $n_{u_0} = 9 \pm 3$. This accuracy is sufficient for the estimation of the trial number. Following Equation 50, substituting $u_0 = 0$ and $u = 5^2 = 25$, we find

$$p_{global} = O(10^{-7}) + 9 \times e^{-25/2} = 3.3 \times 10^{-5} \quad (51)$$

The trial number is about $trial\# \approx \frac{10^{-5}}{10^{-7}} \approx 100$ and it reduces the significance from 5σ to 4σ .

7.2 The LEE with two parameters (m, Γ) undefined under the null hypothesis.

In cases where there are two parameters undefined under the null hypothesis, such as mass (m) and width (Γ) the Look Elsewhere Effect is broader. Ref [13] solved the case for a multi-dimensional search.

Suppose we would like to estimate the global significance of some observed excess. When allowing both the mass and the width float, we observe that the highest significance of $Z\sigma$ occurs for some specific mass and width. This observation corresponds to a local background fluctuation with a p -value of p_{local} . However, any fluctuation at any mass and width in the 2D search plane of m and Γ would have drawn our attention. The increased probability to observe a fluctuation of $Z\sigma$ or more anywhere in the mass-width plane $A = (m, \Gamma)$ (LEE) is given by the global p -value, p_{global} . The local p -value is based on scanning the $q_0(m, \Gamma)$ test statistic, $q_0(m, \Gamma)$ given by

$$q_0(m, \Gamma) = -2 \log \frac{L(0, m, \Gamma, \hat{\theta})}{L(\hat{\mu}, \hat{m}, \hat{\Gamma}, \hat{\theta})}. \quad (52)$$

The distribution of the maximum local significance $u = Z^2 = \max_{m, \Gamma} q_0(m, \Gamma)$ was studied in [13]. The global p -value is given by

$$p_{global} \approx E[\phi(A_u)] = p_{local} + e^{-u/2}(N_1 + \sqrt{u}N_2) \quad (53)$$

where N_1 and N_2 are coefficients that are estimated by calculating the average Euler characteristic of the plane A . To solve for N_1 and N_2 , it is convenient to set two reference levels u_0 and u_1 , find the Euler characteristics for each level, and solve the consequent system of two linear equations. In a 2D manifold with closed islands, some with holes, each disconnected full island takes the value $+1$. Each hole contributes -1 . In that sense a full round shape has the Euler characteristic of $+1$. If you dig a hole in it, its Euler characteristics becomes $+1 - 1 = 0$ (Figure 12).

An example can be taken from the search for di-photon in ATLAS [14]. In Figure 13 one sees the 2D $(m_X, \Gamma_X/m_X)$ plane. The manifold A_u is obtained by slicing this plane at a level $u = Z^2$. The Euler characteristic is the number of "disconnected" islands in that slice.

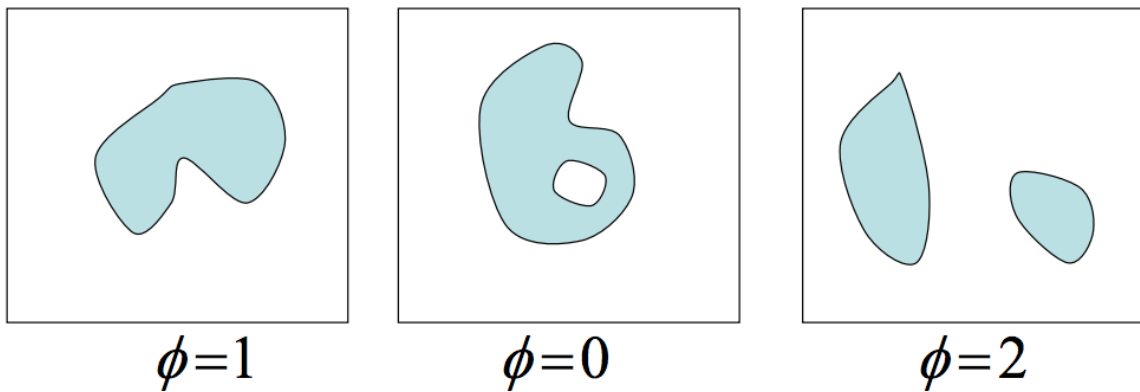


Fig. 12: Illustration of the Euler characteristic of some 2-dimensional manifold.

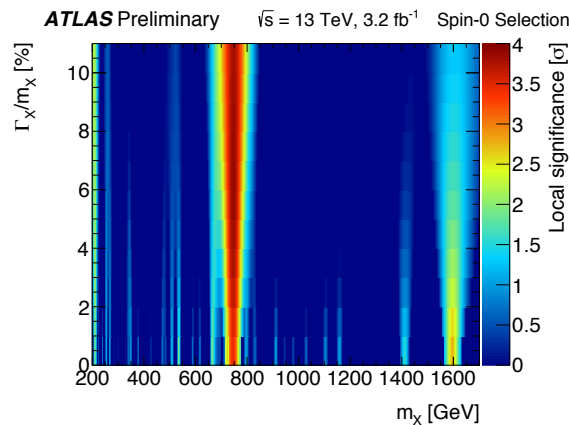


Fig. 13: The 2D $(m_X, \Gamma_X/m_X)$ plane. The colors are the significance Z , where the level u is given by $u = Z^2$

Acknowledgements

The author would like to thank Jonathan Shlomi for helping to produce some of the Figures shown and for his careful reading of the manuscript. His comments were very useful. The author would also like to thank the organisers of ESPHEP, Nick Ellis and Martijn Mulders for the wonderful opportunity to prepare these lectures.

References

- [1] G. Cowan, K. Cranmer, E. Gross and O. Vitells, *Eur. Phys. J. C* **71** (2011) 1554 [*Eur. Phys. J. C* **73** (2013) 2501] doi:10.1140/epjc/s10052-011-1554-0, 10.1140/epjc/s10052-013-2501-z [arXiv:1007.1727 [physics.data-an]].
- [2] E. Gross and O. Vitells, *Eur. Phys. J. C* **70**, 525 (2010) doi:10.1140/epjc/s10052-010-1470-8 [arXiv:1005.1891 [physics.data-an]].
- [3] Neyman, Jerzy; Pearson, Egon S. (1933). "On the Problem of the Most Efficient Tests of Statistical Hypotheses". *Philosophical Transactions of the Royal Society A: Mathematical, Physical and Engineering Sciences* 231 (694i&j;706): 289i&j;337. Bibcode:1933RSPTA.231..289N. doi:10.1098/rsta.1933.0009. JSTOR 91247.
- [4] Birnbaum, Allan (1962). "On the foundations of statistical inference". *Journal of the American Statistical Association* 57 (298): 269i&j;326. doi:10.2307/2281640. JSTOR 2281640. MR 0138176.

- [5] Presentation of search results: the CLs technique, A L Read 2002 J. Phys. G: Nucl. Part. Phys. 28 2693-2704, doi:10.1088/0954-3899/28/10/313
- [6] G. J. Feldman and R. D. Cousins, Phys. Rev. D **57** (1998) 3873 doi:10.1103/PhysRevD.57.3873 [physics/9711021 [physics.data-an]].
- [7] R. D. Cousins and V. L. Highland, “Incorporating systematic uncertainties into an upper limit,” Nuclear Instruments and Methods A.320 (1992) 331-335
- [8] S.S. Wilks, *The large-sample distribution of the likelihood ratio for testing composite hypotheses*, Ann. Math. Statist. **9** (1938) 60-2.
- [9] A. Wald, *Tests of Statistical Hypotheses Concerning Several Parameters When the Number of Observations is Large*, Transactions of the American Mathematical Society, Vol. **54**, No. 3 (Nov., 1943), pp. 426-482.
- [10] [ATLAS Collaboration], “Observation of an Excess of Events in the Search for the Standard Model Higgs boson with the ATLAS detector at the LHC,” ATLAS-CONF-2012-093.
- [11] G. Cowan, K. Cranmer, E. Gross and O. Vitells, “Asymptotic distribution for two-sided tests with lower and upper boundaries on the parameter of interest,” arXiv:1210.6948 [physics.data-an].
- [12] R. B. Davies, *Hypothesis testing when a nuisance parameter is present only under the alternative*, Biometrika **74** (1987), 33-43.
- [13] O. Vitells and E. Gross, “Estimating the significance of a signal in a multi-dimensional search,” Astropart. Phys. **35**, 230 (2011) doi:10.1016/j.astropartphys.2011.08.005 [arXiv:1105.4355 [astro-ph.IM]].
- [14] The ATLAS collaboration, “Search for resonances in diphoton events with the ATLAS detector at $\sqrt{s} = 13$ TeV,” ATLAS-CONF-2016-018.

Organizing Committee

T. Donskova (Schools Administrator, JINR)
N. Ellis (CERN)
M. Mulders (CERN)
A. Olchevsky (JINR)
K. Ross (Schools Administrator, CERN)
G.. Zanderighi (CERN & Oxford Univ., UK)

Local Organizing Committee

P. Iaydjuev (INRNE, Bulgaria)
I. Ilchev (Sofia Univ., Bulgaria)
L. Kostov (BNRA, Bulgaria)
G. Mitkova (BNRA, Bulgaria)
B. Pavlov (Sofia Univ., Bulgaria)
D. Tonev (INRNE, Bulgaria)
R. Tsenov (Sofia Univ., Bulgaria)
G. Vankova-Kirilova (Sofia Univ., Bulgaria)

International Advisors

R. Heuer (CERN)
V. Matveev (JINR)
A. Skrinsky (BINP, Novosibirsk, Russia)
N. Tyurin (IHEP, Protvino, Russia)

Lecturers

A. Arbuzov (JINR)
S. Floerchinger (CERN)
S. Gori (Perimeter Inst., Canada)
E. Gross (Weizmann Inst., Israel)
A. Mitov (Univ. of Cambridge, UK)
T. Nakada (EPFL, Switzerland)
S. Petcov (SISSA, Italy)
F. Riva (CERN)
A. De Simone (SISSA, Italy)
A. Wulzer (INFN, Italy)

Discussion Leaders

S. Alioli (CERN)
A. Bednyakov (JINR)
S. Demidov (INR, Russia)
V. Filev (DIAS, Ireland)
M. Garny (CERN)
E. Ginina (HEPHY, Austria)

Students

Thea AARRESTAD	Andrew FERRANTE	Roger NARANJO
Marharyta ALOKHINA	Simon FINK	Daniel NARRIAS VILLAR
Damian ALVAREZ PIQUERAS	Nils FLASCHEL	Ivan ORLOV
Brian AMADIO	Camilla GALLONI	Josef PACALT
Ivan ANGELOZZI	Andrea GAUDIELLO	Joao PELA
Juan Pedro ARAQUE ESPINOSA	Aysenur GENCER	Sebastien PRINCE
Francisco ARDUH	Nikolay GERAKSIEV	Yang QIN
William ASTILL	Francesco GIULI	Georgiy RAZUVAEV
Nikolay ATANOV	Olga GRZYMKOWSKA	Othmane RIFKI
Nada BARAKAT	Ali HARB	Jonatan ROSTEN
Cristovao BEIRAO DA CRUZ E SILVA	Tobias HECK	Violetta SAGUN
Sophie BERKMAN	Rachel HINMAN	Daniel SALERNO
Christian BOURJAU	Maria HOFFMANN	Daria SAVRINA
Elvire BOUVIER	Mikhail ILIUSHIN	Balthasar SCHACHTNER
Eldwan BRIANNE	Andrew JOHNSON	Marco SESSA
Carsten BURGARD	Goran KACAREVIC	Muhammad SHOAIB
Daniel BUSCHER	Oleh KIVERNYK	Milan STOJANOVIC
Michael BUTTIGNOL	Nicolas KOEHLER	Thomas STREBLER
Luca CADAMURO	Nataliia KONDRASHOVA	Stanislav SUCHEK
Leonor CERDA ALBERICH	Nataliia KOVALCHUK	Rishat SULTANOV
Daniel CERVENKOV	Anna KOWALEWSKA	Mohamad TARHINI
Zakaria CHADI	Dmytro LEVIT	El Sayed Abdelftah TAYEL
Shirin CHENARANI	Matic LUBEJ	Royer TICSE TORRES
Irina CIOARA	Anna LUPATO	Malika TOUIL
Orjan DALE	Daniele MADAFFARI	Nikolozi TSVERAVA
Baishali DUTTA	Anna MAKSYMCHUK	Emanuele USAI
Katharina ECKER	Christine MC LEAN	Tsvetan VETSOV
Imad EL BOJADDAINI	Philipp MILLET	Oleksandr VIAZLO
Abdelali EL JAUDI	Stefan MLADENOV	Vytautas VISLAVICIUS
Esmaeel ESKANDARI TADAVANI	Adam MORRIS	Michael ZIEGLER
	Miha MUSKINJA	Joze ZOBEC

Posters

Poster title	Author
Search for heavy resonances in the W/Z-tagged dijet mass spectrum at CMS	AARRESTAD, T.
Multijet Black Hole Search Using 13 TeV p-p Collisions at the ATLAS Detector	AMADIO, B.
Evidence of Higgs boson decay to a pair of τ leptons with ATLAS detector in Run I	ALVAREZ PIQUERAS, D.
Search for LFV $\tau \rightarrow \mu\gamma\gamma$ channel in ATLAS	ANGELOZZI, I.
Search for vector-like quark decaying to a Z boson with the ATLAS experiment	ARAQUE, J. P.
Search for monotops at the LHC	BUTTIGNOL, M.
The CMS Level-1 τ algorithm for the LHC Run II	CADAMURO, L.
Search for di-Higgs production in the $\gamma\gamma bb$ channel with the ATLAS detector	CERDA ALBERICH, L.
Search for Chargino pair production in the Electron-Muon Channel	CHENARANI, S.; BAKHSHIAN, H.; ESKANDARI, E.; FAHIM, A.; JAFARI, A.; PAKTINAT, S.; ZEINALI, M.
ATLAS Run 2 HVV coupling measurements in the EFT framework	ECKER, K.; BURGARD, C.
The CALICE Technological Prototype of the Analog Hadronic Calorimeter for ILC	ELDWAN, B.
Search for Chargino Pair Production Decaying to Stau in Di-Electron Final States with $\sqrt{s} = 8$ TeV CMS data	ESKANDARI, E.; BAKHSHIAN, H.; CHENARANI, S.; FAHIM, A.; JAFARI, A.; PAKTINAT, S.; ZEINALI, M.
FPGA Based Data Read-Out System of the Belle 2 Pixel Detector	LEVIT, D.; KONOROV, I.; BAI, Y.; PAUL, S.

Poster title	Author
Belle II Physics Analysis Tools	LUBEJ, M.
Search for $H \rightarrow b\bar{b}$ in Association with Single Top Quarks as a Test of Higgs Boson Couplings	FINK, S.
Search for heavy resonances decaying $X \rightarrow HH \rightarrow \tau\tau b\bar{b}$ final state at CMS	GALLONI, C.
Defocusing beam line for an irradiation facility at the TAEA SANAEM Proton Accelerator Facility	GENCER, A.; DEMIRKÖZ, M. B.; EFTHYMIPOULOS, I.; YIGITOGU, M.
Inclusive Study of Charmed Mesons in $B \rightarrow D^* D_{s(J)}^*$ Decays at Belle Experiment	GRZYMKOWSKA, O.
Test Beam of the first CMS P_T -module using the CBC2 read-out Chip for the Phase-II Upgrade	HARB, A.; HAUKE, J.; MUSSGILLER, A.
A search for $t\bar{t}$ resonances using lepton plus jets events in proton-proton collisions at $\sqrt{s} = 8$ TeV with the ATLAS detector	HECK, T.
ATLAS Pixel Detector Performance	HINMAN, R.
Production of Cumulative Particles and Light Nuclear Fragments at High p_T Values beyond the Fragmentation Region of Nuclei in pA Collisions at a Proton Energy of 50 GeV	ILIUSHIN, M.
Plans to test scintillator strips for the muon system at ILC	KACAREVIC, G.
Muon reconstruction performance in ATLAS at LHC Run-II	KÖHLER, N.
Jet Energy Corrections at CMS	KOVALCHUK, N.; STOEVEER, M.; STADIE, H.
Charged Higgs boson searches in $H^\pm \rightarrow \tau\nu$ channel in the ATLAS experiment at the LHC	KOWALEWSKA, A.
Semileptonic Decays at LHCb	LUPATO, A.
HyperNIS TOF System	MAKSYMCHUK, A.

Poster title	Author
Search for resonant slepton production in R-parity violating SUSY scenarios with CMS	MILLET, P.
Non-abelian T-duality in string theory	MLADENOV, S.; RASHKOV, R.; VETSOV, T.
Measurement of the $B_s^0 \rightarrow \phi\phi$ branching fraction and search for $B_d^0 \rightarrow \phi\phi$	MORRIS, A.
$ZZ \rightarrow 4l$ at 13 TeV with ATLAS	ROSTEN, J.
The study of the $e^+e^- \rightarrow \pi^0\gamma, \eta\gamma \rightarrow 3\gamma$ processes with the CMD-3 detector at the VEPP-2000 collider	RAZUVAEV, G.P.
Measurement of the $t\bar{t}W/Z$ production cross-sections using events with same-sign leptons at 8 TeV with the ATLAS detector	RIFKI, O.
Non-equilibrium of Strange Hadrons and Λ -anomaly during Chemical Freeze-out Stage	SAGUN, V.
Search for standard model $t\bar{t}H(bb)$ production in the all hadronic final state using the Matrix Element Method	SALERNO, D.; CAMINADA, L.; PROF. CANELLI, F.
Search for the associated production of the Higgs boson with a top quark pair in multi-lepton final states with the ATLAS detector	SESSA, M.
Level-1 trigger selection of electrons and photons with CMS for LHC Run-II	STREBLER T.
Studies of Identified Charged Jets in ALICE Experiment	SULTANOV R.
Search for $t\bar{t}H(H \rightarrow bb)$ channel and identification of jets containing two B hadrons with the ATLAS detector.	TICSE TORRES, R.E.
Search for the decay $B^0 \rightarrow \tau^+\tau^-$ at Belle	ZIEGLER, M.